Treatment of the Cyanotoxin Anatoxin-a via Activated Carbon Adsorption

by

Silvia Vlad

A thesis
presented to the University of Waterloo
in fulfillment of the
thesis requirement for the degree of
Master of Applied Science
in
Civil Engineering

Waterloo, Ontario, Canada, 2015

©Silvia Vlad 2015

AUTHOR'S DECLARATION

I hereby declare that I am the sole author of this thesis. This is a true copy of the thesis, including any required final revisions, as accepted by my examiners.

I understand that my thesis may be made electronically available to the public.

Silvia Vlad

Disclaimer

The mention of trade names or commercial products does not constitute endorsement of or recommendation for their use.

Abstract

Cyanobacteria are bloom-forming aquatic microorganisms that impact many drinking water sources and can produce a variety of toxins, eponymously termed cyanotoxins. Three cyanotoxins are of particular concern in a North American context, as indicated by their inclusion on the USEPA's third iteration of the Candidate Contaminant List (CCL3): microcystin, cylindrospermopsin and anatoxin-a. Of these, anatoxin-a (a potent neurotoxin) cannot be effectively oxidized by chlorine, indicating that conventional drinking water treatment plants may not have an effective barrier to this toxin. Investigation into treatment alternatives is needed; activated carbon removal of anatoxin-a has not previously been thoroughly studied, though granular and powdered activated carbon (GAC and PAC) are frequently used to remove other cyanobacterial metabolites. The primary objective of this research was to elucidate anatoxin-a adsorption behaviour during treatment with activated carbon.

Two analytical methods for the quantification of anatoxin-a were evaluated: an enzyme-linked immunosorbent assay (ELISA) which had only recently become available, and a liquid-chromatography tandem mass spectrometry (LC-MS/MS) method. The ELISA method was deemed unsuitable for the planned treatment study, as it could not quantify (-)-anatoxin-a (one of the two stereoisomers present in the racemic (±)-anatoxin-a standard), had a relatively high variability in toxin detection, and was time-intensive. Comparatively, the LC-MS/MS method established was rapid, reproducible and capable of quantifying environmentally-relevant toxin concentrations (method detection limit of 0.65 µg/L) without sample pre-treatment.

Anatoxin-a adsorption in ultrapure water was investigated using six virgin carbons: coal-based F400 and F300 GACs (Calgon Carbon), coconut-based Aqua Carb GAC (Siemens), wood-based C Gran and WV B-30 (Norit and WMV, respectively) GACs, and finally coal-based Watercarb 800 PAC (Standard Purification). The coal-based GACs (F400 and F300) required the greatest amount of time

to reach equilibrium (up to 90 days for F300, the larger of the two carbons), but had the highest capacity of the virgin GACs. Conversely, the more mesoporous wood-based carbons were the fastest of the GACs to attain equilibrium (within 14 days), but had lower ultimate capacity at the concentrations examined (approximately 50% less than the coal-based GACs at 1 µg/L aqueous anatoxin-a concentration). Unsurprisingly given its microporous structure, the coconut-based Aqua Carb was relatively slow to reach equilibrium (45 days); its capacity was similar to those of the wood-based GACs at 1 µg/L aqueous anatoxin-a. The one coal-based PAC included in this study had both faster kinetics and higher capacity than the GACs, although depending on its application, the capacity of PAC may not always be fully utilized. Furthermore, intact cyanobacterial cells may be able to bypass PAC treatment only to be lysed and release intracellular toxin later in the treatment train.

The five GACs were preloaded with natural organic material (NOM) at pilot scale for approximately 40,000 bed volumes, using post-sedimentation water from a full-scale southern Ontario surface water treatment plant. Based on bench-scale studies using the preloaded carbons in ultrapure water, the coal-based GACs retained the greatest capacity at aqueous anatoxin-a concentrations below 20 µg/L. A second sample of preloaded F300 carbon was obtained from a full-scale treatment plant where it had been in use for approximately 100,000 bed volumes, and isotherm studies indicated its capacity was approximately 40% lower than that of the pilot-preloaded F300, and 60% lower than that of the virgin F300. Interestingly, the preloaded GACs had slightly faster toxin uptake than their virgin counterparts; F400 and F300 in particular saw an increase in removal rate, an effect partially attributable to changes in carbon surface charge. It is postulated that the NOM-preloading resulted in lower repulsive interactions between the positively-charged coal-based GACs and the cationic anatoxin-a.

Adsorption of anatoxin-a by the virgin carbons was also investigated in Grand River water (GRW), although difficulties with toxin degradation were encountered. In GRW (pH 8.0), anatoxin-a degraded

by approximately 60% over 21 days, while positive controls in ultrapure water (pH 6.3) remained relatively stable. The observed change in stability may be partially attributed to pH sensitivity, as anatoxin-a becomes deprotonated at higher pHs and the deprotonated, neutral form is less stable than the cationic, protonated form. Based on equilibrium isotherms the five GACs had very similar capacity to one another in GRW, while the kinetic data show that the coal-based carbons again had the slowest toxin removal. Capacity reductions compared to the virgin carbons ranged from 15% (WV B-30, wood-based) to 69% (F400, coal-based), at a 1 µg/L aqueous anatoxin-a concentration.

Overall, the findings indicated that adsorption of anatoxin-a using PAC and GAC is a promising treatment option, although further investigation is needed to confirm findings in other surface waters, and at a larger scale (i.e. pilot-scale). This research has implications for drinking water providers impacted by cyanobacteria, and may be a valuable aid in analyzing the advantages of different carbon types.

Acknowledgements

Firstly, I would like to thank my supervisions, Drs. William B. Anderson, Peter M. Huck and Sigrid Peldszus for their guidance and support throughout my Master's program. I am grateful for the opportunities you have given me to learn and experience new aspects of research, your valuable and thoughtful counsel, and for your undaunted tenacity in tackling challenging research problems.

I offer my heartfelt thanks to my family and friends for helping me to reach this point – your cheerful support and encouragement made all the difference. I am grateful to my parents, my sister and my fiancé for lending me perspective and for their patience and optimism.

I also wish to thank the many students and staff at the University of Waterloo and in the NSERC Chair in Water Treatment who offered their immeasurable help in ways great and small throughout the course of my degree. My profound thanks go to Dr. Feisal Rahman for his help at every stage; his passion for scientific inquiry and vision of human potential continue to inspire me. I am grateful to Dr. Monica Tudorancea for her help with the LC-OCD analysis and for always being willing to help graduate students overcome challenges in lab work, and to Victoria Chennette for sharing the results of her work determining activated carbon surface charges. Thanks to my fellow graduate students and friends, Jonathan Bradley Reginald Pettifer Wilson, Lizanne Pharand, Michael (Yulang) Wang, Alex (Fei) Chan, Ahmed El-Hadidy, Helen (Yanting) Liu, Michelle Cho, Cailin Hillier and Nathanael Couperus – it has been a pleasure and a privilege to work with you all. Special thanks go to Dana Herriman for all her assistance.

I would like to acknowledge Dr. Detlef Knappe for his suggestion to normalize kinetic data so as to exclude particle size effects. I gratefully acknowledge the support of Mark Merlau, Mark Sobon and Terry Ridgeway, who were always ready and able to help with lab troubleshooting. I would also like to offer my thanks to Dr. Souleymane Ndiongue, Dr. Xiaohui Jin and Tory Hewlett of the Walkerton

Clean Water Centre for their feedback and perspectives on cyanobacterial research, to the Region of Waterloo for their assistance in setting up a pilot preloading system, and to the Cities of Barrie and London for providing carbon samples for use in this study.

Finally, I wish to thank the Water Institute at the University of Waterloo for giving me the opportunity to meet others passionate about water, and to acknowledge their efforts to facilitate interactions between students of different disciplines and promote collaboration.

Funding for this project was provided by the Natural Sciences and Engineering Research Council of Canada (NSERC) in the form of an Industrial Research Chair in Water Treatment at the University of Waterloo. The current Chair partners include: the Region of Waterloo, Walkerton Clean Water Centre, City of Brantford, City of Hamilton, Lake Huron and Elgin Area Water Supply Systems, Region of Halton, City of Ottawa, City of Guelph, Region of Niagara, Region of Durham, City of Barrie, City of Toronto, Ontario Clean Water Agency (OCWA), Conestoga-Rovers & Associates Ltd., Associated Engineering Group Ltd., GE Water & Process Technologies Canada, MTE Consultants Inc., EPCOR Water Services, and RAL Engineering Ltd. This work was produced as part of a project conducted in partnership with the Walkerton Clean Water Centre.

Dedication

In light of the many divisions we face as professionals and as global citizens, I find it profoundly heartening to have seen first-hand that distinctions between academic disciplines, nationalities and backgrounds can all be set aside, as strangers become colleagues and colleagues become friends.

In that spirit, this thesis is dedicated to the ideals of collaboration and cooperation, in the hope that together we can achieve the great endeavors we have set ourselves, and find greater-still ambitions to which we can aspire.

Table of Contents

AUTHOR'S DECLARATION ii
Disclaimer iii
Abstract iv
Acknowledgements vii
Dedication ix
Table of Contents x
List of Figures xiii
List of Tables xvi
List of Acronyms xvii
Chapter 1 Introduction 1
1.1 Problem Statement 1
1.2 Research Objectives 4
1.3 Research Approach and Thesis Structure 4
Chapter 2 Removal of the Cyanotoxin Anatoxin-a by Drinking Water Treatment Processes: A Review 7
2.1 Summary 7
2.2 Introduction 7
2.3 Analogues, Chemical Properties and Stability 9
2.4 Toxicity, Occurrence and Regulations 11
2.5 Water treatment processes for extracellular anatoxin-a removal or degradation 12
2.5.1 Oxidation 12
2.5.2 Membrane filtration 25
2.5.3 UV Irradiation 26
2.5.4 Adsorption 27
2.5.5 Biofiltration/Slow Sand Filtration 30
2.5.6 Other treatment options 31
2.6 Best Practices 32
2.7 Conclusions 35
Chapter 3 Analytical Considerations for Anatoxin-a 36
3.1 Summary 36
3.2 Introduction 36

3.3 Materials and Methods 40
3.3.1 Standards and solutions 40
3.3.2 Anatoxin-a Receptor Binding Assay 41
3.3.3 LC-MS/MS 42
3.4 Anatoxin-a Receptor Binding Assay Validation 43
3.4.1 Standard Protocol 43
3.4.2 Enhanced Sensitivity Protocol 44
3.5 LC-MS/MS Method Development and Validation 46
3.6 Analytical Method Comparison 49
3.7 Conclusions 50
Chapter 4 Anatoxin-a Adsorption by Virgin Carbon in Ultrapure Water 52
4.1 Summary 52
4.2 Introduction 52
4.3 Materials and Methods 54
4.3.1 Materials 54
4.3.2 Carbon Analysis 55
4.3.3 Sample Preparation and Handling 56
4.3.4 Anatoxin-a Analysis by LC-MS/MS 57
4.4 Results and Discussion 57
4.4.1 Carbon Properties 57
4.4.2 Kinetics 62
4.4.3 Isotherms 68
4.4.4 Equilibrium Column Model 77
4.5 Conclusions 79
Chapter 5 Adsorption of Anatoxin-a by Preloaded Carbon in Ultrapure Water 82
5.1 Summary 82
5.2 Introduction 82
5.3 Materials and Methods 83
5.3.1 Materials 83
5.3.2 Carbon Preloading 83
5.3.3 Sample Preparation and Handling 86
5.3.4 Anatoxin-a Analysis by LC-MS/MS 86

5.4 Results and Discussion 86
5.4.1 Carbon Preloading 86
5.4.2 Kinetics 88
5.4.3 Isotherms 94
5.4.4 Equilibrium Column Model 101
5.5 Conclusions 103
Chapter 6 Adsorption of Anatoxin-a by Virgin Carbon in Natural Water 105
6.1 Summary 105
6.2 Introduction 105
6.3 Materials and Methods 106
6.3.1 Materials 106
6.3.2 Sample Preparation and Handling 106
6.3.3 Anatoxin-a Analysis by LC-MS/MS 107
6.4 Results and Discussion 108
6.4.1 Natural Water Characterization 108
6.4.2 Anatoxin-a Stability 108
6.4.3 Kinetics 109
6.4.4 Isotherms 111
6.4.5 Equilibrium Column Model 122
6.5 Conclusions 123
Chapter 7 Conclusions and Recommendations 125
7.1 Summary of Conclusions 126
7.1.1 Anatoxin-a Analytical Methods (Chapter 3) 126
7.1.2 Anatoxin-a Adsorption Behaviour (Chapters 4 – 6) 126
7.2 Recommendations for Future Research 129
References 131
Appendix A Additional LC-MS/MS Method Validation Data 143
Appendix B Linearly Determined Kinetic Parameters 144
Appendix C Confidence Intervals and Joint Confidence Regions for Freundlich Isotherms 146
Appendix D Kinetic Data 149
Appendix E Equilibrium Data 154
Appendix F Details of Surface Area and Pore Volume Distribution Analysis 163

List of Figures

Figure 1.1: NASA Modis sensor satellite image of Lake Erie from Oct. 9, 2011. 2
Figure 1.2: Cyanobacterial toxins on the USEPA's contaminant candidate list. 3
Figure 1.3: Thesis structure and relevance of the thesis chapters 6
Figure 2.1: Molecular structures: a) protonated (+)-anatoxin-a, b) deprotonated (+)-anatoxin-a, c) homoanatoxin-a 9
Figure 2.2: Anatoxin-a species distribution based on pH. 10
Figure 2.3: pH dependence of the rate constants for the reaction of cyanotoxins with ozone. Reprinted with permission from Onstad et al. (2007). Copyright 2007 American Chemical Society. 18
Figure 4.1: Cumulative pore area with increasing pore width, for the 6 carbons investigated 61
Figure 4.2: Pore volume represented at a range of pore widths, for the 6 carbons investigated 61
Figure 4.3: Anatoxin adsorption as a function of time 63
Figure 4.4: GAC removal kinetics, normalized by average effective particle size 64
Figure 4.5: Pseudo-second order kinetic model fits using virgin carbon in ultrapure water. 67
Figure 4.6: Anatoxin-a Freundlich isotherms for virgin F400 and F300 (coal-based) GACs in ultrapure water 69
Figure 4.7: Anatoxin-a Freundlich isotherm, for virgin Aqua Carb (coconut-based) GAC in ultrapure water 70
Figure 4.8: Anatoxin-a Freundlich isotherm, for virgin C-Gran (wood-based) GAC in ultrapure water 70
Figure 4.9: Anatoxin-a Freundlich isotherm, for virgin WV B-30 (wood-based) GAC in ultrapure water 70
Figure 4.10: Anatoxin-a Freundlich isotherm, for virgin PAC (coal-based) in ultrapure water 71
Figure 4.11: Anatoxin-a Freundlich isotherms for six carbons investigated 72
Figure 4.12: Freundlich adsorption coefficient (K_F) non-linear fit with 95% confidence intervals 74
Figure 4.13: Freundlich model parameter (1/n) non-linear fit with 95% confidence intervals 74
Figure 4.14: 95% joint confidence regions and point estimates for the Freundlich parameters of isotherms generated with virgin carbon in ultrapure water 75
Figure 4.15: Comparison of Freundlich isotherms for anatoxin-a, MIB and geosmin by virgin coal-based carbons in ultrapure water. 76
Figure 4.16: ECM predicted total treated volume to breakthrough 79
Figure 5.1: GAC preloading design 85

Figure 5.2: GAC preloading setup 85
Figure 5.3: TOC of influent and effluents for the five GAC contactors used for preloading 87
Figure 5.4: Anatoxin adsorption by preloaded carbons as a function of time 89
Figure 5.5: GAC removal kinetics, normalized by average effective particle size 89
Figure 5.6: F400 kinetics - preloaded and virgin carbons in ultrapure water 90
Figure 5.7: F300 kinetics - preloaded and virgin carbons in ultrapure water 91
Figure 5.8: Aqua Carb kinetics - preloaded and virgin carbons in ultrapure water 91
Figure 5.9: C Gran kinetics - preloaded and virgin carbons in ultrapure water 91
Figure 5.10: WV B-30 kinetics - preloaded and virgin carbons in ultrapure water 92
Figure 5.11: Pseudo-second order kinetic model fits using preloaded carbon in ultrapure water. 93
Figure 5.12: Anatoxin-a Freundlich isotherms for virgin and preloaded F400 and F300 (coal-based) GAC in ultrapure water 95
Figure 5.13: Anatoxin-a Freundlich isotherms for virgin and preloaded Aqua Carb (coconut-based) GAC in ultrapure water 95
Figure 5.14: Anatoxin-a Freundlich isotherms for virgin and preloaded C-Gran and WV B-30 (wood-based) GAC in ultrapure water 96
Figure 5.15: Anatoxin-a Freundlich isotherms for six preloaded GACS 97
Figure 5.16: Freundlich adsorption coefficient (K_F) non-linear fit with 95% confidence intervals 98
Figure 5.17: Freundlich model parameter (1/n) non-linear fit with 95% confidence intervals 99
Figure 5.18: 95% joint confidence intervals and point estimates for the Freundlich parameters of isotherms generated with preloaded carbon in ultrapure water 100
Figure 5.19: Comparison of Freundlich isotherms for anatoxin-a and MIB by preloaded wood- and coconut-based carbons.. 101
Figure 5.20: ECM predicted total treated volume to breakthrough 102
Figure 6.1: Anatoxin-a positive controls in ultrapure water (UW) and Grand River water (GRW), degradation over 21 days 109
Figure 6.2: Anatoxin % removal by virgin carbons in GRW as a function of time 110
Figure 6.3: Anatoxin-a removal time series, normalized by average effective particle size 111
Figure 6.4: Anatoxin-a Freundlich isotherms for virgin F400 and F300 (coal-based) GAC in ultrapure water (UW) vs. Grand River water (GRW) 113
Figure 6.5: Anatoxin-a Freundlich isotherms for virgin Aqua Carb (coconut-based) GAC in ultrapure water (UW) vs. Grand River water (GRW) 113

Figure 6.6: Anatoxin-a Freundlich isotherms for virgin C-Gran and WV B-30 (wood-based) GAC in ultrapure water (UW) vs. Grand River water (GRW) 114
Figure 6.7: Anatoxin-a Freundlich isotherms for virgin (coal-based) PAC in ultrapure water (UW) vs. Grand River water (GRW) 114
Figure 6.8: Anatoxin-a Freundlich isotherms for six virgin carbons in Grand River water 115
Figure 6.9: Freundlich adsorption coefficient (K_F) non-linear fit with 95% confidence intervals, in Grand River water 116
Figure 6.10: Freundlich model parameter (1/n) non-linear fit with 95% confidence intervals, in Grand River water 117
Figure 6.11: 95% joint confidence regions and point estimates for the Freundlich parameters of isotherms generated with virgin carbon in Grand River water. A – all carbons; B – GACs 118
Figure 6.12: Comparison of Freundlich isotherms for anatoxin-a and the cyanotoxins microcystin-LR (MC-LR) and cylindrospermopsin (CYN) by virgin coal-based carbons in natural water 120
Figure 6.13: Comparison of Freundlich isotherms for anatoxin-a, microcystin-LR (MC-LR) and MIB by virgin coconut-based carbons in natural water.. 121
Figure 6.14: Comparison of Freundlich isotherms for anatoxin-a, microcystin-LR (MC-LR), microcystin-LA (MC-LA), cylindrospermopsin (CYN), and MIB by virgin wood-based carbons in natural water. 122
Figure 6.15: ECM predicted total treated volume to breakthrough in GRW. 123

List of Tables

Table 2.1: Regulations and guidelines for anatoxin-a concentration in drinking water 12
Table 2.2: Second order rate constants reported for the oxidation of anatoxin-a in ultrapure water ... 13
Table 2.3: Percent anatoxin-a degradation reported for various water treatment oxidants..... 15
Table 2.4: Summary of treatment process efficacy for anatoxin-a removal 33
Table 2.5: Recommended anatoxin-a study parameters 34
Table 3.1: Commercially available cyanotoxin ELISA microtitre plate kits..... 39
Table 3.2: MS parameters for the MRM quantitation of ANTX, 1,9-diaminonane and c(RADvF).... 42
Table 3.3: Percentage recoveries of (+)-anatoxin-a 44
Table 3.4: Recoveries of (+)-anatoxin-a in three identical samples extracted in parallel using SPE .. 46
Table 4.1: Carbon properties..... 60
Table 4.2: Pseudo-second order kinetic model parameters for virgin carbon in ultrapure water 68
Table 4.3: Freundlich isotherm parameters for virgin carbon in ultrapure water 71
Table 4.4: Comparison of anatoxin-a adsorption capacities for the carbons evaluated at different aqueous concentrations 72
Table 5.1: Point of zero charge for virgin vs. preloaded GACs..... 88
Table 5.2: Average effective particle sizes for the GACs based on manufacturer documentation..... 90
Table 5.3: Pseudo-second order kinetic model parameters for preloaded carbon in ultrapure water .. 93
Table 5.4: Freundlich isotherm parameters for preloaded carbon in ultrapure water 96
Table 5.5: Comparison of anatoxin-a adsorption capacities for the preloaded carbons evaluated at different aqueous concentrations 98
Table 6.1: Raw river water parameters 108
Table 6.2: Freundlich isotherm parameters for virgin carbon in Grand River water..... 112
Table 6.3: Comparison of anatoxin-a adsorption capacities for the virgin carbons evaluated at different aqueous concentrations in natural water 116

List of Acronyms

ANTX – anatoxin-a

BET – Brunauer, Emmett and Teller

CCL – candidate contaminant list

c(RADfV) – Cyclo-(Arg-Ala-Asp-D-Phe-Val)

CYN – cylindrospermopsin

DOC – dissolved organic carbon

DFT – density functional theory

ECM – equilibrium column model

ELISA – enzyme-linked immunosorbent assay

ESI – electro-spray ionization

GAC – granular activated carbon

GRW – Grand River water

GTX – gonyautoxin

homoANTX – homoanatoxin-a

HPLC – high-performance liquid chromatography

JCR – joint confidence region

LC-MS/MS – liquid chromatography tandem mass spectrometry

MC-LA – microcystin-LA

MC-LR – microcystin-LR

MC-YR – microcystin-YR

MDL – method detection limit

MIB – 2 methylisoborneol

MRM – multiple reaction monitoring

NOD – nodularin

NOM – natural organic material

PAC – powdered activated carbon

pH_{PZC} – pH at the point of net zero surface charge

pKa – acid dissociation constant

PSP – paralytic shellfish poison

RBA – receptor binding assay (an ELISA)

RSD – relative standard deviation

SPE – solid phase extraction

STX – saxitoxin

TOC – total organic carbon

USEPA – United States Environmental Protection Agency

UW – ultrapure water

VFDF – very fast death factor

Chapter 1
Introduction

1.1 Problem Statement

Cyanobacterial blooms can produce numerous toxins, and these cyanotoxins are of increasing concern to drinking water providers as eutrophication of source waters continues to stimulate bloom formation. Worldwide occurrence of cyanobacteria can vary considerably – in warmer climates, blooms can be present year-round, whereas in more temperate climates they are considered a seasonal concern. Anthropogenic nutrient loading has resulted in an increase in the frequency and severity of cyanobacterial blooms, and global climate change has the potential to further promote cyanobacterial dominance over competing organisms in aquatic ecosystems (Paerl & Paul, 2012, Merel et al., 2013).

In southern Ontario, cyanobacterial blooms occur in many surface waters, including those used for drinking water; in 2011, the largest cyanobacterial bloom on record formed in Lake Erie (Figure 1.1), covering an estimated area greater than 5,000 km^2 at its peak – nearly one fifth of the surface of the lake (Michalak et al., 2013). Cyanobacterial blooms on Lake Erie have impacted drinking water providers on both sides of the US-Canadian border, and between August 1 and 4, 2014, the presence of the cyanotoxin microcystin-LR resulted in a highly-publicized do-not-drink advisory for the City of Toledo, Ohio, which left 500,000 residents without direct access to potable water (Department of Public Utilities, 2014).

Figure 1.1: Centers for Coastal Ocean Science, NASA Modis sensor satellite image of Lake Erie from Oct. 9, 2011. NOAA Harmful Algal Blooms, <http://oceanservice.noaa.gov/hazards/hab>

Anatoxin-a is a low molecular weight alkaloid neurotoxin, previously referred to as VFDF (very fast death factor) and is one of three cyanotoxins on the USEPA's third iteration of the Candidate Contaminant List (CCL3), along with cylindrospermopsin and the more commonly-regulated microcystin, shown in Figure 1.2 (USEPA, 2012). It has also been recommended for inclusion on the fourth CCL iteration (Adams et al., 2014). Neurotoxic analogues of anatoxin-a include homoanatoxin-a, although anatoxin-a is the most prevalent and most potent of the analogues in North America (Rellan et al., 2007). Several anatoxin-a-producing cyanobacterial species have been identified, including *Anabaena flos aquae, Anabaena planktonica, Aphanizomenon flos aquae, Cylindrospermum,* benthic *Oscillatoria, Planktothrix rubescens, Arthrospira fusiformis* (Rellán et al., 2007) and more recently, *Tychonema bourrellyi* (Rellan et al., 2007; Shams et al., 2015).

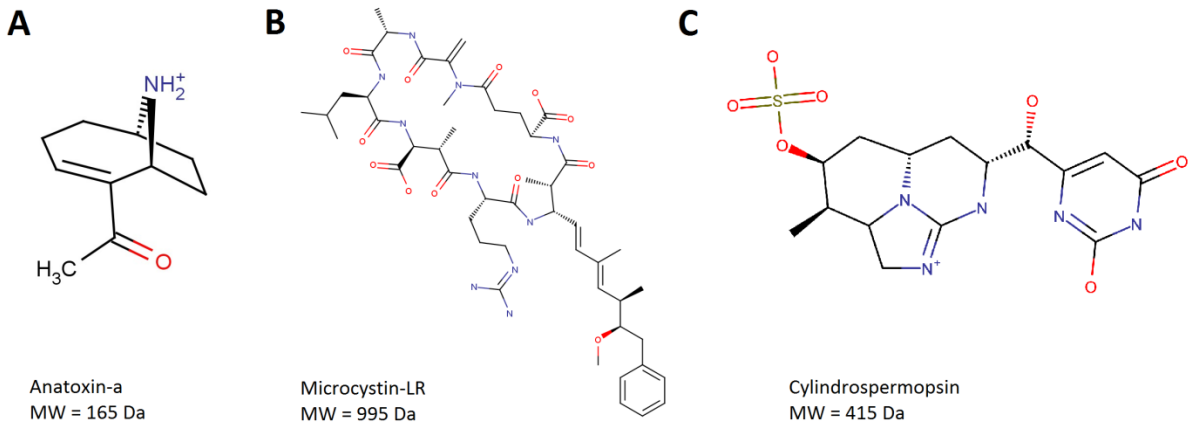

Figure 1.2: Cyanobacterial toxins on the USEPA's contaminant candidate list: a) anatoxin-a; b) microcystin-LR; c) cylindrospermopsin. Figure produced with Marvin-Sketch software © 2013 by ChemAxon Ltd.

While there are currently no US or Canadian regulations for anatoxin-a in drinking water, a 3.7 µg/L provisional guideline has been proposed in the province of Quebec (Institut National de Santé Publique du Québec, 2005) and concentrations of up to 5.6 µg/L anatoxin-a have been detected in Canada, in addition to numerous reports of animal poisoning and death (Manitoba Water Stewardship, 2011). Anatoxin-a has also been reported in western Lake Erie, Lake Ontario, Lake Champlain (in New York state) and throughout the lower Great Lakes watershed (Yang, 2005).

Although oxidation with ozone (Onstad et al., 2007), permanganate (Rodriguez et al., 2007a) and advanced oxidation processes (AOPs, Afzal et al., 2010) have been shown to be capable of inactivating anatoxin-a. Chlorine, the most commonly applied oxidant in water treatment, is not effective (Rodríguez et al., 2007a). Several reviews of cyanotoxin treatment options have remarked on the lack of available information on the adsorption of anatoxin-a (Westrick et al., 2010, Global Water Research Coalition, 2012, Vlad et al., 2014) and it has been suggested that in the absence of other data, microcystin-LR could be used as an indicator for anatoxin-a adsorption behaviour; however, the two molecules are markedly different in size and structure, as shown in Figure 1.2 and strategies for optimizing removals of the two toxins by activated carbon adsorption may differ.

1.2 Research Objectives

The primary goal of this research was to evaluate the viability of activated carbon adsorption as a treatment process for the removal of anatoxin-a from drinking water at environmentally relevant concentrations. The following objectives were identified to achieve this goal:

- Evaluate existing analytical methods for the quantification of aqueous anatoxin-a concentrations at environmentally relevant concentrations, including enzyme-linked immunosorbent assays (ELISAs) and liquid chromatography tandem mass spectrometry (LC-MS/MS), and implement the most suitable method.
- Select a representative range of carbons based on commercially available products and investigate the impact of physico-chemical properties of the activated carbons on anatoxin-a removal in ultrapure and a southern Ontario surface water.
- Establish equilibrium isotherm parameters for adsorption of anatoxin-a on virgin activated carbons in ultrapure and a southern Ontario surface water and compare the adsorption capacities with those of other cyanobacterial metabolites, including other North American cyanotoxins, and the common cyanobacterial taste and odour compounds geosmin and MIB.
- Study the kinetics of anatoxin-a adsorption by virgin carbons in ultrapure and natural water.
- Evaluate the effect of carbon preloading with background natural organic matter (NOM) on the equilibrium capacity and adsorption rates for anatoxin-a.

1.3 Research Approach and Thesis Structure

This thesis contains seven chapters, with Chapters 2, 3, 4, 5 and 6 formatted as journal articles (i.e. a paper-based thesis) (Figure 1.3). Chapter 2 provides an overview of current knowledge and research on the removal of aqueous anatoxin-a in drinking water treatment, and has been published in the Journal of Water and Health (Vlad et al., 2014). Chapter 3 presents the results of an assessment of the ELISA and LC-MS/MS analytical methods for quantifying aqueous anatoxin-a. Following the development and

implementation of an LC-MS/MS method, six activated carbons from three source materials were selected for inclusion in subsequent treatment studies – five granular activated carbons (GACs) and one powdered activated carbon (PAC). Chapter 4 describes the results of characterization tests for each of the six carbons, as well as the investigation of anatoxin-a adsorption under idealized conditions using virgin carbon in ultrapure water. The five GACs under investigation were then preloaded with NOM in parallel using pilot-scale flow-through contactors at a southern Ontario surface water treatment plant and samples of a preloaded GAC were extracted from another operating drinking water treatment plant in Ontario. Chapter 5 details subsequent studies to elucidate the impact of carbon preloading on anatoxin-a adsorption, again in ultrapure water. Chapter 6 considers the adsorptive behaviour of anatoxin-a in a surface water using the six virgin activated carbons. Finally, Chapter 7 summarizes the outcomes and findings of this research, as well as proposing several recommendations for future studies into the treatment of anatoxin-a in drinking water. The references from all chapters are compiled in a comprehensive list at the end of the thesis, and several appendices are included for additional detail.

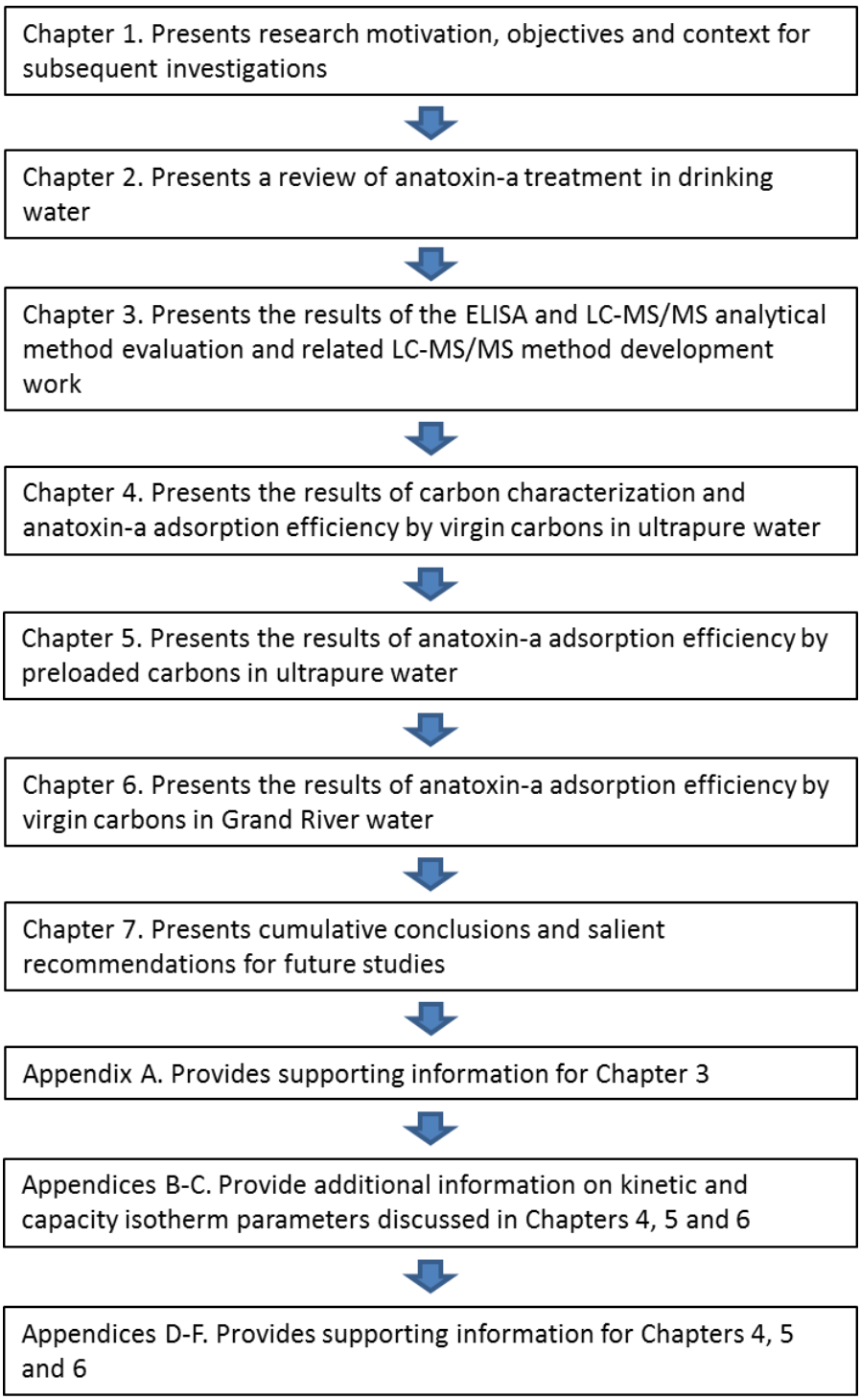

Figure 1.3: Thesis structure and relevance of the thesis chapters

Chapter 2
Removal of the Cyanotoxin Anatoxin-a by Drinking Water Treatment Processes: A Review

This chapter was published under the same title in the Journal of Water and Health (December, 2014) volume 12, issue 4, pages 601-617. Cited references are included in the cumulative reference list at the end of this thesis.

2.1 Summary

Anatoxin-a is a potent alkaloid neurotoxin, produced by several species of cyanobacteria and detected throughout the world. The presence of cyanotoxins, including anatoxin-a, in drinking water sources is a potential risk to public health. This article presents a thorough examination of the cumulative body of research on the use of drinking water treatment technologies for extracellular anatoxin-a removal, focusing on providing an analysis of the specific operating parameters required for effective treatment and on compiling a series of best-practice recommendations for owners and operators of systems impacted by this cyanotoxin. Of the oxidants used in drinking water treatment, chlorine-based processes (chlorine, chloramines, and chlorine dioxide) have been shown to be ineffective for anatoxin-a treatment, while ozone, advanced oxidation processes and permanganate can be successful. High-pressure membrane filtration (nanofiltration and reverse osmosis) is likely effective, while adsorption and biofiltration may be effective but further investigation into the implementation of these processes is necessary. Given the lack of full-scale verification, a multiple-barrier approach is recommended, employing a combination of chemical and non-chemical processes.

2.2 Introduction

Historically referred to as Very Fast Death Factor (VFDF) (Carmichael & Gorham, 1978), the neurotoxic alkaloid anatoxin-a (ANTX-a) was first identified in the prairie region of Canada, and has subsequently been detected at low µg/L concentrations in surface waters throughout North America, South America,

Europe, Africa, Asia and New Zealand (Carmichael & Gorham, 1978; Park et al., 1998; Ballot et al., 2003; Carrasco et al., 2007; Kotak & Zurawell, 2007; Wood et al., 2007; Faassen et al., 2012; Ruiz et al., 2013). It can be produced by several genera of cyanobacteria, including *Anabaena*, *Oscillatoria*, *Cylindrospermum*, *Aphanizomenon*, and in some instances *Microcystis*, *Raphidiopsis*, *Arthrospira*, *Nostoc* and *Phormidium* (Osswald et al., 2007; van Apeldoorn et al., 2007), and can co-occur with other cyanotoxins and/or taste and odour compounds produced by cyanobacteria (Ruiz et al., 2013). During the growth phase of cyanobacterial blooms cyanotoxins exist predominantly intracellularly. However, weakening or rupture of the cell membrane due to bacterial aging, physical stresses placed on the cells, or exposure to chemicals such as the oxidants used in drinking water treatment can all cause toxins to be released (Hart et al., 1998; WHO, 1999; Ho et al., 2012).

The presence of cyanotoxins in drinking water sources has been a cause of concern as they have the potential to compromise public health, and many treatment processes have been investigated for their ability to remove the various classes of toxins which can be produced (Westrick et al., 2010; Merel et al., 2013b; Pantelic et al., 2013).The majority of studies on cyanotoxins and their fate during drinking water treatment have focused on microcystins and particularly the microcystin-LR variant (Merel et al., 2013b). The lack of information on treatment options for ANTX-a, and other cyanotoxins including cylindrospermopsin, nodularin and beta-methylamino-L-alanine (BMAA), has been noted frequently (WHO, 1999; Hitzfeld et al., 2000; Westrick et al., 2010; Global Water Research Coalition, 2012; Merel et al., 2013a). Of the studies undertaken into the treatment of ANTX-a, some have provided contradictory results and no comprehensive review has been presented to date to reconcile these results. All published studies have been at the bench- or pilot-scale, with no full-scale data available. This review aims to discern the necessary practices and operating parameters for optimal extracellular toxin removal, and highlight areas where further study is required to allow a treatment strategy to be implemented with confidence. Numerous studies have been published regarding the potential for cell lysis during water

treatment, and operational considerations for removing intact cyanobacterial cells; however, removal of intracellular ANTX-a is not within the scope of this review.

2.3 Analogues, Chemical Properties and Stability

ANTX-a is a relatively low molecular weight molecule (MW = 165) with a pK_a of 9.36; at pH levels relevant to drinking water (pH 6-9) it exists predominantly in the more stable protonated, cationic form, shown in Figure 2.1a (van Apeldoorn et al., 2007). However, some portion of the toxin does exist in the neutral form (Figure 2.1b), as illustrated in Figure 2.2, which shows that at pH 6, ANTX-a is completely protonated (less than 1% deprotonated), while at pH 8.5, approximately 12% is deprotonated and at pH 9, 24% is deprotonated.

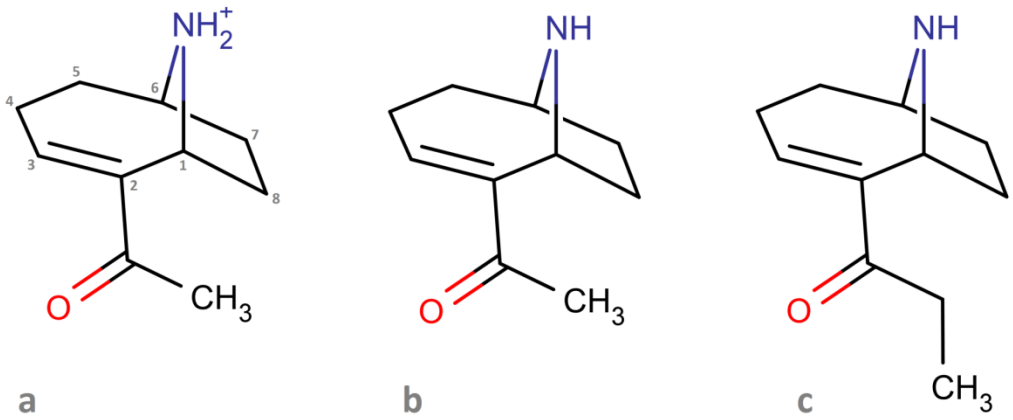

Figure 2.1: Molecular structures: a) protonated (+)-anatoxin-a stereoisomer (asymmetric centers at carbons 1 and 6, the secondary aminogroup for the (-)-anatoxin-a stereoisomer is located below the plane of the carbon ring), b) deprotonated (+)-anatoxin-a, c) homoanatoxin-a

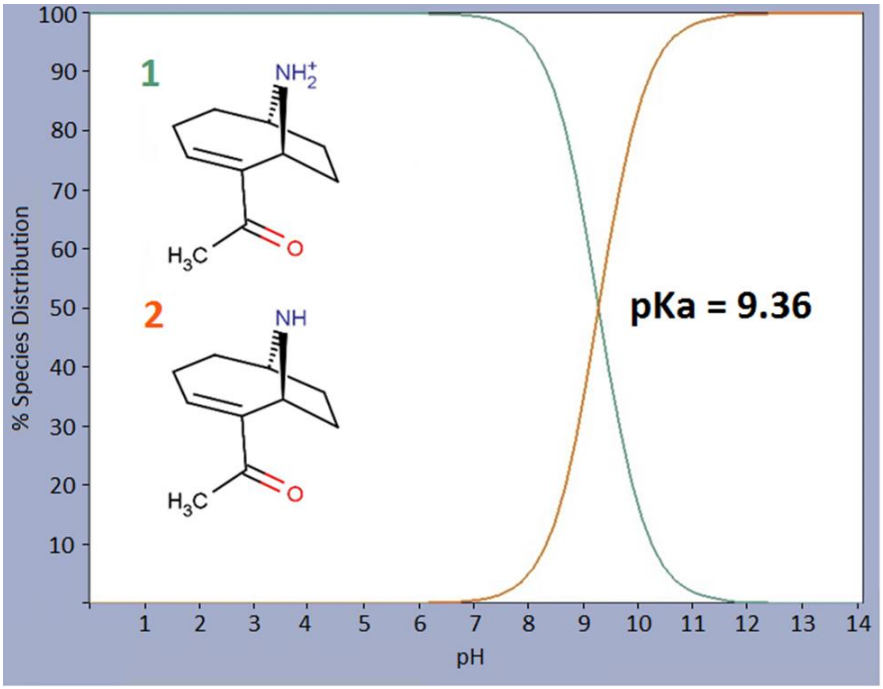

Figure 2.2: Anatoxin-a species distribution based on pH. Figure produced with MarvinSketch software ©2013 by ChemAxon Ltd.

Kaminski et al. (2013) indicated that increasing the pH of a solution accelerated the decomposition of ANTX-a under a variety of conditions including increased temperature (100^{o}C) and UV-B exposure. They noted that at acidic pH (3.5), 1 hour exposure to 100^{o}C temperature or 36 µmol m^{-2} s^{-1} UV-B radiation both caused minimal degradation of ANTX-a (<10%), while the same treatments at pH 9.5 resulted in a toxin reduction of nearly 80%. It should be noted, however, that the initial toxin concentration used in this study (25 mg/L) is several orders of magnitude greater than would typically be detected in natural waters, as will be discussed subsequently. These results imply that pH can be a critical factor in the treatment of ANTX-a, however, most studies do not differentiate between the treatment efficiency for the protonated and deprotonated forms of the toxin.

Conflicting results exist regarding the decomposition of ANTX-a in direct sunlight; Stevens and Krieger (1990) found that sunlight accelerates decay kinetics (1-2 hour half-lives observed), while Kaminski et al. (2013) observed only 3% toxin degradation following 5 hours of irradiation with photosynthetically

active radiation (1500 µmol m^{-2} s^{-1}). However, in dark conditions (as in most drinking water treatment plants and distribution systems) the toxin can persist for weeks or months (Stevens & Krieger, 1990; van Apeldoorn et al., 2007; Yang, 2007).

It should be noted that of the two stereoisomers of the ANTX-a molecule, only (+)-ANTX-a is produced naturally as a cyanobacterial metabolite (Valentine et al., 1990); this isomer is the more potent of the two forms of the toxin, with over 10 times greater toxicity than (-)-ANTX-a (Adeyemo & Siren, 1992; Valentine et al., 1990). The (+)-ANTX-a stereoisomer is shown in Figure 2.1, with the asymmetric centers at carbons 1 and 6. In the (-)-ANTX-a stereoisomer the secondary amino group is located beneath the plane of the carbon ring. It should be noted that most commercially available ANTX-a standards contain both stereoisomers in a racemic (50%-50%) mixture.

One commonly identified analogue of ANTX-a is known as homoanatoxin (MW = 179), and differs from ANTX-a by one additional methyl unit on the side chain (Figure 2.1c). Although homoanatoxin is also highly neurotoxic (Wonnacott & Swanson, 1992; Watanabe et al., 2003; Faassen et al., 2012), it is less frequently detected, and its treatment has not been investigated; this review therefore focuses on treatment of the more common analogue ANTX-a.

Anatoxin-a(s), while similar in name, is not structurally related to ANTX-a and homo-anatoxin-a. This compound should not be confused with ANTX-a and its treatment is not considered in this review.

2.4 Toxicity, Occurrence and Regulations

ANTX-a is a nicotinic agonist whose toxicity has been well documented, resulting in a number of animal deaths globally (Edwards et al., 1992; Hitzfeld et al., 2000; Cadel-Six et al., 2007; Puschner et al., 2008; Environment Canada - Manitoba Water Stewardship, 2011; Faassen et al., 2012). It is an acutely toxic compound with a LD_{50} of 380 µg/kg (i.p. mouse) (Valentine et al., 1990), known to cause muscular paralysis and death due to respiratory arrest; however, the effects of chronic, low-level exposure are unknown, particularly with regard to human and animal reproduction (Osswald et al., 2007).

When detected, ANTX-a generally occurs at low concentrations environmentally (below 5 µg/L) (Robert et al., 2005; Fristachi et al., 2008); however, concentrations of up to 156 µg/L have been reported and in one case, a concentration of approximately 10 µg/L was detected in a post-treatment drinking water in Florida (Burns, 2005). Based on current knowledge of the toxicity, potential health effects, and frequency of detection of ANTX-a, some regulatory bodies have set maximum concentrations for ANTX-a in drinking water (Table 2.1) and in recreational waters (Chorus, 2012). Furthermore, a 1 µg/L drinking water guideline value has been recommended in the scientific literature, calculated to provide a safety margin of three orders of magnitude to protect against adverse effects of sub-lethal doses (Fawell et al., 1999). Although no regulations exist in the US, ANTX-a is one of three cyanotoxins on the USEPA Candidate Contaminant List 3 (USEPA, 2012), indicating a need for further study into its occurrence, effects and treatment, and the potential for forthcoming regulations.

Table 2.1: Regulations and guidelines for anatoxin-a concentration in drinking water

Location	Regulation/Guideline	Status	Source
Quebec (Canada)	3.7 µg/L	Provisional	Institut national de santé publique du Québec, 2005
Oregon (USA)	3 µg/L	Adopted guideline	Oregon Health Authority, 2013
New Zealand	6 µg/L	Provisional	New Zealand Ministry of Health, 2008

2.5 Water treatment processes for extracellular anatoxin-a removal or degradation

2.5.1 Oxidation

The ability to oxidize ANTX-a is highly dependent on the type and dose of oxidant used, the pH and background water characteristics, and the contact time provided for the reaction to occur. Rodríguez et al. (2007a) demonstrated that second order rate constants can accurately represent the relative reactivity of various oxidants with ANTX-a, and these constants therefore serve as a general guideline to

implementation requirements. A compendium of rate constants reported in the literature for ANTX-a oxidation in ultrapure water is presented in Table 2.2. The apparent reaction rates observed in natural water applications will differ from the values given in Table 2.2 due to water quality effects. Rate constants collected in Table 2.2 have been given for the overall oxidation of ANTX-a at a stated pH.

Table 2.2: Second order rate constants reported for the oxidation of anatoxin-a in ultrapure water

Oxidant	Rate Constant – Second Order ($M^{-1}s^{-1}$)	Conditions	Source
Cl_2	0.71	pH 7	Rodríguez et al., 2007b
NH_2Cl	< 1	pH 8	Rodríguez et al., 2007a
ClO_2	Low	pH 8	Rodríguez et al., 2007a
O_3	5.6×10^4	pH 7	Bernazeau et al., 1995; Bruchet et al., 1998
O_3	6.4×10^4	pH 8	Onstad et al., 2007
O_3	9.7×10^5	pH 9	Onstad et al., 2007
AOP – $OH^{\cdot}$	3.0×10^9	pH 7	Onstad et al., 2007
AOP – $OH^{\cdot}$	5.2×10^9	pH 4.5 – 9.5	Afzal et al., 2010
MnO_4^-	2.3×10^4	pH 8	Rodríguez et al., 2007a

Based on the data in Table 2.2, AOPs are the most effective oxidation process for ANTX-a degradation with a second order rate constant four orders of magnitude greater than that reported for any other oxidant (5.2×10^9 $M^{-1}s^{-1}$). Ozone has the second highest rate constant for ANTX-a oxidation, and appears particularly effective at higher pH, with the rate constant increasing by an order of magnitude between pH 8 and pH 9. Permanganate has a similar (but slightly lower) rate constant to ozone, while the chlorine based oxidants (chlorine, chloramines and chlorine dioxide) all have very low rate constants (less than 1 $M^{-1}s^{-1}$). These rate constants are consistent with redox potential of the various oxidative species considered, which is a fundamental indicator of the oxidising power of each chemical, and ranks the oxidants as follows: OH· radical > ozone > permanganate > chlorine dioxide > chlorine (Zhou & Smith, 2002). The relative reactivity with ANTX-a established by these constants is largely supported by the toxin degradation studies carried out to date.

Compared to other cyanotoxins, ANTX-a is relatively recalcitrant to oxidation. The second order rate constants with ozone, OH· radicals, and chlorine are all higher for both microcystin-LR and

cylindrospermopsin than for ANTX-a (Acero et al., 2005; Onstad et al., 2007; Rodríguez et al., 2007a,b), although the second order rate constant for ANTX-a oxidation with permanganate (2.3×10^4 $M^{-1}s^{-1}$) is several orders of magnitude higher than those for microcystin-LR (357 $M^{-1}s^{-1}$) and cylindrospermopsin (0.9 $M^{-1}s^{-1}$) (Rodríguez et al., 2007a).

Numerous studies have reported some degree of ANTX-a oxidation, and their results, as well as the relevant factors listed above, are summarized in Table 2.3. However, little consideration has been given to the possible creation of toxic by-products from these oxidation reactions, and degradation of the parent toxin may not always be synonymous with reduction of overall toxicity. Complete mineralization of micropollutants is usually not achievable under conditions employed in water treatment practice, and therefore further investigation is required into the intermediate products of this toxin with the various oxidants. Monitoring of the toxicological endpoint in addition to the reduction of the parent compound may allow conclusions to be drawn regarding the toxicity reduction, without the need to examine individual intermediates. This approach has been employed for oxidative treatment of hormones using a screening assay to determine changes in estrogenic activity (Huber et al, 2004), and may be appropriate for cyanobacterial toxicity studies. However, the possibility that the by-products of ANTX-a oxidation may have a different toxicological effect should also be considered.

Table 2.3: Percent anatoxin-a degradation reported for various water treatment oxidants

Oxidant	% Toxin Reduction	pH	Water Matrix[a]	Oxidant Dose (mg/L)	Contact Time (min)	Initial Anatoxin Concentration (µg/L)	Detection Limit (µg/L)	Study
Cl_2	16%	6-7	N	15 (4.5 residual)	30	20	5	Newcombe & Nicholson, 2004
Cl_2	15%	8	N (DOC 3.6 mg/L)	3	-	166	-	Rodríguez et al., 2007a
Cl_2	8%	7	N (DOC 6.7 mg/L)	3	24 h	165	-	Rodríguez et al., 2007b
Cl_2	0%	-	N	0.5	-	22[b]	-	Keijola et al., 1988
O_3	46%	7	U	1.8	3	1000	0.2	Al Momani, 2007
	63%	11	U	2.0		1000		
O_3	>90%	-	T	2.0	-	2.4 – 4.3	-	Hall et al., 2000
O_3	92%	7	T	0.11 residual (after 60 s)		24	-	Rositano et al., 1998
O_3	96%	-	N	1	-	22[b]	-	Keijola et al., 1988
O_3	>95%	7.9	N (DOC 1.6 mg/L)	0.8	30	150	-	Onstad et al., 2007
	95%	7.2	N (DOC 13.1 mg/L)	>2.0	30	150		
O_3	95%	8	N (DOC 3.6 mg/L)	0.75	-	166	-	Rodríguez et al., 2007a
O_3	100%	7.8	N (DOC 5.3 mg/L)	1.1	5	20	0.01	Rositano et al., 2001
	100%	7.5	N (DOC 4.6 mg/L)	1.7	5	20		
	100%	7.8	N (DOC 5.7 mg/L)	1.5	5	20		
	100%	7.1	N (DOC 15.5 mg/L)	>2.2	5	20		
AOP – H_2O_2/Fe(II)	100%	7	U	0.1 Fe(II), 0.02 H_2O_2	1.5	1000	0.2	Al Momani, 2007
AOP – O_3/H_2O_2	>98%	7	U	0.001 H_2O_2, 2.0 O_3	3	1000	0.2	Al Momani, 2007

	100%	7	U	0.01 H_2O_2, 1.0 O_3	3	1000		
AOP – O_3/Fe(II)	85%	7	U	1.0 O_3, 0.5 Fe(II)	3	1000	0.2	Al Momani, 2007
AOP – LP UV/H_2O_2	70%	7	D	250 mJ/cm^2 UV 30 mg/L H_2O_2	-	600	33	Afzal et al., 2010
AOP – VUV	>95%	7	D	96 mJ/cm^2	-	600	33	Afzal et al., 2010
	85%	6.9	S (TOC 6.63 mg/L)	192 mJ/cm^2		600		
	70%	7.3	N (TOC 3.94 mg/L)	192 mJ/cm^2		600		
AOP – TiO_2/UV	100%	-	U	1% m/v slurry TiO_2 (UV unspecified)	30	5000	-	Robertson et al., 1999
MnO_4^-	>90%	-	T	2.0	-	2.4 – 4.3	-	Hall et al., 2000
MnO_4^-	100%	8	N (DOC 3.6 mg/L)	0.5	-	166	-	Rodríguez et al., 2007a

[a] water matrix classification: U – ultrapure, T – treated drinking water, N – natural, D – deionised, S – synthetic/modelled

[b] influent concentration approximated based on cyanobacterial biomass

- indicates parameter not reported

2.5.1.1 Chlorine

It has been established repeatedly that chlorine is ineffective for the treatment of ANTX-a (Keijola et al., 1988; Hart et al., 1998; Hall et al., 2000; Newcombe & Nicholson, 2004; Rodríguez et al., 2007a). A range of concentrations, contact times and pH levels relevant to drinking water treatment have been examined in various natural water sources (as detailed in Table 2.3) resulting in a consensus within the scientific literature that the oxidation of ANTX-a by chlorine is too slow a process to be considered an effective treatment barrier. This is a significant finding as most other cyanotoxins are well oxidised by this standard disinfectant.

Conventional treatment plants employing chlorine as primary disinfectant may therefore be facing a greater risk from ANTX-a. Although in general the water industry is moving away from using chlorine for this purpose, many jurisdictions in the world require the maintenance of a disinfectant residual (typically chlorine or chloramines) in the distribution system. While plants doing this could rely on this application of chlorine at the end of the treatment process to remove other cyanotoxins, this step would not contribute to the removal of ANTX-a.

2.5.1.2 Chloramines and Chlorine Dioxide

Similarly to chlorine, chloramines cannot effectively oxidize the ANTX-a molecule, and the reaction rate is prohibitively slow with an apparent second order rate constant of less than 1 $M^{-1}s^{-1}$ (Rodríguez et al., 2007a). Minimal oxidation of ANTX-a is observed in the presence of chlorine dioxide; indeed, the reactivity is so low that the second-order rate constant is not measureable (Rodríguez et al., 2007a). As a result of these findings, neither of these disinfectants is considered a feasible barrier to ANTX-a in drinking water treatment, nor to the other common microcystins and cylindrospermopsin (Merel et al., 2010; Westrick et al., 2010).

2.5.1.3 Ozone

Ozone is believed to selectively attack both the double bond and the deprotonated amine moiety of the ANTX-a molecule (Onstad et al., 2007) and it has been shown that the two species have different reaction

rates with the deprotonated form reacting somewhat faster with molecular ozone than the protonated form (Onstad et al., 2007) (Figure 2.3). It can be challenging to distinguish changes in degradation efficiency due to differences in reaction rates between the species from the increased degradation of the deprotonated form at high pH values. In addition, as discussed below, ozone degradation produces OH radicals, which occurs more readily at higher pH values. This will also impact the observed reduction in ANTX-a concentrations during ozonation as it reacts more readily with OH radicals than molecular ozone.

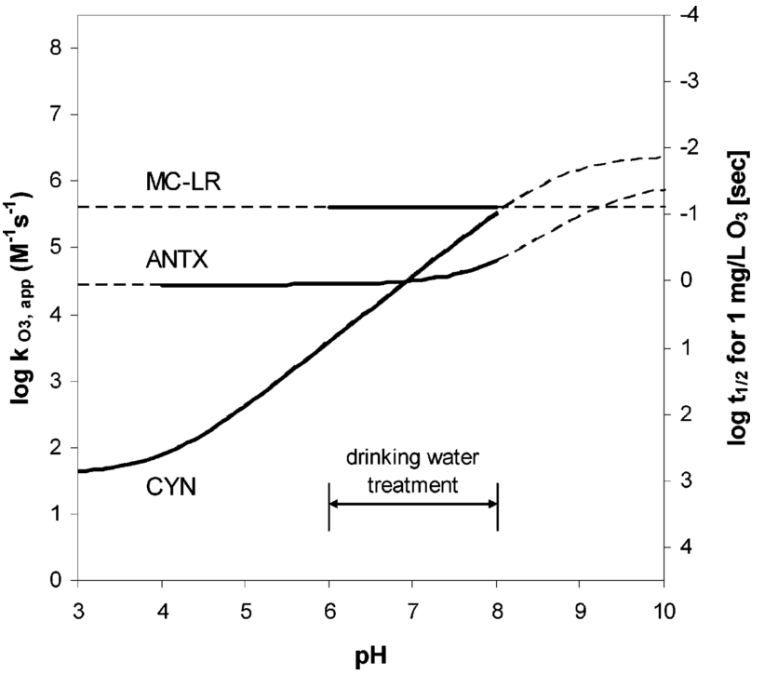

Figure 2.3: pH dependence of the rate constants for the reaction of cyanotoxins with ozone. Half-life times are given for an ozone concentration of 1 mg/L. MC-LR, microcystin; CYN, cylindrospermopsin; ANTX, anatoxin-a. Reprinted with permission from Onstad et al. (2007). Copyright 2007 American Chemical Society.

Several studies have investigated the use of ozone for treatment of ANTX-a; while most have reported good- to excellent toxin degradation, the degree of oxidation has been variable in some cases. These findings imply that optimal operating conditions have to be determined carefully in order to achieve a reliable reduction in ANTX-a toxicity utilizing ozone.

In ultrapure water, a 0.11 mg/L ozone residual after 60 seconds contact time has been shown to reduce ANTX-a concentrations of 24 µg/L by 92%, although the initial dose required to achieve that residual was not noted (Bernazeau et al., 1995; Rositano et al., 1998). In another study, 63% toxin reduction was achieved from a starting concentration of 1000 µg/L ANTX-a, with ozone doses up to 2 mg/L, ozone residuals were not given, also in ultrapure water (Al Momani, 2007). The extremely high initial ANTX-a concentration used in this study should be noted, as the lower percentage of ANTX-a degraded can be explained by examining the reactants on the basis of molar ratios. An additional issue regarding this study is the lack of ozone residual data which is needed to estimate inactivations (e.g. CT calculations).

Further supporting the case for ozone use, high reductions have been attained in natural waters. Using 1 mg/L ozone, Keijola et al. (1988) achieved complete toxin elimination from an approximate starting concentration of 22 µg/L in natural water, although the water quality was undisclosed. In a lake water with 1.6 mg/L of DOC, an ozone dose of 0.8 mg/L was capable of oxidizing over 95% of ANTX-a (Onstad et al., 2007), and results reported by Hart et al. (1998) and Hall et al. (2000) showed greater than 90% toxin reduction with a 2 mg/L dose, from 2.4 – 4.3 µg/L initial toxin concentrations in treated natural water. Although the Hart et al. (1998) and Hall et al. (2000) results are very encouraging, the kinetic parameters such as the contact time were not reported, and there was no indication of what processes were used to prepare the "treated" water matrix.

In more organic-rich raw waters, toxin degradation diminishes severely, as expected for ozone operation; at the same 2 mg/L O_3 dose approximately 50% toxin degradation was noted by Hall et al. (2000). Furthermore, Onstad et al. (2007) showed that in waters with high organic content (13.1 mg/L DOC), ozone doses above 2 mg/L were required to oxidize 95% of ANTX-a. These results indicate a scavenging effect from other natural water constituents and emphasize the importance of appropriate, source-specific pretreatment leading up to the oxidation process.

More conclusively, Rositano et al. (2001) endeavoured to determine the effects of different background water characteristics on ozone oxidation of ANTX-a by applying the oxidant to four toxin-spiked natural

waters with varying properties, including DOC (4.6 – 15.5 mg/L), alkalinity (30 – 133 mg/L as $CaCO_3$), pH (7.1 – 7.8) and specific UV absorption (SUVA) (140 – 210 cm^{-1} $(mg/L)^{-1}$ at 254 nm). They noted that complete elimination of the influent toxin (20 µg/L) was attainable, and relied on the maintenance of an ozone residual of approximately 0.05 – 0.06 mg/L after 5 minutes (CT = 0.25 mg min/L), which in three of the four waters, was attainable with ozone doses below 2 mg/L. Moreover, they found that in each of the waters examined, complete oxidation of ANTX-a required a higher ozone dose than was necessary for the destruction of an equal influent concentration of microcystin-LR. The findings for ANTX-a degradation in natural water and the associated ozone dose requirements are consistent with the reported second order rate constants for microcystin-LR, cylindrospermopsin and ANTX-a (Onstad et al., 2007).

The efficiency of the ozone-ANTX-a reaction has been shown to be pH dependent with better toxin degradation achieved at higher pH for the same dose (Al Momani, 2007; Onstad et al., 2007). At pH 8, Onstad et al. (2007) reported an apparent second order rate constant of $6.4 \times 10^4 M^{-1}s^{-1}$ for the oxidation of ANTX-a (combined species) with ozone, which increased to 9.7×10^5 $M^{-1}s^{-1}$ at pH 9 (Table 2.2). The observed pH dependence for ANTX-a degradation by ozonation is likely the result of three effects co-occurring: firstly, the degradation of molecular ozone increases at higher pH, thereby forming more hydroxyl radicals which are more reactive towards ANTX-a than molecular ozone as indicated by their second order rate constants presented in Table 2.2; further, the deprotonated toxin is less stable and degradation of this species may be another removal pathway; finally, at high pH, the proportion of the deprotonated neutral ANTX-a species increases, which is more reactive than the protonated form with a reported second order rate constant of 8.7×10^5 $M^{-1}s^{-1}$ (Onstad et al., 2007). The last of these effects is well illustrated by Figure 2.3, reproduced from Onstad et al. (2007), which shows the rate constants for molecular ozone with three cyanotoxins, and their pH dependence. This study used a radical scavenger to suppress any reactions with OH radicals in order to measure the rate constants for molecular ozone alone which are illustrated in Figure 2.3. ANTX-a is evidently more reactive at higher pH values with this oxidant.

Disinfection by-product formation as a result of oxidant doses required for toxin degradation is another factor which needs to be considered when implementing ozonation. Rodríguez et al. (2007a) found only 1 µg/L bromate formation when ozone was applied to a natural water with 50 µg/L spiked bromide, for complete oxidation of 165 µg/L influent ANTX-a. However, the oxidation intermediates which may be produced from the ozone-anatoxin reaction sequence remain to be investigated, and the potential toxicity of those intermediate species is unknown.

Overall, most studies agree that ozone has the ability to oxidize ANTX-a effectively, provided oxidant scavenging by background natural organic matter (NOM) constituents, pH and temperature are duly accounted for. As with most ozone applications, the precise dose and contact time required to achieve the desired level of toxin degradation will depend upon local water quality and treatment conditions, but published material can serve as a guide for expected operation. The poorer performance (only 63% toxin degradation) observed by Al Momani (2007), was from a study which employed extremely high ANTX-a concentrations (several orders of magnitude above those normally observed in natural waters); studies which examined more environmentally relevant toxin concentrations all achieved greater than 90% oxidation. Ozone doses typically employed in drinking water disinfection (less than 2 mg/L) appear to be appropriate for this application, and greater than 99.9% (3-log) degradation of ANTX-a is predicted for systems meeting the ozone dose and contact time requirements for E. coli, viruses, and *Giardia lamblia* disinfection (Onstad et al., 2007). However, care should be taken to validate attainment of the expected toxin degradation.

2.5.1.4 Advanced Oxidation Processes

Advanced oxidation processes (AOPs) are considered an effective treatment for many micropollutants and emerging contaminants, including cyanotoxins, due to the non-specificity of the oxidizing hydroxyl radical (Jin et al., 2012; Lee & von Gunten, 2012). The second order rate constants for the reaction of the hydroxyl radical with organic micropollutants are typically very fast i.e. in the range of $10^9 M^{-1}s^{-1}$ and provided that hydroxyl radicals are present in excess reaction rates are essentially diffusion controlled.

However, when employing AOPs in natural water hydroxyl radicals are not necessarily available in excess. Hydroxyl radical formation and concentrations are dependent on the operating parameters employed for a particular AOP and on the natural water matrix. Various AOPs have been studied for their ability to reduce ANTX-a concentrations, including O_3/H_2O_2, UV/H_2O_2, the Fenton process, O_3/Fe(II) and titanium dioxide photocatalysis. Generally, O_3/H_2O_2, and UV/H_2O_2 have been employed at full-scale for other contaminants in drinking water treatment whereas the other processes have been applied either in groundwater remediation or at bench-scale.

ANTX-a degradation efficiency is increased by the addition of OH· radical-promoting chemicals to an ozone process, such as hydrogen peroxide (H_2O_2) or ferrous ions (Fe(II)). In ultrapure water hydrogen peroxide and ozone combined can achieve 100% elimination of ANTX-a in less than 180 seconds, with increased H_2O_2 doses (0.001 – 0.01 mg/L) increasing degradation efficacy (Al Momani, 2007), although this H_2O_2 dose (0.1 mg/L with 1 mg/L ozone) was relatively low – an approximate stoichiometric ratio of 0.3 g H_2O_2 : 1 g O_3 is more typical (Crittenden et al., 2012). The increased degradation observed was likely due to enhanced formation of hydroxyl radicals. In the O_3/Fe(II) process, addition of Fe(II) in excess of 0.5 mg/L did not result in improved toxin degradation, although at 1 mg/L ozone and 0.5 mg/L Fe(II), 85% toxin degradation was achieved (Al Momani, 2007).

In the same study, use of the Fenton process (a combination of H_2O_2 and Fe(II)) also yielded complete oxidation of ANTX-a, with the H_2O_2 concentration controlling the total degradation, likely enhancing hydroxyl radical production, and an inverse relationship between pH and toxin degradation. With the application of 0.005 mg/L H_2O_2 and 0.1 mg/L Fe(II), the toxin degradation increased from 60% at pH 7 to 73% at pH 3, at a contact time of 180 s. This pH relationship is the opposite of what was observed for ozone, and is likely attributable to the fact that the Fenton process is more effective in producing hydroxyl radicals at acidic pH values (Chang et al., 2008). Of the AOPs investigated by Al Momani (2007), the Fenton process had the highest apparent (first order) rate constant for oxidation of ANTX-a, followed by O_3/H_2O_2 and O_3/Fe(II), with all of the AOPs studied showing much higher apparent rate constants than

ozone alone. This relative reactivity is consistent with the difference in magnitude between the second order rate constants for reactions with OH• radicals and molecular ozone as shown in Table 2.2. Similarly, preliminary work conducted by Robertson et al. (1999) with titanium dioxide photocatalysis showed complete toxin decomposition within 30 minutes. This was validated by comparison with toxin destruction under control conditions – illumination without the catalyst present – which showed less than 5% degradation. The limited toxin degradation observed in this control (UV irradiation) is in agreement with the results discussed in the section on UV treatment.

Although the removals observed by Robertson et al. (1999) and Al Momani (2007)in ultrapure water are promising, no investigation was made in either study into the effects of natural water conditions; scavenging of the oxidants by NOM and the impact of excess alkalinity need to be considered when applying AOPs at full scale as a barrier to cyanotoxins. Furthermore, the ANTX-a concentrations used in both studies (0.5-5 mg/L) are several orders of magnitude higher than those relevant for naturally occurring blooms and therefore the applicability of these results to typical source waters needs to be assessed under natural water conditions.

Afzal et al. (2010) examined two UV-based AOPs – vacuum UV photolysis (VUV) at 172 nm, and low pressure (LP) UV/H_2O_2– and found both to be effective in the oxidation of ANTX-a. VUV was capable of reducing a 600 µg/L ANTX-a concentration to below the 33 µg/L detection limit (>95% removal) in deionised water; however, as expected investigations in model and natural waters showed a reduction in the process efficiency, with only 70-85% removals observed for double the UV dose (Afzal et al., 2010). A similar trend was observed for the LP UV/H_2O_2 process, with decreased removals in natural and synthetic water, although only 70% toxin reduction was reported in deionised water. A possible dose-response relationship was observed between H_2O_2dose and ANTX-a removal with UV/H_2O_2, up to a 40 mg/L dose (Afzal et al., 2010). As H_2O_2 alone does not appear to effectively oxidize ANTX-a, with only 5% reduction in toxin concentration reported by Al Momani (2007), this relationship is attributed to increased production of the OH· radical.

Table 2.2 presents the two pseudo-second order rate constants which have been reported for the reaction of ANTX-a with the OH· radical: 3.0 x 10^9 $M^{-1}s^{-1}$ at pH 7 (Onstad et al., 2007), and 5.2 ± 0.3 × 10^9 $M^{-1}s^{-1}$. The latter was reported to be independent of pH (4.5 – 9.5) and temperature (8 – 48 ^oC) (Afzal et al., 2010). There is good agreement between these rate constants given that they were established independently by different labs using different methodologies.

Collectively these results indicate that although AOPs are capable of achieving complete removal of ANTX-a, the operating conditions and selection of the OH· radical generation process play critical roles in determining the toxin degradation efficacy and efficiency. Furthermore, all the studies presented in the literature have used initial concentrations of ANTX-a higher than would be expected in environmental conditions. The effects of oxidant scavenging in natural waters would likely be more severe for lower influent toxin concentrations, and this issue should be addressed by future studies.

2.5.1.5 Permanganate

Potassium permanganate has been used as an effective oxidative barrier to numerous emerging contaminants, including cyanotoxins (Hart et al., 1998; Hall et al., 2000; Rodríguez et al., 2007a). A 2 mg/L dose may be sufficient to reduce a starting ANTX-a concentration of 2.4 – 4.3 µg/L by over 90% in treated water, although the necessary contact time and pretreatment employed have not been indicated (Hall et al., 2000). Between pH 6 and 8, the reaction appears constant, but reactivity increases markedly between pH 8 and 10 (Rodríguez et al., 2007a). The apparent second-order rate constant is provided in Table 2.2, and indicates that permanganate is slightly less reactive with ANTX-a than ozone, and much less reactive than the hydroxyl radical. In natural water with 3.6 mg/L DOC, 0.5 mg/L permanganate was able to completely eliminate 166 µg/L influent toxin, indicating this oxidant is very well suited to treatment of ANTX-a, even in the presence of background NOM (Rodríguez et al., 2007a). Other studies have shown better removal with permanganate than ozone, an unexpected result based on the second order rate constants (Hart et al. 1998; Hall et al., 2000; Rodríguez et al., 2007a). In the case of Rodriguez

et al. (2007), the authors attributed the higher removals to the impacts of the natural water matrix, indicating that it increased the stability of permanganate resulting in increased oxidant exposure.

2.5.2 Membrane filtration

Due to the small molecular size of ANTX-a, low pressure membranes (microfiltration and ultrafiltration) are generally not considered a barrier to the dissolved, extracellular toxin, although they can be used effectively to remove intact cyanobacterial cells under appropriate operating conditions (Global Water Research Coalition, 2012). As a result, this review considers only high pressure membranes, namely nanofiltration and reverse osmosis.

Based on molecular weight cut-offs (150-700 Da), nanofiltration can be a promising candidate for ANTX-a removal. At low molecular weight cut-offs < 165Da (i.e. the molecular weight of ANTX-a) complete removal would be expected based on size exclusion. But even where the molecular weight cut-off of a membrane (Trisep TS80 4040) is slightly higher than the molecular weight of the target compound (200 Da vs. 165 Da), removal efficiency of greater than 96% can be achieved indicating that mechanisms other than size exclusion are important for removal (Gijsbertsen-Abrahamse et al., 2006). ANTX-a adsorption to nanofiltration membranes has been observed in multiple studies (Gijsbertsen-Abrahamse et al., 2006; Teixeira & Rosa, 2011, 2012), and therefore accurate removal values can only be determined after an appropriate acclimation period of at least 48h. Although these effects were considered in the Gijsbertsen-Abrahamse et al. (2006) study, some limitations still apply to their results: in this bench-scale investigation, recovery was only 10% of the feed water, which is significantly lower than the >75% recoveries often employed in full-scale operation where multiple stages are employed. The initial ANTX-a concentration (4.6 – 4.8 µg/L) was within a relevant range for impacted source waters; however, with increased recovery, the feed water toxin concentration will increase and lower removals may result.

Teixeira & Rosa (2006) demonstrated removals up to 96.6% from an electrolyte solution spiked with 10 µg/L ANTX-a using a negatively charged nanofiltration membrane (Alfa Laval NFT50) operating with 10 bar transmembrane pressure and 0.91 m/s crossflow. While the molecular weight cut-off of the NFT50

(150 Da) is lower than the molecular weight of ANTX-a (165 Da), the two values are quite close and size exclusion was likely not the only mechanism for removal as observed removals changed with changes in operating conditions. Teixeira & Rosa (2006) found that lower pH (pH 4-8) and the presence of $CaCl_2$ both enhanced the achievable toxin removals. At low pH, addition of 1 mM $CaCl_2$ resulted in an increase in removal efficiency from 83.3% (pH 4.3) to 96.6% (pH 4.0) and at higher pH the removal increased from 67.9 % (pH 8.2) to 88.7% (pH 7.7) with the addition of calcium. High rejection (95%) continued to be achievable even in clarified natural waters with NOM present. At recovery rates of up to 90%; indeed, the presence of background organics, including other cyanotoxins, removed the pH dependence observed in electrolyte solution, which was attributed to increased steric hinderances thereby increasing toxin rejection.

Nanofiltration membranes appear to be an effective treatment process for ANTX-a, although the scarcity of studies indicates a need for validation of these results, in particular for removal by nanofiltration membranes with higher molecular weight cut-offs. It should be noted that although high removals of ANTX-a have been observed, removal of microcystins was higher still, as expected given the molecular size differential. Removals for the tighter reverse osmosis membranes would be expected to be complete, given the ability of those membranes to reject even monovalent ions in desalination processes; however, this has not yet been demonstrated.

2.5.3 UV Irradiation

Unlike UV irradiation employed for disinfection and AOPs using UV to generate hydroxyl radicals for contaminant degradation, direct photolysis degradation of ANTX-a using UV irradiation requires very high fluences (doses) (Hall et al., 2000; Afzal et al., 2010) although studies differ on how high. A study published by Hall et al. (2000) showed that doses in the range of 20,000 mJ/cm^2 were required to achieve toxin degradation, although toxin removal values were not given in this study, and the type of lamp used (medium vs. low pressure UV) was not noted. As the maximum absorbance for ANTX-a occurs at 227 nm, low pressure (LP) UV emitting only at 254 nm has been deemed ineffective (Afzal et al., 2010).

Medium pressure lamps emit light over a wide wavelength spectrum and in their study using medium pressure (MP) lamps, Afzal et al. (2010) achieved 88% and 50% toxin reductions from starting concentrations of 0.6 mg/L and 1.8 mg/L respectively, using a UV fluence of 1285 mJ/cm^2. Higher fluences will have to be employed to achieve removals greater than 90% which is well above the 20 – 100 mJ/cm^2 range typically employed for disinfection in drinking water treatment (Crittenden et al., 2012).

As the Afzal et al. (2010) study was conducted in ultrapure water at bench-scale, and although fluence determinations take the character of the particular water characteristics into account, it is expected that the reported removals will be impacted by the presence of shielding and competing compounds in full-scale operations. Overall, this process is not an effective treatment barrier for ANTX-a as the high fluences required are economically unfeasible.

2.5.4 Adsorption

As was previously noted, ANTX-a exists both intra- and extracellularly, with the toxin predominantly found within intact cells during the bloom growth phase until cell lysis occurs as a result of aging or other water treatment processes. While activated carbon may not be appropriate for the treatment of toxins bound within the intact cells, it may play a role in the removal of extracellular ANTX-a .

Activated carbon adsorption is considered a primary treatment barrier for many extracellular cyanotoxins (microcystin-LR,-RR,-YR, cylindrospermopsin, saxitoxin, etc.), although its effectiveness for removal of ANTX-a is less well understood (Cook & Newcombe, 2002; Carrière et al., 2010). Few studies have investigated the use of powdered or granular activated carbon (PAC or GAC) for ANTX-a control and no adsorption isotherm parameters have been reported in the literature to-date. The type of carbon used can strongly impact the removals obtained, as carbons produced from varying source materials (coconut, coal, wood, etc.) and activated via diverse techniques (steam activated, chemically activated, etc.) can exhibit different characteristics including surface charge and pore size distribution. Based on the properties of a target compound, a more microporous or more mesoporous carbon may be optimal for different

microcontaminants, and based on background water characteristics, some carbons may perform better when the competitive and preloading effects of NOM are considered.

To manage the lack of available research results, some authors have suggested using microcystin adsorption as an indicator of potential ANTX-a removal (Carrière et al., 2010; Global Water Research Coalition, 2012). However, given the differences in chemical structures, charge, and molecular weight, microcystin may not be an appropriate surrogate for the adsorption behaviour of ANTX-a (Newcombe & Nicholson, 2004), and impacts of NOM competition and carbon properties may be quite different for the two toxins. ANTX-a has a molecular weight of 165 Da, and is therefore more comparable in size to 2-methylisoborneol (MIB) (MW = 168 Da) and geosmin (MW = 182 Da) – two taste and odour compounds produced by cyanobacteria – than to microcystin (MW = 995 Da, microcystin-LR variant). Given the much greater availability of data regarding the removal of geosmin and MIB, these compounds may potentially serve as appropriate gauges of the feasibility of activated carbon processes for treatment of ANTX-a. Activated carbon is also seen as a primary barrier against taste and odour compounds, with high removals potentially achievable and further study into the ANTX-a application is therefore warranted.

2.5.4.1 Granular Activated Carbon (GAC)

Some preliminary work has been conducted using GAC, although the studies were limited in scope and results were somewhat contradictory. Hart et al. (1998) used a coal-based GAC rapid small scale column with an empty bed contact time of 6 minutes, and achieved greater than 90% initial removal but found 80% breakthrough of the 8.2 µg/L influent after 35,000 bed volumes (equivalent to approximately 18 weeks' operation). However, no information was given regarding the water matrix used, nor was any consideration given to competitive effects. Another study also noted ANTX-a removal using GAC at pilot scale, but was unable to distinguish between removals due to adsorption and the possibility of biological degradation within the active biofilm (UKWIR, 1996).

2.5.4.2 Powdered Activated Carbon (PAC)

Due to the seasonal and sporadic nature of blooms in many parts of the world, PAC is a more popular adsorptive treatment method for cyanobacterial metabolites (i.e., geosmin and MIB) as it allows operators greater flexibility and suffers less from the effects of pre-loading of carbon sites than does GAC. However, during the bloom growth phase much of the toxin present may be contained intracellularly. The usefulness of PAC applied at the front end of the plant (as is typical) would therefore be limited, as only the extracellular toxin fraction at the plant intake would be accessible. Intracellular ANTX-a would be unaffected by the PAC, but could be released as the result of cell lysis in a later stage of the treatment train.

PAC removal studies for ANTX-a have also been limited; two studies reported 50 – 60% removal of ANTX-a using a 5 mg/L PAC dose, one from an influent with approximately 22 µg/L anatoxin (Keijola et al., 1988), and the other from an unspecified influent concentration (Bruchet et al., 1998). In both studies, contextual information was lacking: no information was given on the type of PAC, contact time, or water matrix investigated.

A more promising result showed 90% toxin removal from 10 µg/L ANTX-a influent, but required 11 mg/L PAC, and 60 mg/L was required to remove 98% of ANTX-a from a 50 µg/L influent, although the contact time allotted was again unspecified (Mouchet & Bonnelye, 1998); In contrast, typical PAC doses employed in drinking water treatment would be in the 5-25 mg/L range (Crittenden et al., 2012). The total organic carbon (TOC) of the water matrix studied varied between 4 and 6 mg/L, and therefore the adsorption process included competition from background organics, but only one carbon type (F400 coal based, Calgon Carbon) was considered, and as discussed above, carbon selection is a critical consideration for effective adsorption of micropollutants.

A systematic optimization of this treatment process could yield favourable results, but further information is required to be able to accurately and confidently determine PAC doses and contact times, based on the

background water NOM concentration and composition, temperature, carbon type and influent toxin concentration.

2.5.5 Biofiltration/Slow Sand Filtration

Similarly to adsorption, despite being considered one of the more effective treatment processes for removal of cyanotoxins from drinking water, there is limited information available on the use of biofiltration or slow sand filtration as a barrier to dissolved ANTX-a (Ho et al., 2012). ANTX-a degrading microorganisms seemingly occur naturally in various lake environments (Rapala et al., 1994), although only one such organism – a *Pseudomonas sp*. Gram-negative bacteria – has been identified (Kiviranta et al., 1991). The ANTX-a degradation rate in natural waters via this bacterium was determined to be 6 – 30 µg/mL over a 3 day period.

Rapala et al. (1994) noted biodegradation of ANTX-a in a batch sediment experiment, but only following a 4 day lag-phase; studies examining removal of other cyanotoxins – primarily microcystin-LR – using biofiltration have shown that an extended lag phase (up to 16 days) can be required prior to establishment of degrading microorganisms within the biofilm (Cousins et al., 1996; Ho et al., 2012), and based on the above findings, similar concerns may be anticipated for ANTX-a. As such, biodegradation may be limited to application in warmer climates where cyanobacterial blooms are a continual issue, rather than a seasonal and episodic concern as in more temperate regions.

There is a lack of information on studies dealing directly with degradation of the toxin within a biofilm, and no bench-, pilot-, or full-scale biofiltration studies are reported in the peer-reviewed literature. In the only study directly dealing with drinking water treatment processes, Keijola et al. (1988) reported 68-74% reduction of the neurotoxin from *Anabaena flos-aquae* culture (presumed to be ANTX-a), using pilot-scale slow sand filters with an approximate empty bed contact time of 100 minutes, and implicated biological activity by microscopic verification of the presence of biofilm.

There is evidence for the potential for biodegradation-based processes to contribute to a multiple-barrier treatment approach for ANTX-a, albeit the effects of temperature, empty bed contact time, and background water quality remain unknown. Further validation of achievable removals within different operating conditions is required to confidently rely on biofiltration or slow sand filtration processes.

2.5.6 Other treatment options

Bank filtration intakes may provide ancillary benefits for cyanotoxin removal; Klitzke et al. (2011) noted that ANTX-a sorption to sediments was higher for clay- and organic-rich sediments than to sandy sediments, and reported various Langmuir sorption model parameters based on 10 different sediment types. This study may serve as a guide for the type of ANTX-a removals which could be achieved in a bank-filtration scenario, considering local soil and sediment compositions.

The majority of treatment options studied and presented in this review are intended to represent municipal-scale operations; as such a knowledge gap exists for technologies implemented at smaller scale. While high-pressure membrane filtration and oxidation processes can be expected to perform similarly to those operations detailed above, other technologies such as home filtration devices – including both ion exchange and activated carbon filtration – are not well characterised, and their performance with respect to ANTX-a removal is therefore unknown. No studies have examined home carbon filtration devices for ANTX-a control and further investigation of the prospects of these systems may be of value to owners of small-community or point-of-entry/point-of-use systems.

To the authors' knowledge, no studies have been published examining the use of ion exchange for removal of ANTX-a. Monosov et al. (2012) found that microcystin-LR was well removed but suffered from competitive effects of background NOM concentrations, and similar concerns can be expected for ANTX-a. Although due to the molecular differences between the two toxins, as discussed above, it would be inapt to extrapolate specific operating parameters such as resin types.

2.6 Best Practices

Physical removal via high-pressure membrane filtration and chemical elimination via oxidants such as ozone, AOPs and permanganate are the only processes which can presently be considered effective for the treatment of extracellular ANTX-a from drinking water, as summarized in Table 2.4. Various studies have validated the ability of each of the above treatments to remove or degrade over 90% of the toxin, and the impacts of diverse treatment conditions including different background water quality parameters such as TOC and pH have been reported and are considered manageable. While treatment with membranes, ozone and permanganate has been investigated at environmentally relevant toxin concentrations, the studies examining the various AOPs have dealt with high initial ANTX-a levels. Furthermore, often only one or two studies have been published on the different hydroxyl radical-producing processes, as Table 2.3 demonstrates; therefore, while AOPs are considered effective, further validation is recommended.

Conventional plants which employ none of these processes may be more vulnerable to this toxin than other cyanobacterial toxins including the more prevalent microcystins. In a survey of treatment plants in the Canadian province of Quebec, it was projected that under a climate change scenario (15 µg/L influent ANTX-a concentrations) no plants using chlorine as the exclusive treatment barrier would be able to conform to the 3.7 µg/L provisional provincial guideline (Carrière et al., 2010).

Table 2.4: Summary of treatment process efficacy for anatoxin-a removal

Process	Treatment Barrier Efficacy	Operational Considerations/Comments
Membranes – NF/RO	Likely effective	Adsorption of toxin on membrane surface occurs, rejection efficiency governed by electrostatic interactions and steric hindrance, 90% recovery achievable. However, no RO data to support theoretical rejection and only some NF membranes have been investigated. NF membranes with higher molecular weight cut-offs may not be as effective and need to be investigated.
Oxidation – Ozone	Effective	1 – 2 mg/L doses resulted in >90% degradation in 6 studies, dependent on water quality
Oxidation – Permanganate	Effective	Efficiency increases above pH 8, 0.5 – 2 mg/L doses resulted in >90% degradation in 2 studies
Oxidation – AOPs	Effective	$OH^{\cdot}$ generation process impacts efficiency, efficacy needs to be quantified for lower toxin concentrations and in natural water
Adsorption – PAC/GAC	May be effective	Not frequently investigated, effects of carbon type unknown, competition from background NOM may reduce efficacy (high PAC doses and short GAC run times may be required)
Biofiltration	May be effective	Not frequently investigated, temperature, pH, water quality effects unknown, lag phase may occur prior to establishment of anatoxin-degrading species (may not be suitable for seasonal cyanobacterial outbreaks)
Oxidation – Chlorine	Ineffective	Reaction is prohibitively slow (k_{app} <1 $M^{-1}s^{-1}$ at pH 8)
Oxidation – Chloramine	Ineffective	Reaction is prohibitively slow (k_{app} <1 $M^{-1}s^{-1}$ at pH 8)
Oxidation – Chlorine Dioxide	Ineffective	Reaction is prohibitively slow
UV	Ineffective at disinfection doses	Very high fluences required (1285 – 20000 mJ/cm^2)
Home Filtration (POU) Devices (Carbon)	Unknown	Further research needed
Ion Exchange	Unknown	Further research needed

Among the physical and chemical processes discussed, some challenges remain to be considered including the potential for toxic by-product formation in oxidative treatment, and the management of residuals produced in high-pressure membrane treatment. Due to the uncertainty associated even with those treatment processes considered effective for ANTX-a removal, and the lack of full-scale data, a

multiple treatment barrier approach is recommended to ensure that public health is safeguarded and that potential future regulations and guidelines can be met. A combination of oxidation and physical or sometimes biological removal has been employed for other cyanotoxins; however, in the absence of applicable information for activated carbon and biofiltration, non-chemical processes for ANTX-a are limited to high-pressure membrane filtration.

It was noted in several instances that important information was missing to assist with the interpretation of some studies. Table 2.5 presents suggestions for parameters which should be monitored and included in published materials, to allow drinking water practitioners to gauge the re-applicability of study results to similar conditions.

Table 2.5: Recommended anatoxin-a study parameters

Study Type	Parameters
Oxidation – Cl_2, O_3, AOPs, Permanganate	CT (time of exposure, oxidant residual at time of anatoxin-a sample collection and at T_0 – if applicable), pH, temperature
UV-based (including AOPs)	UV-fluence/dose, type of lamp (low pressure/medium pressure), reactor configuration, if MP wavelengths are blocked below 200 nm, water flow rate, pH, temperature
PAC	Carbon type (porosity/pore size distribution, source material, particle size, surface charge), contact time, type and dose of coagulant used (if any), pH, temperature
GAC	Hydraulic loading, empty bed contact time, media/carbon type (as above), effective size, uniformity coefficient, media depth, pH, temperature
Biofiltration	Hydraulic loading, empty bed contact time, media/carbon type (as above), effective size, uniformity coefficient, media depth, pH, temperature, biomass parameters e.g. ATP
Studies considering natural waters	Alkalinity, pH, temperature, TOC, DOC, UV_{254}, SUVA, turbidity, NOM

2.7 Conclusions

Further work is needed to ascertain the conditions under which the treatment processes discussed herein can be applied successfully at full-scale for the removal of ANTX-a. Oxidation via permanganate or ozone, and AOPs have all been repeatedly identified as processes effective for ANTX-a treatment, but especially for AOPs, studies in natural water and at environmentally relevant ANTX-a concentrations are still required. There is a consensus that UV, chlorine, chloramine and chlorine dioxide have been acknowledged as ineffective under drinking water treatment conditions. High pressure membrane filtration is likely effective, with excellent results for some nanofiltration membranes, although removals for NF membranes with larger molecular weight cut-offs need to be validated; furthermore the assumption that reverse osmosis membranes will be capable of achieving high rejection of ANTX-a has not yet been substantiated. Preliminary results for activated carbon adsorption (particularly PAC) and biofiltration show good potential, but indicate a need for further investigation, while the potential of other processes or process combinations, including ion-exchange and home treatment units, remains unknown. A multiple-barrier approach is suggested for utilities impacted by this toxin, to mitigate the uncertainties related to process optimization.

Chapter 3
Analytical Considerations for Anatoxin-a

3.1 Summary

Two analytical methods for the quantification of aqueous anatoxin-a concentrations, enzyme-linked immunosorbent assay (ELISA) and liquid chromatography tandem mass spectrometry (LC-MS/MS) were evaluated for use in a planned treatment study. An anatoxin-a ELISA which had only become commercially available at the time of this study was found to have high relative standard deviation, and detected only the naturally-occurring (+)-anatoxin-a stereoisomer. While detection of only the naturally occurring isomer seems advantageous the only dependably cost-effective standards available for treatment studies are a racemic mixture of (±)-anatoxin-a. Furthermore, it necessitated the use of a solid phase extraction sample preconcentration step to measure environmentally-relevant toxin concentrations. By contrast, the LC-MS/MS method developed was rapid, reproducible, and sufficiently sensitive to measure concentrations in the 1-100 µg/L range of the racemic mixture of (±)-anatoxin-a. However, the laboratory equipment and operator training requirements of the LC-MS/MS method are much greater than those of the ELISA method. Ultimately, the LC-MS/MS method was deemed to be better suited to the requirements of the planned studies.

3.2 Introduction

A review of analytical methods for the measurement of cyanotoxins in drinking water and surface water studies revealed that enzyme-linked immunosorbent assays (ELISA) and liquid chromatography tandem mass spectrometry (LC-MS/MS) were the most frequently used (Fortin et al. 2010).

ELISA analysis typically employs a colorimetric reaction to quantify the amount of an antigen bound to a fixed quantity of receptors in the assay vessel. In the most sophisticated applications, test wells within a microtitre plate are used as the assay vessel and the results are measured using a spectrophotometer.

ELISA assays for microcystins (MC) are well established and produced by numerous manufacturers, as shown in Table 3.1. They have been used in a range of monitoring and water treatment studies, including Delgado et al. (2012), Fortin et al. (2010), Fromme et al. (2000), Haddix et al. (2007), Hoeger, et al. (2005), Ou et al. (2012), Rodríguez et al. (2008), Sorlini, et al. (2013), Xagoraraki and Harrington (2006), and Zamyadi et al. (2012, 2013). Several formats of the assay are available for microcystin detection, including some that can target multiple variants of the toxin and even target microcystin and nodularin (NOD) in the same assay. In most cases, the sensitivity varies for the different congeners, as shown in Table 3.1; therefore many assays are calibrated to the most common variant, microcystin-LR, and report the concentration in microcystin-LR equivalents, rather than providing absolute concentrations. However, cross-reactivity of the toxin variants also depends on the antibodies employed, and therefore assays from different manufacturers can produce different results for the same sample (Triantis et al. 2010). Several issues can further impact the efficacy of microcystin and nodularin ELISA assays, including matrix effects such as the potential suppression of test sensitivity by methanol extract matrices, and over-reporting resulting from seawater matrices (Triantis et al. 2010), although these impacts are now better understood and some manufacturers have developed guidelines for managing challenging sample matrices (for example, Abraxis, 2015c).

ELISA kits for many of the other common cyanotoxins including cylindrospermopsin (CYN), as well as the brackish- and seawater toxins nodularin and saxitoxin (STX) are also available. These tests are capable of providing both presence-absence detection, in their simplest forms, and quantification at environmentally relevant concentrations, in their more extensive forms, typically without any sample pre-concentration. In 2013, an anatoxin-a receptor binding assay (RBA) based on similar principles became available from Abraxis (PA, USA). While issues of cross-reactivity are not anticipated, given the limited number of anatoxin-a congeners detected in surface waters, the anatoxin-a assay operates in a concentration range several orders of magnitude greater than that of most cyanotoxin ELISA kits (up to 500 µg/L anatoxin-a), and much greater than typical environmental concentrations. The discrepancy

between the assay range and environmental sample concentrations necessitated the addition of a pre-concentration step, using solid phase extraction (SPE).

Triantis et al. (2010) and Spoof (2005) recommended ELISA for microcystin and nodularin be used as a screening tool in combination with more sensitive methods such as LC-MS/MS, particularly in critical cases. While the low capital and operational costs of ELISA are attractive as compared to LC-MS/MS, these must be weighed against the limitations in reproducibility, accuracy and specificity.

In LC-MS/MS quantification the contents of a sample are first separated by an LC column, wherein some compounds are more attracted to the column packing material (or stationary phase) than others, resulting in a longer retention time prior to elution. Peaks eluting from the column are then ionized, detected by the MS quadrupoles and identified based on their m/z or mass-to-charge number ratio. The use of two quadrupoles in tandem (MS/MS) allows compounds to be more selectively differentiated than with a single quadrupole; ions detected by the first quadrupole (precursor ions) are subsequently fragmented, and the resulting product ions are detected by the second quadrupole, producing a fragmentation pattern which can be used to confirm compound identification based on the precursor ions.

LC-MS/MS methods for cyanotoxins, including anatoxin-a, are extremely sensitive, capable of differentiating between variants and typically highly reproducible (Furey et al. 2003, Oehrle et al., 2010); however, these methods require costly laboratory equipment and extensive operator training. In this study, both the RBA and LC-MS/MS methods for anatoxin-a quantification were evaluated, to determine their applicability to laboratory water treatment investigation.

Table 3.1: Commercially available cyanotoxin ELISA microtitre plate kits

Manufacturer	Trade Name	Cyanotoxins detected[1]	Assay range (µg/L)	Cross-reactivity range	Source
Abraxis & Enzo Life Sciences[2]	Microcystins-ADDA ELISA	MC-LR, -LF, -LW, -RR, -YR NOD	0.15 – 5.0 MC-LR equivalents	100% MC-LR 50% (MC-RR) – 167% (MC-YR) 100% NOD	Fischer et al. 2001; Abraxis 2015c; Enzo Life Sciences 2012
Abraxis	Microcystins (ADDA)-Direct Monoclonal ELISA	MC-LR, -LA, -LF, -LW, -LY, -RR, -YR NOD	0.15 – 5.0 MC-LR equivalents	100% MC-LR 66% (MC-LA) – 102% (MC-LW) 78% NOD	Abraxis 2015b
Biorbyt[3]	Microcystin ELISA Kit	MC-LR, RR, -YR NOD	0.1 – 5.0 MC-LR equivalents	100% MC-LR 12% (MC-RR) – 72% (MC-YR) 27% NOD	Biorby, 2015
Envirologix[3]	QuantiPlate™ Kit	MC-LR,- LA, -RR,- YR NOD	0.16 – 2.5 MC-LR equivalents	100% MC-LR 35% (MC-YR) – 62% (MC-LA) 68% NOD	Envirologix 2010
Abnova & Aviva Systems Biology[2]	Microcystin-LR ELISA Kit	MC-LR (monoclonal)	0.1 – 2.5 MC-LR	-	Abnova 2015; Aviva Systems Biology 2015
Abraxis	Cylindrospermopsin ELISA	CYN, deoxy-CYN	0.05 – 2.0 CYN	100% CYN 112% deoxyCYN	Abraxis 2015a
Abraxis	Saxitoxin (PSP) ELISA	STX, decarbamoyl STX, neoSTX, decarbamoyl neoSTX, gonyautoxins (GTX) 1, 2, 3, 4 & 5B, lyngbyatoxin, sulfo GTX 1 & 2, decarbamoyl GTX 2 & 3)	0.02 – 0.40 STX	100% STX <0.2% (GTX 1 & 4) – 29% (decarbamoyl STX)	Abraxis 2015d
Abraxis	Anatoxin-a Receptor Binding Assay	ANTX, homoANTX	5 – 500 ANTX	100% ANTX 22% homoANTX	Abraxis 2013b; Rubio et al. 2014
Abraxis	Anatoxin-a Enhanced Sensitivity Kit	ANTX, homoANTX	0.4 – 20 ANTX	100% ANTX 22% homoANTX	Abraxis 2013a; Rubio et al. 2014

[1] Variants noted are those confirmed in kit documentation. Assays may also detect (with variable cross-reactivity) other congeners of toxins listed.

[2] Assays produced by both manufacturers have identical patent numbers, documented properties and descriptions

[3] Where assay sensitivity to different congeners was expressed as the 50% inhibition of binding level (50% B/B_o) for each compound, cross reactivity of a compound X (CR_x) was calculated as follows: $CR_x = B_{MC\text{-}LR}/B_X$

3.3 Materials and Methods

3.3.1 Standards and solutions

Two types of anatoxin-a standards are commercially available –the synthetically-derived (±)-anatoxin-a fumarate, which is available from a number of manufacturers worldwide, and a (+)-anatoxin-a standard extracted directly from a cyanobacterial cell culture and purified, which is only available from one source, the National Research Council of Canada. While it would be ideal to use the second form, which contains only the naturally occurring (+)-anatoxin-a stereoisomer, this standard is two orders of magnitude more expensive than the synthetic version and as such is cost-prohibitive for a spiking study. Furthermore, given the low production levels of this standard, it would be not be feasible to obtain even the relatively small quantities necessary for spiking at an environmentally relevant concentration. The (+)-anatoxin-a standard is intended for use as a certified calibration solution in laboratory analysis validation, and that is how it was employed here. The (±)-anatoxin-a standard is synthesized via a process which results in a consistent racemic (50/50) mixture of the two stereoisomers, as confirmed by the manufacturer using optical rotation measurements (personal communication, Klein, 2013).

Solid (±)-anatoxin-a fumarate standard was obtained from Abcam (MA, USA), and a 30 µM (+)-anatoxin-a standard solution in methanol and water (9:91, v/v) was obtained from the National Research Council of Canada (ON, Canada). The two potential internal standards (ISs) investigated, Cyclo-(Arg-Ala-Asp-D-Phe-Val) (aka c(RADfV)) and 1,9-diaminononane, were obtained from Peptides International (KY, USA) and Sigma-Aldrich (WI, USA), respectively.

LC-MS grade formic acid was obtained from Sigma–Aldrich. Acetonitrile and methanol were of liquid chromatography mass spectrometry (LC-MS) grade. High purity water was acquired from a Millipore Milli-Q® UV PLUS water system (MA, USA). Syringe filters were 0.2 µm polyethersulphone from VWR International (PA, USA). Surface water was obtained from a local creek and filtered using 0.45µm filters prior to use.

(±)-anatoxin-a stock solutions were prepared by dissolving 5 mg of (±)-anatoxin-a fumarate in 25 mL of high purity water. A (+)-anatoxin-a working solution was prepared by diluting 0.2 mL of the 30 µM standard solution to 3 mL using high purity water. A 2.5 mg/mL stock solution of c(RADfV) was prepared using high purity water, and was further diluted to a working solution concentration of 100 µg/mL. Similarly, a 1 mg/mL stock solution of 1,9-diaminononane was prepared using high purity water, and was further diluted to a working solution concentration of 50 µg/mL. Stock solutions were prepared fresh monthly, and stored in amber vials at -20^{o}C.

3.3.2 Anatoxin-a Receptor Binding Assay

Anatoxin-a RBA and enhanced sensitivity kits were obtained from Abraxis (PA, USA), and employed as per the manufacturer's procedure provided with the kit (Abraxis 2013a, 2013b). Briefly, toxin present in buffered samples and standards competes with biotinylated alpha-bungarotoxin for binding sites of the nicotinic acetylcholine receptor coated on the bottom of a 96-well microtitre plate. Two further compounds are added in excess, streptavidin-horseradish peroxidase and a colour substrate solution, which produce a colourimetric reaction with the biotinylated alpha-bungarotoxin, with the colour signal inversely proportional to the amount of toxin present. This reaction is halted after a specified time by the addition of a stopping solution and the colour signal is evaluated by reading the absorbance at 450 nm. A four-point calibration curve was included in each run, and sample concentrations were interpolated from a 4-parameter logistic fit. All samples and standards included three or more replicates, as recommended.

A ChroMate® computer-controlled microplate reader from Awareness Technologies (FL, USA) and accompanying software were used to read the absorbance of microplate wells and construct the calibration curves.

For the enhanced sensitivity protocol, the pH of samples was adjusted to 10.5 +/- 0.05 using 6 N NaOH, just prior to SPE extraction. SPE columns used were those included in the kit (the type and amount of SPE resin are proprietary), and all flow rates were approximately 1 mL/min. The columns were conditioned with 3 mL methanol followed by 3 mL high purity water, and then 25 mL of sample were

passed through the column. Samples were eluted using 1.5 mL 0.1% formic acid in methanol, evaporated to dryness under a gentle stream of nitrogen and finally, reconstituted using 1 mL of the provided "Anatoxin-a Sample Diluent," resulting in a 25x concentration factor. Concentrated samples were then run through the normal RBA process, though without the use of buffers.

3.3.3 LC-MS/MS

A Shimadzu 8030 liquid chromatography tandem mass spectrometer (Shimadzu, KYT, Japan) was used. The liquid chromatograph (LC) componentry consisted of a Shimadzu DGU-20A3R degassing unit, a Shimadzu LC-20 ADXR pump with a 100 µL mixing loop, and a Pinnacle DB C18 (50 mm x 2.1 mm internal diameter, 1.9 µm packing) analytical column (Restek, PA, USA), regulated at a temperature of 35^{o}C. The eluent was an isocratic mixture of 95% aqueous mobile phase (0.1% formic acid in water) and 5% organic mobile phase (0.1% formic acid in acetonitrile), with a flow rate of 0.3 mL/min and 10 µL sample injection volume. Quantification and analysis were conducted using the Shimadzu LabSolutions (version 5.60 SP2) analysis software provided with the hardware package. The MS was operated in multiple reaction monitoring (MRM) mode, following electrospray ionization (ESI), with the MS parameters indicated in Table 3.2. Standards and samples were prepared for analysis by adding 50 µL of the appropriate internal standard working solution to a 1 mL sample aliquot, resulting in a concentration of 2.4 µg/mL in samples and standards when 1,9-diaminononane was used as the internal standard.

Table 3.2: MS parameters for the MRM quantitation of ANTX, 1,9-diaminonane and c(RADvF)

Compound	Molecular Weight	Transition (m/z)	Collision Energy (eV)
Anatoxin-a	165	166.1 > 43.0	-25.0
		166.1 > 149.1	
1,9-diaminononane	159	159.1 > 142.2	-17.0
c(RADvF)	589	589.3 > 120.1	-52.0

3.4 Anatoxin-a Receptor Binding Assay Validation

3.4.1 Standard Protocol

Numerous trials of the receptor binding assay were conducted using spiked anatoxin samples in both high-purity and surface waters, to determine the assay's performance parameters. The racemic (±)-anatoxin-a standard was used for preliminary trials, and recoveries were confirmed using the (+)-anatoxin-a standard. Given that the toxin-detection mechanism is based on molecular configuration only the naturally-occurring (+)-anatoxin-a stereoisomer is detected by the RBA, and the (-)-anatoxin-a stereoisomer concentration was not included in the analysis of recoveries. Each standard and spiked sample was analyzed in triplicate, as recommended in the assay protocol, and the triplicate average response was used to calculate concentrations (i.e. three wells of a microtitre plate constitute one analysis of a sample). The 4-parameter logistic calibration curve generally yielded acceptable fits for ELISA, with $R^2 > 0.9$ in all cases.

The recoveries and relative standard deviations (RSD) obtained in both high-purity and surface water are presented in Table 3.3. Within the operating range (10 – 500 µg/L) the assay documentation notes that the 50% inhibition level (the concentration of anatoxin-a required to bind 50% of the available receptor sites) is approximately 87 µg/L, and that determinations closer to the middle of the calibration range will yield the most accurate results. This assertion is borne out by the lower average error and RSD of the 50 µg/L and 125 µg/L levels in both high-purity and surface water, when compared to the 10 µg/L spiking level. However, when the (+)-anatoxin-a standard was used, the 250 µg/L level resulted in better recovery and RSD than the 100 µg/L level.

Table 3.3: Percentage recoveries of (+)-anatoxin-a

Standard	Spiked Concentration (µg/L)	Level (µg/L) (+)-anatoxin-a	High Purity Water			Surface Water		
			N (each in triplicate)	% Recovery of (+)-anatoxin-a	% RSD	N (each in triplicate)	% Recovery of (+)-anatoxin-a	% RSD
(±)-anatoxin-a[1]	20	10	11	109%	68%	3	75%	49%
	50	50	18	113%	35%	3	147%	21%
	250	125	20	94%	26%	3	124%	17%
(+)-anatoxin-a[2]	100	100	7	71%	23%			
	250	250	7	90%	11%			

[1] spiked with the racemic mixture
[2] spiked with the naturally occurring isomer only

The average recoveries of the (+)-anatoxin-a stereoisomer from the (±)-anatoxin-a standard were 106% in high purity water and 115% in surface water. Recoveries of the (+)-anatoxin-a standard were lower on average, possibly indicating that the (-)-anatoxin-a stereoisomer, while not targeted by the assay, may also be detected at some lower cross-reactivity level.

While the observed average recoveries are adequate for many applications, very high RSD values were obtained in both matrices (particularly for the 10 µg/L level), calling into question the reliability of any single value. The assay documentation advises that anatoxin-a samples be analyzed in triplicate; by contrast, the better established microcystin ELISA protocols advise analysis in duplicate, indicating better reproducibility at the individual well-level in those assays. As a consequence of the triplicate analysis requirement, the cost per sample is also greater compared to other ELISA kits, as fewer samples can be processed using one plate. Indeed, only 11 samples can be processed in triplicate at a time, as the documentation advises using a maximum of 48 wells (half of the 96-well plate) in a single analytical run. Furthermore, in this study analysis in septuplicate (i.e. using the average response of seven wells in a microtitre plate for each sample) was required to consistently obtain RSD values below 20%.

3.4.2 Enhanced Sensitivity Protocol

One advantage of many ELISA analyses is the lack of pre-concentration requirements, which reduces preparation time and analytical complexity and has the added benefit of requiring relatively small sample

volumes. Compared to ELISA kits available for other cyanotoxins, the anatoxin-a RBA operates at a much higher concentration range, which necessitates the use of a sample extraction step to analyze environmentally relevant concentrations and determine compliance or exceedance of proposed regulations in the 3 – 6 µg/L range (Vlad et al., 2014). Via the "Enhanced Sensitivity" protocol, the target concentration range is lowered from 5-500 µg/L to 0.4-20 µg/L.

A 5 µg/L (+)-anatoxin-a sample was prepared using the (±)-anatoxin-a standard, split into three 25 mL aliquots, and extracted in parallel using the Enhanced Sensitivity protocol for the anatoxin-a receptor binding assay (Abraxis 2013a). Each of the three resulting 25x concentrated samples was analyzed three times (each in triplicate for a total of nine wells per sample), and the tabulated recoveries are presented in Table 3.4. The average recovery was fairly consistent (57 – 61%), with a RSD of 17% between the three samples (a measure of the consistency of the extraction procedure, within a single day and with a single operator). This trial demonstrated an average of 42% loss through extraction; however, the setup of the assay is such that 100% recovery of the toxin through the SPE step is assumed. No internal standard is used, no positive control is provided and the standards provided to construct the calibration curve are not subjected to the same SPE process – the same standards are used as for the standard protocol, simply dividing their nominal concentration by 25 for the analysis. Following the Enhanced Sensitivity protocol as directed, toxin losses through extraction are not determinable, nor is it possible to determine the consistency of extraction between days or between different users. A further draw-back of the Enhanced Sensitivity protocol is that the plating of samples differs slightly (buffers vs. no buffers), therefore un-concentrated and concentrated samples cannot be analyzed concurrently. Given the challenges of stereoisomer detection, reproducibility and sensitivity, the anatoxin-a RBA kit was deemed unsuitable for reliably quantifying anatoxin-a in the planned adsorption study.

Table 3.4: Recoveries of (+)-anatoxin-a in three identical samples extracted in parallel using SPE

Standard used	Spiked concentration (µg/L)	Level (µg/L) (+)-anatoxin-a	N (analysis, each in triplicate)	% Recovery of (+)-anatoxin-a	% R.S.D.
(±)-anatoxin-a	10	5	3	57%	20%
	10	5	3	57%	9%
	10	5	3	61%	23%
			Cumulative:	**58%**	**17%**

3.5 LC-MS/MS Method Development and Validation

Subsequent to the evaluation of the anatoxin-a RBA kit, LC-MS/MS instrumentation became available in the University of Waterloo Environmental Engineering research labs and the development of a rapid, sensitive and reproducible LC-MS/MS method for anatoxin-a determination was undertaken. The (±)-anatoxin-a standard was used, as the compound identification and quantification is based on molecular mass and can detect both stereoisomers. The method employed multiple reaction monitoring (MRM) using electrospray ionization (ESI), and the MS/MS parameters including transition monitoring (m/z values) and collision energy were optimized using LabSolutions' integrated optimization tool, as reported in Table 3.2. The MS parameters were developed using direct injection of standards to the MS/MS detector, prior to optimizing the separation by LC.

The method developed by Oehrle et al. (2010) for the LC-MS/MS analysis of multiple cyanotoxins was used as a preliminary source, and adapted to suit the needs of the current project. The Acuity UPLC HSS T3 column (100 mm x 2.1 mm ID, 1.8 µm particle size) (Waters, MA, USA) used in the Oehrle et al. (2010) paper, was deemed unnecessarily long at 10 cm for the current application – as the original study required the separation of 12 compounds, while this project only required the analysis of anatoxin-a and one internal standard. A shorter column with similar properties was obtained from Restek (Pinnacle DB C18, 50 mm x 2.1 mm internal diameter, 1.9 µm packing), and determined to be sufficient to the separation needs of the analysis. As per Oehrle et al. (2010), c(RADfV) was investigated as a preliminary

choice for an internal standard, and 0.1% formic acid in water and 0.1% formic acid in acetonitrile were used as the mobile phases in a binary gradient beginning with 2% acidified acetonitrile for 1 minute then increasing to 70% over 8 minutes, before flushing with 80% acetonitrile for 1 minute, then re-equilibrating at 2% acetonitrile for 3 minutes. The gradient was adjusted to elute the anatoxin-a and internal standard peaks more quickly, while maintaining separation.

Problems with retention time variability were encountered, and were more pronounced for the internal standard than for the anatoxin-a peak. Subsequently, the method was modified to operate the LC isocratically (with no gradient), and 1, 9-diaminononane was investigated as an alternate internal standard, as used by Bogialli et al. (2006). Adjustments to the isocratic mix of mobile phases were made to ensure that peaks did not elute at less than one column void volume. Ultimately, a stable method was developed using 5% aqueous mobile phase (0.1% formic acid in ultrapure water) and 95% organic mobile phase (0.1% formic acid in acetonitrile) isocratically, at a flow rate of 0.3 mL/minute. Both (+)-anatoxin-a and (-)-anatoxin-a eluted within one peak, as the column did not separate the stereoisomers. 1,9-diaminonane was selected as the internal standard, as it was closer in retention time to the anatoxin-a peak, and under these conditions, the retention times were 0.78 minutes for 1,9-diaminononane, and 1.08 minutes for anatoxin-a, as shown in Figure 3.1. This method employs direct injection of the aqueous samples into the LC-MS/MS. No sample pretreatment was used, other than filtration through a 0.45 µm cartridge filter to remove particulates when required, making it much less time consuming than the anatoxin-a RBA.

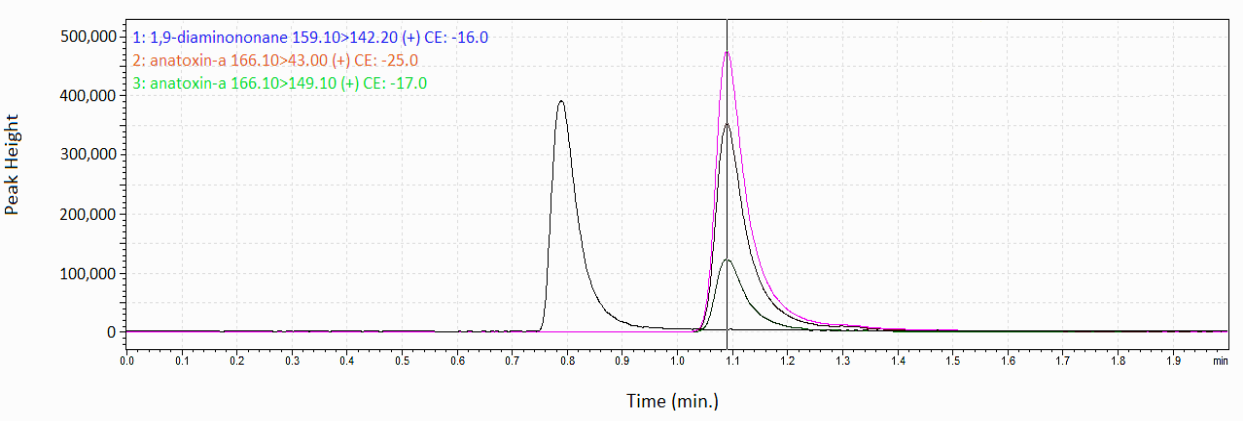

Figure 3.1: Sample chromatogram. 1- Internal standard (1,9-diaminononane); 2- Anatoxin-a

An eight-point calibration curve in the range of 0.5-100 µg/L ANTX was used, yielding a linear fit with an R^2 of 0.999. All samples and standards were analyzed using triplicate measurements (i.e. 3 injections per sample vial). Seven samples in ultrapure water at a 5 µg/L concentration were prepared independently of one another, and analyzed (with three injections per sample; i.e. 21total injections) to determine the method detection limit (MDL), as per Standard Methods for the Examination of Water and Wastewater (2012):

$$MDL = 3.14 \times s \quad \ldots\ldots (1)$$

where *s* is the standard deviation of seven replicates, with recoveries of 100 ± 50% and less than 20% RSD. The process was repeated with seven samples at a concentration of 10 µg/L anatoxin-a, and the results of this analysis are shown in Table 3.5. The relatively low RSD indicates acceptable reproducibility and the MDL of 0.65 µg/L anatoxin-a – calculated using the lower concentration samples (5 µg/L) – is sufficient to detect environmentally relevant concentrations, without a preconcentration step.

Table 3.5: LC-MS/MS method detection limit determination

	Spiked Anatoxin-a Concentration	
	5 µg/L	10 µg/L
Average concentration (µg/L)	4.45	9.84
Standard deviation	0.21	0.125
RSD	4.7%	1.27%
MDL (µg/L)	0.65	

3.6 Analytical Method Comparison

Table 3.6 presents a comparison of the properties of anatoxin-a analysis via the two methods investigated. The LC-MS/MS method developed provides a rapid and sensitive analysis of anatoxin-a concentrations, and is capable of detecting both stereoisomers of the toxin, yet requires expensive analytical equipment and substantial operator training. Although the use of SPE in combination with LC-MS/MS has not been investigated for anatoxin-a specifically, it is anticipated that even greater sensitivity could be achieved using this combination, if necessary.

Conversely, the RBA method without pre-concentration of samples is fairly simple to utilize, but is not sufficiently sensitive to determine compliance with proposed anatoxin-a regulations below the 10 µg/L level. The pairing of the RBA with a SPE pre-concentration step lowers the assay detection range, but increases the complexity of the assay and introduces a source of considerable error, while providing no method by which to account for losses during SPE when running the assay as directed.

Table 3.6: Comparison of anatoxin-a analytical methods

	RBA (standard protocol)	RBA with SPE (enhanced sensitivity protocol)	LC/MS/MS
Sample pre-concentration	Not required	Required	Not required
Calibration range	10 – 500 µg/L	0.4 – 20 µg/L	1-100 µg/L
Sample volume required	0.3 mL	25 mL	1 mL
Equipment requirements and expense	Limited (multi-channel pipetters, incubator, plate reader)	Moderate (multi-channel pipetters, incubator, plate reader, SPE extraction manifold, nitrogen drying rack)	Substantial (LC-MS/MS system, appropriate column)
Operator training requirements	Limited	Moderate	Substantial
Analysis time	Long (> 4 hours/11 samples)	Extensive (> 8 hours/ 11 samples)	Rapid (<6 min/sample)
Stereoisomers detected	100% (+)-anatoxin-a Unknown cross-reactivity with (-)-anatoxin-a		(+)-anatoxin-a (-)-anatoxin-a
Variability & Reproducibility	Relatively high inherent assay variability	Increased variability from pre-concentration step	Excellent reproducibility
Internal standard	Not used	Not used	Used
Applicability	Potential for high-concentration screening of environmental samples	Environmental monitoring/sample screening	Laboratory spiking studies at environmentally relevant concentrations (e.g., treatment studies) Environmental monitoring

3.7 Conclusions

High RSD values were obtained for the RBA, and it was unable to quantify the (-)-anatoxin-a stereoisomer, which makes up half of the more cost-effective standard as they are racemic mixtures of (+)

and (-)-anatoxin-a. Furthermore, difficulties were encountered in quantifying losses through the preconcentration step necessary to measure the low environmentally relevant toxin concentrations. These findings indicate that in its current form the RBA may not be appropriate for scientific quantification requirements, although it may be a useful semi-quantitative tool for environmental monitoring and screening applications. It is highly recommended that a positive control, processed alongside samples, be included in trials using SPE as per the Enhanced Sensitivity protocol, to allow losses due to this extraction step to be quantified. The LC-MS/MS method developed was capable of quantifying anatoxin-a at environmentally relevant concentrations, and was significantly faster than the RBA. Given the analytical requirements of the planned study, which included relatively small sample volumes, high throughput and a toxin concentration range which extended to low µg/L levels, the LC-MS/MS method was selected as the most appropriate, and subsequent treatment investigations utilized the method as described herein.

Chapter 4
Anatoxin-a Adsorption by Virgin Carbon in Ultrapure Water

4.1 Summary

The adsorption of anatoxin-a in ultrapure water by five GACs and one PAC in virgin state was examined using the bottle point technique. As expected PAC outperformed all of the GACs in terms of both kinetics and capacity; despite this promising result, the potential for intracellular toxin to bypass PAC and then be released downstream limits the applicability of PAC as a treatment barrier to dissolved cyanotoxins. Of the GACs, the wood-based carbons (C-Gran and WV B-30) adsorbed anatoxin-a most rapidly, followed by the coconut-based (Aqua Carb CX) and finally the coal-based carbons (F400 and F300). Conversely, the coal-based carbons had the greatest capacity at equilibrium (1.8 – 6.9 µg/mg adsorbent and an aqueous anatoxin-a concentration of 1 µg/L), while the coconut- and wood-based carbons had lower capacity at environmentally relevant toxin concentrations (1.2 µg/mg and 0.9 – 1 µg/mg for coconut and wood respectively, at an initial 1 µg/L aqueous anatoxin-a). In surface water applications competition with natural organic matter for adsorption sites and preloading of carbons should be further considered to elucidate expected reductions in capacity and potential changes in kinetic behaviour.

4.2 Introduction

The capacity and kinetics of adsorption for virgin carbons in ultrapure water can provide a baseline measure of adsorption behaviour. While this information does not account for adsorptive competition from natural organic matter (NOM) in natural waters, or for capacity loss from NOM preloading prior to a cyanobacterial toxin event, it is produced under replicable conditions, making the values directly comparable with information found in the literature.

The adsorptive capacity of an activated carbon for a particular adsorbate is dependent on the carbon properties, the water matrix, temperature, the properties of the adsorbate in question, and the concentration of the adsorbate in the aqueous phase. In a batch adsorption reaction where carbon with no prior exposure to the adsorbate is used, the mass balance can be expressed as follows:

$$q_e = \frac{V}{m_A} (C_0 - C_e) \quad \text{..... (1)}$$

where q_e is the carbon loading (or amount of adsorbate in solid phase) at equilibrium in µg adsorbate per mg carbon, V is the volume of solution in L, m_A is the mass of carbon in mg, and C_0 and C_e are respectively the initial and equilibrium aqueous adsorbate concentrations in µg/L. Such data are typically obtained using the bottle point technique (Droste, 1997).

Isotherms describe equilibrium data for adsorbent loading as a function of the aqueous phase adsorbate concentration, assuming constant temperature. Numerous equations have been used to describe adsorption isotherms, both theoretical and empirically derived. Among these, the most common are the Langmuir and Freundlich isotherms, both two-parameter equations (Crittenden et al. 2012). The theoretically derived Langmuir equation is predicated upon several assumptions, including the chemical binding of adsorbate molecules in a single layer upon the adsorbent surface and constant free-energy change across all adsorption sites, which do not hold for most activated carbon applications (Crittenden et al. 2012). Consequently, it is often inappropriate for describing isotherm data for aqueous solutions, particularly when using activated carbon as the adsorbent (Crittenden et al. 2012; Worch, 2012).

The empirically-derived Freundlich model is generally found to best represent experimental data for adsorption in aqueous solutions, particularly for heterogeneous adsorbents such as activated carbon (Crittenden et al. 2012); its recurring use in water treatment studies has established it as a kind of standard (Worch, 2012). The Freundlich equation is expressed as follows:

$$q_e = K_F C_e^{\,1/n} \quad \text{.....(2)}$$

where K_F and n are model parameters, indicative of adsorption strength and energetic heterogeneity of the adsorbent surface, respectively (Worch, 2012). It should be noted that it is also possible to arrive at the Freundlich equation by combining a suite of Langmuir isotherms for different adsorption site free-energy levels (Crittenden et al. 2012).

To date, no adsorption isotherms have been published for the removal of anatoxin-a. In their review of water treatment processes for cyanotoxin removal, Westrick et al (2010) noted that activated carbon adsorption of anatoxin-a has not been frequently studied and requires further investigation. A past study (UKWIR, 1996) examined removal of anatoxin-a in a granular activated carbon (GAC) biofilter; however, the distinction between adsorption and biodegradation removal mechanisms could not be made (Ho et al., 2012; WHO, 1999). While the coal-based GAC was found to reduce influent anatoxin-a concentrations of 1.5 – 9.2 µg/L to below 0.5 µg/L, there was limited information on the GAC capacity or adsorption kinetics (UKWIR, 1996). Hart et al. (1998) investigated the removal of anatoxin-a in a coal-based GAC rapid small scale column, attaining greater than 90% removal of a 8 µg/L influent, with 80% breakthrough after 35,000 bed volumes; however, these results cannot be substantiated by replication, as no characterizing information was provided for the water matrix studied. The International Guidance Manual for the Management of Toxic Cyanobacteria (Global Water Research Coalition, 2012) also indicated that there is limited data available on anatoxin-a removal using powdered activated carbon (PAC) or GAC, but that removals similar to those of microcystin-LR could be expected. However, given the differences in molecular structure between microcystin and anatoxin, it is not evident that they would have similar adsorption characteristics.

It was the objective of this study to investigate anatoxin-a adsorption by a range of activated carbons under replicable conditions, producing kinetic data and isotherms which could be compared with literature values to provide a preliminary indication of the adsorption behaviour of this neurotoxin. Batch adsorption studies were undertaken with six activated carbons, and the performance of each carbon was evaluated based on kinetics and equilibrium capacity.

4.3 Materials and Methods

4.3.1 Materials

F400 and F300 GACs were provided by Calgon Carbon (PA, USA), WV B-30 GAC was provided by MWV (SC, USA), C-Gran GAC was provided by Norit (TX, USA) and Aqua Carb CX 1230 GAC was

provided by Evoqua (PA, USA). All GACs were donated by the manufacturers at no charge, and a sample of unused AC Watercarb 800 PAC from Standard Purification (FL, USA) was provided by a municipality in southern Ontario (Canada), where it is used seasonally for taste and odour control.

± Anatoxin-a fumarate standard (>98% purity) was acquired from Abcam (MA, USA), and HPLC-grade 1,9-diaminononane and formic acid from Sigma–Aldrich (WI, USA). Acetonitrile was of liquid chromatography mass spectrometry (LC-MS) grade. A Millipore Milli-Q® UV PLUS water system (MA, USA) was used to produce ultrapure water. Syringe filters were 0.2 µm polyethersulphone from VWR International (PA, USA).

5 mg of anatoxin-a fumarate was dissolved in 25 mL of high purity water to prepare stock solutions. A 1 mg/mL stock solution of 1,9-diaminononane was prepared using high purity water, and was diluted to a working solution concentration of 50 µg/mL. Stock and working solutions were prepared fresh monthly, and stored in amber vials at -20^{o}C.

4.3.2 Carbon Analysis

4.3.2.1 Pore Volume and Surface Area Determination

The virgin carbons were analyzed by an external lab (Quantachrome Instruments, FL, USA), to determine surface area and porosity.

4.3.2.2 Point of Zero Charge (PZC) Analysis

The pH at which the carbons carry a net-zero surface charge density, or the point of zero charge (pH_{PZC}) was determined as per Summers (1986). A series of Erlenmeyer flasks containing 20 mL of 0.1 M NaCl solution were adjusted to pH values ranging from 2 to 12 using 0.1 M hydrochloric acid or 0.1 M sodium hydroxide. 100 mg of carbon was then added, and the flasks were sealed, placed on orbital shakers at 120 rpm for 24 hours and their equilibrium (final) pH was then measured. The final pH of the solution was plotted against the initial pH, and the pH_{PZC} was determined as the point on the resulting curve where the final and initial pH are equivalent.

4.3.3 Sample Preparation and Handling

The bottle point method was used to investigate the adsorption of anatoxin-a by virgin carbon in Milli-Q® ultrapure water at bench scale, as described in Droste (1997). The GACs were repeatedly washed with ultrapure water to remove fines, dried at 110^{o}C for 24-36 hours, and subsequently stored in desiccators to ensure the dry weight of adsorbent could be measured, following recommendations by Worch (2012) adapted from Sontheimer (1988).

Ultrapure water was collected as a batch and allowed to equilibrate overnight, with no pH adjustment (pH 6.4). Uncrushed carbon was used, and doses ranging from 4 – 50 mg/L GAC and 7 – 16 mg/L PAC were added to 0.5 L samples, each individually spiked with 100 µg/L anatoxin-a. A starting concentration of 100 µg/L was selected as a conservative estimate of potential influent anatoxin-a levels, while remaining within environmentally observed concentrations. 7–9 bottles with different carbon doses were used for each of the 6 carbons. Three positive controls were included to monitor potential toxin degradation, two replicates with a concentration of 100 µg/L, and one with a concentration of 20 µg/L anatoxin-a. Six negative controls (one for each carbon) containing only ultrapure water and 50 mg/L GAC or 16 mg/L PAC, and one blank containing only ultrapure water, were also included to preclude the possibility of any compounds present being misidentified as anatoxin-a. The positive controls with an initial concentration of 100 µg/L remained relatively stable throughout the study, and retained an average concentration of 94 µg/L after 90 days.

All samples and controls were placed on orbital shakers at 150 rpm, under an opaque cover to reduce exposure to light. The sample bottles with the highest carbon doses (50 mg/L for GACs, 16 mg/L for PAC) were monitored regularly by removing a 1 mL aliquot from the bottle to measure the anatoxin-a concentration. Equilibrium was defined as a change in aqueous concentration of less than 1% per day. At equilibrium, the aqueous toxin concentration in each of the sample bottles was determined, and used to generate Freundlich adsorption isotherms. Data points with a final concentration below the reporting limit

of the LC-MS/MS method were not included in isotherm estimation (approximately 5% of the data points).

4.3.4 Anatoxin-a Analysis by LC-MS/MS

Anatoxin-a concentrations were quantified using a Shimadzu 8030 liquid chromatography tandem mass spectrometer (LC-MS/MS) system, composed of a Shimadzu DGU-20A3R degassing unit, a Shimadzu LC-20 ADXR pump with a 100 µL mixing loop, and a Pinnacle DB C18 analytical column (50 mm x 2.1 mm internal diameter, 1.9 µm packing) (Restek, PA, USA), heated to 35^{o}C. An internal standard 1,9-diaminononane at a sample concentration of 2.4 µg/mL, was used as per Bogialli et al. (2006), and a single mobile phase composed of 95% water, 5% acetonitrile and 0.1% formic acid additive was employed, adapted from Oehrle et al. (2010). The flow rate was 0.3 mL/min, with an injection volume of 10 µL. Detection was by multiple reaction monitoring following electrospray ionization. An eight-point linear calibration in the range of 0.5-100 µg/L anatoxin-a was established, using an external standard calibration. Internal standard quantification was used only in the analysis of the equilibrium data, as problems with the stability of the internal standard retention time had not yet been resolved at the time the kinetic data was acquired. No sample preconcentration was required to achieve a method detection limit of 0.65 µg/L, when using the internal standard.

4.4 Results and Discussion

4.4.1 Carbon Properties

Five GACs and one PAC were selected to provide a cross-section of available products for drinking water treatment, representing a range of source materials, porosities, activation methods, and particle sizes (Table 4.1). The two coal-based, steam-activated GACs, F400 and F300, differed predominantly in their effective particle size. Two wood-based, chemically activated GACs, WV B-30 and C-Gran, and one coconut-based carbon with enhanced activation, Aqua Carb CX 1230, were included to round out the portfolio of GACs investigated, and one PAC was also included to provide an indication of the efficacy obtainable with the finer particle-size.

Carbons were not crushed, as it was the goal of this study to produce kinetic data which could be compared with further investigations using preloaded carbons, which cannot be crushed without changing their properties and opening previously inaccessible pores. Furthermore, it was desired to provide a comparison of the carbons in circumstances as close as possible to those found in full-scale GAC contactors, including an examination of the impact of effective particle size. Finally, Worch (2012) notes that grinding of activated carbons to speed the equilibration time can be problematic as isotherms determined with the smaller material may not be exactly equivalent to those of the original product.

4.4.1.1 Porosity and Surface Area

Based on the reported carbon properties, the two coal-based GACs, F400 and F300, have very similar properties, as expected, with only small differences in their Brunauer, Emmett and Teller (BET) surface areas, pore volumes, pore size distribution and micropore percentage. Figures 4.1 and 4.2 further show that F400 and F300 had nearly analogous pore volume distributions. The coal-based PAC also had similar parameters, although its pore volume profile showed some differences in the primary and secondary micropore ranges, with lower PAC pore volumes in both ranges. Likewise, the two wood-based carbons, C-Gran and WV B-30, were similar, although there was greater variability in BET surface area. Figures 4.1 and 4.2 reveal comparable profiles for the wood-based carbons, with larger peaks in the secondary micropore range (0.8 – 2 nm, Rouquerol *et al*., 1994) than those of the coal-based carbons, and the greatest portion of pore volume contained in the mesopores. Interestingly, the coconut-based Aqua Carb shared some properties with both the coal- and wood-based carbons; it had a high BET surface area similar to the wood-based carbons, but its pore volume was much closer to the coal-based carbons. It had the highest micropore volume per gram, both in absolute terms and as a percentage of total pore volume, but very little volume in the mesopore range (Figure 4.2). The molecular dimensions of anatoxin-a were calculated to be 6.07 Å in width and 9.96 Å in length, using the MarvinSketch chemical editor (ChemAxon, Budapest, Hungary). These dimensions indicate that anatoxin-a is on the cusp of the primary micropore size range, and would fit within the 8-20 Å secondary micropore range; depending on

orientation, the primary micropores may still play a role in anatoxin-a adsorption as the shorter dimension (6 Å) is within the 0-8 Å range.

4.4.1.2 pH Point of Zero Charge

Oxygen-containing functional groups on the surface of activated carbons can display either acidic or basic character; at different pH levels, these functional groups can shift between protonated and deprotonated states – as such, the carbon surface charge is pH dependent (Worch, 2012). Carbon surface charges can result in additional interactions (attraction or repulsion) between the adsorbent and ionic adsorbates such as anatoxin-a. At low pH carbons typically have a positive surface charge, and inversely, at high pH, a negative surface charge. The pH_{PZC} indicates the pH at which the carbon has a net zero surface charge, and it can be used to determine the charge of the carbon at pH values employed in this study.

The pH_{PZC} values for the various carbons are also reported in Table 4.1. The two chemically-activated wood-based carbons had the lowest point of zero charge, unsurprising given the use of acid in their production. As expected, the two coal-based GACs and the coal-based PAC all had very similar pH_{PZC} values, and the coconut-based Aqua Carb had the highest point of zero charge, indicating that its surface would be positively charged below pH 10. At pH levels typical of drinking water treatment (approximately 6-8), the virgin coal- and coconut-based carbons have positive surface charges, while the wood-based WV B-30 is negatively charged. The wood-based C-Gran would have a slightly negative or near-neutral surface charge, as its pH_{PZC} is within the stated pH operating range.

Table 4.1: Carbon properties

Product name	Manufacturer	Base material	Activation	Effective size[1] (mm)	pH_{PZC}[2]	BET surface area[3] (m^2/g)	DFT method pore volume[3] (cm^3/g)	DFT pore size distribution[3]			% of pore volume in micropores[3, 4]
								Primary micropores <0.8 nm (cm^3/g)	Secondary micropores 0.8-2 nm (cm^3/g)	Mesopores 2-24 nm (cm^3/g)	
Watercarb 800 PAC	Standard Purification	Coal	Steam	-	9.4	744	0.416	0.15	0.08	0.13	70%
F400	Calgon	Coal	Steam	0.55 – 0.75	9.6	963	0.503	0.21	0.16	0.13	74%
F300	Calgon	Coal	Steam	0.80 – 1.00	9.2	1057	0.551	0.23	0.19	0.14	74%
AquaCarb CX 1230	Siemens (now Evoqua Water Technologies)	Coconut	Enhanced	0.60 – 0.85	10.1	1568	0.672	0.33	0.31	0.08	94%
WV B-30	MWV	Wood	Chemical	0.80 – 1.10	4.6	1565	1.130	0.06	0.33	0.72	35%
C-Gran	Norit	Wood	Chemical	[d_{50} = 1mm]	6.3	1813	1.444	0.12	0.40	0.89	36%

[1] from manufacturer documentation; [2] experimentally determined at the University of Waterloo; [3] experimentally determined at external lab; [4] micropores defined as <2 nm (Rouquerol *et al.*, 1994)
BET – Brunauer–Emmett–Teller adsorption theory
DFT – density functional theory

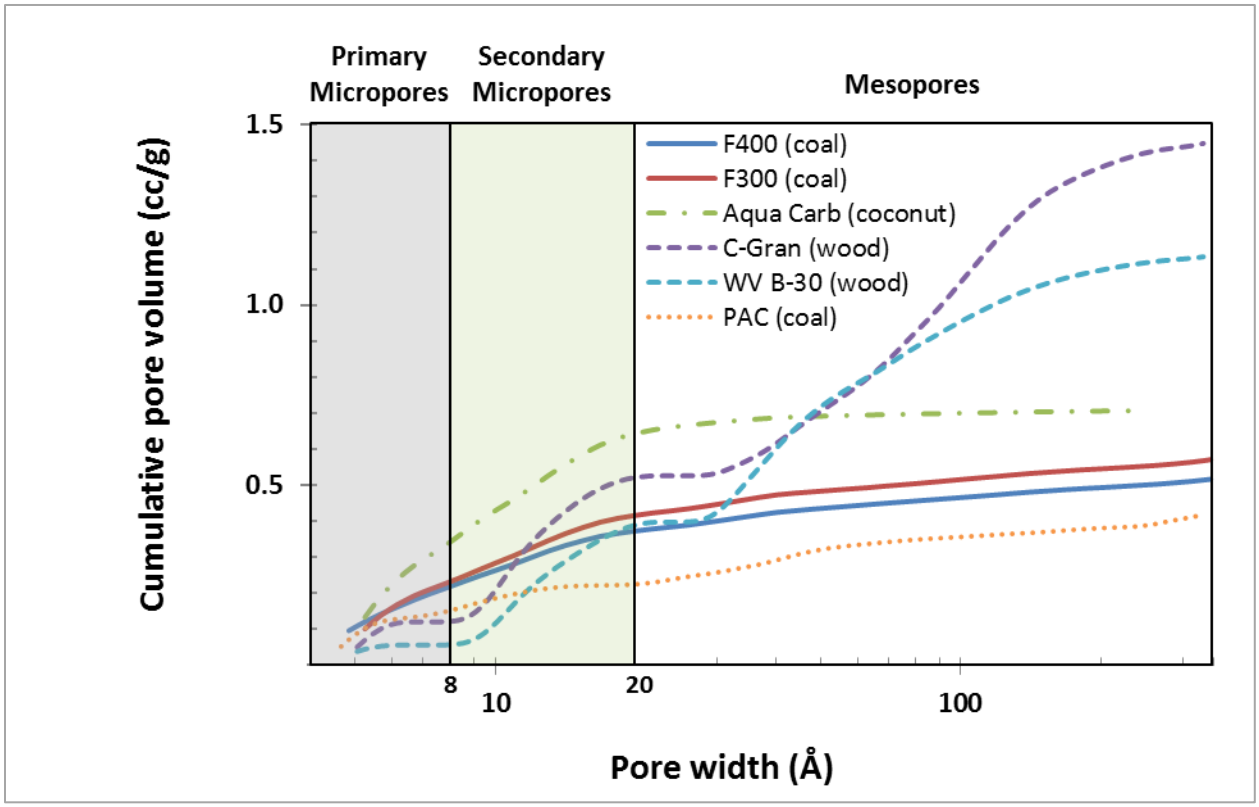

Figure 4.1: Cumulative pore area with increasing pore width, for the 6 carbons investigated

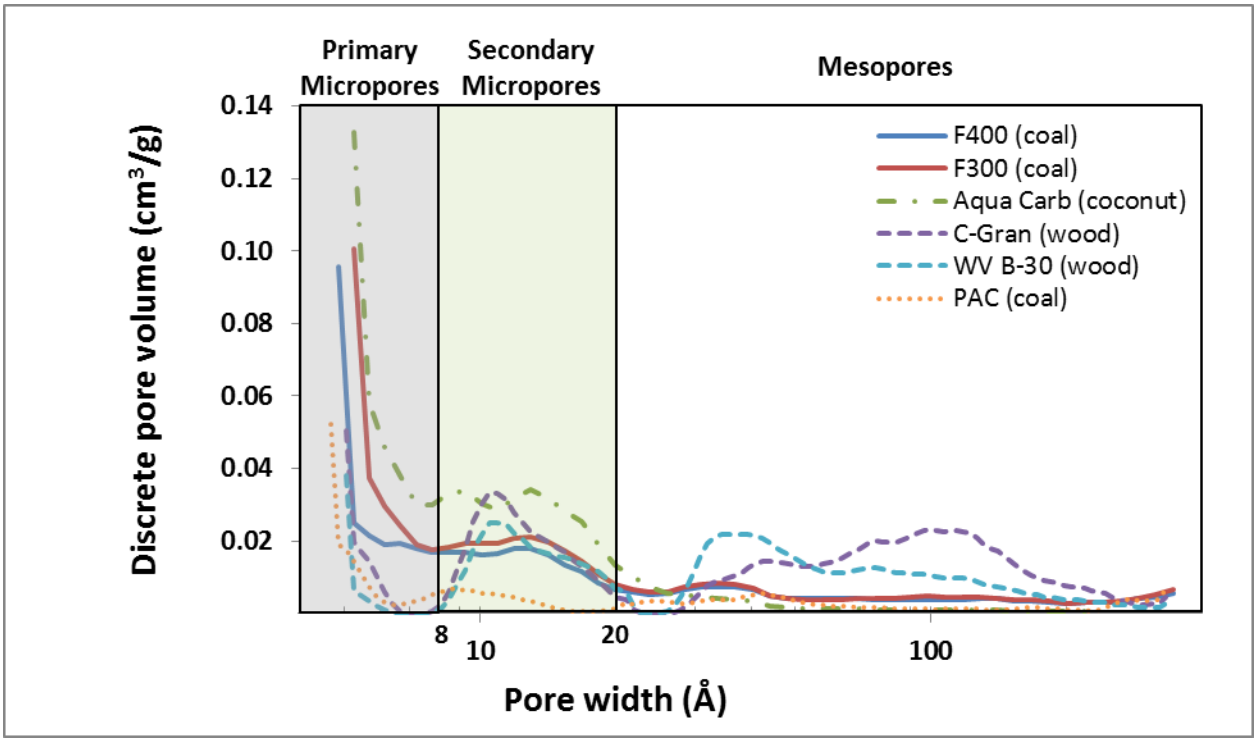

Figure 4.2: Pore volume represented at a range of pore widths, for the 6 carbons investigated

4.4.2 Kinetics

The results of kinetic studies on the adsorption of anatoxin-a in ultrapure water using the six carbons are presented in Figure 4.3. Over the 90-day period of the study, all six carbons appeared to achieve near-complete removal of the toxin, although this occurred at markedly different rates. Within the first hour of the study, the PAC vastly outpaced the GACs, as expected, though it should be noted that this process was examined using a batch system, which differs significantly from a flow-through contactor and may favour PAC over GAC adsorption. In a slurry system, such as that used in this study, pore (or intraparticle) diffusion may dominate the kinetics as the rate of film diffusion is increased by the rapid stirring, and particle size will impact the pore diffusion as a result of the shorter diffusion paths (mainly impacting the macro- and mesopores) (Worch, 2012).

The five GACs began to show differentiable rates of removal within the first twelve hours (Figure 4.3a). The two wood-based carbons had the fastest toxin removal of the GACs, and both performed very similarly, achieving equilibrium within 14 days (Figure 4.3b). This can be partially attributed to the higher proportion of mesopores in the wood-based carbons (0.7 – 0.9 cm^3/g) as compared to the coal- and coconut-based carbons (0.08-0.14 cm^3/g) (Table 4.1), providing easier transport to the adsorption sites. The rates of toxin adsorption by the two coal-based carbons were also quite close, with the smaller effective particle size of the F400 resulting in slightly faster toxin removal than the larger F300. A plot of toxin removal over time was normalized by the average effective particle size of each GAC (calculated as the average of the effective size range reported in Table 4.1), to compare kinetic behaviour on the basis of material rather alone (Figure 4.4). The observed trends for virgin carbon in ultrapure water remain unchanged when the effect of particle size can be neglected, with wood-based GACs adsorbing anatoxin-a more rapidly than coconut-based GAC, which in turn is a faster adsorber than the coal-based GACs.

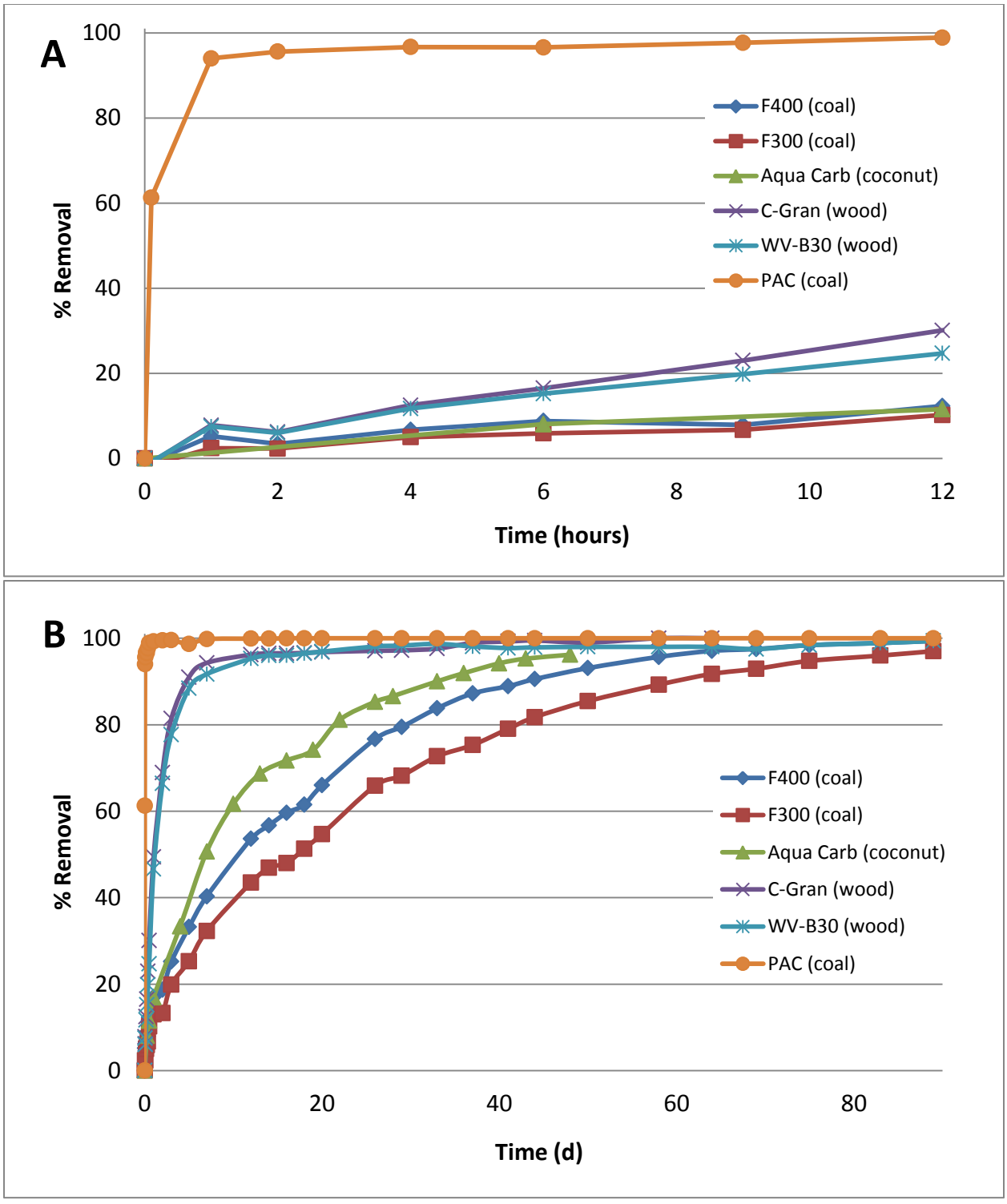

Figure 4.3: Anatoxin adsorption as a function of time; 100 µg/L initial anatoxin-a concentration, 50 mg/L adsorbent dose. A) 12 hour exposure; B) 90 day exposure

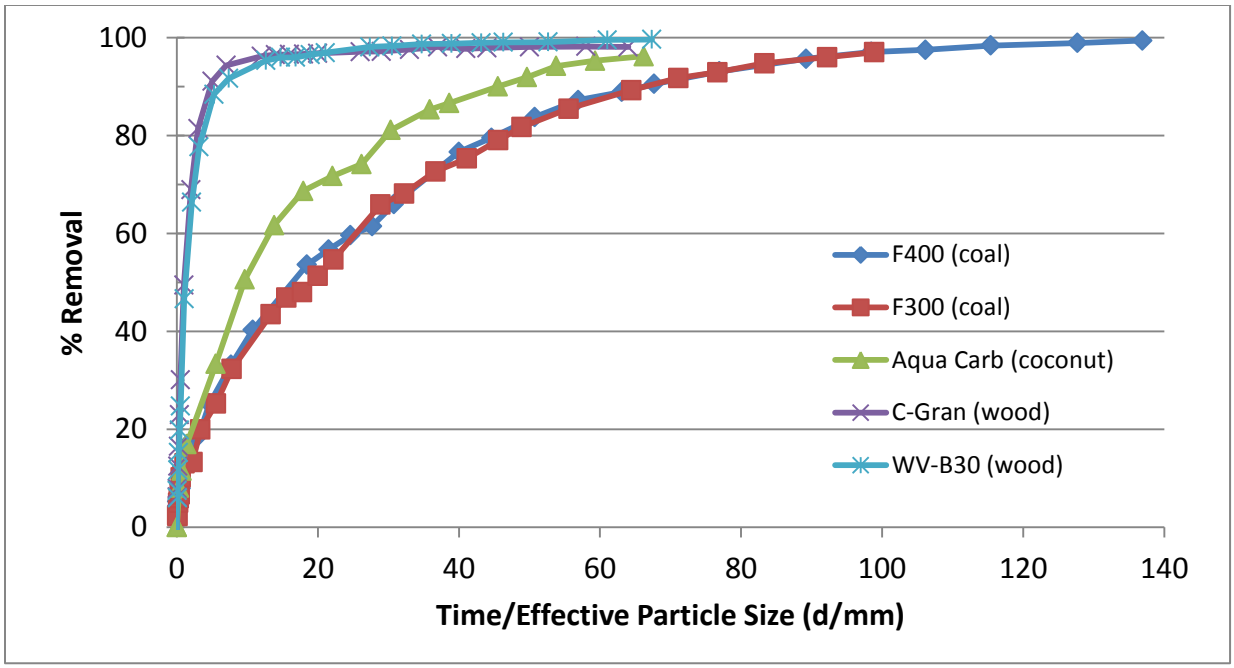

Figure 4.4: GAC removal kinetics, normalized by average effective particle size

The lower pH_{PZC} of the wood-based carbons may also contribute to their faster kinetics – at the pH of the ultrapure water (6.4), anatoxin-a (pKa = 9.4) exists predominantly in its protonated, positively-charged state, and the wood-based carbons are negatively charged or very close to neutral as previously noted; conversely, the coal- and coconut-based carbons are positively charged, producing the potential for repulsive interactions that may slow transport to adsorption sites.

A pseudo-second order model has previously been used to describe the kinetics of activated carbon adsorption of a wide range of compounds (Ho & McKay, 1999). While this type of adsorption model is effectively empirical (Worch, 2012), it can provide useful kinetic descriptors for comparatively evaluating different carbons. As per Ho and McKay (1999), the rate of adsorption in a batch process can be modeled as:

$$\frac{dq_t}{dt} = k_2(q_e - q_t)^2 \quad \text{.....(3)}$$

where t is the number of days elapsed, q_t (µg/mg) is the amount of solute adsorbed at time t, k_2 is the rate constant of adsorption and q_e is the total amount of solute adsorbed at equilibrium.

Equation 3 can be integrated over time (t) and amount adsorbed (q_t) to yield:

$$q_t = \frac{q_e^2 k_2 t}{(1+q_e k_2 t)} \quad \text{.....(4)}$$

which can be rearranged into a linear form as follows:

$$\frac{t}{q_t} = \frac{1}{k_2 {q_e}^2} + \frac{1}{q_e} t \quad \text{.....(5)}$$

The kinetic data are plotted in this form (Figure 4.5) and exhibit excellent linearity for all datasets; furthermore, the model fits all result in R^2 values greater than 0.99, indicating the pseudo-second order model described the data well. It should be noted that although the R^2 values are high, there appear to be systematic errors underlying the fit for many of the carbons (i.e. analysis of the residuals does not bear out the assumption that they are randomly distributed – there is a systematic trend to the residuals) indicating that the underlying mechanism implied by the pseudo-second order model is not completely representative of the adsorption system as observed in this study. Nevertheless, it is possible to use the parameters of this model to provide a good approximate description which can be used to compare the kinetic behaviour of the different carbons in adsorbing anatoxin-a.

The pseudo-second order model was fitted to the kinetic data for each carbon using an iterative non-linear least squares method, and the model parameter values are shown in Table 4.2.

An expression of the initial adsorption rate, ϑ (µg/mg/day) can be also be determined using the pseudo-second order model, providing a numeric indicator of performance at low contact times. This parameter can be calculated according to Equation 5:

$$\vartheta = k_2 {q_e}^2 \quad \text{.....(6)}$$

The experimentally determined q_e values were calculated using Equation 4:

$$q_e(experimental) = \frac{C_o - C_e}{m/V} \quad \text{.....(7)}$$

Where C_o is the initial anatoxin-a concentration (µg/L), C_e is the liquid-phase concentration at equilibrium (µg/L), and m/V is the carbon dose (mg/L).

Based on the initial adsorption rate (ϑ) (Table 4.2), the PAC dramatically outperformed all of the GACs by 2 – 3 orders of magnitude, at 751 µg/mg/day. Among the five GACs, the wood-based carbons were the fastest by an order of magnitude with initial rates of 2.00 µg/mg/day (C-Gran) and 1.72 µg/mg/day (WV B-30). Of the two coal-based carbons, F400 outperformed the larger F300 (0.17 vs. 0.11 µg/mg/day respectively), while the coconut-based Aqua Carb slightly outperformed them both at 0.26 µg/mg/day.

The experimental and modeled q_e values were quite similar, and all have values near 2 µg/mg. While the modeled q_e estimates were higher than the experimentally determined q_e values, this could be attributed to a slight overdosing of carbon relative to the anatoxin-a concentration (as previously noted, all carbons achieved nearly complete removal of 100 µg/L anatoxin-a with a carbon dose of 50 mg/L).

A pseudo-first order model was also fitted to the kinetic data, to determine which model was most appropriate (refer to Appendix B); the R^2 values for the pseudo-first order model were lower or very similar to those of the pseudo-second order model, while the predicted q_e deviated further from the experimentally determined values, indicating that the pseudo-second order model better described the observed data. As such, only this model was used to compare adsorption kinetics for the various carbons investigated.

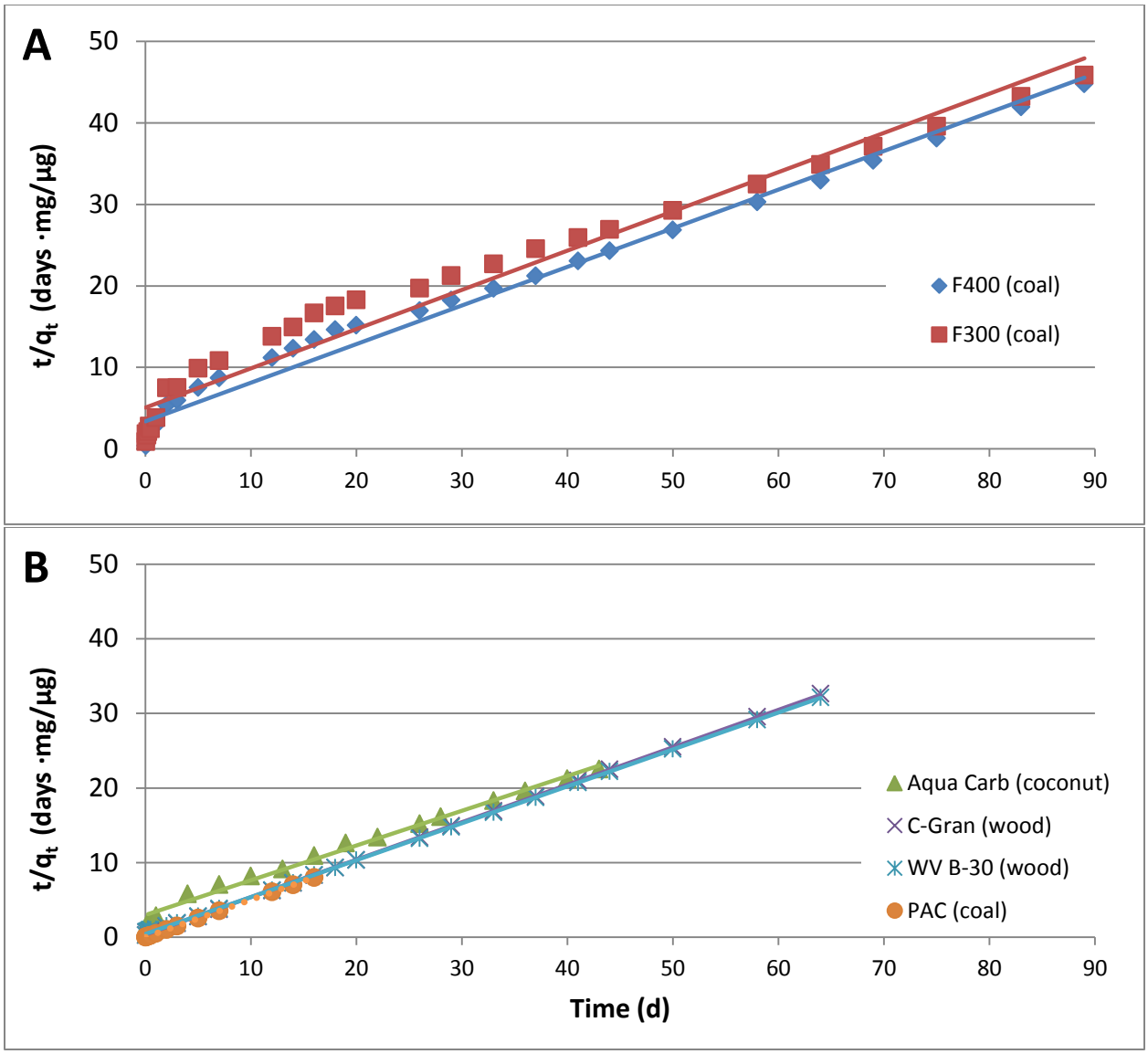

Figure 4.5: Pseudo-second order kinetic model fits using virgin carbon in ultrapure water. A) F400 and F300, B) Aqua Carb, C-Gran, WV B-30 and PAC.

Table 4.2: Pseudo-second order kinetic model parameters for virgin carbon in ultrapure water

Carbon	Equilibrium Carbon Capacity, q_e experimental (µg/mg)	Equilibrium Carbon Capacity, q_e predicted (µg/mg)	k_2 (mg/µg/day)	ϑ (µg/mg/day)	R^2
F400	1.99	2.31	0.033	0.17	0.99
F300	1.99	2.42	0.019	0.11	0.99
Aqua Carb	1.91	2.27	0.051	0.26	1.00
C-Gran	1.96	2.04	0.481	2.00	1.00
WV B-30	1.99	2.06	0.404	1.72	1.00
PAC	2.00	2.00	186	751	1.00

4.4.3 Isotherms

4.4.3.1 Freundlich parameter determination

Worch (2012) noted that knowledge of equilibrium adsorption data is necessary for selecting suitable adsorbents; in this study, six carbons were investigated in parallel, to provide a direct comparison between the available adsorbents. The Freundlich model (Equation 2) was applied to the equilibrium data obtained using the bottle point technique, for each carbon in ultrapure water, as shown in Figures 4.6 – 4.10. The model parameters and confidence intervals summarized in Table 4.3 were determined using non-linear least squares regression, as advised by both Crittenden et al. (2012) and Worch (2012), as certain assumptions made in linear regression, including that errors are normally, identically and independently distributed about zero, may not hold following transformation of the data to a linear form.

The adsorption coefficient (K_F), is an indicator of the achievable carbon loading – higher K_F values imply greater capacity if all other terms are equal (Crittenden et al., 2012). The 1/n value is indicative of the dependence of a carbon's capacity on the aqueous phase adsorbate concentration – i.e., the curvature of the isotherm (or the slope, on a log-log plot). All other terms being equal, a low 1/n value would indicate greater capacity at low aqueous adsorbate concentration, with little increase in capacity associated with an

increase in the aqueous phase adsorbate concentration. Conversely, a high 1/n value would signify lower capacity at low aqueous adsorbate concentrations, with a large capacity increase corresponding to increases in the aqueous adsorbate concentration.

Again, the PAC was the best-performing carbon, with a K_F value several times greater than those of the GACs (Table 4.3). Of the GACs, the two coal-based carbons had the highest K_F values, while the two wood-based carbons had the lowest K_F values. The 1/n value was quite low for the PAC (0.07), and comparable for the wood- and coal-based carbons (0.4-0.6), with the coconut-based Aqua Carb having the lowest 1/n of the GACs (0.28). In the case of the F300 isotherm, one aberrant data point may be an outlier (identified in Figure 4.6); while this data point cannot be excluded on the basis of any experimental consideration, it is anomalous when considered alongside the other data. An analysis of isotherm parameters both with and without this outlier is provided, and it can be seen that by removing the outlier the goodness of fit (R^2) for the non-linear regression increases by 9%. More compellingly, the F300 adsorption coefficient (K_F) draws closer to that of the F400 isotherm; it was anticipated that the isotherms of these two carbons would be nearly equivalent, as the differing particle size is be expected to have a greater impact on the kinetics of adsorption than the equilibrium capacity.

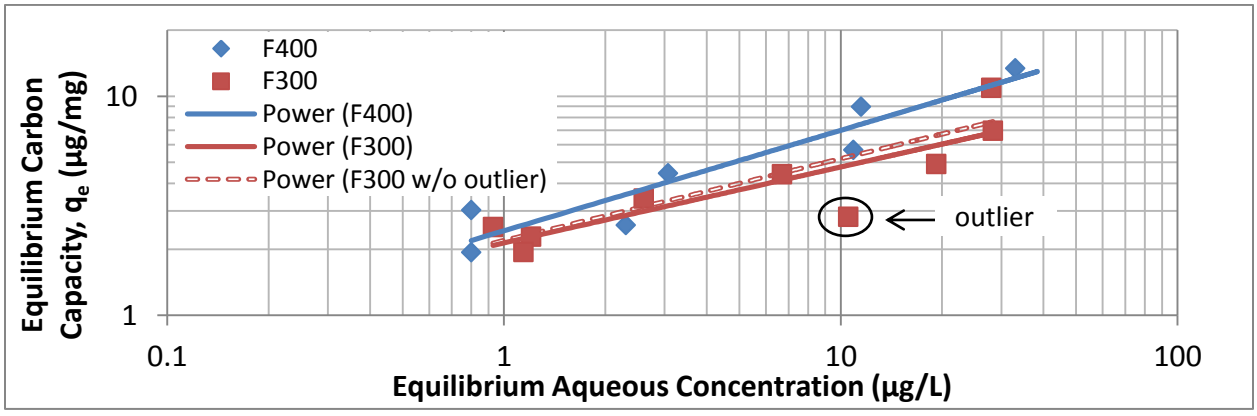

Figure 4.6: Anatoxin-a Freundlich isotherms for virgin F400 and F300 (coal-based) GACs in ultrapure water

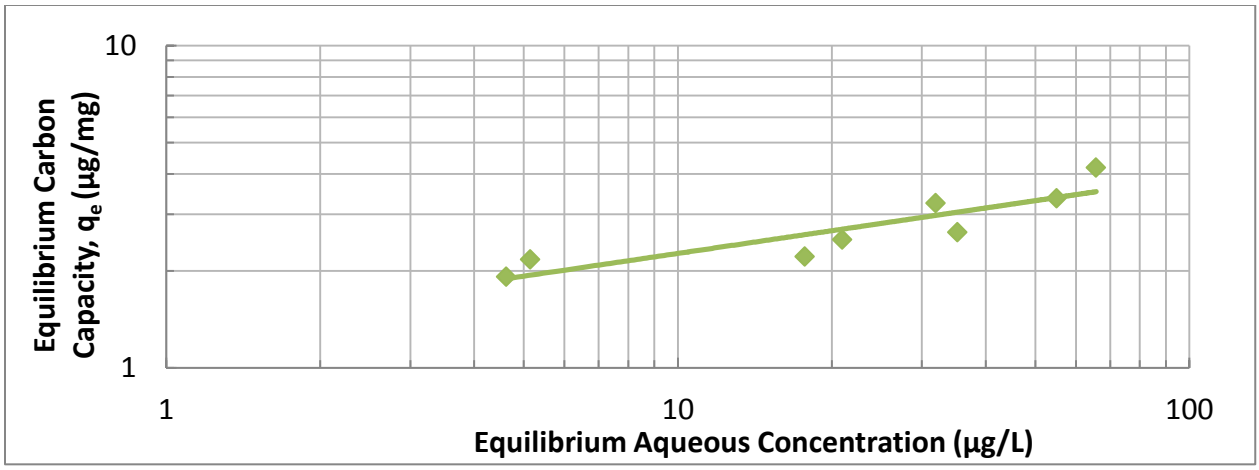

Figure 4.7: Anatoxin-a Freundlich isotherm, for virgin Aqua Carb (coconut-based) GAC in ultrapure water

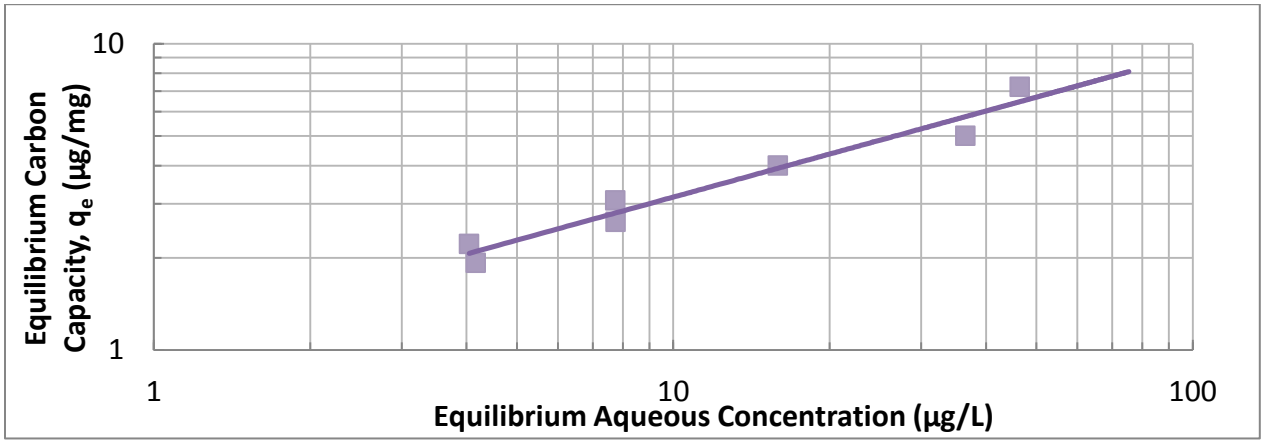

Figure 4.8: Anatoxin-a Freundlich isotherm, for virgin C-Gran (wood-based) GAC in ultrapure water

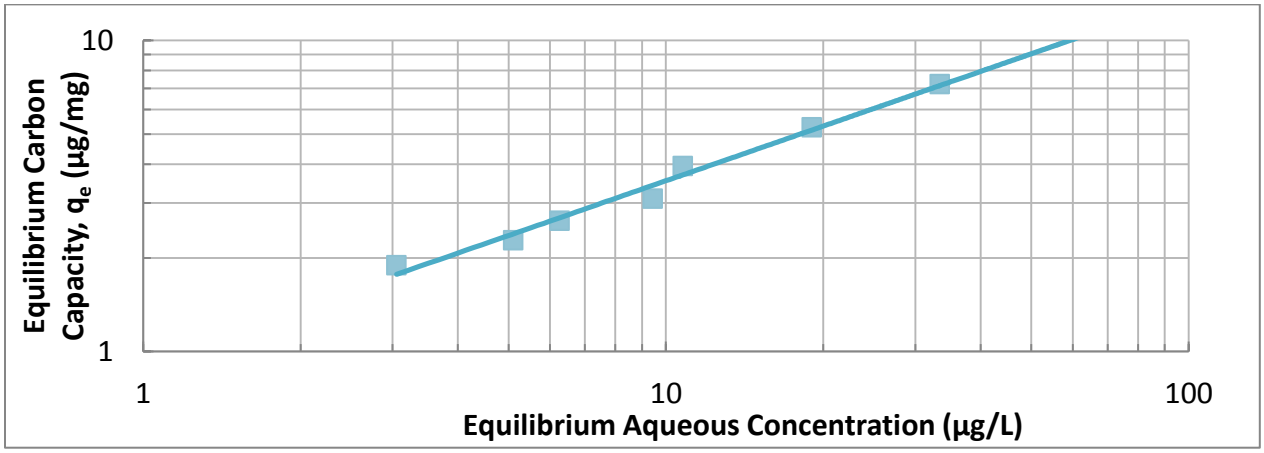

Figure 4.9: Anatoxin-a Freundlich isotherm, for virgin WV B-30 (wood-based) GAC in ultrapure water

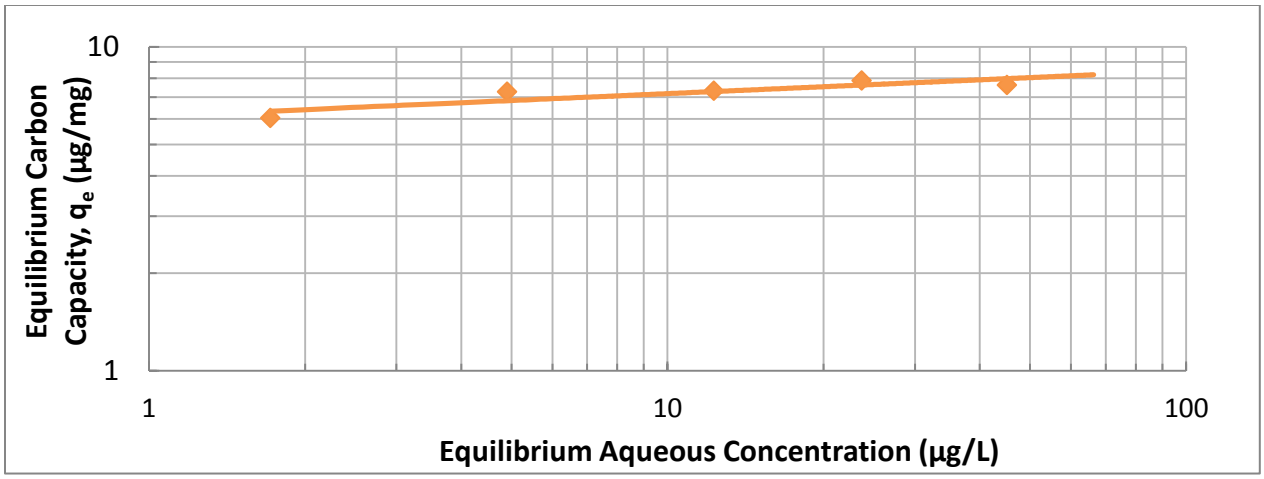

Figure 4.10: Anatoxin-a Freundlich isotherm, for virgin PAC (coal-based) in ultrapure water

Table 4.3: Freundlich isotherm parameters for virgin carbon in ultrapure water

Carbon		K_f (µg/mg) (µg/L)$^{-1/n}$	1/n	R^2
F400	N = 7	2.19 *(1.00 – 3.38)*	0.51 *(0.33 – 0.70)*	0.94
F300	N = 9	1.78 *(0.33 – 3.23)*	0.43 *(0.16 – 0.71)*	0.74
F300 w/o outlier	N = 8	2.08 *(0.71 -3.46)*	0.40 *(0.17 – 0.52)*	0.83
Aqua Carb	N = 8	1.15 *(0.52 – 1.78)*	0.28 *(0.12 – 0.43)*	0.78
C-Gran	N = 7	1.04 *(0.51 – 1.56)*	0.48 *(0.33 – 0.64)*	0.94
WV B-30	N = 7	0.89 *(0.71 – 1.07)*	0.60 *(0.58 – 0.66)*	0.99
PAC	N = 5	6.17 *(4.90 – 7.44)*	0.07 *(0– 0.14)*	0.74

(95% confidence interval)
N – number of data points

Figure 4.11and Table 4.4 provide a comparison of anatoxin-a adsorption capacities at different aqueous anatoxin-a concentrations. At 1 µg/L aqueous anatoxin-a the carbon loadings (q_e) are equal to the adsorption coefficients (K_F), wherein WV B-30 has the lowest carbon loading and PAC has the highest. Evaluating the isotherms at 5 µg/L anatoxin-a, the order of the carbons in terms of carbon loading changes slightly, with Aqua Carb having the lowest q_e (1.8 µg/mg), while PAC maintains the highest

loading (6.9 µg/mg), while at 20 µg/L anatoxin-a aqueous concentration the F400 GAC overtakes the PAC with a q_e of 10.2 µg/mg. As can be seen, the aqueous adsorbate concentration can be a critical factor in selecting the optimal carbon, due to the different 1/n values of the Freundlich isotherms.

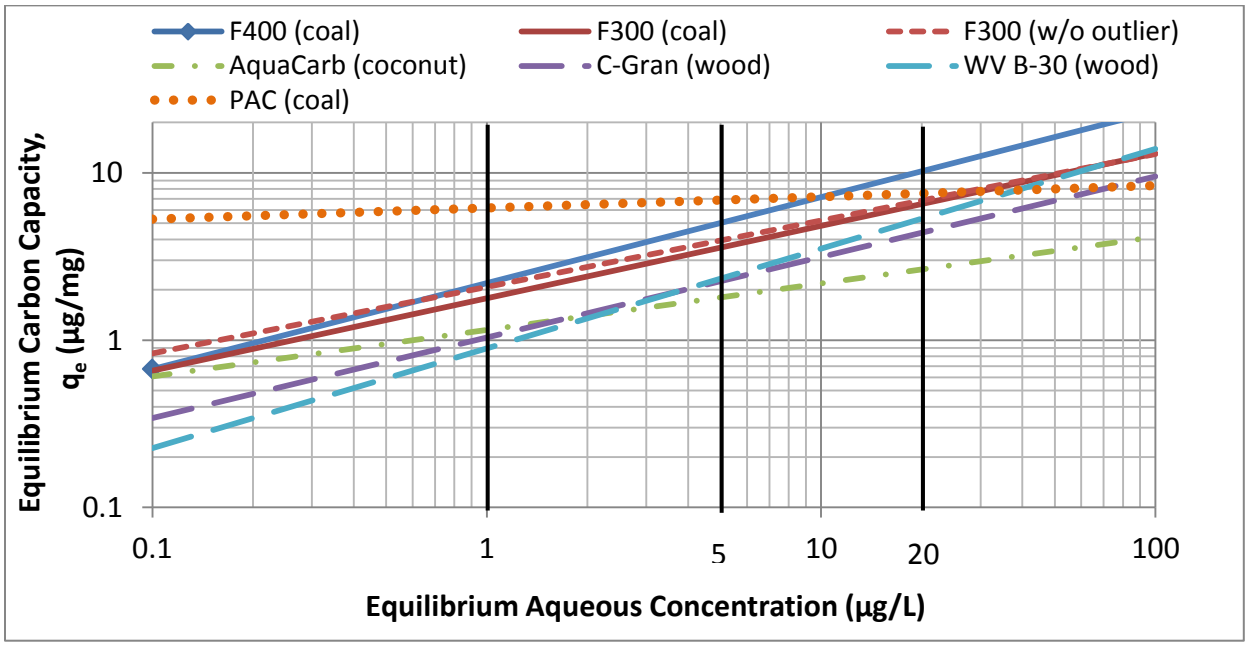

Figure 4.11: Anatoxin-a Freundlich isotherms for six carbons investigated

Table 4.4: Comparison of anatoxin-a adsorption capacities for the carbons evaluated at different aqueous concentrations

Carbon	C = 1 µg/L	C = 5 µg/L	C = 20 µg/L
F400	2.2	5.0	10.2
F300	1.8	3.6	6.5
F300 w/o outlier	2.1	3.9	6.8
Aqua Carb	1.2	1.8	2.6
C-Gran	1.0	2.2	4.4
WV B-30	0.9	2.3	5.3
PAC	6.2	6.9	7.5

Adsorption capacity, q_e unit = µg(anatoxin-a)/mg(carbon)

Based on the best-fit Freundlich adsorption coefficient values, the more microporous coal- and coconut-based carbons appear to have a greater capacity than the more meso- and macroporous wood-based carbons, particularly at low concentrations. However, an examination of the 95% confidence intervals for K_F (Figure 4.12) indicates that while the GACs had a range of best-fit values, at the 95% confidence level they cannot be concluded to be significantly different. The K_F value for F400 can be said to be different from the coconut- and wood-based carbons with 80% confidence (refer to Appendix C), however given the increased scatter in the F300 data, its K_F value can only be said to be different from those of the wood-based carbons at a 60% confidence level. An examination of the GAC data pooled by carbon source material indicates a difference between coal- and wood-based carbons at a 70% confidence level, though neither source material could be differentiated from the coconut-based carbon at that confidence level.

A similar picture is presented for 1/n (Figure 4.13), although for that parameter, WV B-30 (wood-based) and the coconut-based Aqua Carb appear to be statistically different with 95% confidence. The PAC isotherm had a much lower 1/n value than those of the GAC isotherms; this is indicative of relatively high capacity at low aqueous anatoxin-a concentrations, with little capacity increase at higher aqueous concentrations. Analogously, the aqueous concentration is the mass transfer driving force in the equilibrium between aqueous and adsorbed toxin: with a low 1/n value, an increase in this driving force does not result in a large effect on the adsorbed toxin capacity. Theoretically, 1/n can be greater than or equal to 1; however, values of less than 1 are typical, and are considered “favourable” as they show relatively high carbon loading capacity at low concentrations (Crittenden et al., 2012). All Freundlich equations determined in this study had a 1/n value of less than 1, and as such are all termed favourable isotherms.

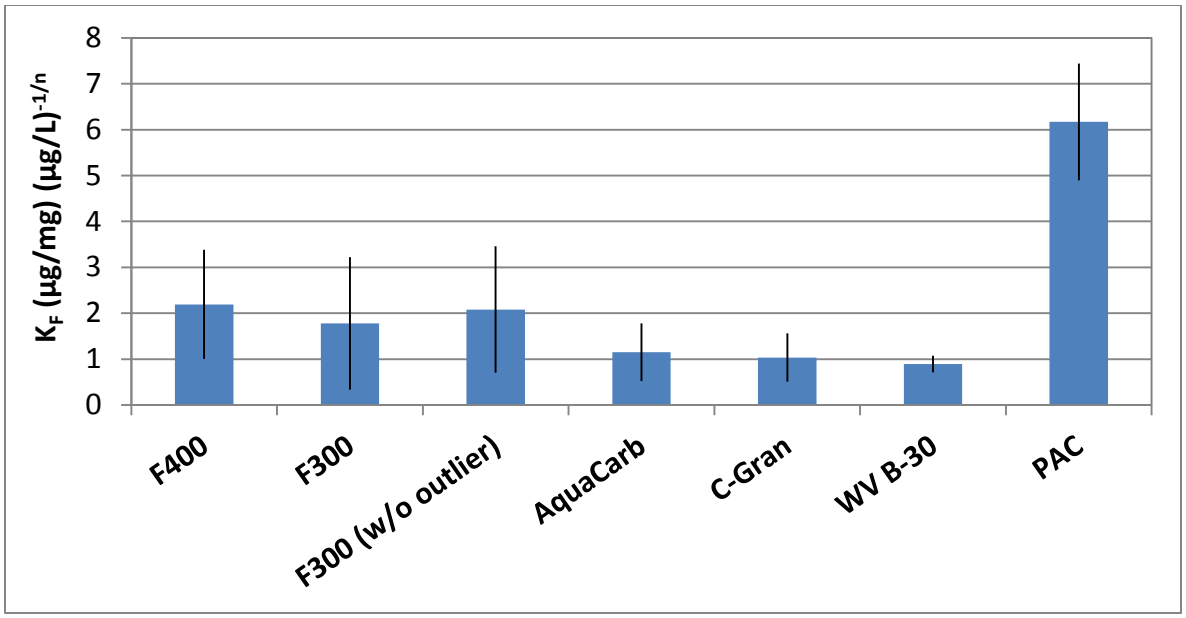

Figure 4.12: Freundlich adsorption coefficient (K_F) non-linear fit with 95% confidence intervals

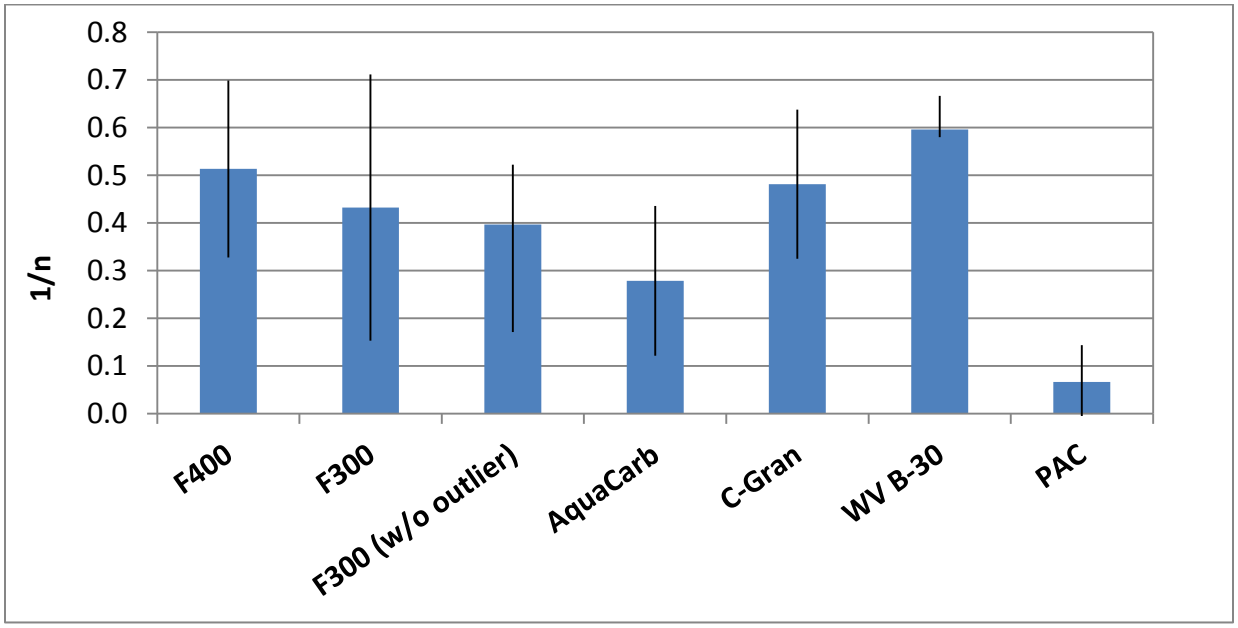

Figure 4.13: Freundlich model parameter (1/n) non-linear fit with 95% confidence intervals

4.4.3.2 Freundlich Parameter Joint Confidence Regions

Because of the mathematical structure of the Freundlich equation, the two parameters (K_F and 1/n, Equation 2), are closely linked – estimates of one parameter directly impact the possible values of the second parameter, therefore confidence intervals for individual parameters may not provide a complete

picture of the range of model fits implied by the data. Joint confidence regions (JCRs) for K_f and 1/n were calculated for each carbon at a 95% confidence level, and are shown in Figure 4.14, demonstrating the high level of correlation between the two parameters. Details of the calculation are provided in Appendix C. While the JCRs for the PAC isotherm parameters and the Aqua Carb isotherm parameters are distinct from those of the other carbons, those of coal-based F400 and F300 overlap, and the F300 joint confidence region also overlaps with those of the two wood-based carbons C Gran and WV B-30. Thus caution should be exercised in comparing the parameter estimates for F300 with those of F400 or the two wood-based carbons.

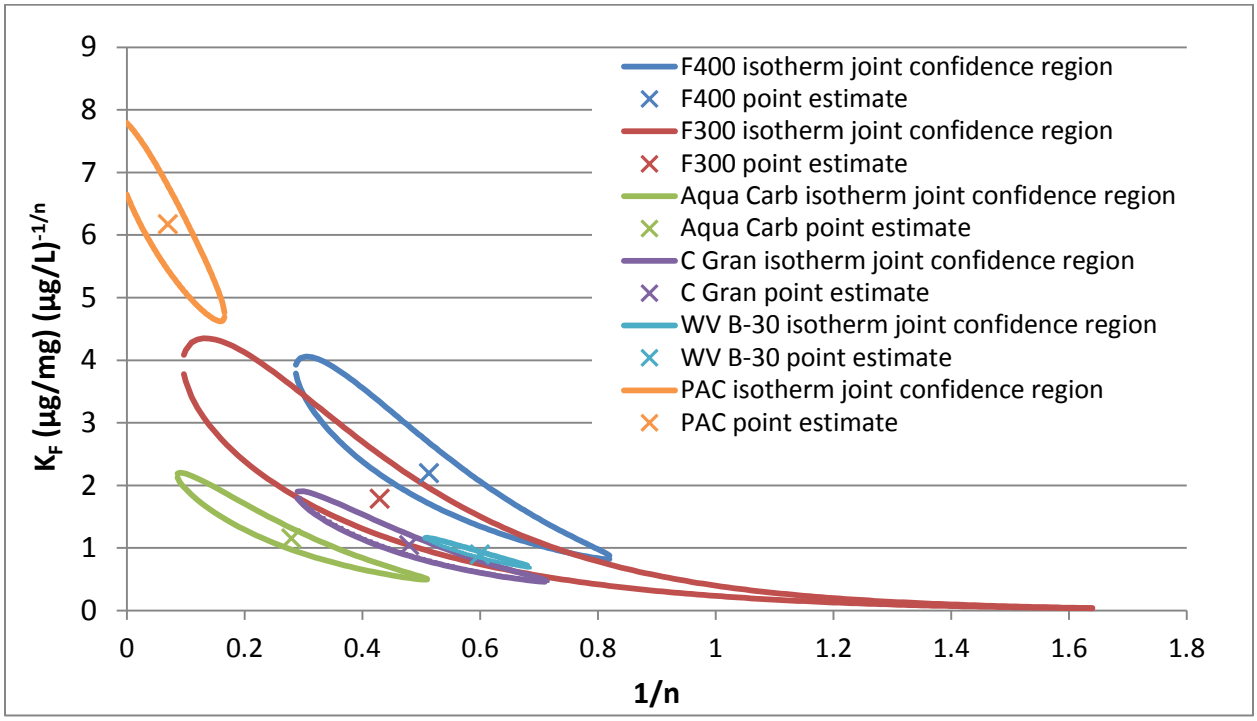

Figure 4.14: 95% joint confidence regions and point estimates for the Freundlich parameters of isotherms generated with virgin carbon in ultrapure water

4.4.3.3 Comparison with literature values

No previously-determined isotherm data exist in the literature for anatoxin-a adsorption. As such, anatoxin-a adsorption isotherms were compared to literature values for microcontaminants acquired under similar conditions (virgin carbon in ultrapure water), to provide a measure of relative adsorbability.

Figure 4.15 presents the F400 and F300 anatoxin-a isotherms determined in this study alongside Freundlich isotherms obtained using F400 (Pirbazari et al., 1993) and F200 (Chen, Dussert, & Suffet, 1997) for two cyanobacterial taste and odour compounds, geosmin and MIB. F400 is commonly used in drinking water treatment applications and is therefore frequently included as a benchmark in adsorption studies, while F200 is a similar coal-based product from Calgon Carbon, which has similar effective particle size (0.55 – 0.75 mm) to F400.

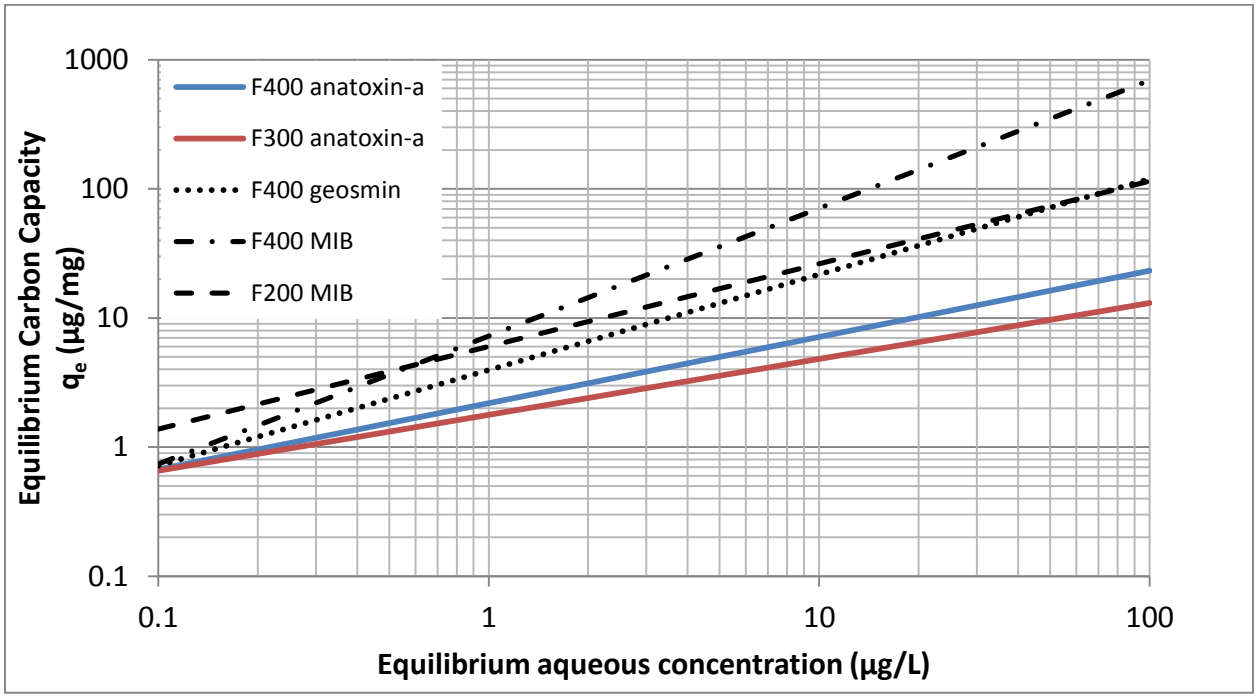

Figure 4.15: Comparison of Freundlich isotherms for anatoxin-a, MIB and geosmin by virgin coal-based carbons in ultrapure water. Anatoxin-a isotherms are based on data from the current study, while MIB and geosmin isotherms were drawn based on Freundlich parameters obtained from the literature (F400 geosmin & MIB from Pirbazari et al. (1993); F200 MIB from Chen, Dussert, & Suffet (1997)).

As noted by Vlad et al. (2014), anatoxin-a (MW = 165 Da) is a much smaller molecule than other common cyanotoxins such as microcystin (995 Da) and cylindrospermopsin (415 Da), and is in fact much closer in size to geosmin (182 Da) and 2-methylisoborneol (MIB, 168 Da). These microcontaminants are also produced by cyanobacteria, and can co-occur with cyanotoxins including anatoxin-a (Graham et al., 2010). It should be noted that as geosmin and MIB are typically detected at sub-microgram per liter

levels, their isotherms were determined in lower concentration ranges (0.01 – 1 µg/L (Pirbazari et al., 1993) and 0.001 – 0.1 µg/L (Chen, Dussert, & Suffet, 1997), respectively) and the resulting Freundlich equations were extrapolated to allow comparison with those determined for anatoxin-a. While MIB and geosmin are not charged molecules, they are quite close to anatoxin-a in size, as all three compounds have a molecular weight between 165 and 182 Daltons.

Based on Figure 4.15, anatoxin-a is less well adsorbed than either MIB or geosmin by virgin, coal-based carbon in ultrapure water. The F400 and F200 MIB isotherms have similar K_F values (as would be expected), with the F400 adsorption coefficient slightly greater than the F200 coefficient, and the 1/n value of the F400 isotherm is greater than that of the F200 isotherm. At an aqueous contaminant concentration of 1 µg/L, F400 carbon has nearly twice the capacity for geosmin (4.0 µg/mg) and over three times the capacity for MIB (7.3 µg/mg), as for anatoxin-a (2.2 µg/mg).

4.4.4 Equilibrium Column Model

A chief consideration in the application of GAC via fixed-bed adsorbers is the time to breakthrough or operational life of the carbon. Unlike batch reactors, fixed-bed flow-through absorbers do not experience a decline in the mass transfer driving force over time, as they are continually exposed to the influent aqueous adsorbate concentration. In a fixed-bed adsorber, the adsorbate solution passes through three zones: a spent-carbon zone (already at a carbon loading in equilibrium with the inlet concentration), a mass transfer zone (where adsorption takes place with adsorbate concentration declining as depth increases), and finally a fresh-carbon zone, which has not yet been exposed to the adsorbate. As such, fixed-bed adsorbers assure near-complete removal of the adsorbate prior to breakthrough, when the mass transfer zone reaches the bottom of the adsorber. Once the mass-transfer zone reaches the bottom and progresses out of the adsorber bed, increasing concentrations of adsorbate are left unadsorbed, and the effluent concentration increases until the adsorption capacity is completely exhausted; this produces the typical ‘S’ shaped breakthrough curve (Crittenden, 2012).

The equilibrium column model (ECM) is a simplified breakthrough curve prediction model. It uses only the single-solute Freundlich isotherms of the solution components as inputs, assuming instantaneous equilibrium and neglecting kinetic considerations. These simplifications assume that the mass transfer zone is of negligible depth – that there is no resistance to mass transfer and minimal dispersion. The ECM is therefore limited to predicting ideal breakthrough curves as concentration steps, neglecting the 'S' shape of typical breakthrough curves (Worch, 2012). These are major simplifications, the consequences of which are discussed below, alongside the implications of the model results. Despite these limitations, the ECM can be useful in approximating the maximum service life of a theoretical adsorber as a preliminary design calculation (Hand et al., 1997). In a single-solute system, the model produces calculations similar to the "carbon usage rate," with the total volume of water treated prior to breakthrough calculated as:

$$V = \frac{q_i m_A}{C_i} \quad \text{(8)}$$

where C_i is the influent adsorbate concentration, q_i is the carbon loading in equilibrium with the influent concentration, and m_A is the mass of adsorbent in use. Applying the Freundlich equation to obtain q_i yields:

$$V = \frac{K_F C_i^{1/n} m_A}{C_i} \quad \text{(9)}$$

The approximate treated volumes to breakthrough were calculated for all GACs, assuming an influent anatoxin-a concentration of 2 µg/L and a carbon mass of 1000 kg (one metric tonne), and ranged from 675 to 1564 million litres (Figure 4.16). In this setup, F400 and F300 were the best performing, treating nearly twice the volume of the coconut and wood-based carbons.

While the ECM can be extended to include multisolute systems, it was applied as a single-solute analysis in this case. As this implies no other compounds are present to compete with anatoxin-a for adsorption sites, it should be noted that the service life predicted will be an approximate maximum, and would

decline in the presence of NOM. It should be further noted that in non-idealized systems, slower adsorption kinetics result in a wider S-curve at breakthrough; the ECM more closely approximates rapid adsorption scenarios, where the assumption of instantaneous equilibrium is less severely violated. Initial breakthrough would be expected to occur earlier than predicted for all carbons, but particularly for those with slower adsorption. In kinetic studies the coal-based F400 and F300 carbons were the slowest to reach equilibrium and as such the ECM breakthrough prediction is especially suspect in their case.

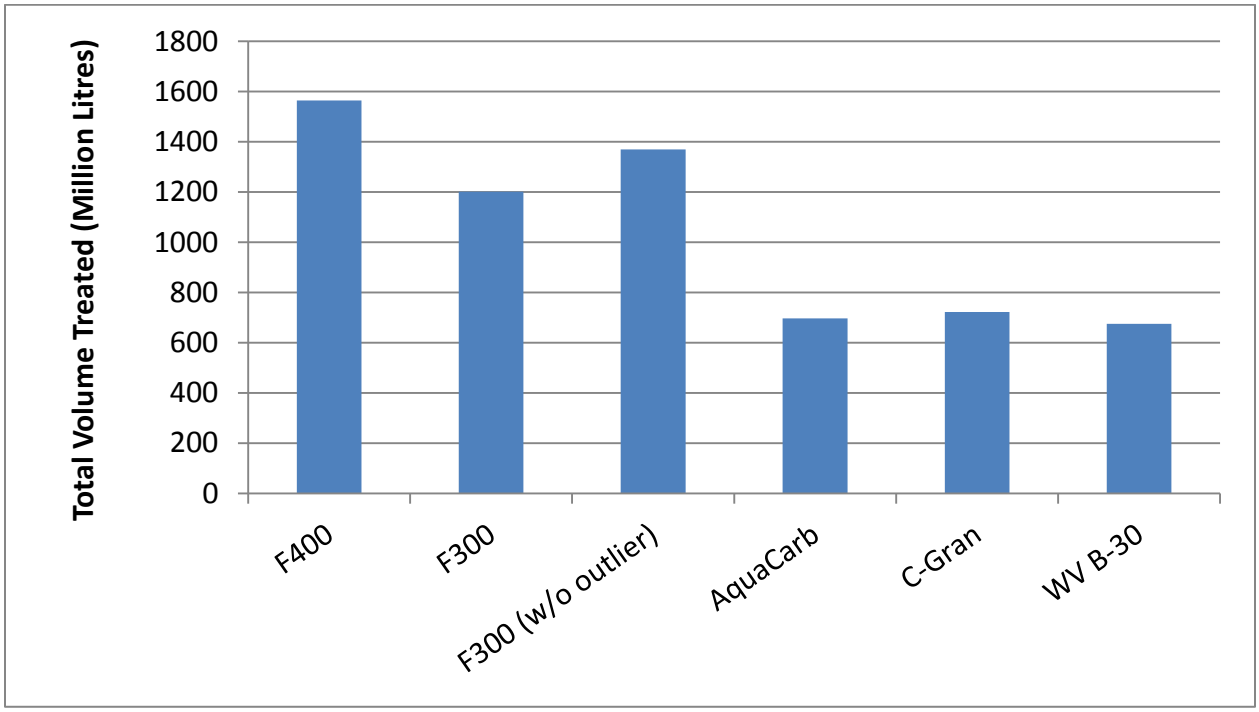

Figure 4.16: ECM predicted total treated volume to breakthrough, for 1,000 kg of GAC in a single-solute system with an influent anatoxin-a concentration of 2 µg/L

4.5 Conclusions

The adsorption of anatoxin-a by five GACs and one PAC in virgin state was examined using the bottle point technique. In both kinetics and capacity, the PAC, as expected, outperformed all of the GACs in ultrapure water batch experiments. It delivered a significant increase in the Freundlich isotherm adsorption coefficient, K_F, over all of the GACs at a 95% confidence level, and had an initial adsorption rate 2–3 orders of magnitude greater than those of the GACs. However, as noted by Vlad et al. (2014),

there are stringent limitations to the applicability of PAC for the removal of dissolved, extracellular anatoxin-a, as intact cells containing the toxin may shield it from PAC adsorption, allowing it to bypass this treatment process. As PAC is typically applied at the front end of a drinking water treatment train, it is possible that intact cells entering the plant would later be lysed through oxidation or cell accumulation and aging within the plant, thereby releasing the contained toxin.

In terms of influence of the adsorbent properties on the kinetics, clear trends were discernable once kinetics data normalized over particle size were used. While all five GACs investigated were able to adsorb anatoxin-a, the wood-based C-Gran and WV B-30 carbons most quickly adsorbed the toxin, likely due to their high surface area, more meso- and macroporous structure and interactions between the positively-charged anatoxin-a and the slightly negative or nearly neutral carbon surface charges at the operating pH. Conversely, these carbons appeared to have the lowest overall capacity at the concentrations investigated, although their isotherms could only be said to be statistically different from those of F400 and Aqua Carb at a 95% confidence level, based on the joint confidence regions.

The coal-based F400 and F300 GACs removed anatoxin-a at the slowest rate, with a discernible impact from the different effective particle sizes, while the coconut-based Aqua Carb adsorbed anatoxin-a faster than the coal-based and slower than the wood-based carbons. The slower adsorption of the F400, F300 and Aqua Carb carbons may be partly attributed to their microporous structure and positive carbon surface charge at the operating pH resulting in repulsive interactions with the positively-charged anatoxin-a. The coal-based carbons demonstrated the highest capacity of the GACs investigated, although at a 95% confidence level only the F400 isotherm could be distinguished from the isotherms of the wood- and coconut-based GACs, as the F300 joint parameter space overlapped with those of the wood-based carbons.

Using the ECM, the coal-based GACs were predicted to achieve nearly double the total treatment volume of the wood- and coconut-based carbons prior to breakthrough, under single-solute conditions; however, the ECM estimates a maximum value for carbon usage rate, and the true treatment volume to

breakthrough would be expected to be much less. Furthermore, these values must be interpreted with the understanding that preloading, NOM competition, and kinetic parameters were not taken into consideration.

Chapter 5
Adsorption of Anatoxin-a by Preloaded Carbon in Ultrapure Water

5.1 Summary

Exposure to background organic material in water results in preloading of granular activated carbons, and can impact the capacity and kinetics of adsorption by those carbons. Five GACs were preloaded in parallel with approximately 40,000 bed volumes of settled water at a surface water treatment plant. The adsorption of anatoxin-a in ultrapure water by the five preloaded GACs was investigated using the bottle point technique. Unsurprisingly, preloading impacted the surface properties of the carbons, and resulted in changes to adsorption kinetics as well as reduced capacity at equilibrium. Unexpectedly, the coal-based F400 and F300 carbons adsorbed the toxin much more rapidly once preloaded than in their virgin states, but the wood-based C Gran and WV B-30 GACs still had the fastest kinetics of the preloaded carbons. At lower toxin concentrations, the coal-based preloaded carbons (F400 and F300) retained the greatest equilibrium capacity (1.2 µg/mg at 1 µg/L aqueous anatoxin-a), with the coconut-based carbon capacity being slightly less at 1.0 µg/mg at 1 µg/L aqueous anatoxin-a, and the wood-based carbons having the lowest capacity (0.6 µg/mg at 1 µg/L aqueous anatoxin-a). However, at equilibrium concentrations greater than 20 µg/L anatoxin-a, the wood-based carbons had greater toxin capacity than all other preloaded carbons. Further consideration should be given to NOM competition for adsorption sites when treating surface water, to determine the potential impacts on kinetics and carbon capacity.

5.2 Introduction

Activated carbons can be effective in removing a wide range of microcontaminants in drinking water, and previous investigations have shown adsorption to be a viable technology for removal of the cyanobacterial neurotoxin, anatoxin-a. The exposure of activated carbons to natural organic material (NOM) prior to a cyanobacterial event may reduce the capacity of a carbon for anatoxin-a, both directly by occupying appropriate adsorption sites and indirectly by blocking access to still-available sites in

obstructed pores (Newcombe et al. 2002; Yu et al. 2009; Crittenden et al. 2012). Further, preloading can change surface properties of activated carbons, notably the surface charge, significantly impacting the removal of charged adsorbates (de Ridder et al. 2011). The degree to which the adsorption kinetics and capacity of a carbon are impacted by preloading depends on the nature of the preloading (the duration, contact time, and water quality), the target adsorbate, and activated carbon type (Crittenden et al. 2012). However, to date, the effects of carbon preloading for anatoxin-a adsorption have not been studied.

The objective of this study was to evaluate the impact of preloading on activated carbons used for the adsorption of anatoxin-a. Five GACs – Calgon F400, Calgon F300, Seimens Aqua Carb CX, Norit C Gran and MWV WV B-30 – were preloaded in parallel using post-sedimentation water at a Southern Ontario surface water treatment plan. An additional sample of preloaded F300 carbon was obtained from a GAC contactor at a full-scale surface water treatment plant, which had been in use for approximately 100,000 bed volumes. The kinetic properties and capacities of the preloaded GACs were investigated in batch experiments with ultrapure water, to provide complementary data sets comparable to those produced in prior investigations using virgin carbon in ultrapure water, which described adsorption of anatoxin-a under ideal conditions.

5.3 Materials and Methods

5.3.1 Materials

Virgin carbons and HPLC-grade chemicals were obtained as noted in Section 4.3.1. A sample of F300 carbon from a full-scale GAC contactor in use for approximately 3 years (approximately 100,000 bed volumes) was obtained from a southern-Ontario utility treating lake water.

5.3.2 Carbon Preloading

Virgin carbons prepared as per Section 4.3.3 were preloaded with natural organic material (NOM) in a pilot setup at the Mannheim Water Treatment Plant in the Region of Waterloo, Ontario, which uses the Grand River as a source. As shown in Figures 1 and 2, post-sedimentation water from the full-scale

treatment train was first filtered via a pair of 5 cm internal diameter pre-columns, operating in parallel, with a bed composition of 5 cm gravel, 10 cm sand, and 10 cm anthracite. The pre-columns were necessary to remove floc from the post-sedimentation water prior to GAC treatment. The flow was then split among five up-flow GAC contactors with internal diameters of 2.5 cm and 15 cm bed depth. A 12 m/h hydraulic loading rate was targeted, and the pre-columns were backwashed as necessary to maintain flow in the preloading system, approximately once every 24 hours. The total organic carbon (TOC) of the influent (after the pre-column filtration) and of the effluent from each GAC contactor was monitored 5 times over the course of 21 days (approximately 40,000 bed volumes) from late-August to mid-September 2014. The preloaded carbons were freeze-dried over 72 hours and stored in a desiccator prior to use.

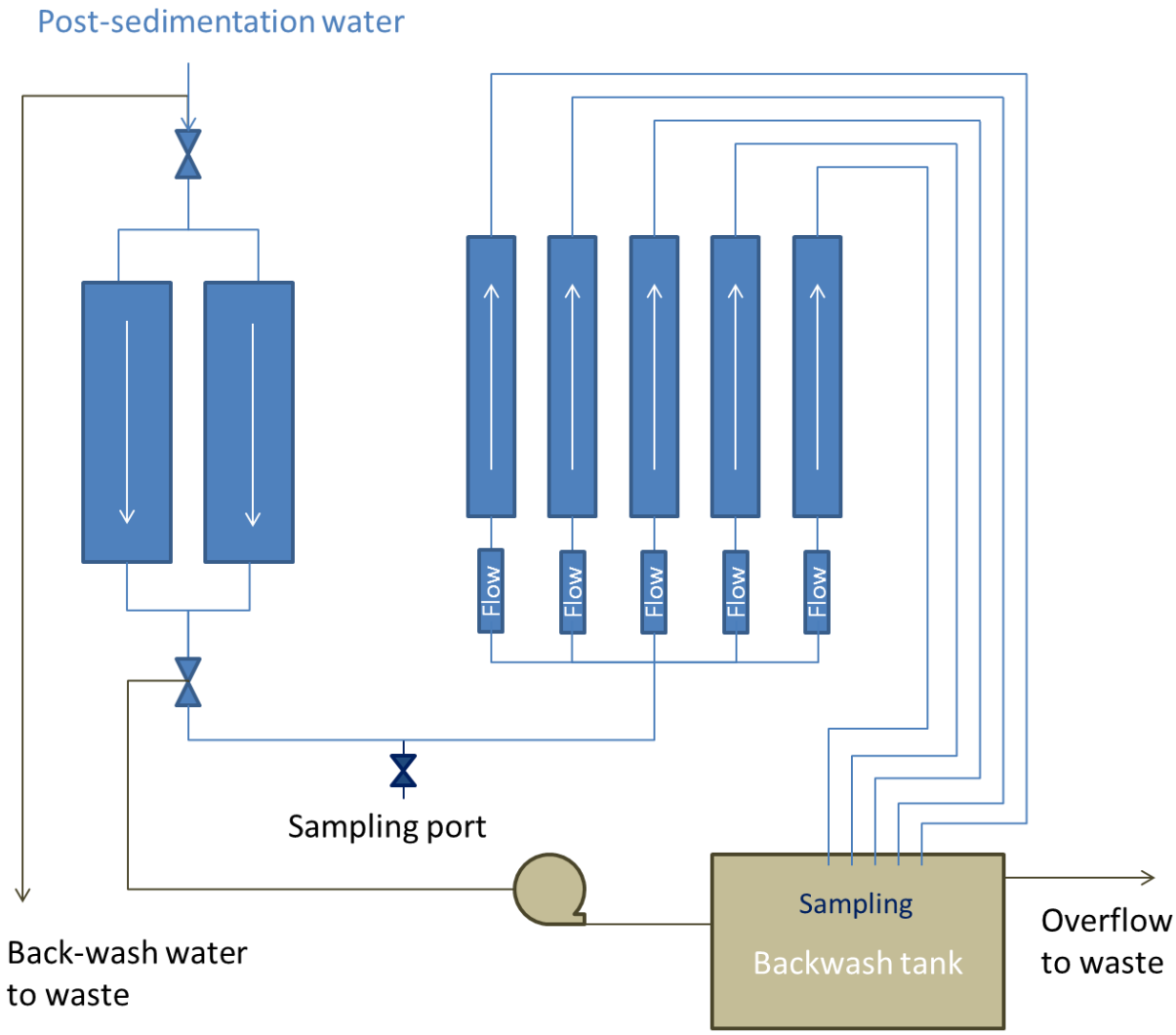

Figure 5.1: GAC preloading design

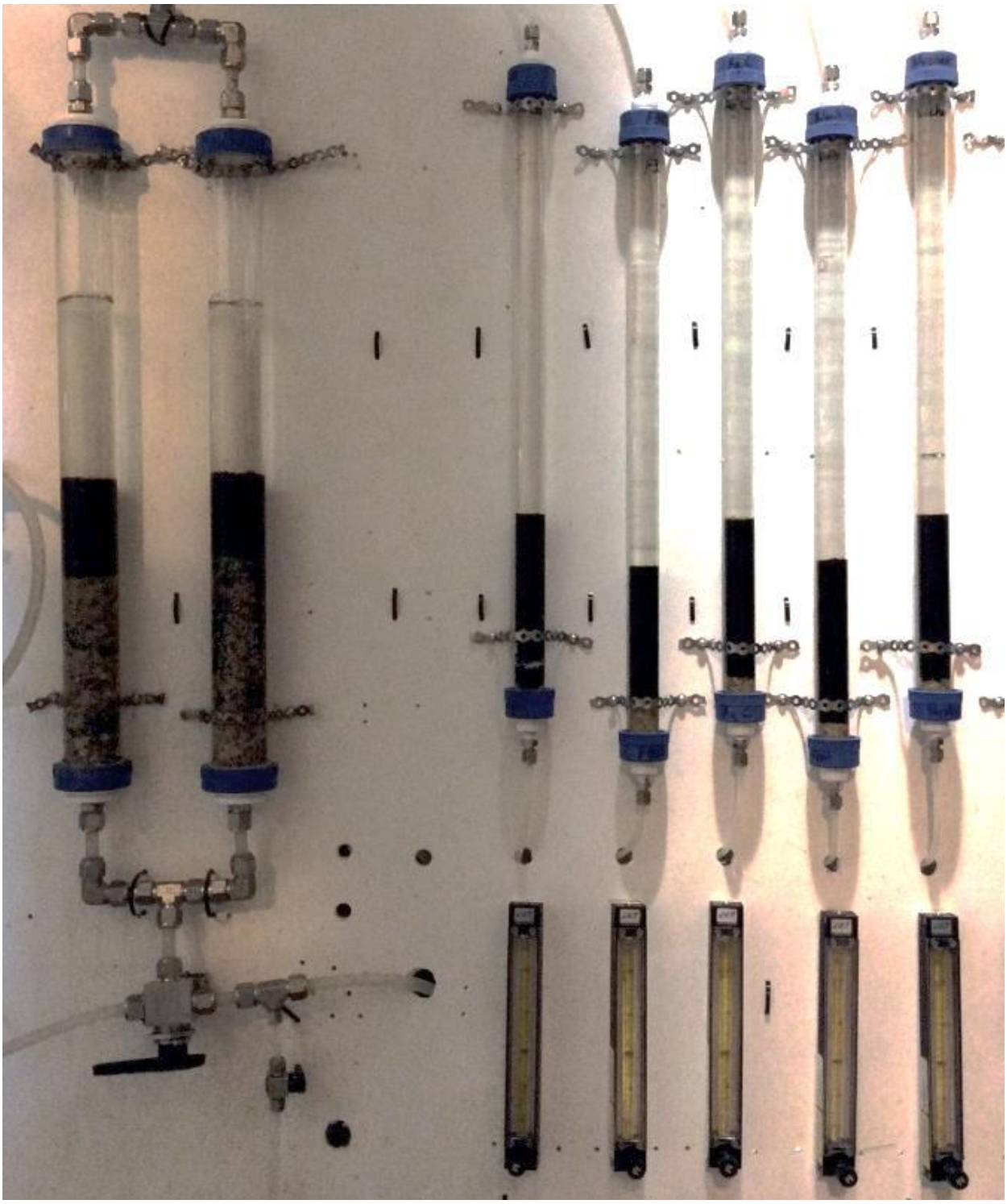

Figure 5.2: GAC preloading setup

5.3.3 Sample Preparation and Handling

Anatoxin-a adsorption by the preloaded carbons in ultrapure water (pH 6.3) was investigated via the bottle point method, as described in Section 4.3.3. For each carbon preloaded as part of this study, 8 x 500-mL glass bottles with carbon doses ranging from 4 – 50 mg/L were used, while for the utility-preloaded F300 carbon sample, 3 bottles were used with doses in the 4 – 25 mg/L range. Three positive controls were included with only ultrapure water and spiked anatoxin-a – two at the 100 µg/L anatoxin-a concentration and one at a 20 µg/L concentration. Six negative controls with only ultrapure water and the preloaded carbons were included, one for each carbon, at a 50 mg/L dose. One blank was also included containing only ultrapure water. A 500 mL volume was used for all samples and controls. The anatoxin-a concentration in the bottles which contained the carbon dose for each carbon, as well as each of the controls, was monitored at intervals throughout the experiment by removing a 1 mL aliquot to measure the toxin concentration. Equilibrium was defined as a change in aqueous concentration of less than 1% per day. The two positive controls with an initial concentration of 100 µg/L anatoxin-a remained relatively stable throughout the study, and retained an average concentration of 97.5 µg/L after 43 days.

5.3.4 Anatoxin-a Analysis by LC-MS/MS

Analysis of aqueous anatoxin-a concentration was conducted using the LC-MS/MS instrumentation and methodology detailed in Section 4.3.4. 1,9-diaminononane was employed as an internal standard in the acquisition of both the kinetic and equilibrium data.

5.4 Results and Discussion

5.4.1 Carbon Preloading

Total organic carbon (TOC) content was monitored during preloading, both at the influent to the 5 GAC contactors (following the two pre-filtration columns) and at the effluent of each contactor. As shown in Figure 5.3, breakthrough of the background organics began within 3 days for all of the carbons, although the two wood-based carbons (C Gran and WV B-30) had a greater breakthrough concentration after 3 days than the coal- or coconut-based carbons (F400, F300, and Aqua Carb) . After 21 days, or

approximately 40,000 bed volumes treated, all five carbons had nearly complete breakthrough of TOC, and were taken out of service.

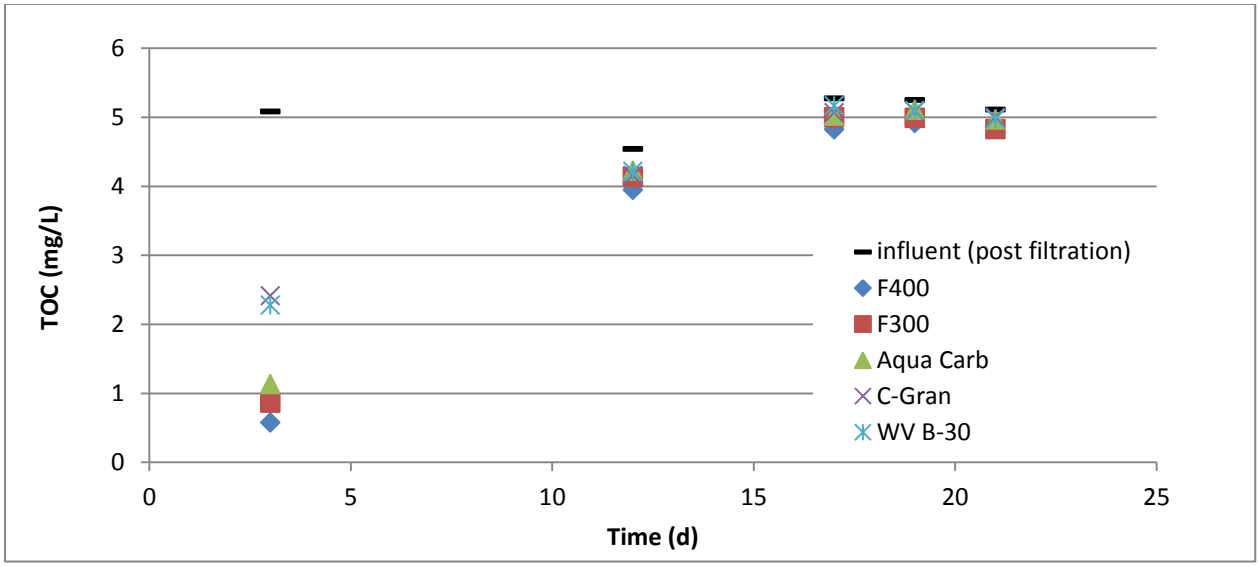

Figure 5.3: TOC of influent and effluents for the five GAC contactors used for preloading

The point of zero charge (pH_{PZC}) of each preloaded carbon was then determined to provide an indication of surface charge. While the virgin carbons showed a range of values – the wood-based carbons having pH_{PZC} values below 7, with the coal- and coconut-based carbons above 9 – the exposure to natural water and preloading with NOM resulted in converging surface properties (Table 5.1). All of the preloaded carbons had pH_{PZC} values in the 6.9-7.2 range, indicating that the adsorption of NOM (major components of which are typically negatively charged at neutral pH) altered the carbon characteristics; similar effects have been observed for membranes after fouling – while internal heterogeneity is retained, the fouling layer governs most surface properties (Makdissy et al. 2010).

Table 5.1: Point of zero charge for virgin vs. preloaded GACs

Carbon	pH_{PZC}	
	Virgin	Preloaded
F400	9.6	7.2
F300	9.2	7.2
Aqua Carb	10.1	7.1
C Gran	4.6	7.1
WV B-30	6.3	6.9

5.4.2 Kinetics

Figure 5.4 shows the results of the kinetic investigations of anatoxin-a adsorption by preloaded GACs in ultrapure water, using a batch system. Similarly to the virgin carbon ultrapure water results, the wood-based C Gran and WV B-30 carbons achieved equilibrium most rapidly, although the smaller of the preloaded coal-based carbons, F400, reached equilibrium before the preloaded coconut-based Aqua Carb (unlike the virgin carbons). Again, F400 adsorbed anatoxin-a faster than F300 due to its smaller particle size; Figure 5.5 presents the kinetic data normalized by the average effective particle size shown in Table 5.2. The difference between the F400 and F300 was minimized and the remaining difference in the normalized kinetics implies that preloading impaired the rapid access to adsorption sites more extensively for the larger F300 grains than for F400.

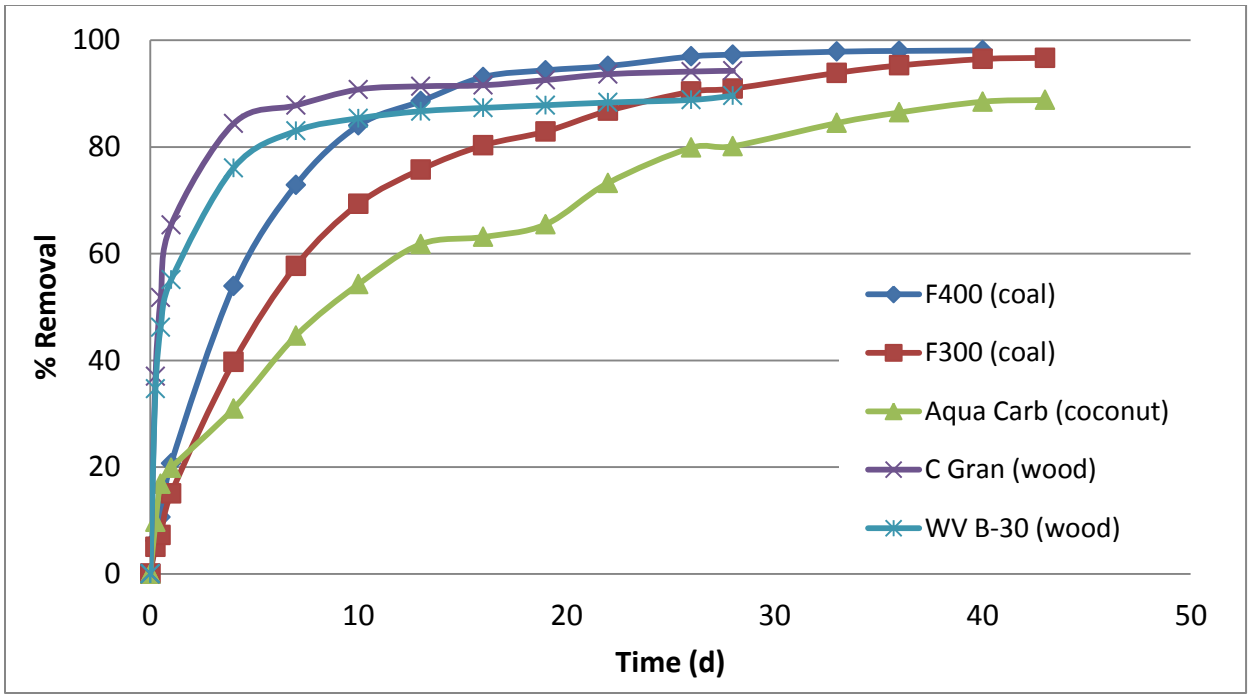

Figure 5.4: Anatoxin adsorption by preloaded carbons as a function of time; 100 µg/L initial anatoxin-a concentration, 50 mg/L GAC dose

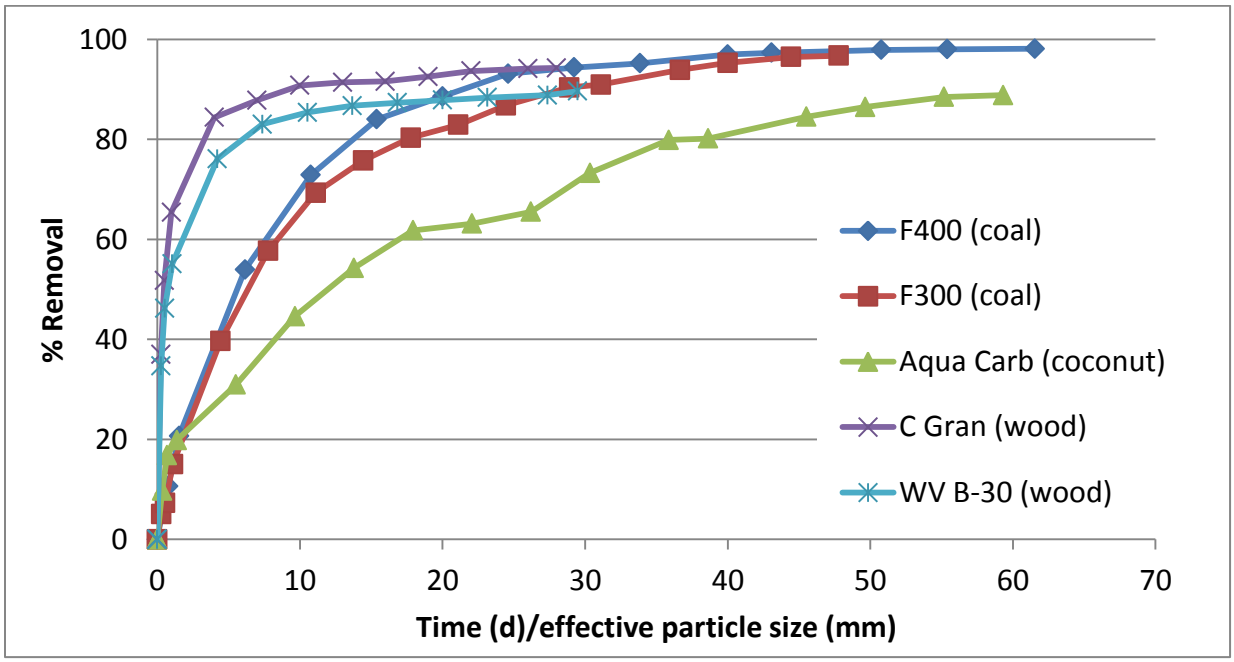

Figure 5.5: GAC removal kinetics, normalized by average effective particle size

Table 5.2: Average effective particle sizes for the GACs based on manufacturer documentation

Carbon	Average Effective Particle Size (mm)
F400	0.65
F300	0.90
Aqua Carb	0.73
C Gran	1.00
WV B-30	0.95

Interestingly, in a direct comparison of the kinetics of anatoxin-a adsorption by preloaded and virgin GACs in ultrapure water (as shown in Figures 5.6 – 5.10), the preloaded coal-based carbons (F400, Figure 5.6 and F300, Figure 5.7) reach equilibrium faster than their virgin counterparts (albeit with lower equilibrium capacity). The change in pH_{PZC} offers one possible explanation: at pH 6.3, the virgin carbons (pH_{PZC} > 9) have a more strongly positive surface charge than the preloaded carbons (pH_{PZC} = 7.2), resulting in greater electrostatic repulsion of the cationic anatoxin-a molecule.

The preloaded wood-based carbons C Gran (Figure 5.9) and WV B-30 (Figure 5.10) also had slightly faster initial adsorption than their virgin counterparts, although the time to reach equilibrium was comparable, while the coconut-based Aqua Carb (Figure 5.8) had very similar kinetics of adsorption in both virgin and preloaded states.

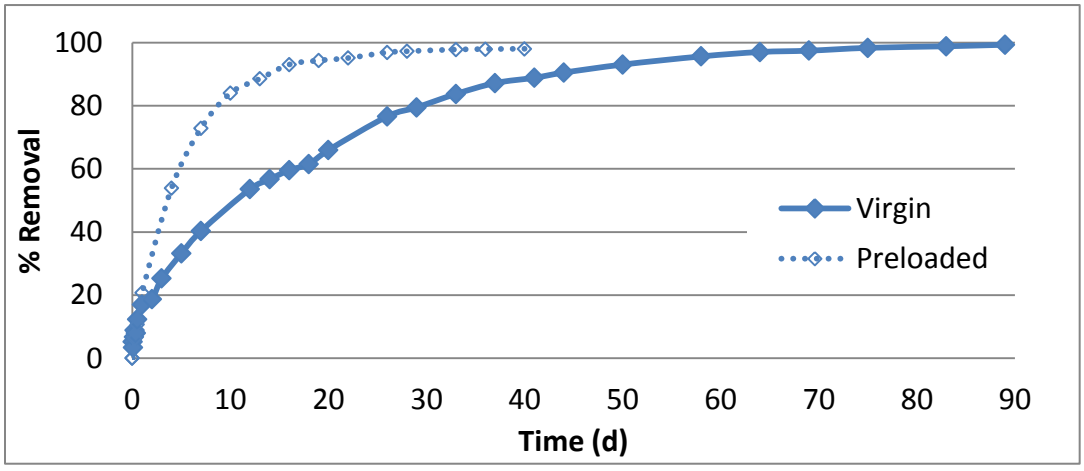

Figure 5.6: F400 kinetics - preloaded and virgin carbons in ultrapure water

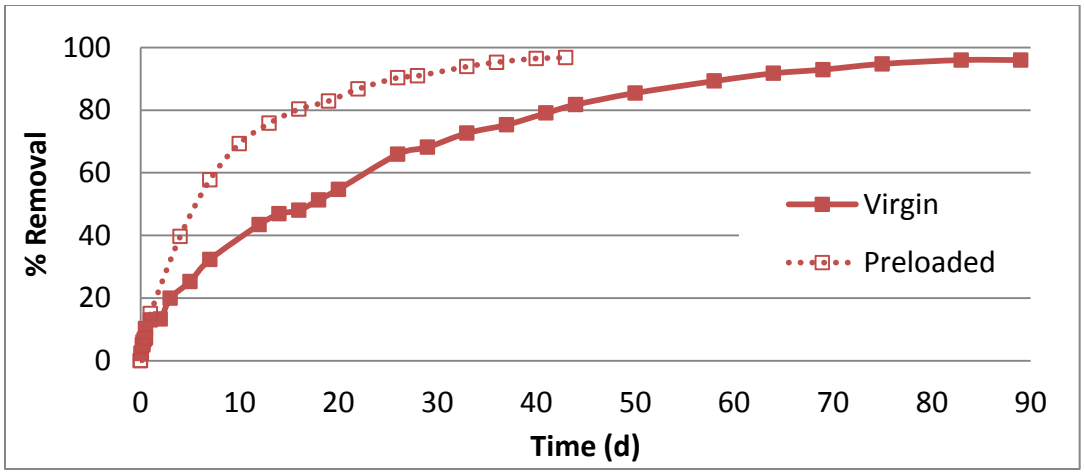

Figure 5.7: F300 kinetics - preloaded and virgin carbons in ultrapure water

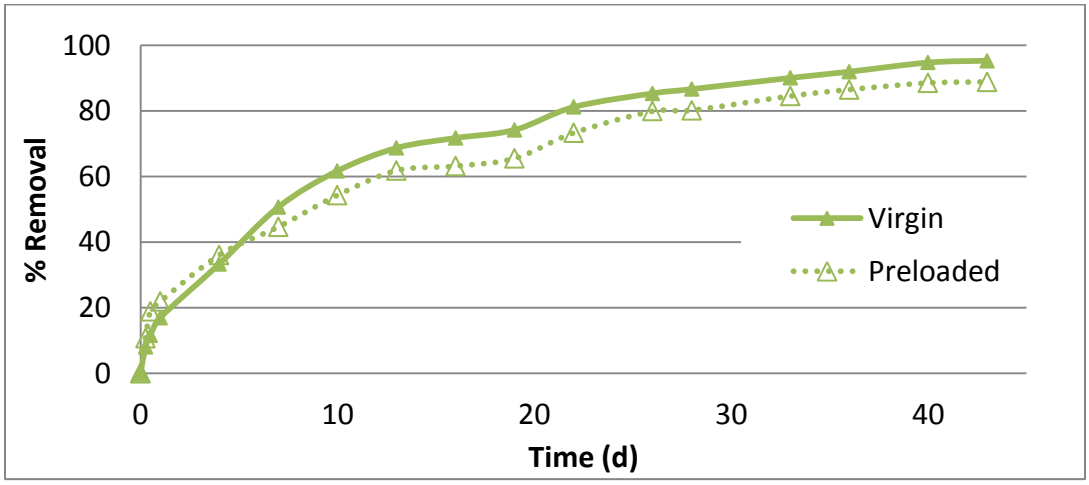

Figure 5.8: Aqua Carb kinetics - preloaded and virgin carbons in ultrapure water

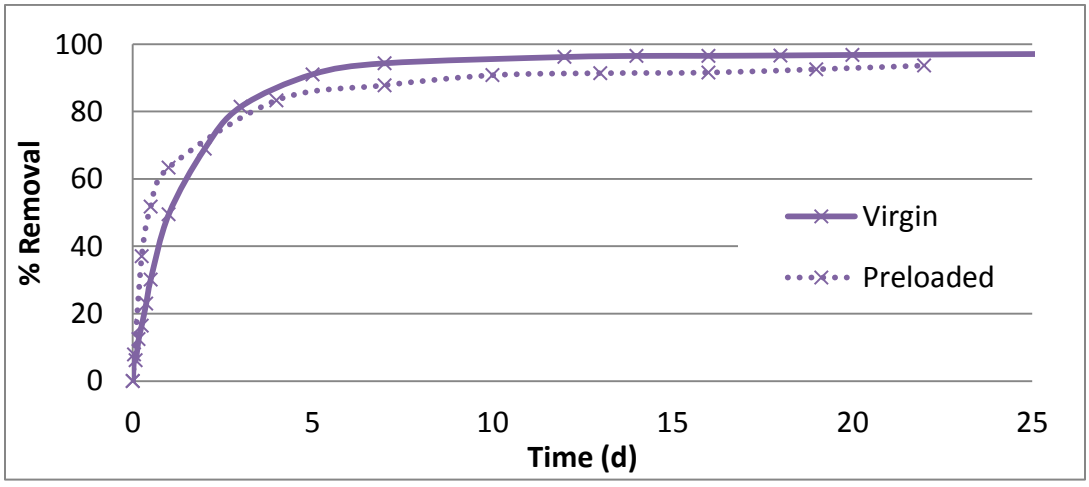

Figure 5.9: C Gran kinetics - preloaded and virgin carbons in ultrapure water

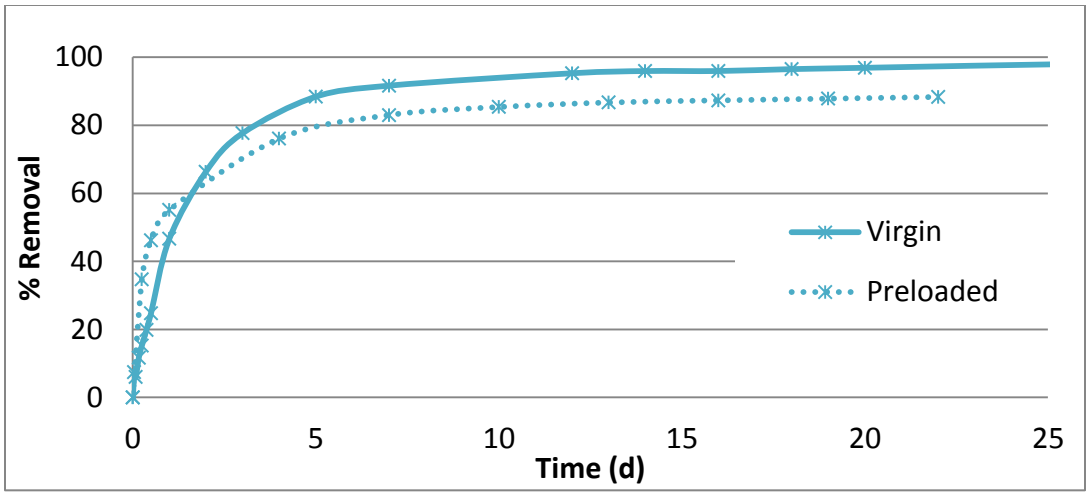

Figure 5.10: WV B-30 kinetics - preloaded and virgin carbons in ultrapure water

The pseudo-second order model outlined in Section 4.4.2 was applied to the kinetic data from the preloaded carbons, with excellent fits ($R^2 > 0.99$), as depicted in Figure 5.11 and Table 5.3, although systematic trends in the residuals were again observed, indicating that while the model may approximate the data well in this case, the underlying mechanisms of adsorption are not completely described. However, the model provides a basis for comparing characteristics of the data sets for the various carbons, and it is to this end that it is employed herein. The pseudo-second order parameters were estimated using an iterative non-linear least squares method, as linear methods require data transformation and may not produce equally accurate fits.

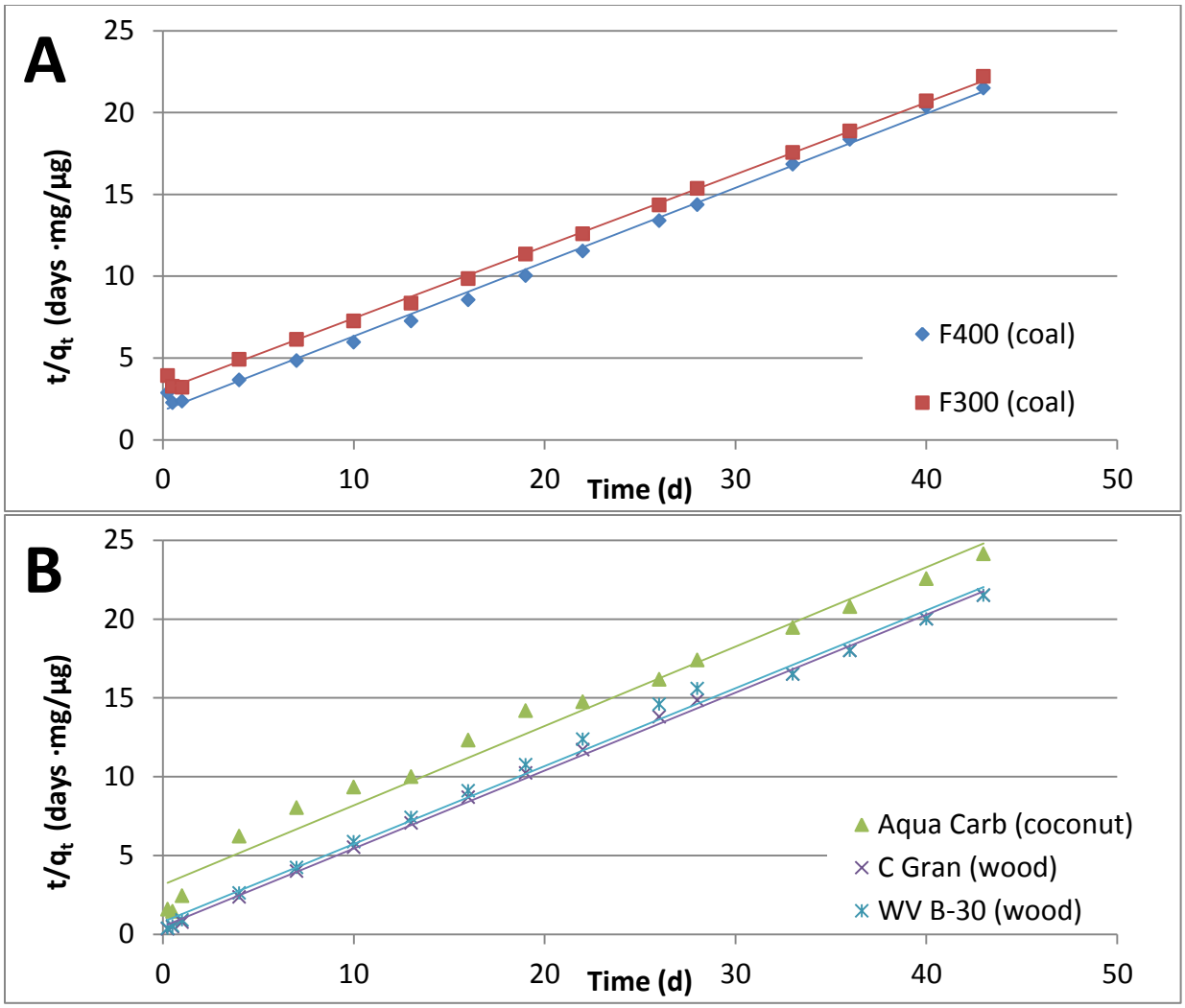

Figure 5.11: Pseudo-second order kinetic model fits using preloaded carbon in ultrapure water. A) F400 and F300, B) Aqua Carb, C-Gran, and WV B-30.

Table 5.3: Pseudo-second order kinetic model parameters for preloaded carbon in ultrapure water

Carbon	Equilibrium Carbon Capacity, q_e experimental (µg/mg)	Equilibrium Carbon Capacity, q_e predicted (µg/mg)	k_2 (mg/µg/day)	ϑ (µg/mg/day)	R^2
F400	1.96	2.22	0.12	0.59	1.00
F300	1.93	2.25	0.07	0.34	1.00
Aqua Carb	1.78	2.08	0.06	0.24	0.99
C-Gran	1.89	1.89	1.23	4.40	1.00
WV B-30	1.79	1.79	1.13	3.62	1.00

A comparison of the initial adsorption rate (ϑ) fits the observation made earlier that the wood-based carbons outperform the coal- and coconut-based carbons, by an order of magnitude. Compared to the equivalent values obtained for virgin carbons in ultrapure water, the F400 and F300 initial adsorption rate, ϑ, and overall rate constant, k_2, are both more than 3 times greater when preloaded. While the preloaded wood-based carbons also showed some increase in these parameters, it was less than half that of the coal-based carbons.

The experimental and modeled q_e values were quite similar, and in the case of the wood-based carbons, were identical. The modeled q_e estimates for the coal- and coconut-based carbons were slightly higher than the experimentally determined q_e values, though in every case the preloaded carbon q_e values were lower than those of the virgin carbons, as expected.

5.4.3 Isotherms

5.4.3.1 Freundlich parameter determination

The equilibrium anatoxin-a adsorption of the preloaded carbons in ultrapure water was modelled using the Freundlich isotherm equation, as described in Section 4.4.3.1 with the parameters determined by non-linear least squares regression given in Table 5.4. Figures 5.12 – 5.14 present a comparison of the preloaded carbon isotherms with those of the virgin carbons; while the equilibrium capacity of all carbons deteriorated following preloading, the capacity reduction varied among the carbons, with K_F values changing by as little as 12% (Aqua Carb) and as much as 44% (C Gran).

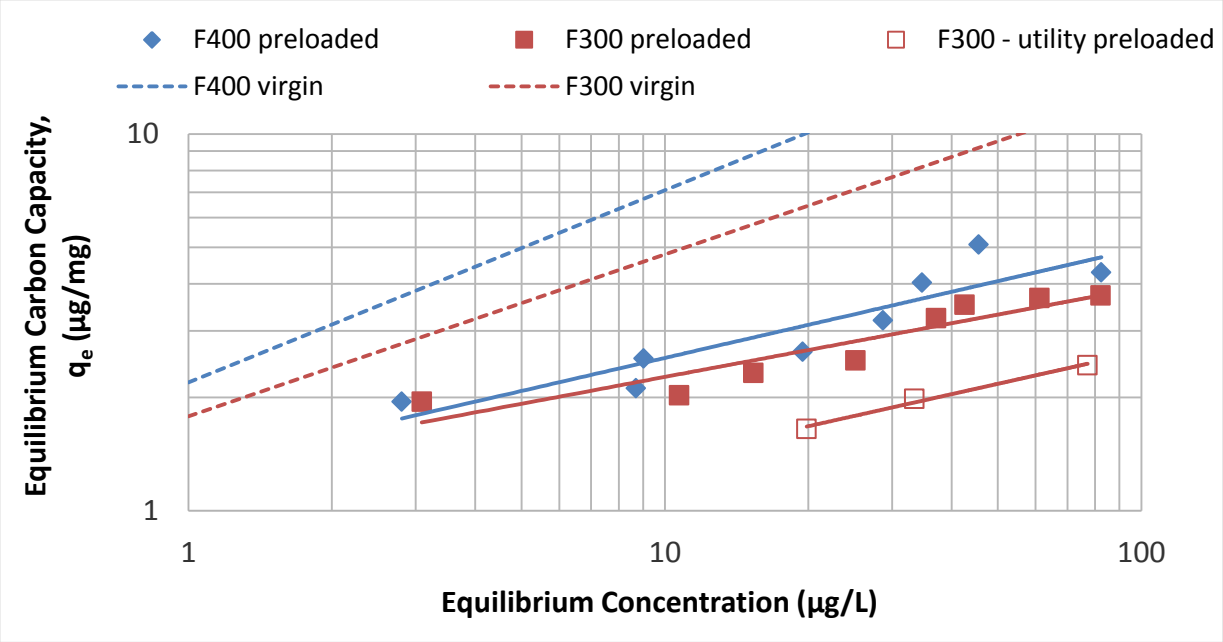

Figure 5.12: Anatoxin-a Freundlich isotherms for virgin and preloaded F400 and F300 (coal-based) GAC in ultrapure water

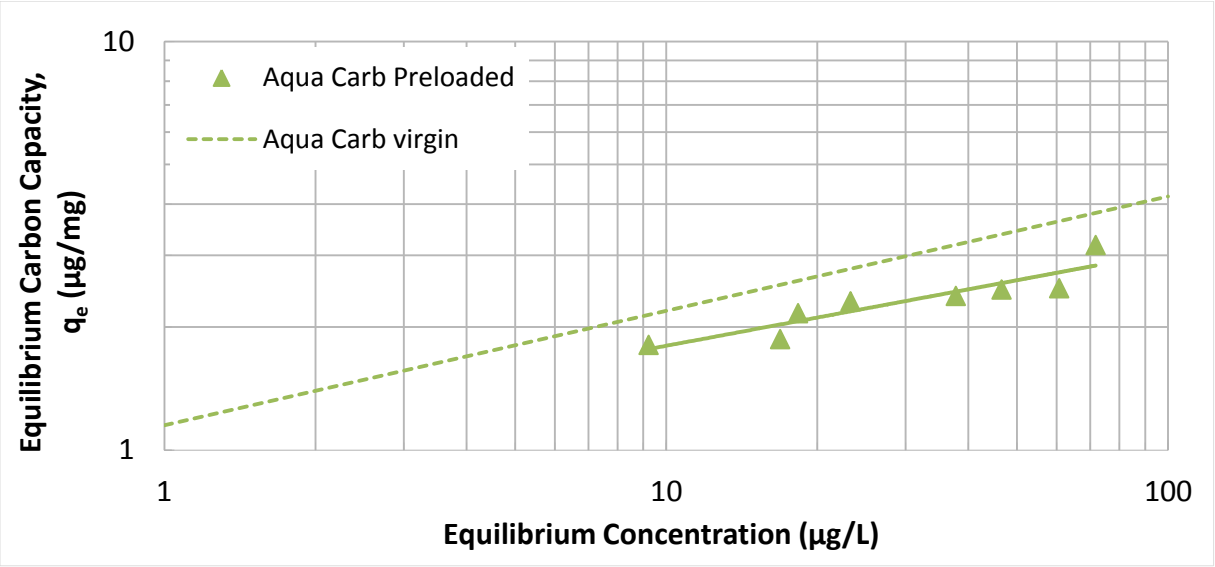

Figure 5.13: Anatoxin-a Freundlich isotherms for virgin and preloaded Aqua Carb (coconut-based) GAC in ultrapure water

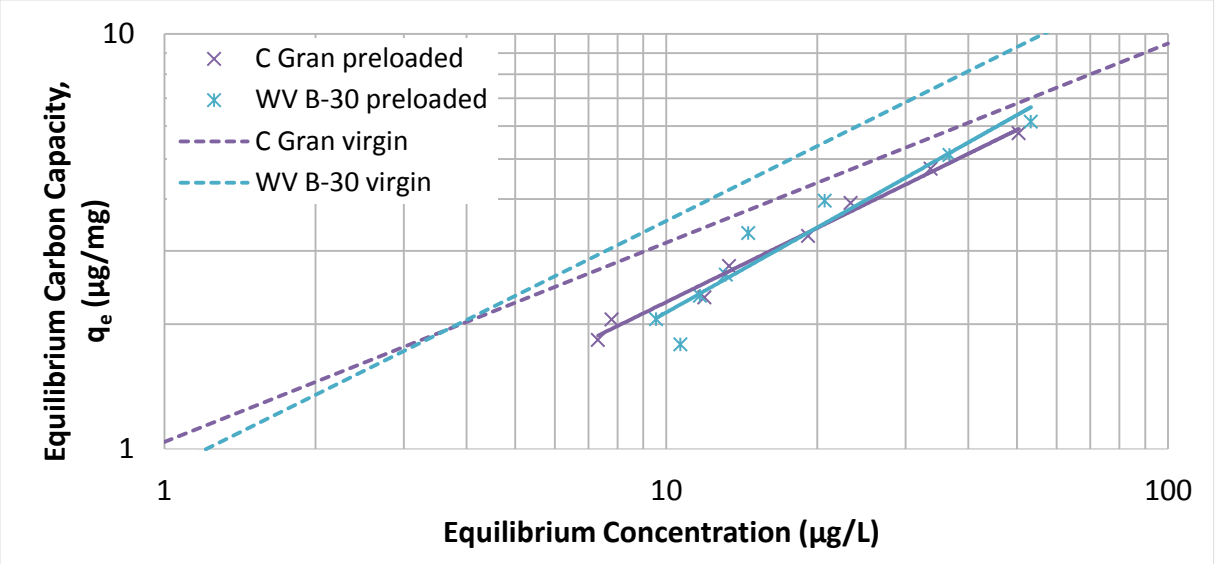

Figure 5.14: Anatoxin-a Freundlich isotherms for virgin and preloaded C-Gran and WV B-30 (wood-based) GAC in ultrapure water

Table 5.4: Freundlich isotherm parameters for preloaded carbon in ultrapure water

Carbon		K_f (µg/mg) (µg/L)$^{-1/n}$	1/n	R^2
F400	N = 8	1.24 *(0.44 – 2.03)*	0.31 *(0.13 – 0.49)*	0.78
F300	N = 8	1.18 *(0.76 – 1.59)*	0.27 *(0.17- 0.36)*	0.91
F300 - utility	N = 3	0.72 *(0 – 2.56)*	0.28 *(0 – 0.95)*	0.97
Aqua Carb	N = 8	1.01 *(0.60 – 1.46)*	0.24 *(0.13 – 0.36)*	0.82
C-Gran	N = 8	0.58 *(0.48 – 0.69)*	0.59 *(0.54 – 0.64)*	0.99
WV B-30	N = 8	0.55 *(0.29 – 0.81)*	0.61 *(0.47 – 0.75)*	0.95

(95% confidence interval)
N – number of data points

Of the coal-based carbons (Figure 5.12), preloaded F400 again had slightly higher capacity than F300 in the concentration range investigated, and as expected, the F300 sample preloaded after 3 years' operation in a full-scale surface water treatment plant had even lower capacity, with a K_F value 60% lower than that of the virgin F300. Both the preloaded wood-based carbons again produced very similar isotherms (Figure 5.14), with K_F values 38-44% lower than in their virgin states, while the coconut-based Aqua

Carb (Figure 5.13) had the lowest capacity reduction following preloading, with a change in K_F of only 12%.

A comparison of the capacities of the various preloaded carbons at three aqueous anatoxin-a concentrations, 1, 5 and 20 µg/L, is provided in Table 5.5, along with an indication of the change in capacity as compared to virgin carbon at the same toxin concentration. While the coal-based carbons underwent relatively large capacity reductions through preloading, they retain the highest capacity at lower concentrations (<10 µg/L), whereas the preloaded wood-based carbons appear to perform more favourably at higher concentrations (>20 µg/L).

It should be noted that at a 95% confidence level, only the F300 and C Gran isotherms can be differentiated from one-another, as demonstrated in Figures 5.16 and 5.17. The coal- and coconut-based preloaded carbon isotherms can only be distinguished from those of the wood-based carbons at an 80% confidence level, for both the K_F and 1/n parameter values.

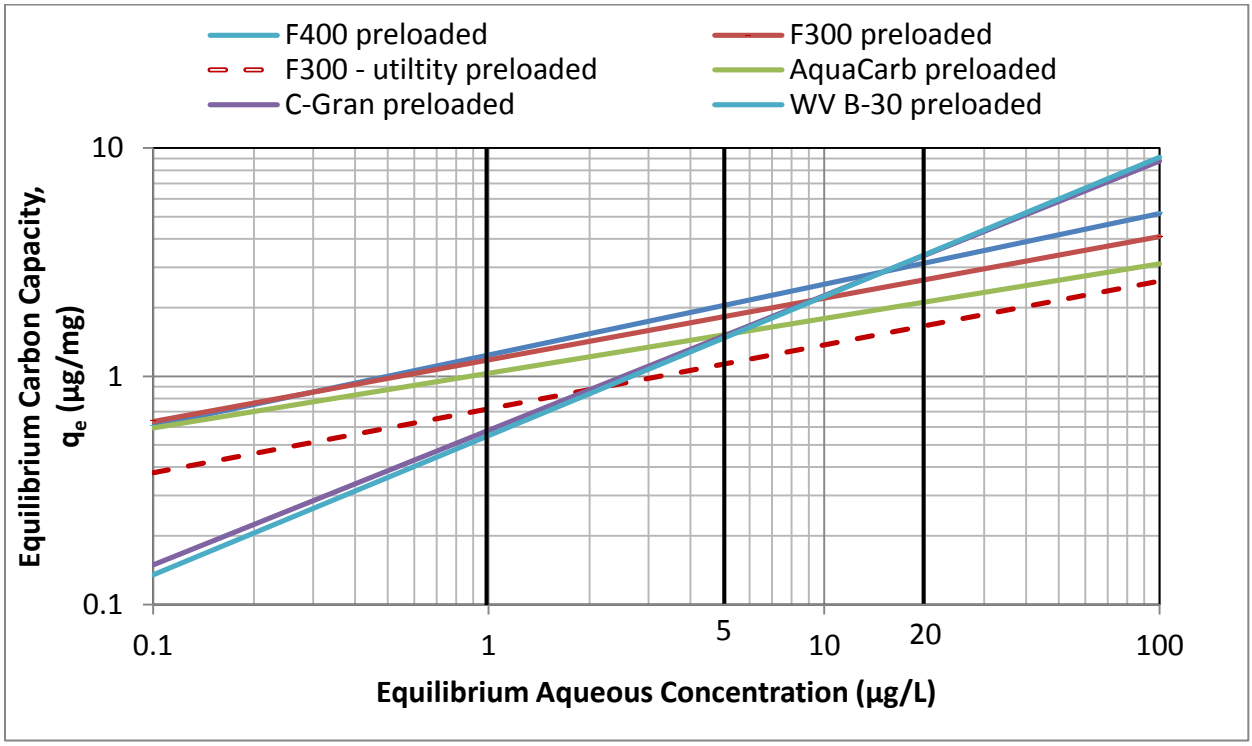

Figure 5.15: Anatoxin-a Freundlich isotherms for six preloaded GACS

Table 5.5: Comparison of anatoxin-a adsorption capacities for the preloaded carbons evaluated at different aqueous concentrations

	Aqueous anatoxin-a concentration		
Carbon	C = 1 µg/L	C = 5 µg/L	C = 20 µg/L
F400 preloaded	1.2 *(-43%)*	2.0 *(-59%)*	3.1 *(-69%)*
F300 preloaded	1.2 *(-34%)*	1.8 *(-49%)*	2.6 *(-59%)*
F300 – utility preloaded	0.7 *(-60%)*	1.1 *(-68%)*	1.7 *(-74%)*
Aqua Carb preloaded	1.0 *(-12%)*	1.5 *(-18%)*	2.1 *(-22%)*
C-Gran preloaded	0.6 *(-44%)*	1.5 *(-33%)*	3.4 *(-22%)*
WV B-30 preloaded	0.6 *(-38%)*	1.5 *(-37%)*	3.4 *(-36%)*

Adsorption capacity, q_e unit = µg(anatoxin-a)/mg(carbon)
(% change from virgin carbon capacity)

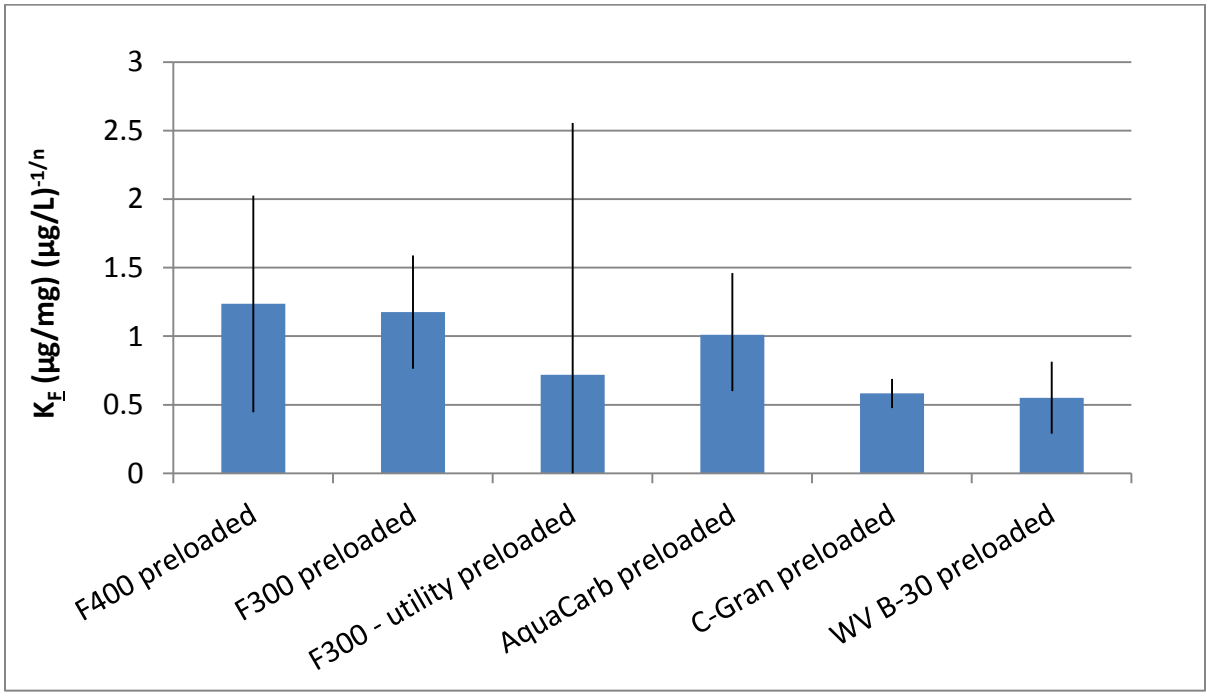

Figure 5.16: Freundlich adsorption coefficient (K_F) non-linear fit with 95% confidence intervals

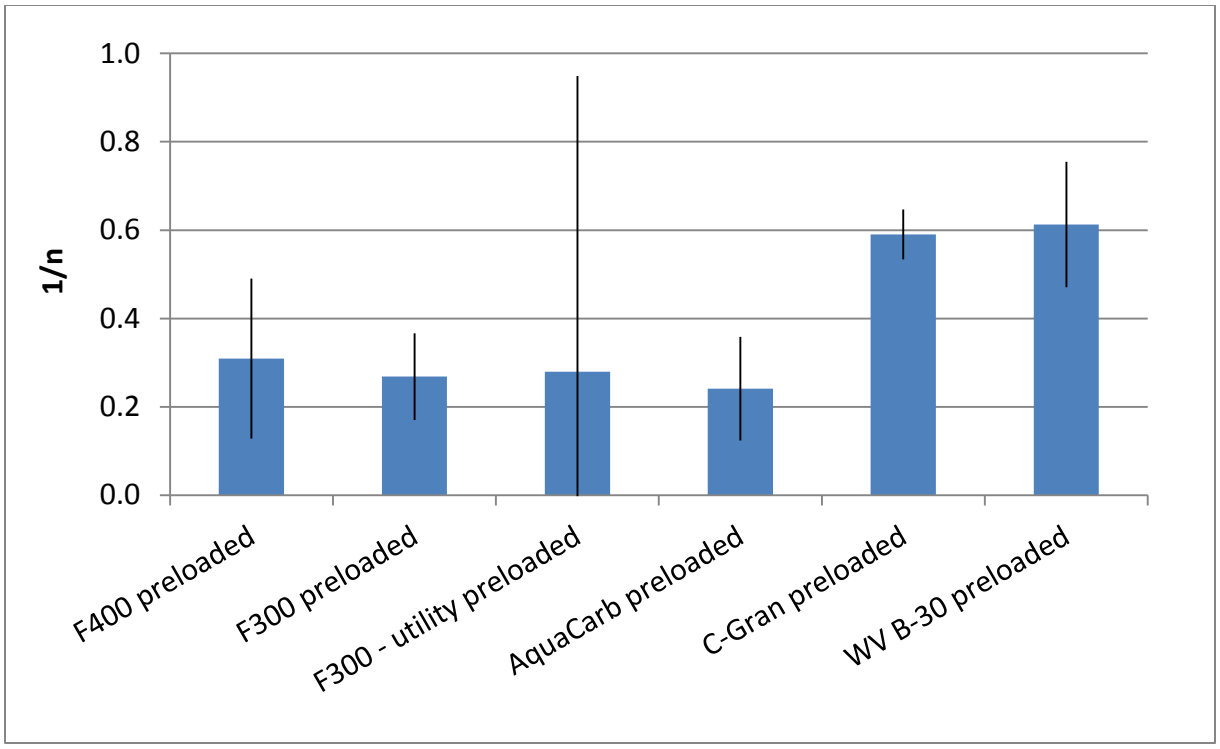

Figure 5.17: Freundlich model parameter (1/n) non-linear fit with 95% confidence intervals

5.4.3.2 Freundlich Parameter Joint Confidence Regions

Joint confidence regions (JCRs) for the two Freundlich isotherm parameters, K_F and 1/n were calculated at a 95% confidence level, and are shown in Figure 5.18 (details in Appendix C). Unlike the confidence intervals calculated for the individual parameters, JCRs consider the correlation of the two parameters, and the non-orthogonal orientation of the JCRs with respect to the axes confirms that the parameters are not independent. In this analysis, the five isotherms are differentiated clearly by carbon material – the two coal-based carbons have overlapping JCRs, as do the wood-based carbons, but no two JCRs from carbons of different source material coincide. The implication of these results is that isotherms of the F400 and F300 GACs can be said to be statistically different from those of the C Gran and WV B-30, and the Aqua Carb GACs, and vice-versa (with 95% confidence); therefore, comparisons of carbon behaviour based on these isotherms can be expected to represent true differences between the carbon material types.

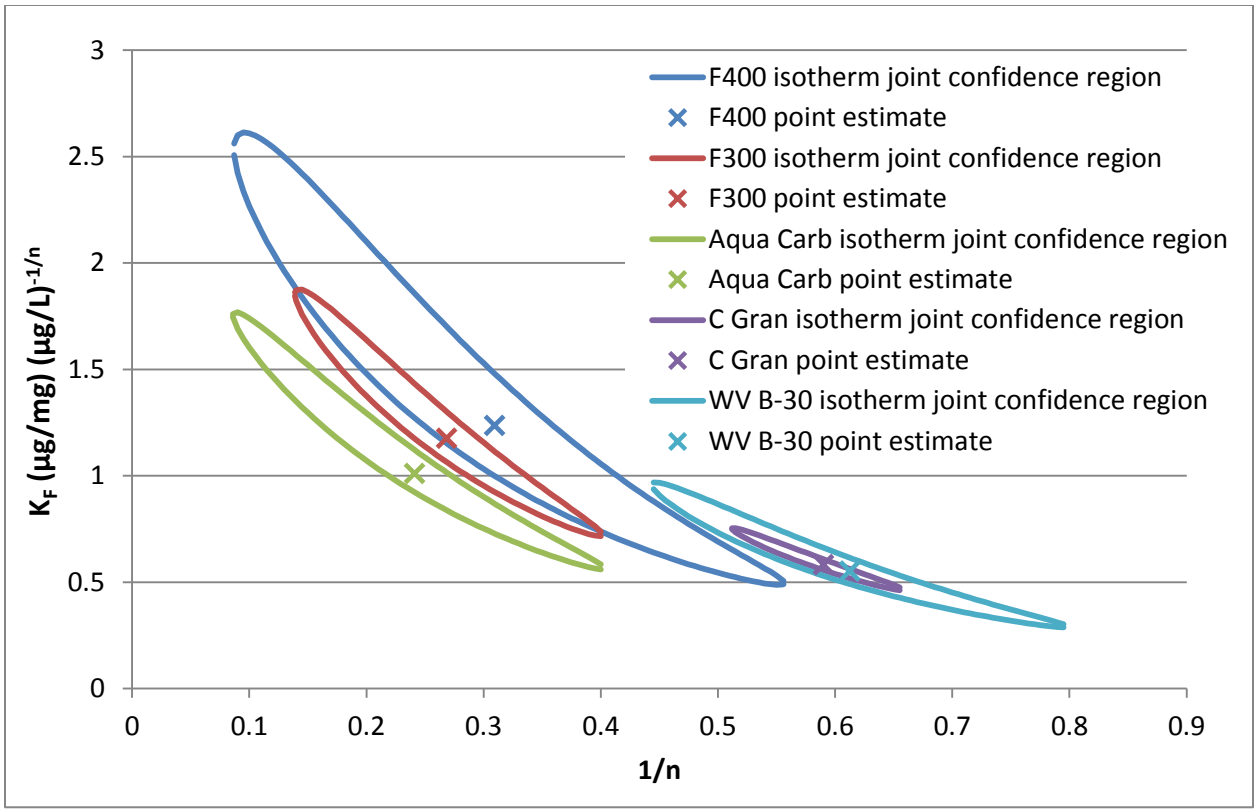

Figure 5.18: 95% joint confidence intervals and point estimates for the Freundlich parameters of isotherms generated with preloaded carbon in ultrapure water

5.4.3.3 Comparison with Literature Values

Given the inherent variability of preloading – differences in hydraulic loading, water quality and contactor design – it is difficult to directly compare isotherms produced using preloaded carbons from different studies. Furthermore, many studies do not provide details of their preloading operation (bed volumes, preloading water characteristics, etc.), rendering it even more difficult to draw any conclusions based on isotherm comparisons. Figure 5.19 presents wood- and coconut-based preloaded carbon isotherms for the adsorption of MIB and the cyanotoxin microcystin in two of its common variants – microcystin-LR (MC-LR) and microcystin-LA (MC-LA) (Ho & Newcombe, 2007; 2010). While preloading information was not provided for the MIB isotherm, the microcystin isotherms used carbon from a preloading setup following approximately 20,000 bed volumes of treated water with 4.9 mg/L DOC. Although the isotherms imply that similar carbons have considerably lower capacities for those

compounds than for anatoxin-a, the literature-based isotherms were generated in natural water, rather than in ultrapure water as done in this study. The implication of this is that anatoxin-a isotherms conducted using natural water would likely be more similar to those shown for MIB and microcystin.

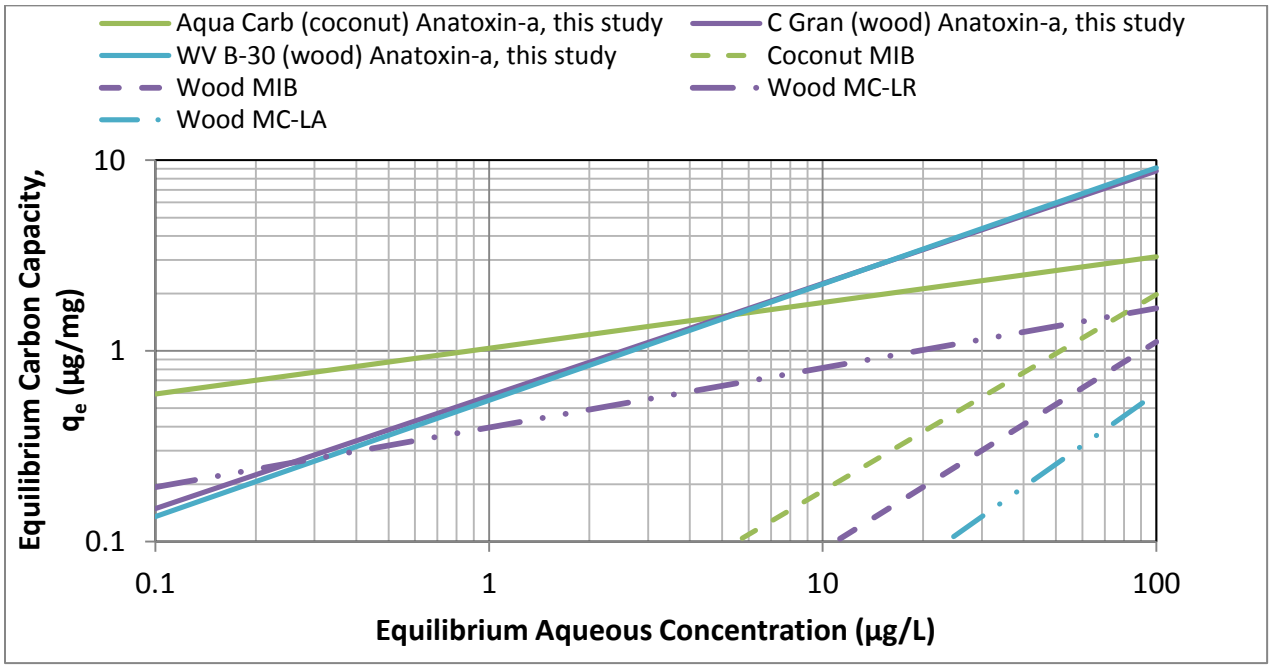

Figure 5.19: Comparison of Freundlich isotherms for anatoxin-a and MIB by preloaded wood- and coconut-based carbons. Anatoxin-a isotherms are based on data from the current study produced in ultrapure water, while MIB and microcystin isotherms were drawn based on Freundlich parameters obtained from the literature and produced in natural water (Ho & Newcombe, 2007; 2010).

5.4.4 Equilibrium Column Model

The Equilibrium Column Model (ECM) was used to estimate the maximum potential usage of the preloaded carbon, as described in Section 4.4.4. It must be noted again that in the single-solute form, the ECM employs several simplifications regarding ideal adsorption kinetics and lack of competition which render its outputs viable only for preliminary performance comparisons. In realistic applications, the presence of NOM fractions competing for adsorption sites and non-instantaneous adsorption results in considerably higher carbon usages than indicated by the model output. However, the model can be useful

in defining the idealized maximum boundary of performance potential, and different carbons may be compared via this maximum.

Assuming conditions identical to those used in Section 4.4.4, namely a 2 µg/L anatoxin-a influent concentration and carbon mass of 1,000 kg within a filter bed, the maximum treated volume to breakthrough was calculated for each of the preloaded carbons, as shown in Figure 5.20. Of the preloaded carbons, the coal-based F400 and F300 again had the highest potential treated volume prior to breakthrough of anatoxin-a (over 700 million litres, corresponding to a carbon usage rate of 1.4 mg carbon/L treated), although their capacity was more greatly reduced by preloading than that of the coconut-based Aqua Carb. The F300 sample from a full-scale treatment plant showed even greater capacity loss resulting from the extended preloading, although relatively high removals were still achievable. As noted previously, further substantial capacity reductions would be expected for adsorption in natural water.

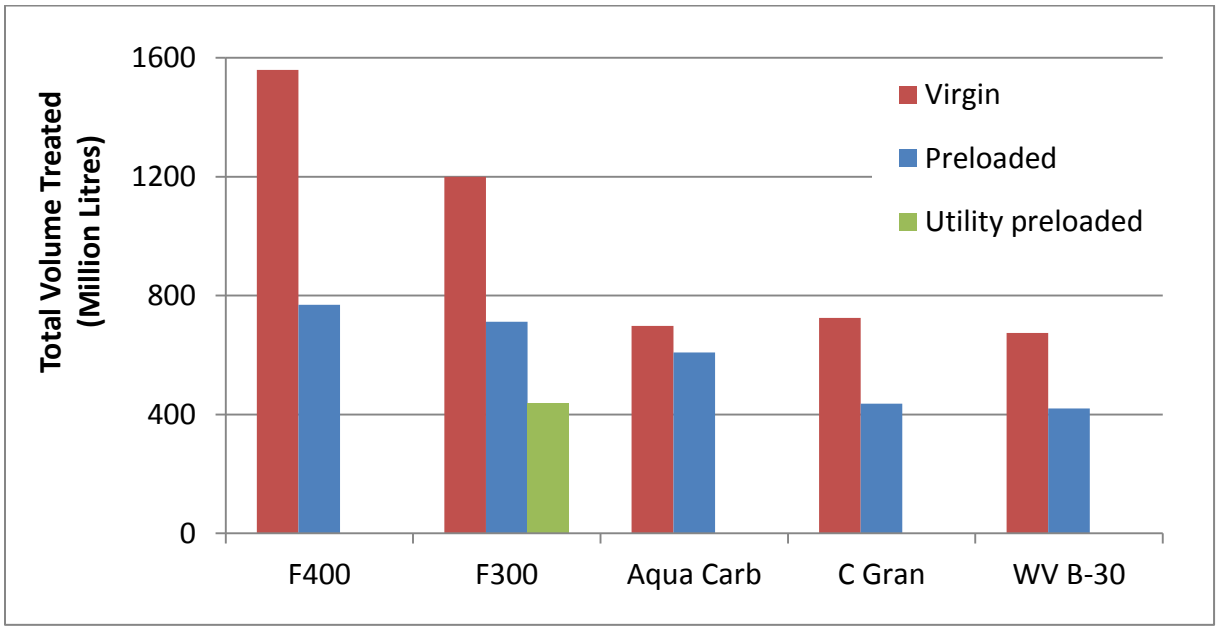

Figure 5.20: ECM predicted total treated volume to breakthrough, for 1,000 kg of GAC in a single-solute system with an influent anatoxin-a concentration of 2 µg/L

5.5 Conclusions

Five GACs were preloaded in parallel with post-sedimentation surface water to allow a direct comparison of changes to adsorption kinetics and equilibrium capacity for anatoxin-a, in ultrapure water. Near-complete breakthrough of the influent TOC (4.5 – 5.2 mg/L) was observed for all of the carbons after 21 days (approximately 40,000 bed volumes, hydraulic loading rate 12 m/h). Converging carbon surface properties, including pH_{PZC} were attributed to the impact of preloading with NOM (which is negatively charged); following preloading, all of the carbons had very similar pH_{PZC} values, within the 6.9 – 7.2 range.

The capacity of all carbons deteriorated following preloading, (as compared to the capacities of the virgin carbons) with the coconut-based Aqua Carb experiencing the smallest reduction. The coal-based F400 and F300 carbons retained the greatest capacity at lower aqueous toxin concentrations (less than 20 µg/L) while at higher concentrations the wood-based carbons had greater capacity. It should be noted that only the coal-based F300 and the wood-based C Gran Freundlich model parameters could be statistically differentiated by their 95% confidence intervals, although JCRs at a 95% confidence level distinguished between the joint parameter spaces of the coal-, wood- and coconut-based carbons, indicating that the isotherms produced by carbons of different source material are distinct from one another.

The adsorption of anatoxin-a by preloaded coal-based GACs (F300 and F400) was much faster than by their virgin counterparts, possibly due to changes in the carbon surface charge. Preloading with negatively-charged NOM reduced the pH_{PZC}, and as a result, at the pH of the ultrapure water (6.3) the repulsive charge interactions between the positively-charged carbon and the cationic toxin were diminished. While the coconut- and wood-based carbons also showed some increase in the initial rate of adsorption, it was considerably smaller than the effect observed for the coal-based carbons. Overall, the preloaded wood-based C Gran and WV B-30 retained the fastest toxin adsorption, while the coal-based F400 and F300 overtook the slower coconut-based Aqua Carb; this material-based ranking was maintained when the kinetics data were normalized by the average particle size.

Chapter 6
Adsorption of Anatoxin-a by Virgin Carbon in Natural Water

6.1 Summary

The adsorption of anatoxin-a from Grand River water by five virgin GACs and one PAC was studied at bench-scale via the bottle point technique. Water from the Grand River in Southern Ontario was characterized using DOC (5.42 mg/L), pH (8.0), SUVA (4.11 L/mg*m) and LC-OCD analysis, and was found to have relatively high humic content (4.69 mg/L). As expected, the presence of background natural organic material (NOM) reduced the equilibrium capacity of all the carbons, compared to their capacities in ultrapure water. The PAC was the fastest adsorber, followed by the coconut- and wood-based carbons, while the coal-based carbons were the slowest – a trend which became increasing apparent when the kinetic data were normalized by average effective particle size, to more closely examine the impact of carbon source material. The PAC also had the greatest capacity in the concentration range investigated, although its application may be limited as intact cyanobacterial cells may permit intracellular toxins to bypass PAC early in the treatment train. Conversely, GAC contactors are typically located later in a treatment train, and would be less likely to encounter intact cyanobacterial cells. All of the GACs produced very similar Freundlich isotherms, and comparison with literature values indicated similar or slightly lower capacities for anatoxin-a as for the more commonly regulated microcystin-LR. Declining toxin concentrations in the natural water controls were noted, and a conservative approach was taken in evaluating the results; nevertheless, trends observed are believed to be valid.

6.2 Introduction

The efficacy of microcontaminant adsorption from drinking water is impacted by the water quality as a result of carbon preloading and NOM competition (e.g. Ho & Newcombe, 2007). Numerous studies have investigated the adsorption of other cyanotoxins (mainly microcystins) and cyanobacterial taste and odour compounds such as geosmin and MIB in natural water (Ho & Newcombe, 2007; Ho & Slyman, 2008; Ho & Newcombe, 2010; Sorlini & Collivignarelli, 2011) however, no analogous anatoxin-a isotherms have

been published to date. This investigation provides an indication of the impact of natural water characteristics on anatoxin-a adsorption and the relative treatability of this neurotoxin, producing kinetic data and isotherms for six carbons which can be compared with literature values available for other cyanobacterial metabolites. However, it is reasonable to consider that the major trends observed would be generally applicable to other waters having similar quality with respect to major parameters such as DOC, pH, etc.

It should be noted that each water matrix will impact the adsorption process to different degrees and results will be specific to a given water matrix; as such, this study aimed to also provide a characterization of the surface water used. Outcomes of this study may not be applicable to different source waters –it must be understood that the specific results pertain to the surface water used in this investigation.

6.3 Materials and Methods

6.3.1 Materials

HPLC-grade chemicals and virgin carbon samples were obtained as detailed in Section 4.3.1. The water used in this study was Grand River water (GRW) collected from the raw water intake of a southern-Ontario utility on December 3, 2014.

6.3.2 Sample Preparation and Handling

GRW was filtered through 0.45 µm nylon filters (Supelco Analytical, PA, USA) to remove solids. The remaining NOM components were characterized using liquid chromatography–organic carbon detection (LC-OCD), which fractionates NOM based on size and can be used to quantify five NOM components: biopolymers (compounds with molecular weight over 10,000 Da, including proteins and polysaccharides), humic substances, building blocks (breakdown products of humic substances), low molecular weight neutrals, and low molecular weight acids (Huber et al., 2011). The UV254, pH, and dissolved organic carbon (DOC) content of the water were also measured, to provide further characterizing information. Specific ultraviolet absorbance (SUVA) was calculated by dividing the

UVA_{254} (m^{-1}) by the dissolved organic carbon (DOC, mg/L) as determined from the bypass peak of the LC-OCD chromatogram.

The bottle point method was used to study anatoxin-a adsorption in GRW by the virgin carbons, as described in Section 4.3.3. The water was autoclaved prior to toxin addition, to discourage microbial growth and reduce biodegradation potential. Six positive controls were included: two ultrapure water controls at 100 µg/L anatoxin-a, one ultrapure water control at 20 µg/L (as used previously), as well as two GRW controls at 100 µg/L and one GRW control at 20 µg/L anatoxin-a. Six additional negative controls were also added to the protocol – one for each carbon in GRW – as well as a GRW blank. All bottles were places on an orbital shaker operating at 150 rpm and shielded from light exposure (again, to minimize toxin degradation). The anatoxin-a concentrations of the sample bottles with the highest doses of each carbon, as well as the positive controls, were monitored by removing a 1 mL aliquot for analysis by LC-MS/MS. The % removal was calculated using the difference in concentrations between the sample bottle and the average of the two GRW positive controls with an initial concentration of 100 µg/L anatoxin-a (at the same sampling time); equilibrium was defined as a change in the toxin removal of less than 1% per day. At equilibrium, the aqueous anatoxin-a concentration of all sample and control bottles was determined; in calculating equilibrium isotherms only data points with a final aqueous concentration greater than the limit of quantification of the LC-MS/MS method (0.65 µg/L) and less than the average of the two 100 µg/L (initial concentration) GRW positive controls were included. In general, this procedure resulted in the exclusion of only approximately 15% of the data.

6.3.3 Anatoxin-a Analysis by LC-MS/MS

The LC-MS/MS method used to quantify aqueous anatoxin-a concentrations is detailed in Section 4.3.4.

6.4 Results and Discussion

6.4.1 Natural Water Characterization

The results of the analyses used to characterize the GRW are summarized in Table 6.1. The humic fraction made up the largest portion of the carbon content (73%), with building blocks and low molecular weight neutrals contributing an additional 24%. SUVA (a ratio of UV absorbance and DOC concentration) is an indicator of the proportion of aromatic organic material (mostly humic), and supports the finding of high humic content in GRW. A past characterization study of Southern Ontario drinking water sources found that the Grand River typically had much greater DOC and humics content than other surface waters, including the Great Lakes (Croft, 2012). In addition, at 8.0, the pH of the GRW used in this study was much higher than that of the ultrapure water used in prior components of this study (6.3).

Table 6.1: Raw river water parameters

DOC (mg/L)	Biopolymers (mg/L)	Humics (mg/L)	Building Blocks (mg/L)	Neutrals (mg/L)	Acids (mg/L)	SUVA (L/mg*m)	pH
5.42	0.16	4.09	0.81	0.54	0.02	4.11	8.0

6.4.2 Anatoxin-a Stability

After 21 days, all carbons had met the equilibrium criteria (a change in removal of less than 1% per day, as compared to the average of the GRW positive controls with a 100 µg/L initial concentration). However, degradation of the spiked anatoxin-a in GRW was observed over the 21 days of this investigation. While the aqueous anatoxin-a concentrations of the positive controls in ultrapure water remained relatively stable throughout, the GRW positive controls which had an initial concentration of 100 µg/L declined gradually to an average of 36.7 µg/L, as shown in Figure 6.1. The third GRW positive control had an initial concentration of 20 µg/L, and declined to a final concentration of 6.7 µg/L, with concentrations equivalent to 18-21% of the 100 µg/L-initial concentration positive controls at each sampling time. In part, the degradation of the toxin in GRW can likely be attributed to the difference in pH values between the GRW (8.0) and the ultrapure water (6.3); it has been previously noted that

anatoxin-a is more stable in the protonated, cationic form, which predominates at lower pH levels (pKa = 9.4), whereas the neutral species degrades more readily (van Apeldoorn et al, 2007; Kaminski et al., 2013). At pH 8, approximately 4% of the toxin would exist in the less stable deprotonated form, in a continuously correcting equilibrium with the protonated form, as opposed to less than 0.1% at pH 6.3. The pH of the GRW was not adjusted prior to spiking with anatoxin-a, as it was desired to examine the adsorption behaviour in an unaltered natural surface water, to maintain conditions as close to realistic as possible; furthermore, the degree of degradation observed was unexpected, given that after six days the toxin concentration in the GRW appeared to level off. Under ideal circumstances, this study would have been repeated at a lower pH level; however, time constraints did not allow for the repetition.

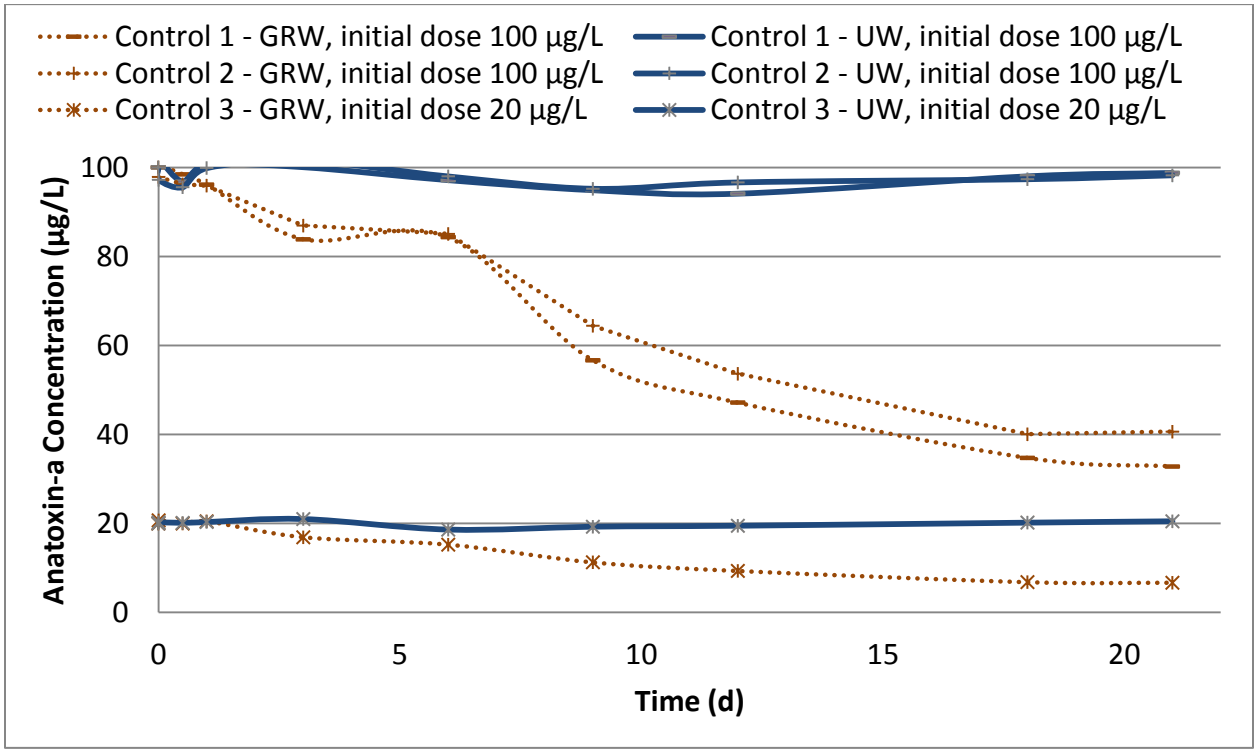

Figure 6.1: Anatoxin-a positive controls in ultrapure water (UW) and Grand River water (GRW), degradation over 21 days

6.4.3 Kinetics

As previously noted in the ultrapure water investigation with virgin carbons, the PAC was the most rapidly adsorbing of the carbons studied for removal of anatoxin-a from GRW. Figure 6.2 shows the

percent removal of each carbon, calculated based on the average concentration of the GRW positive controls at the sampling time. The coconut-based Aqua Carb was the next fastest to reach equilibrium at 18 days, with the wood-based C Gran and WV B30 performing very similarly to the smaller of the coal-based GACs, F400; all of the carbons met the equilibrium criteria (change in removal of less than 1% per day) within 21 days. As noted previously, the larger size of the F300 grains results in somewhat slower adsorption, although normalizing the kinetic data by the average effective particle size, as shown in Figure 6.3, results in nearly overlapping curves, confirming that the difference in particle size is the main differentiating factor for these two carbons.

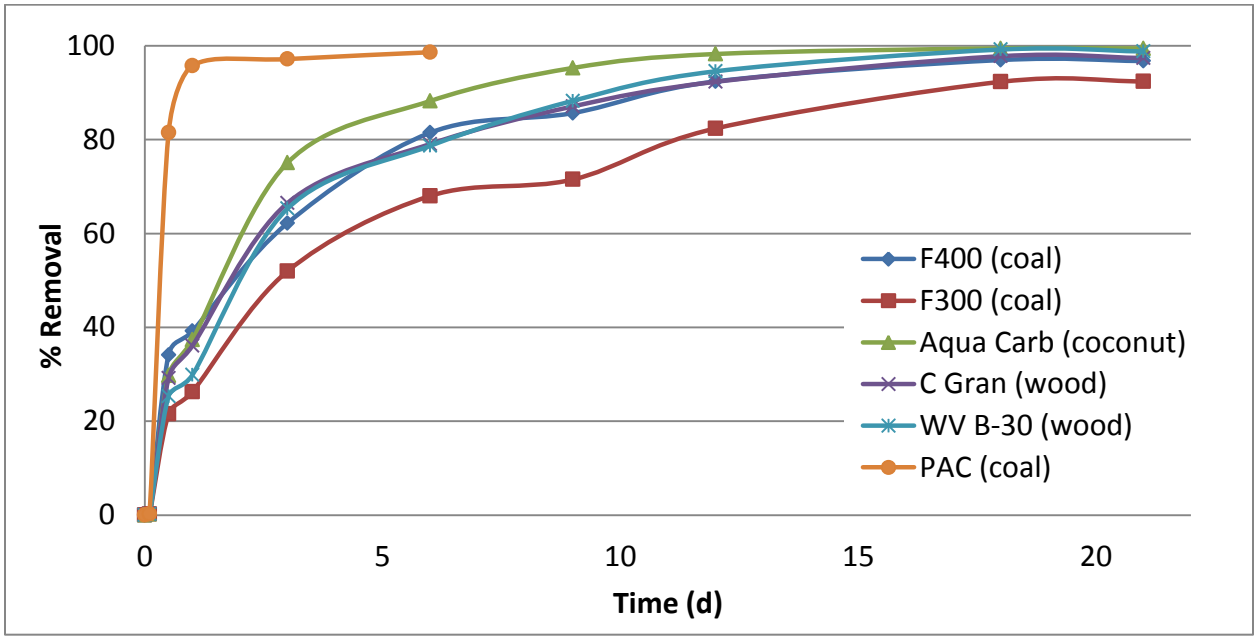

Figure 6.2: Anatoxin % removal by virgin carbons in GRW as a function of time; calculated based on the average GRW control concentration at each sampling time; 50 mg/L adsorbent dose for GACs, 30 mg/L adsorbent dose for PAC.

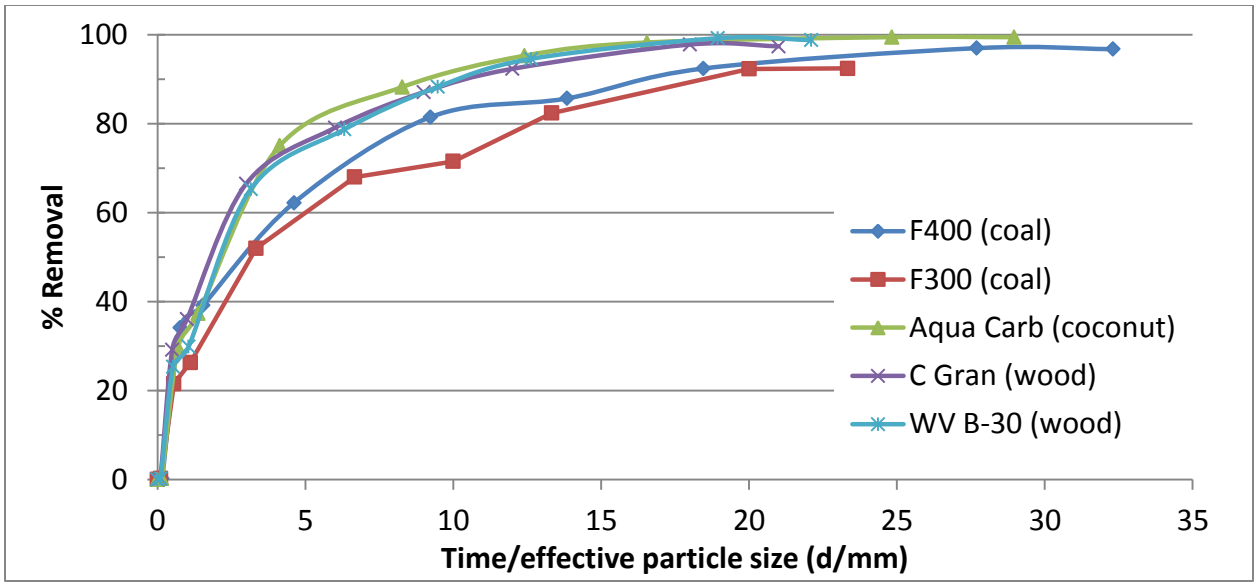

Figure 6.3: Anatoxin-a removal time series, normalized by average effective particle size

Overall, the GACs reached equilibrium faster in GRW than in the past ultrapure water experiments, where one carbon (F300) required nearly 90 days to meet the equilibrium criteria; however, in GRW the aqueous anatoxin-a concentration declined as a result of both degradation and adsorption. The degradation resulted in a diminished driving force for the diffusion of the toxin – as such, results are not directly comparable with those obtained in ultrapure water, where adsorption was the predominant cause of changes in aqueous anatoxin-a concentration.

Due to the degradation of spiked anatoxin-a in GRW, it was not possible to apply the pseudo-second order kinetic model previously used in Sections 4.4.2. and 5.4.2., as the data did not conform to the required input format. The model necessitates the calculation of the amount of the original spiking concentration removed at each sampling time, rather than the percent removal based on available toxin concentration, and assumes no degradation of the target adsorbate – a condition which was not met.

6.4.4 Isotherms

6.4.4.1 Freundlich parameter determination

The Freundlich isotherm model was fitted to the equilibrium adsorption data for each carbon as detailed in Section 4.4.3.1, with the resulting parameter estimates presented in Table 6.2. Given the degradation of

anatoxin-a observed in GRW positive controls, adsorptive capacity (q_e) was calculated as the amount of toxin removed with respect to the amount of toxin available at the time equilibrium was reached – i.e., the difference between the final sample concentration and the average of two GRW positive controls with a 100 µg/L initial concentration.

While the capacity of each carbon was lower in GRW, as expected, the reduction in K_F values varied from 15% (WV B-30) to 69% (F400). Figures 6.4 – 6.7 compare the isotherms in GRW with those previously determined for virgin carbon removal of anatoxin-a in ultrapure water, demonstrating the observed reduction in equilibrium capacity.

Table 6.2: Freundlich isotherm parameters for virgin carbon in Grand River water

Carbon		K_f (µg/mg) (µg/L)$^{-1/n}$	1/n	R^2
F400 (coal)	N = 6	0.67 *(0.55-0.79)*	0.08 *(0.01-0.16)*	0.71
F300 (coal)	N = 5	0.66 *(0.59-0.74)*	0.05 *(0.00-0.10)*	0.80
Aqua Carb (coconut)	N = 6	0.63 *(0.44-0.82)*	0.20 *(0.08-0.33)*	0.85
C-Gran (wood)	N = 6	0.75 *(0.65-0.85)*	0.13 *(0.07-0.18)*	0.88
WV B-30 (wood)	N = 6	0.75 *(0.57-0.94)*	0.15 *(0.04-0.25)*	0.79
PAC (coal)	N = 7	2.14 *(1.51-2.77)*	0.43 *(0.22-0.65)*	0.86

(95% confidence interval)
N – number of data points

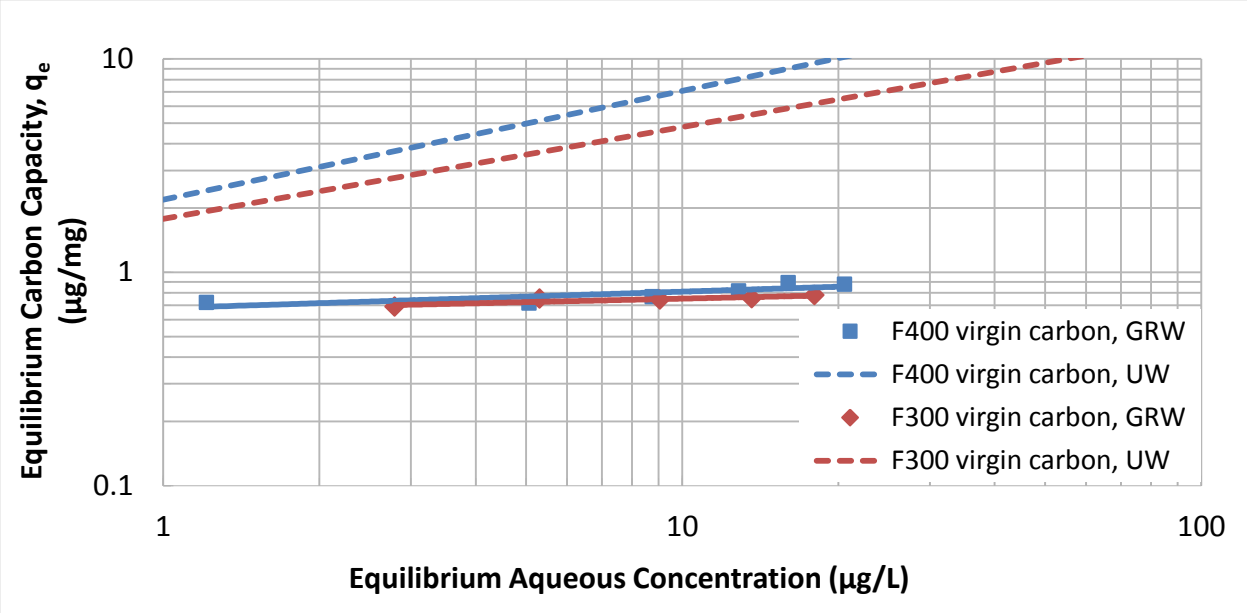

Figure 6.4: Anatoxin-a Freundlich isotherms for virgin F400 and F300 (coal-based) GAC in ultrapure water (UW) vs. Grand River water (GRW)

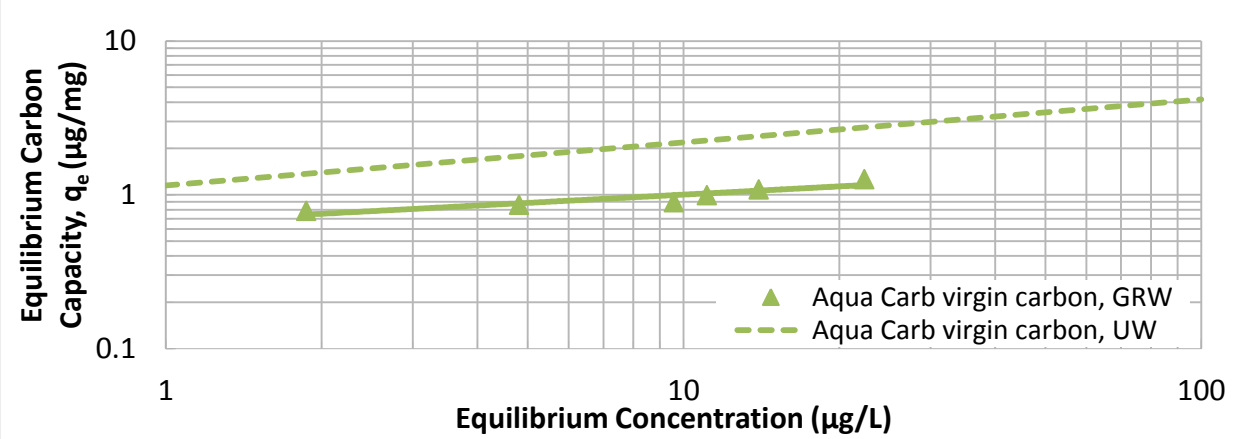

Figure 6.5: Anatoxin-a Freundlich isotherms for virgin Aqua Carb (coconut-based) GAC in ultrapure water (UW) vs. Grand River water (GRW)

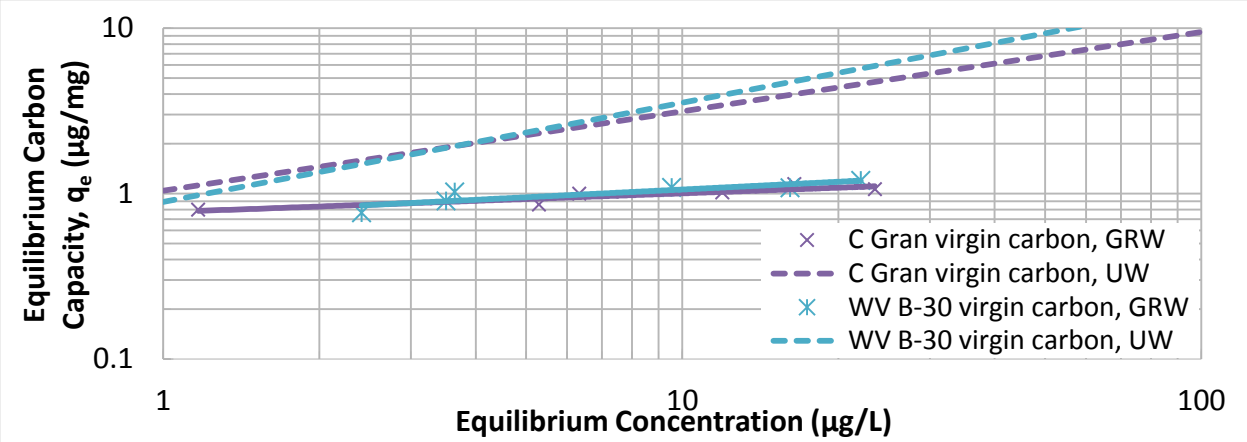

Figure 6.6: Anatoxin-a Freundlich isotherms for virgin C-Gran and WV B-30 (wood-based) GAC in ultrapure water (UW) vs. Grand River water (GRW)

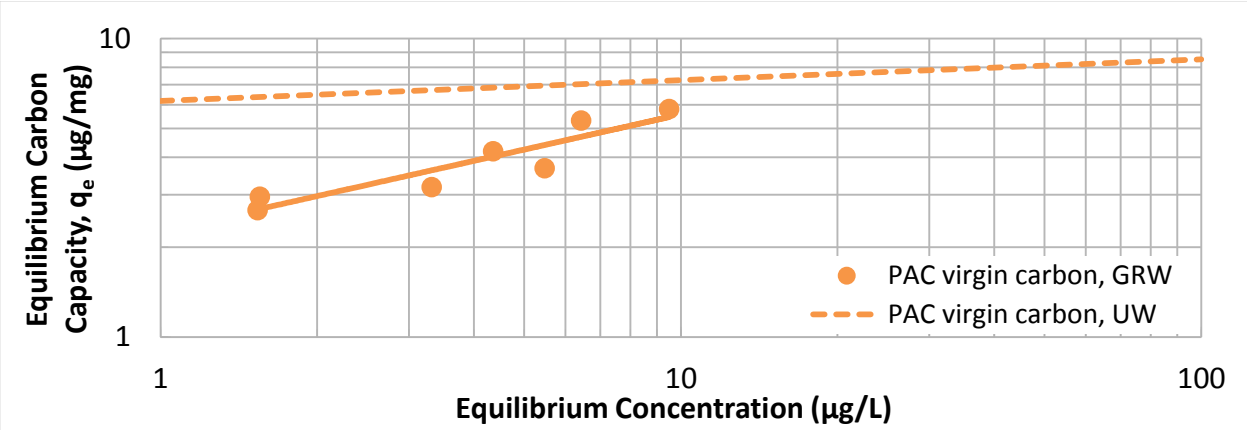

Figure 6.7: Anatoxin-a Freundlich isotherms for virgin (coal-based) PAC in ultrapure water (UW) vs. Grand River water (GRW)

While the GAC isotherms in natural water all had 1/n values comparable to or lower than those determined in ultrapure water, the PAC isotherm shown in Figure 6.7 had a greater 1/n value. Extrapolating the isotherm beyond the concentration range it was determined in implies that the capacity of the PAC could be greater in natural water than in ultrapure water at aqueous concentrations above 11 µg/L. While no explanation is evident from the experimental conditions, the reliability of this unexpected result should be viewed with caution.

The collective GRW isotherms for adsorption of anatoxin-a are shown in Figure 6.8; the GAC isotherms appear very similar, and a calculation of the adsorption capacity of each carbon at different anatoxin-a

concentrations (Table 6.3) demonstrates the resemblance of the GACs. At concentrations above 20 µg/L, the differences become more evident; however, in the range of typical environmental concentrations, the GAC isotherms are similar. Their Freundlich parameter values are also alike, as shown in Figures 6.8 and 6.9; however, the two parameters, K_F and 1/n, are highly linked, as is discussed in Section 6.4.4.2. The capacity reduction in GRW is more pronounced for the coal-based GACs, based on their greater capacity in ultrapure water. Interestingly, the natural water used in this study appears to have an equalizing effect on the GACs – the differences in carbon performance appear far more pronounced in the ultrapure water isotherms.

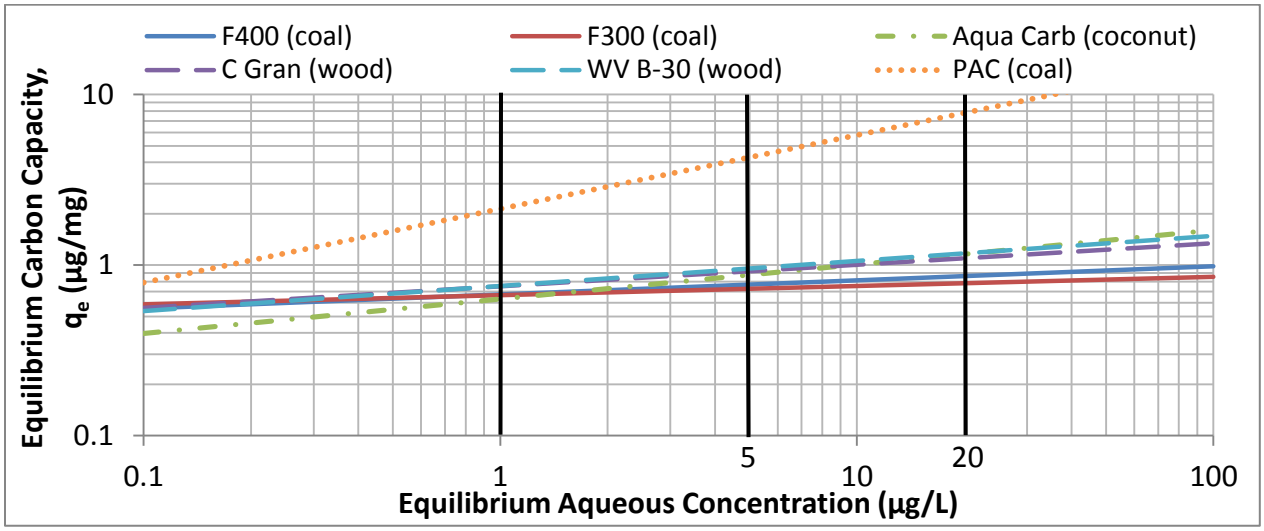

Figure 6.8: Anatoxin-a Freundlich isotherms for six virgin carbons in Grand River water

Table 6.3: Comparison of anatoxin-a adsorption capacities for the virgin carbons evaluated at different aqueous concentrations in natural water

Carbon	C = 1 µg/L	C = 5 µg/L	C = 20 µg/L
F400 natural water	0.7 *(-69%)*	0.8 *(-85%)*	0.9 *(-91%)*
F300 natural water	0.7 *(-63%)*	0.7 *(-80%)*	0.8 *(-88%)*
Aqua Carb natural water	0.6 *(-45%)*	0.9 *(-52%)*	1.2 *(-56%)*
C-Gran natural water	0.7 *(-28%)*	0.9 *(-59%)*	1.1 *(-75%)*
WV B-30 natural water	0.8 *(-15%)*	1.0 *(-59%)*	1.2 *(-78%)*
PAC natural water	2.1 *(-65%)*	4.3 *(-38%)*	7.8 *(3%)*

Adsorptive capacity, q_e unit = µg(anatoxin-a)/mg(carbon)
(% change from ultrapure water capacity)

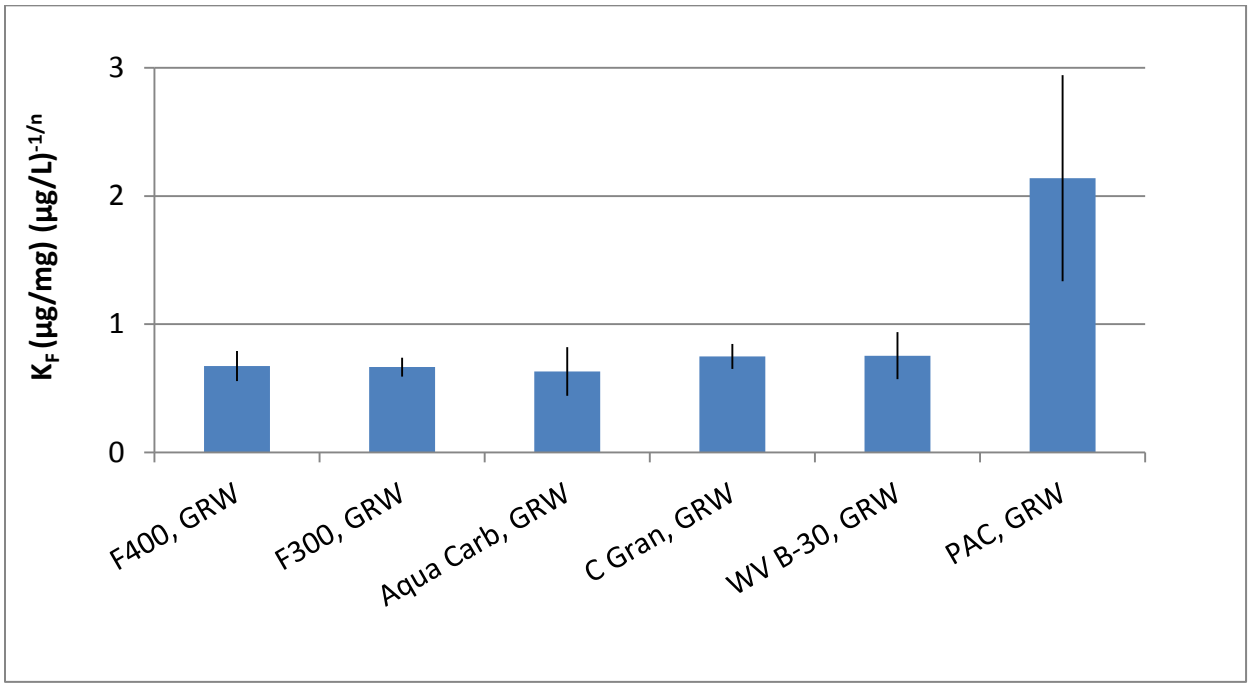

Figure 6.9: Freundlich adsorption coefficient (K_F) non-linear fit with 95% confidence intervals, in Grand River water

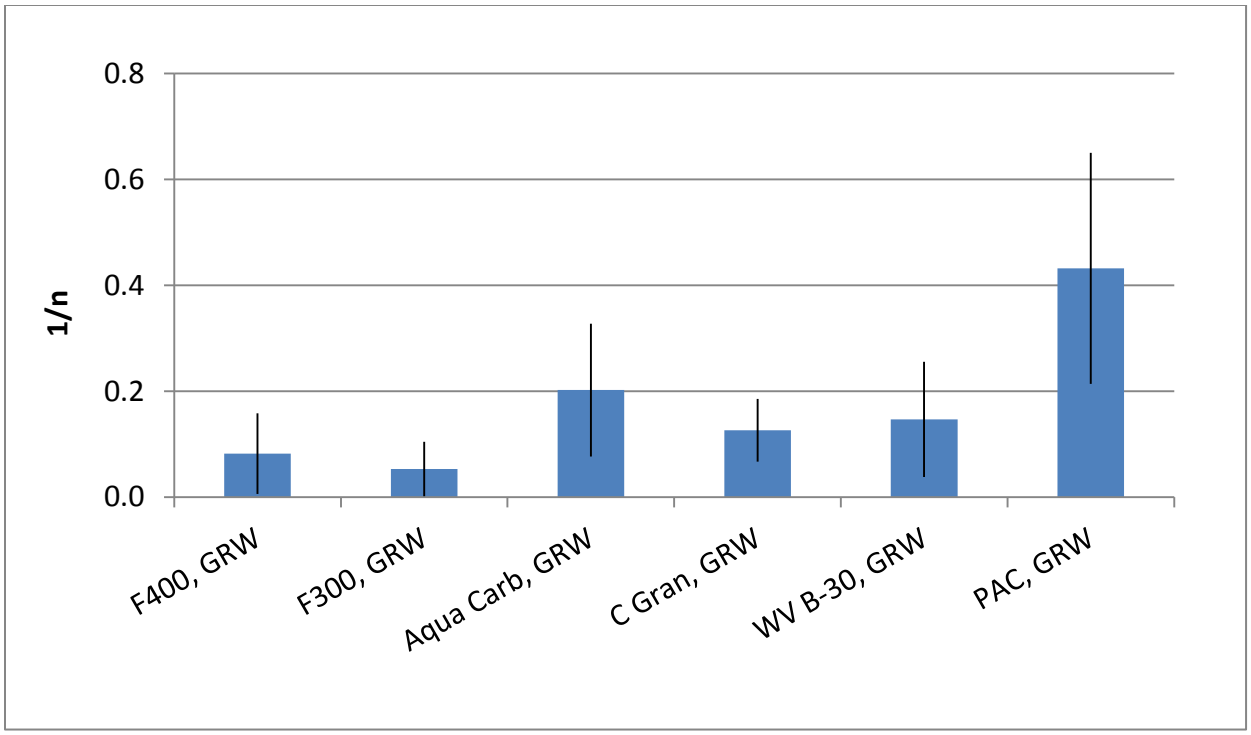

Figure 6.10: Freundlich model parameter (1/n) non-linear fit with 95% confidence intervals, in Grand River water

6.4.4.2 Freundlich Parameter Joint Confidence Regions

Joint confidence regions (JCRs) for the two parameters of the Freundlich isotherm, K_F and 1/n, were determined at a 95% confidence level and are plotted in Figure 6.11. The diagonal orientation of the ellipsoid regions indicates that the parameters are highly correlated, and unlike the 95% confidence intervals for the individual parameters, the JCRs clearly show that the joint parameter regions of the coal-based F400 and F300 do not overlap with those of the wood- and coconut-based GACs. While the coconut-based Aqua Carb and wood-based C Gran and WV B-30 are not differentiable at this confidence level, the PAC shows a large degree of separation from the JCRs of the GACs. In practice, this means that comparisons of adsorption behaviour based on these isotherms can be expected to represent true differences between the coal-based carbons, and those derived from wood or coconut.

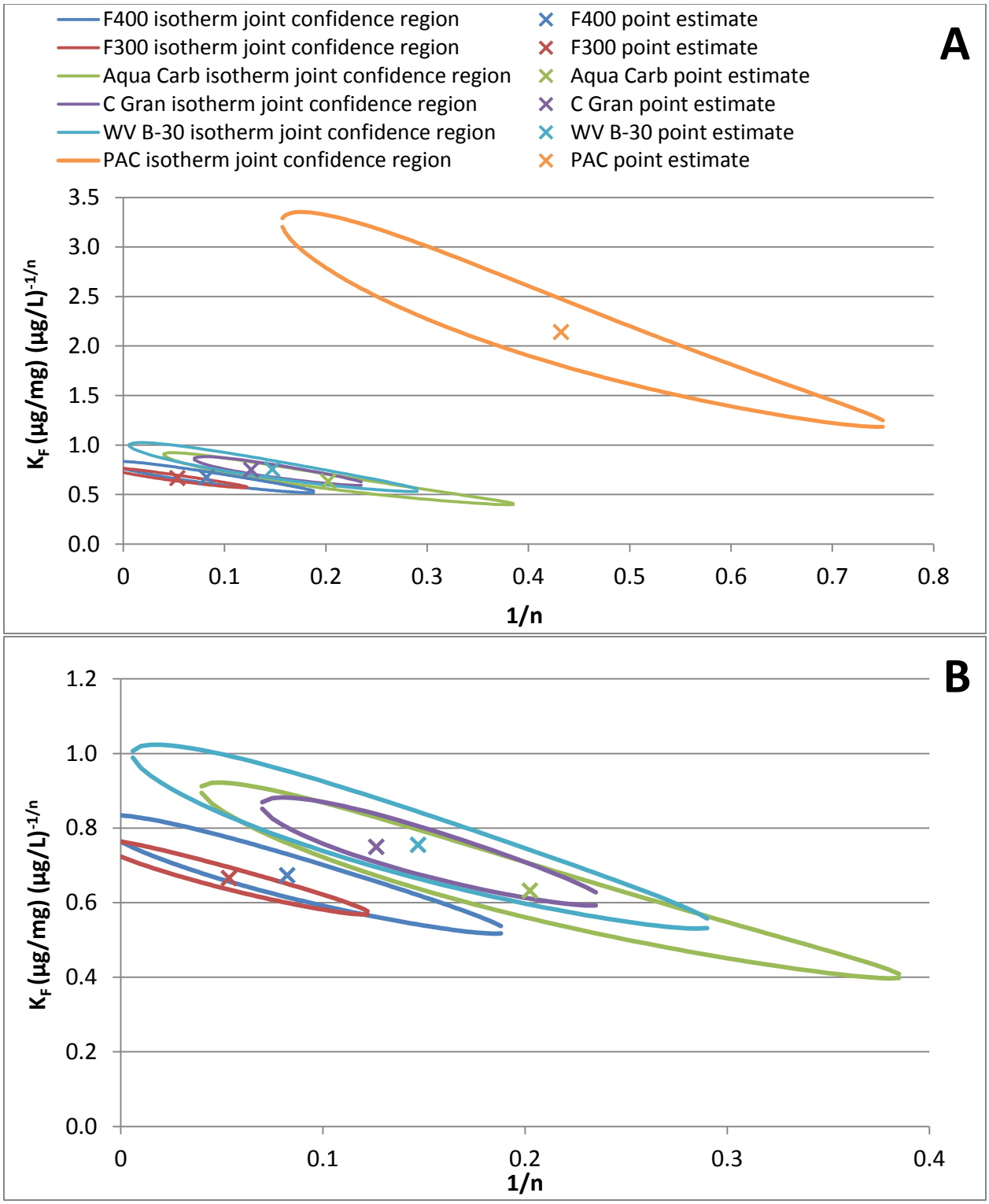

Figure 6.11: 95% joint confidence regions and point estimates for the Freundlich parameters of isotherms generated with virgin carbon in Grand River water. A – all carbons; B – GACs

6.4.4.3 Comparison with Literature Values

The Freundlich isotherms for removal of anatoxin-a from natural water were compared with literature values for other cyanobacterial metabolites – the cyanotoxins microcystin-LR (MC-LR), microcystin-LA (MC-LA) and cylindrospermopsin (CYN), and the cyanobacterial taste and odour compound 2-methylisoborneaol (MIB). The DOC content of the natural waters used in other studies was provided as an indicator of water quality – while it is known that only part of the DOC in natural water competes for adsorption sites, only information on DOC is readily available. The comparison was broken down by activated carbon source material, with coal-based carbon isotherms shown in Figure 6.12, coconut-based carbon isotherms in Figure 6.13 and wood-based carbon isotherms in Figure 6.14. Where available, the trade names of the carbons used in developing the isotherms are indicated. It should be noted that several limitations exist in comparing these isotherms; without further information on the specific characteristics of carbons used, the NOM composition and the nature of the competing fractions, it is difficult to conclusively evaluate carbon performance.

Based on the coal-carbon isotherms (Figure 6.12), capacity for anatoxin-a was somewhat lower than for MC-LR (Sorlini & Collivignarelli, 2011) and somewhat greater than for CYN (Ho & Slyman, 2008), although it must be noted that the MC-LR isotherm was produced in water with lower DOC content than that used in this investigation, while the natural water used in the CYN isotherm had a very high DOC (10.2 mg/L). Furthermore, the MC-LR and CYN isotherms were determined at different concentration ranges (10-10,000 µg/L and 1-40 µg/L respectively) and were extrapolated to the 1-100 µg/L range.

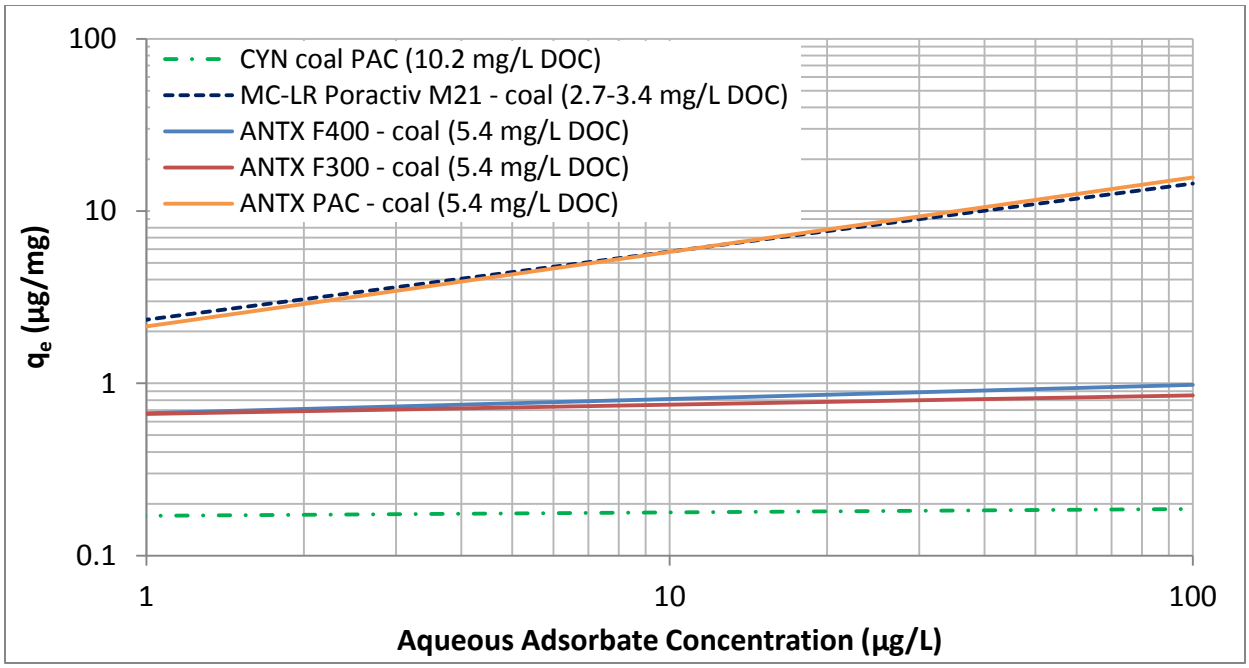

Figure 6.12: Comparison of Freundlich isotherms for anatoxin-a and the cyanotoxins microcystin-LR (MC-LR) and cylindrospermopsin (CYN) by virgin coal-based carbons in natural water. Anatoxin-a isotherms are based on data from the current study produced in Grand River water. The MC-LR isotherm with Poractive M21 GAC and CYN isotherm with coal-based PAC were drawn based on Freundlich parameters obtained from the literature (Sorlini & Collivignarelli, 2011; Ho & Slyman, 2008 respectively).

The anatoxin-a and MC-LR isotherms produced using coconut-based carbons by Sorlini & Collivignarelli (2011), shown in Figure 6.13, appear very similar, although again the MC-LR isotherm was determined in natural water with lower DOC content. The MIB isotherm (Ho & Newcombe, 2010) indicates a greater dependence on the aqueous adsorbate concentration, with greater capacity for anatoxin-a than MIB at lower concentrations (below approximately 4 µg/L), and the reverse at higher concentrations. It should be noted that the MIB isotherm was determined in a lower concentration range (10 – 100 ng/L) while the MC-LR isotherm was determined in a higher concentration range (0.1 – 30 mg/L) and both were extrapolated for the purpose of comparison.

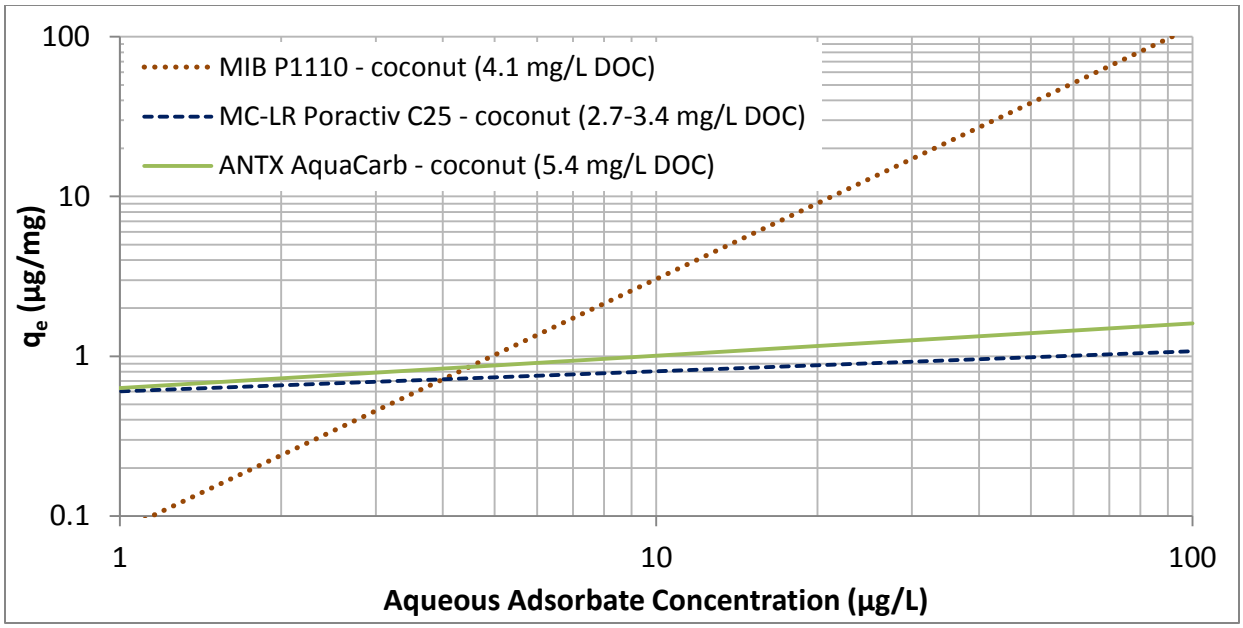

Figure 6.13: Comparison of Freundlich isotherms for anatoxin-a and the cyanotoxin microcystin-LR (MC-LR) and taste and odour compound MIB by virgin coconut-based carbons in natural water. Anatoxin-a isotherms are based on data from the current study produced in Grand River water. The MC-LR isotherm with Poractiv C25 GAC and MIB isotherm with PICA P1100 GAC were drawn based on Freundlich parameters in natural water obtained from the literature (Sorlini & Collivignarelli, 2011; Ho & Newcombe, 2010 respectively).

Wood-based carbon isotherms (Figure 6.14) show a similar trend to coal-based carbons, with greater capacity for MC-LR than anatoxin-a, in this case with similar DOC content in the natural waters used (Ho & Newcombe, 2007). MC-LA, the more recalcitrant microcystin variant, is less well adsorbed than anatoxin-a at most environmentally relevant concentrations, based on data from Ho & Newcombe (2007). For the cases presented, anatoxin-a was better adsorbed than CYN (Ho & Slyman, 2008), although the natural water used to establish the CYN isotherm had extremely high DOC content – therefore, this may not be the case when isotherms obtained under similar conditions are compared. Isotherms for MIB removal from natural water were determined by Ho & Newcombe (2010) in the 3 – 100 ng/L concentration range, and extrapolated for comparison. These isotherms have similar slopes to MC-LR,

and again imply greater capacity for anatoxin-a than MIB at concentrations below 6 µg/L, with the reverse holding at higher concentrations.

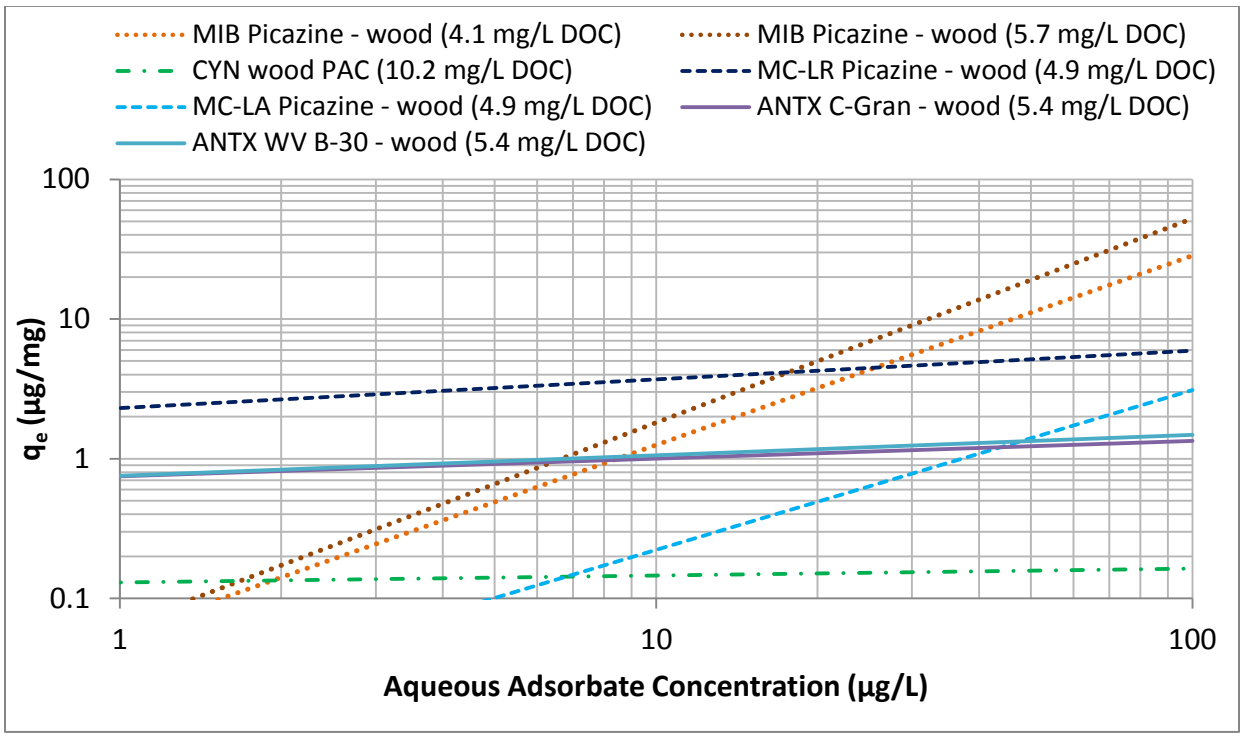

Figure 6.14: Comparison of Freundlich isotherms for anatoxin-a, the cyanotoxins microcystin-LR (MC-LR), microcystin-LA (MC-LA), cylindrospermopsin (CYN), and the taste and odour compound MIB by virgin wood-based carbons in natural water. Anatoxin-a isotherms are based on data from the current study produced in Grand River water. The MC-LR and MC-LA isotherms with PICA Picazine GAC, the CYN isotherm with wood-based PAC and the MIB isotherms with PICA Picazine GAC were drawn based on Freundlich parameters obtained from the literature (Ho & Newcombe, 2007; Ho & Slyman, 2008; Ho & Newcombe, 2010, respectively).

6.4.5 Equilibrium Column Model

The upper-bound of potential treatment volume for each carbon was determined using the Equilibrium Column Model (ECM) detailed in Section 4.4.4. The model was applied in its single-solute form, using the Freundlich parameters determined in natural water to account for NOM competition, although no preloading was considered in this scenario. The results of the ECM for a 1000 kg GAC filter with 2 µg/L anatoxin-a influent are shown in Figure 6.15; in the virgin carbon with natural water scenario, the two

wood-based carbons have the potential for a slightly higher total volume treated than the coal- or coconut-based carbons. Figure 6.15 illustrates the loss in capacity as a reduction in potential treatment volume when operating in natural rather than ultrapure water. In all cases, the natural water isotherms resulted in lower treatment volumes than the preloading study, and it can be anticipated that the combination of preloading with natural water NOM competition would result in still lower capacities. It should also be noted once more that the ECM results must be considered as over-estimations of the true treatment volumes to breakthrough, due to the simplifications regarding kinetic characteristics, NOM competition and preloading effects.

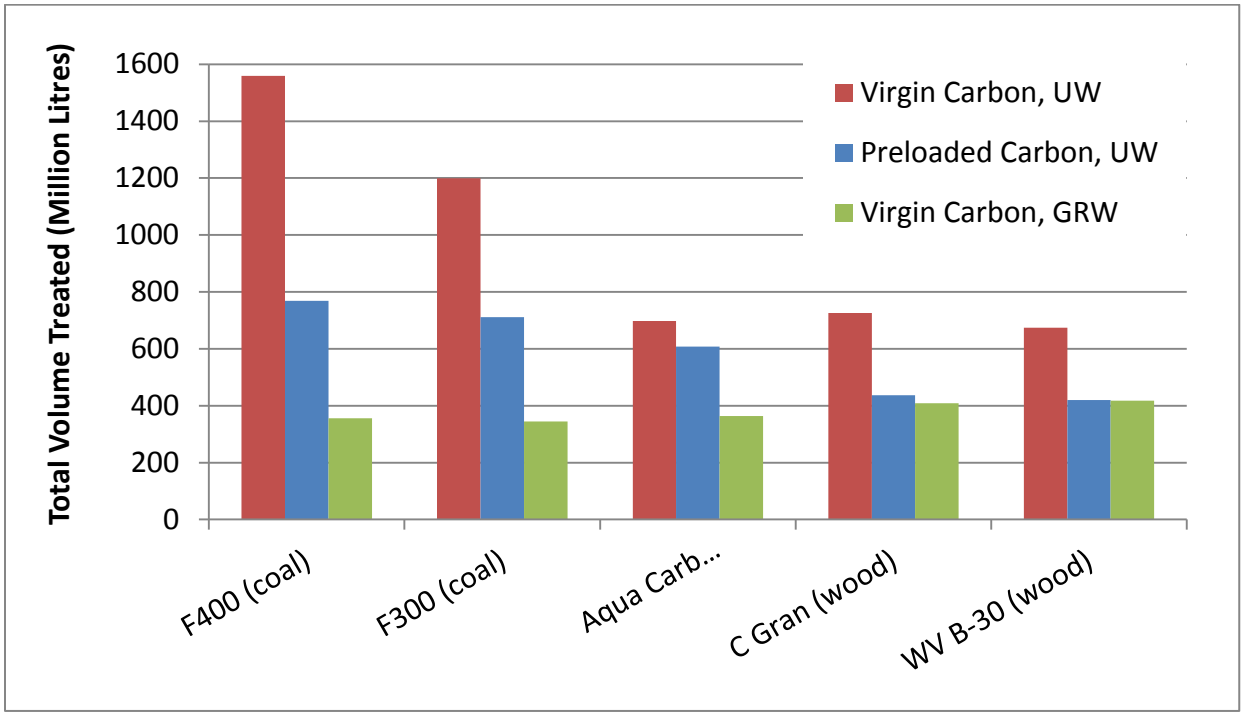

Figure 6.15: ECM predicted total treated volume to breakthrough, for 1000 kg of GAC in a single-solute system with an influent anatoxin-a concentration of 2 µg/L. UW – ultrapure water, GRW – Grand River water

6.5 Conclusions

The adsorption of anatoxin-a from Grand River water by six activated carbons was investigated using the bottle point technique. Based on a comparison of the removal kinetics, the PAC was the fastest adsorbing of the carbons, and its Freundlich isotherm parameters indicate it had the greatest capacity in the

concentration range investigated. However, the differences in application of PAC are such that the full capacity of the PAC may not be utilized, unlike GAC in a flow-through adsorber. Furthermore, the potential for intact cyanobacterial cells to shield toxin from PAC adsorption remains a limitation in the use of PAC for treatment of this toxin. In contrast, GAC is typically located later in a treatment train, and is therefore less likely to encounter cyanobacterial cells which have not yet been lysed, thereby releasing internally contained toxins.

Of the GACs investigated, the coconut- and wood-based carbons had more favourable kinetics than the coal-based carbons when discounting the impact of particle size. All of the carbons had very similar toxin removal at equilibrium, although the isotherms of the coal-based GACs could be distinguished from those of the coconut- and coal based GACs based on the 95% joint confidence regions of the two Freundlich parameters. Compared to other cyanobacterial metabolites in natural water, wood- and coal-based carbons appear to have lower capacity for anatoxin-a than for MC-LR, while the capacities appear comparable (and may even be greater for anatoxin-a) in coconut-based carbons; however, it is important to note the limitations of these comparisons, as isotherms were produced under differing conditions, and changes in background NOM composition, specific carbon properties and adsorbate concentration range can all influence adsorptive capacity. Based on extrapolated Freundlich isotherms, at concentrations below 4 µg/L anatoxin-a is better adsorbed by coconut- and wood-based carbons than MIB.

Considerable toxin losses were observed in the natural water positive controls over the course of the 21-day experiment, and are likely attributable to the higher pH (8.0) of the natural water. Future studies could consider adjusting the pH of the water prior to toxin addition, to minimize degradation of anatoxin-a in its deprotonated, neutral form. Under real world conditions, anatoxin would not appreciably chemically degrade in the less than 30 minutes contact time or so in a GAC contactor. As such, a pH adjustment approach may provide useful information.

Chapter 7
Conclusions and Recommendations

Following a thorough review of drinking water treatment options for the cyanobacterial neurotoxin, anatoxin-a published in the Journal of Water and Health (Vlad et al. 2014), activated carbon adsorption was selected as a promising treatment alternative, which required further investigation. This study examined the adsorptive behaviour of anatoxin-a with six diverse carbons, selected to represent a range of source materials, porosity and grain size: Calgon F400, Calgon F300, Siemens Aqua Carb, Norit C Gran, and MWV WV B-30 granular activated carbons (GACs) and Standard Purification's Watercarb-800 powdered activated carbon (PAC). Initial work compared the available anatoxin-a Receptor Binding Assay (RBA) and LC-MS/MS analytical methods, and led to the establishment of an adaptedliquid chromatography tandem mass spectrometry (LC-MS/MS) method with the reproducibility, specificity, and sensitivity necessary for this treatment investigation. The GACs were assessed based on the rate at which the anatoxin-a was adsorbed (kinetics) and the amount adsorbed at equilibrium (capacity). Both parameters are important in real world applications, one in terms of the ability of the GAC to quickly reduce the anatoxin-a concentration in the event of a substantial contamination event and the other from the point of view of how long the GAC can be depended upon (capacity, as it relates to replacement cost). Isotherm parameters and kinetic data were established under a range of conditions, first using single-solute batch experiments with virgin carbon in ultrapure water, to provide a baseline of adsorption performance and with which to compare to other cyanotoxins and cyanobacterial metabolites. Subsequently, the effects of NOM preloading were studied using GAC preloaded in a pilot setup with post-sedimentation river water in a full-scale drinking water treatment plant in Southern Ontario, and a GAC collected from an operating full-scale GAC adsorber at another plant in Ontario. As with the virgin GAC experiments these were conducted in ultrapure water. Finally, the impact of NOM competition was investigated via batch experiments with virgin carbon, using Grand River water (GRW) as the medium. The findings and summative conclusions which may be drawn from this investigation are outlined below.

7.1 Summary of Conclusions

7.1.1 Anatoxin-a Analytical Methods (Chapter 3)

- Anatoxin-a naturally occurs as the (+)-anatoxin-a stereoisomer; however, most standards are chemically produced as a racemic (50%/50%) mixture of both the (+)- and (-)-anatoxin-a stereoisomers. Therefore, selection of a suitable analytical method must consider the requirements of stereoisomer detection.

- At the present stage of development, the anatoxin-a RBA was not suitable for spiking studies requiring precise and accurate quantification, due to the high variability and non-detection of the (-)-anatoxin-a stereoisomer present in most standards, but may be appropriate for environmental monitoring and presence/absence detection.

- LC-MS/MS methods for anatoxin-a can be rapid, reproducible and sufficiently sensitive to measure environmentally relevant concentrations, but have greater operator training and instrumentation requirements.

- An LC-MS/MS method for anatoxin-a was successfully adapted and implemented, with a method detection limit of 0.65 µg/L without a preconcentration step. This method was capable of detecting, though not separating, both anatoxin-a stereoisomers.

7.1.2 Anatoxin-a Adsorption Behaviour (Chapters 4 – 6)

- In ultrapure water, the virgin coal-based carbons F400 and F300 had the highest equilibrium capacity for anatoxin-a among the tested adsorbents. Preloading reduced the capacity of the coal-based carbons more than that of the other GACs; the relatively low mesopore volume of the coal-based GACs may have led to a proportionately greater pore blockage effect in preloading, as compared to the more mesoporous wood-based GACs. Nevertheless, given their substantially greater initial capacity, the coal-based carbons retained the highest total capacity following preloading, in the anatoxin-a concentration range investigated.

- In GRW, the virgin GAC isotherms were very similar to one another; as expected the PAC isotherm indicated higher capacity for anatoxin-a in the concentration range investigated compared to the GACs.
- The coal-based PAC had the highest capacity and fastest kinetics of any of the carbons investigated in both ultrapure water and GRW; despite this, it is important to note that the experimental conditions used were the same for both the PAC and GAC. In practice, conditions in which PAC is employed differ from those of GAC application, and this has an impact on mass transfer and therefore kinetics. In addition, the full capacity of PAC may not be utilized at full-scale because of the potentially short contact times employed. Furthermore, anatoxin-a contained within intact cyanobacterial cells may not be exposed to PAC applied early in the treatment train, yet may be released if the cells are subsequently lysed, effectively bypassing PAC treatment.
- Of the GACs examined in this study, the wood-based C Gran and WV B-30 adsorbed anatoxin-a most rapidly in ultrapure water in both their virgin and preloaded states. The virgin wood-based carbons had negative or near-neutral surface charges in ultrapure water (pH 6.3) based on their pH_{PZC} values, and were therefore at an advantage in the adsorption of the positively charged anatoxin-a. In GRW, their rate of adsorption was similar to that of the coconut-based Aqua Carb, though still faster than those of the coal-based carbons.
- In all three scenarios examined (virgin carbon in ultrapure water, preloaded carbon in ultrapure water, and virgin carbon in GRW), the coal-based GACs (F400 and F300) required the longest time to reach equilibrium, an observation which may be related to their relatively low mesopore volume (0.13-0.14 cm^3/g, compared to 0.72-0.89 cm^3/g for the wood-based carbons) and in part their surface charge.
- Preloading of GACs with post-sedimentation surface water resulted in reduced capacities for all carbons, as well as converging surface properties. While the virgin carbons had a range of pH_{PZC}

values (4.6 – 10.1), the preloaded GACs all exhibited very similar surface charges (6.9 – 7.2), which impacted the kinetics and adsorptive capacities of the carbons for the cationic anatoxin-a by altering the electrostatic repulsion of positively charged surfaces.

- Preloading increased the rate of anatoxin-a adsorption by the coal-based F400 and F300, compared to their virgin states in ultrapure water. This result may be attributed in part to the effects of changing surface charge; the virgin F400 and F300 had more strongly positive surface charges at the pH level of the ultrapure water than their NOM-preloaded counterparts. This trend was observed to a lesser degree for the other carbons.

- Viewed collectively, the equilibrium results imply that coal-based carbons may be an appropriate selection when targeting anatoxin-a removal. While coal-based carbons had less-favourable kinetics than other carbons under the conditions investigated (indicating a longer mass transfer zone would develop in a GAC bed) this could be mitigated via appropriate contactor design (ensuring sufficient bed depth) and operation.

- Based on preliminary comparisons with other surface water isotherm studies, anatoxin-a may be somewhat less well-removed than microcystin-LR, although it appears to be removed better than the adsorption-recalcitrant microcystin-LA. It is critical to note, however, that differing NOM background concentrations and compositions in the surface waters used to produce the cyanotoxin isotherms, as well as differences in carbon properties, can impact isotherm results. This conclusion is therefore somewhat tentative, given the differing conditions used in the various isotherm studies surveyed as part of this investigation.

- Normalizing kinetic data by mean effective particle size allowed comparisons to be made while disregarding the effects of particle size – isolating the impact of other factors, such as carbon source material (porosity).

- Joint confidence regions (JCRs) can provide valuable information regarding correlated parameter estimates, allowing model fits to be distinguished from one another with greater validity than when using single-parameter confidence intervals.
- Anatoxin-a stability was impacted by the pH of the water matrix tested – while positive controls in ultrapure water (pH 6) remained relatively stable, parallel positive controls in GRW (pH 8) deteriorated by more than 60% over the course of 21 days.

7.2 Recommendations for Future Research

Several issues which may merit further investigation were noted over the course of this research, and future studies may wish to consider the following:

- Batch experiments were used to investigate the adsorption behaviour of anatoxin-a under varying conditions. The trends and effects observed in this study should be validated using column flow-through experiments at pilot scale to confirm adsorption performance, optimize operational parameters and determine scale-up factors as necessary. However, at present the cost of anatoxin-a may be prohibitive in terms of the concentrations required to conduct pilot-scale research.
- While this research included virgin and preloaded carbon, and ultrapure and natural water, there was not sufficient time to explore the adsorption of anatoxin-a by preloaded carbons in natural water. This combination should be investigated for various water matrices.
- Experiments using surface water in this study were conducted using a relatively high-pH water, and experienced significant toxin loss. Future studies should consider adjusting the pH of natural waters to a pH comparable to that of the ultrapure water (6 – 7) prior to the addition of toxin standards.
- Comparisons with adsorption of other cyanobacterial metabolites were drawn based on literature values; however, the different experimental conditions used in determining isotherm values

render conclusive statements regarding relative adsorbability untenable. Multi-solute adsorption experiments containing both anatoxin-a and other cyanotoxins (such as microcystin-LR), and/or single-solute experiments conducted in parallel under identical conditions could provide more definitive evidence of the relative treatability of each compound using activated carbon.

- The adsorptive behaviour of the anatoxin-a analogue, homoanatoxin-a, has not yet been considered; while anatoxin-a is the more prevalent of the two, homoanatoxin-a is also a globally-detected neurotoxin.
- Biodegradation of anatoxin-a using biofiltration may be a viable treatment option, although limited information is available in the peer-reviewed literature. An understanding of biofiltration potential for treating anatoxin-a may help to provide a more complete picture of the value of biologically active filters.
- A positive control, processed alongside samples, could be included in trials using SPE as per the Enhanced Sensitivity protocol of the anatoxin-a RBA method, to allow losses due to this extraction step to be quantified.
- Finally, the LC-MS/MS protocol utilized in this study may be extended to include a solid-phase extraction (SPE) preconcentration step, prior to LC-MS/MS analysis, if greater sensitivity is required.

References

Abnova. 2015. Microcystin-LR ELISA Kit. Catalog No. KA1496, Version 6 1–12. Available at: <www.abnova.com/protocol_pdf/KA1496.pdf> (accessed February 15, 2015).

Abraxis. 2013a. Anatoxin-a in Freshwater Enhanced Sensitivity (ES) Kit. Product No. 520051 (Version 05/14/13):1–2. Available at: <www.abraxiskits.com/uploads/products/docfiles/428_Anatoxin-a Sample Conc_Bulletin R060513.pdf> (accessed August 02, 2013).

Abraxis. 2013b. Anatoxin-a Receptor-Binding Assay (Microtiter Plate). Product No. 520050, Update 04/09/13 1–2. Available at: <http://www.abraxiskits.com/uploads/products/docfiles/425_Anatoxin-a Receptor Binding Assay Insert 040913.pdf> (accessed August 02, 2013).

Abraxis. 2015a. Cylindrospermopsin ELISA (Microtiter Plate). Product No. 522011 1–2. Available at: <www.abraxiskits.com/wp-content/uploads/2015/02/Cylindrospermopsin-Insert-R021215.pdf> February 15, 2015).

Abraxis. 2015b. Microcystins (ADDA)-DM ELISA (Microtiter Plate). Product No. 522015, (Update 01/26/15):1–2. Available at: <www.abraxiskits.com/wp-content/uploads/2015/01/AMicrocystins-DM-PL-Users-Guide-ETV-R150126.pdf> (accessed February 15, 2015).

Abraxis. 2015c. Microcystins-ADDA ELISA (Microtiter Plate). Product No. 520011 1–2. Available at: <www.abraxiskits.com/wp-content/uploads/2014/08/Microcystin-PL-ADDA-Users-Guide-ETV-R082714.pdf> (accessed February 15, 2015).

Abraxis. 2015d. Saxitoxin (PSP) ELISA , Microtiter Plate. Product No. 52255B (Version 04/24/14):1–2. Available at: <www.abraxiskits.com/wp-content/uploads/2014/04/STXplateinsertR042414.pdf> (accessed February 15, 2015).

Adams, C., Roberson, J. A., Rosen, J., Bench, R. 2014. Development of AWWA's Contaminant Candidate List 4 (CCL4) recommendations. Proceedings of the 2014 Water Quality & Technology Conference, New Orleans, USA.

Adeyemo, O. M., Sirén, a L. 1992. Cardio-respiratory changes and mortality in the conscious rat induced by (+)- and (+/-)-anatoxin-a. Toxicon, vol. 30, no. 8, p.899–905.

Afzal, A., Oppenländer, T., Bolton, J. R., El-Din, M. G. 2010. Anatoxin-a degradation by Advanced Oxidation Processes: vacuum-UV at 172 nm, photolysis using medium pressure UV and UV/H2O2. Water Research, vol. 44, no. 1, p.278–286.

Al Momani, F. 2007. Degradation of cyanobacteria anatoxin-a by advanced oxidation processes. Separation and Purification Technology, vol. 57, no. 1, p.85–93.

Astrachan, N., Archer, B., Hilbelink, D. 1980. Evaluation of the subacute toxicity and teratogenicity of anatoxin-a. Toxicon, vol. 18, p.684–688.

Aviva Systems Biology. 2015. Microcystin-LR ELISA Kit. Catalog No. OKVA00009 1–5. Available at: <www.avivasysbio.com/media/pdf/products/OKVA00009.pdf> (accessed February 15, 2015).

Ballot, A., Pflugmacher, S., Wiegand, C., Kotut, K., Krienitz, L. 2003. Cyanobacterial toxins in Lake Baringo, Kenya. Limnologica - Ecology and Management of Inland Waters, vol. 33, no.1, p.2–9.

Bernazeau, F., Baudin, I., Pieronne, P., Bruchet, A., Anselme, C. 1995. Traitement des problèmes des toxines générées par les algues. TSM. Techniques sciences méthodes, génie urbain génie rural, vol. 10, p.747–748.

Biorbyt. 2015. Microcystin ELISA Kit. Catalog No. orb59527 1–3. Available at: <www.biorbyt.com/ProductDatasheet/orb59527/554> (accessed February 15, 2015).

Bogialli, S., Bruno, M., Curini, R., Di Corcia, A., & Laganà, A. 2006. Simple and rapid determination of anatoxin-a in lake water and fish muscle tissue by liquid-chromatography-tandem mass spectrometry. Journal of Chromatography. A, vol.1122, no.1-2), p.180–5.

Bruchet, A., Bernazeau, F., Baudin, I., Pieronne, P. 1998. Algal toxins in surface waters: analysis and treatment. Water Supply, vol. 16, no.1/2, p.611–623.

Burns, J. 2005. CyanoHABs – The Florida Experience. In International Symposium on Cyanobacterial Harmful Algal Blooms. Durham, NC, USA, 09/6–09/10.

Cadel-Six, S., Peyraud-Thomas, C., Brient, L., de Marsac, N. T., Rippka, R., Méjean, A. 2007. Different genotypes of anatoxin-producing cyanobacteria coexist in the Tarn River, France. Applied and Environmental Microbiology, vol. 73, no. 23, p.7605–7614.

Carlile P.R. 1994. Further studies to investigate microcystin-LR and anatoxin-a removal from water. Foundation for Water Research Report, FR 0458, Swindon, UK.

Carmichael, W., Gorham, P. 1978. Anatoxins from clones of Anabaena flos-aquae isolated from lakes of western Canada. Mitteilungen Internationale Vereinigung für Theoretische und Angewandte Limnologie, vol. 21, p.285–295.

Carrasco, D., Moreno, E., Paniagua, T., Hoyos, C. De, Wormer, L., Sanchis, D., Cires, S., Martin-del-Pozo, D., Codd, G., Quesada, A. 2007. Anatoxin-a occurrence and potential cyanobacterial anatoxin-a producers in Spanish reservoirs. Journal of Phycology, vol. 43, no. 6, p.1120–1125.

Carrière, A., Prévost, M., Zamyadi, A., Chevalier, P., Barbeau, B. 2010. Vulnerability of Quebec drinking-water treatment plants to cyanotoxins in a climate change context. Journal of Water and Health, vol. 8, no. 3, p.455–465.

Chang, C.-Y., Hsieh, Y.-H., Cheng, K.-Y., Hsieh, L.-L., Cheng, T.-C., Yao, K.-S. 2008. Effect of pH on Fenton process using estimation of hydroxyl radical with salicylic acid as trapping reagent. Water Science and Technology, vol. 58, no. 4, p. 873–879.

Chen, G., Dussert, B., Suffet, I. 1997. Evaluation of granular activated carbons for removal of methylisoborneol to below odor threshold concentration in drinking water. Water Research, vol. 31, no. 5, p. 1155-1163.

Chorus, I., 2012. Current approaches to cyanotoxin risk assessment, risk management and regulations in different countries. Federal Environment Agency, Germany, Dessau-Roßlau. Available at: <http://www.uba.de/uba-info-medien-e/4390.html> (accessed February 25, 2014).

Cook, D., Newcombe, G. 2002 Removal of microcystin variants with powdered activated carbon. Water Science and Technology, vol. 2, no.5-6, p. 201-207.

Cousins, I., Bealing, D., James, H., Sutton, A. 1996. Biodegradation of microcystin-LR by indigenous mixed bacterial populations. Water Research, vol. 30, no. 2, p. 481–485.

Crittenden, J. C., Trussell, R. R., Hand, D. W., Howe, K. J., Tchobanoglous, G. 2012. MWH's Water Treatment Principles and Design. 3rd Edition. John Wiley & Sons.

Croft, J., 2012. Natural organic matter characterization of different source and treated waters; implications for membrane fouling control. Master's thesis, Department of Civil Engineering, University of Waterloo, Waterloo, Canada.

Delgado, L. F., Charles, P., Glucina, K., Morlay, C. 2012. The Removal of Endocrine Disrupting Compounds, Pharmaceutically Activated Compounds and Cyanobacterial Toxins during Drinking Water Preparation Using Activated Carbon--a Review. Science of the Total Environment, vol. 435-436, p. 509–525.

Department of Public Utilities. 2014. Micrycistin Event Preliminary Summary, Monday, August 4, 2014. City of Toledo. Available at: <http://toledo.oh.gov/media/132055/Microcystin-Test-Results.pdf> (accessed April 11, 2015).

Droste, R. L. 1997. Theory and Practice of Water and Wastewater Treatment. Hoboken, NJ: John Wiley & Sons, Inc.

Edwards, C., Beattie, K., Scrimgeour, C. M., Codd, G. 1992. Identification of anatoxin-A in benthic cyanobacteria (blue-green algae) and in associated dog poisonings at Loch Insh, Scotland. Toxicon, vol. 30, no. 10, p. 1165–1175.

Envirologix. 2010. QuantiPlate(TM) Kit for Microcystins. Catalog No. EP 022, Rev 07-01-10 1–7. Available at: <www.envirologix.com/library/ep022insert.pdf> (accessed February 15, 2015).

Environment Canada - Manitoba Water Stewardship. 2011. State of Lake Winnipeg: 1999 to 2007. Report of Environment Canada. Ottawa, ON, Canada, p. 1–209.

Enzo Life Sciences. 2012. Product Manual - Microcystins-ADDA ELISA (Microtiter Plate). Catalog No. ALX-850-319, Rev. 01/31/2015 1–12. Available at: <static.enzolifesciences.com/fileadmin/files/manual/ALX-850-319_insert.pdf> (accessed February 15, 2015).

Faassen, E. J., Harkema, L., Begeman, L., Lurling, M. 2012. First report of (homo)anatoxin-a and dog neurotoxicosis after ingestion of benthic cyanobacteria in The Netherlands. Toxicon, vol. 60, no. 3, p. 378–384.

Fawell, J. K., Mitchell, R. E., Hill, R. E., Everett, D. J. 1999. The toxicity of cyanobacterial toxins in the mouse: II anatoxin-a. Human & Experimental Toxicology, vol. 18, no. 3, p. 168–173.

Fischer, W. J., Garthwaite, I., Miles, C. O., Ross, K. M., Aggen, J. B., Chamberlin, A. R., Towers, N.R., Dietrich, D. R. 2001. Congener-Independent Immunoassay for Microcystins and Nodularins. Environmental Science and Technology, vol. 35, p.4849–4856.

Fortin, N., Aranda-Rodriguez, R., Jing, H., Pick, F., Bird, D., Greer, G. W. 2010. Detection of Microcystin-Producing Cyanobacteria in Missisquoi Bay, Quebec, Canada, Using Quantitative PCR. Applied and Environmental Microbiology, vol. 76, no.15, p.5105–5112.

Fristachi, A., Sinclair, J. L., Hall, S., Berkman, J. A. H., Boyer, G., Burkholder, J., Burns, J., Carmichael, W., DuFour, A., Frazier, W., Morton, S., O'Brien, E.,Walker, S. 2008. Occurrence of Cyanobacterial Harmful Algal Blooms Workgroup Report. In K. H. Hudnell (Ed.), Cyanobacterial Harmful Algal Blooms: State of the Science and Research Needs. Springer Press. Triangle Park, NC, USA, p. 45–103.

Fromme, H., Kohler, A., Krause, R., Fuhrling, D. 2000. Occurrence of Cyanobacterial Toxins — Microcystins and Anatoxin-a — in Berlin Water Bodies with Implications to Human Health and Regulations. Environmental Toxicology, vol. 15, no.2, p.120–130.

Furey, A., Crowley, J., Lehane, M., James, K. J. 2003. Liquid chromatography with electrospray ion-trap mass spectrometry for the determination of anatoxins in cyanobacteria and drinking water. Rapid Communications in Mass Spectrometry, vol. 17, no. 6, p. 583-588.

Graham, J. L., Loftin, K. A., Meyer, M. T., & Ziegler, A. C. 2010. Cyanotoxin mixtures and taste-and-odor compounds in cyanobacterial blooms from the Midwestern United States. Environmental Science & Technology, vol. 44, no. 19, p.7361-7368

Gijsbertsen-Abrahamse, A., Schmidt, W., Chorus, I., & Heijman, S. 2006. Removal of cyanotoxins by ultrafiltration and nanofiltration. Journal of Membrane Science, vol. 276, no.1-2, p. 252–259.

Global Water Research Coalition. 2012. International Guidance Manual for the Management of Toxic Cyanobacteria. IWA Publishing. London, UK.

Haddix, P. L., Hughley, C. J., LeChevallier, M. W. 2007. Occurrence of Microcystins in 33 US Water Supplies. Journal of the American Water Works Association, vol. 99, no. 9, p. 118–125.

Hall, T., Hart, J., Croll, B., Gregory, R. 2000. Laboratory-scale investigations of algal toxin removal by water treatment. Water and Environment, vol. 14, no. 2, p. 143–149.

Hand, D. W., Crittenden, J. C., Hokanson, D. R., & Bulloch, J. L. 1997. Predicting the performance of fixed-bed granular activated carbon adsorbers. Water science and technology, vol. 35, no. 7, p.235-241.

Hart, J., Fawell, J., Croll, B. & Marsalek, B. 1998. Algal toxins in surface waters: origins and removal during drinking water treatment processes. Water Supply, vol. 16, no. 1/2, p. 611–623.

Hitzfeld, B. C., Höger, S. J., Dietrich, D. R. 2000. Cyanobacterial toxins: removal during drinking water treatment, and human risk assessment. Environmental Health Perspectives, vol. 108, (Supplement 1), p. 113–122.

Ho, L., Dreyfus, J., Boyer, J., Lowe, T., Bustamante, H., Duker, P., Meli, T., Newcombe, G. 2012. Fate of cyanobacterial and their metabolites during drinking water treatment sludge management processes. Science of the Total Environment, vol. 424, p. 232-238.

Ho, Y., McKay, G. 1999. Pseudo-second order model for sorption processes. Process Biochemistry, vol. 34, no. 5, p.451-465

Ho, L., Newcombe, G. 2007. Evaluating the adsorption of microcystin toxins using granular activated carbon (GAC). Journal of Water Supply: Research and Technology—AQUA, vol. 56, no. 5, p.281-291

Ho, L., Slyman, N. 2008. Optimizing PAC and chlorination practices for cylindrospermopsin removal. Journal American Water Works Association, vol. 100, no. 11, p.88-96

Ho, L., Newcombe, G. 2010. Granular Activated Carbon Adsorption of 2-Methylisoborneol (MIB): Pilot- and Laboratory-Scale Evaluations. Journal of Environmental Engineering, vol. 136, no. 9, p. 965-974

Ho, L., Sawade, E., Newcombe, G. 2012. Biological treatment options for cyanobacteria metabolite removal - a review. Water Research, vol. 46, no. 5, p. 1536–1548.

Hoeger, S. J., Hitzfeld, B. C., Dietrich, D. R. 2005. Occurrence and elimination of cyanobacterial toxins in drinking water treatment plants. Toxicology and Applied Pharmacology, vol. 203, no. 3, p.231–242.

Huber, S. A., Balz, A., Abert, M., Pronk, W. 2011. Characterisation of aquatic humic and non-humic matter with size-exclusion chromatography – organic carbon detection – organic nitrogen detection (LC-OCD-OND). Water Research, vol. 45, no. 2, p. 879-885.

Huber, M.M., Ternes, T.A., von Gunten, U. 2004. Removal of estrogenic activity and formation of oxidation products during ozonation of 17alpha-ethinylestradiol. Environmental Science and Technology, vol. 38, no. 19, p. 5177-5186.

Institut National de Santé Publique du Québec. 2005. Propositions de critères d'intervention et de seuils d'alerte pour les cyanobactéries. Available at: <http://www.inspq.qc.ca/pdf/publications/348-CriteresInterventionCyanobacteries.pdf> (accessed December 23 2013).

Jin, X., Peldszus, S., Huck, P. M. 2012. Reaction kinetics of selected micropollutants in ozonation and advanced oxidation processes. Water Research, vol. 46, no. 19, p. 6519–6530.

Kaminski, A., Bober, B., Lechowski, Z. & Bialczyk, J. 2013. Determination of anatoxin-a stability under certain abiotic factors. Harmful Algae, vol. 28, p. 83–87.

Keijola, A. M., Himberg, K., Esala, A. L., Sivonen, K., Hiisvirta, L. 1988. Removal of cyanobacterial toxins in water treatment processes: laboratory and pilot scale experiments. Toxicity Assessment, vol. 3, p. 643–656.

Kiviranta, J., Sivonen, K., Lahti, K. 1991. Production and biodegradation of cyanobacterial toxins-a laboratory study. Archiv für Hydrobiologie, vol. 121, no. 3, p. 281–294.

Klein, A. Reply from Abcam to Your Enquiry Regarding ab80369 [CCE1799724]. Personal communication, February 12, 2013.

Klitzke, S., Beusch, C., Fastner, J. 2011. Sorption of the cyanobacterial toxins cylindrospermopsin and anatoxin-a to sediments. Water Research, vol. 45, no. 3, p. 1338–1346.

Kotak, B. G., Zurawell, R. W. 2007. Cyanobacterial toxins in Canadian freshwaters: A review. Lake and Reservoir Management, vol. 23, no. 2, p. 109–122.

Lee, Y., von Gunten, U. 2012. Quantitative structure-activity relationships (QSARs) for the transformation of organic micropollutants during oxidative water treatment. Water Research, vol. 46, no. 19, p. 6177–6195.

Makdissy, G., Huck, P.M., Reid, M.M., Leppard, G.G., Haberkamp, J., Jekel, M., Peldszus, S. 2010. Investigating the fouling layer of polyamide nanofiltration membranes treating two different natural waters: Internal heterogeneity yet converging surface properties. Journal of Water Supply: Research and Technology – AQUA, vol. 59, no. 2-3, p. 164 -178.

Manitoba Water Stewardship. 2011. State of Lake Winnipeg: 1999 to 2007. Environment Canada. p. 1–209.

Merel, S., Clement, M., Thomas, O., 2010. State of the art on cyanotoxins in water and their behaviour towards chlorine. Toxicon, vol. 55, p. 677-691.

Merel, S., Villarín, M.C., Chung, K., Snyder, S., 2013a. Spatial and thematic distribution of research on cyanotoxins. Toxicon, vol. 76, p. 118-131.

Merel, S., Walker, D., Chicana, R., Snyder, S., Baurès, E., & Thomas, O. 2013b. State of knowledge and concerns on cyanobacterial blooms and cyanotoxins. Environment International, vol. 59, p. 303–327.

Michalak,Am. M., Anderson, E. J., Beletsky, D., Boland, S., Bosch, N. S., Bridgeman, T. B., Chaffin, J. D., Cho, K., Confesor, R., Daloglu, I., Depinto, J. V., Evans, M. A., Fahnenstiel, G. L., He, L., Ho, J. C., Jenkins, L., Johengen, T. H., Kuo, K. C., Laporte, E., Liu, X., McWilliams, M. R., Moore, M. R., Posselt, D. J., Richards, R. P., Scavia, D., Steiner, A. L., Verhamme, E., Wright, D. M., Zagorski, M. A. 2013. Record-setting algal bloom in Lake Erie caused by agricultural and meteorological trends consistent with expected future conditions. Proceedings of the National Academy of Sciences of the U.S.A., vol. 110, no. 16, p. 6448–6452.

Monosov, I., Bazri, M., Imoberdorf, G., Vazquez-Rodriguez, G. A., Barbeau, B., Mohseni, M. 2012. Removal of cyanobacterial toxins and NOM using ion exchange resins. Proceedings, AWWA- Water Quality and Technology Conference, November 2012, Toronto, Canada.

Mouchet, P., Bonnelye, V. 1998. Solving algae problems: French expertise and world-wide applications. Journal of Water Supply: Research and Technology—AQUA, vol. 47, no. 3, p. 125–141.

New Zealand Ministry of Health. 2008. Drinking-water Standards for New Zealand 2005 (Revised 2008) 1–163. Available at: < http://www.health.govt.nz/publication/drinking-water-standards-new-zealand-2005-revised-2008-0> (Accessed December 23, 2013).

Newcombe, G., Nicholson, B. 2004. Water treatment options for dissolved cyanotoxins. Journal of Water Supply: Research and Technology—AQUA, vol. 53, no. 4, p. 227–239.

Oehrle, S. A, Southwell, B., Westrick, J. 2010. Detection of various freshwater cyanobacterial toxins using ultra-performance liquid chromatography tandem mass spectrometry. Toxicon, vol. 55, no. 5, p. 965–972.

Onstad, G. D., Strauch, S., Meriluoto, J., Codd, G., Von Gunten, U. 2007. Selective oxidation of key functional groups in cyanotoxins during drinking water ozonation. Environmental Science & Technology, vol. 41, no. 12, p. 4397–4404.

Oregon Health Authority. 2013. Oregon Drinking Water Services Best Management Practices for Harmful Algae Blooms (HABs) for Drinking Water Providers 1-3. Available at: <http://public.health.oregon.gov/HealthyEnvironments/DrinkingWater/Operations/Treatment/Documents/algae/BMP-HABs.pdf> (Accessed February 25, 2014).

Osswald, J., Rellán, S., Gago, A., Vasconcelos, V. 2007. Toxicology and detection methods of the alkaloid neurotoxin produced by cyanobacteria, anatoxin-a. Environment International, vol. 33, no. 8, p. 1070–1089.

Ou, H., Gao, N., Deng, Y., Qiao, J., Wang, H. 2012. Immediate and Long-Term Impacts of UV-C Irradiation on Photosynthetic Capacity, Survival and Microcystin-LR Release Risk of Microcystis Aeruginosa. Water Research, vol. 46, no. 4, p. 1241–1250.

Paerl, H. W., Paul, V. J. 2012. Climate change: links to global expansion of harmful cyanobacteria. Water Research, vol. 46, no. 5, p. 1349-1363.

Pantelić, D., Svirčev, Z., Simeunović, J., Vidović, M., Trajković, I., 2013. Cyanotoxins: Characteristics, production and degradation routes in drinking water treatment with reference to the situation in Serbia. Chemosphere, vol. 91, p. 421-441.

Park, H., Kim, B., Kim, E., Okino, T. 1998. Hepatotoxic microcystins and neurotoxic anatoxin-a in cyanobacterial blooms from Korean lakes. Environmental Toxicology and Water Quality, vol. 13, no. 3, p. 225–234.

Pirbazari, M., Ravindran, V., Badriyha, B. N., Craig, S., McGuire, M. J. 1993. GAC adsorber design protocol for the removal of off-flavors. Water Research, vol. 27, no. 7, p.1153-1166.

Puschner, B., Hoff, B., Tor, E. R. 2008. Diagnosis of anatoxin-a poisoning in dogs from North America. Journal of Veterinary Diagnostic Investigation, vol. 20, no. 1, p. 89–92.

Rapala, J., Lahti, K., Sivonen, K., Niemela, S. I. 1994. Biodegradability and adsorption on lake sediments of cyanobacterial hepatotoxins and anatoxin-a. Letters in Applied Microbiology, vol. 19, p. 423–428.

Rellán, S., Osswald, J., Vasconcelos, V., Gago-Martinez, A. 2007. Analysis of anatoxin-a in biological samples using liquid chromatography with fluorescence detection after solid phase extraction and solid phase microextraction. Journal of Chromatography A, vol. 1156, p.134–140.

Rice, E. W., Baird, R. B., Eaton, A. D., Clesceri, L. S., Editors. 2012. Standard Methods for the Examination of Water and Wastewater. 22nd ed. American Public Health Association.

Robert, C., Tremblay, H., Deblois, C. 2005. Cyanobactéries et cyanotoxines au Québec: suivi à six stations de production d'eau potable (2001-2003), Report of the Québec Ministère du Développement durable, de l'Environnement et des Parcs, p. 1–65.

Robertson, P. K. J., Lawton, L. A., Munch, B., Cornish, B. 1999. The Destruction of Cyanobacterial Toxins by Titanium Dioxide. Journal of Advanced Oxidation Technology, vol. 4, no. 1, p. 20–26.

Rodríguez, E. M., Acero, J. L., Spoof, L., Meriluoto, J. 2008. Oxidation of MC-LR and -RR with Chlorine and Potassium Permanganate: Toxicity of the Reaction Products. Water Research, vol. 42, no.6-7, p.1744–1752.

Rodríguez, E., Onstad, G. D., Kull, T. P. J., Metcalf, J. S., Acero, J. L., & Von Gunten, U. 2007a. Oxidative elimination of cyanotoxins: comparison of ozone, chlorine, chlorine dioxide and permanganate. Water Research, vol. 41, p.3381–3393

Rodríguez, E., Sordo, A., Metcalf, J. S., Acero, J. L. 2007b. Kinetics of the oxidation of cylindrospermopsin and anatoxin-a with chlorine, monochloramine and permanganate. Water Research, vol. 41, no. 9, p. 2048–2056.

Rositano, J., Newcombe, G., Nicholson, B., Sztajnbok, P. 2001. Ozonation of NOM and algal toxins in four treated waters. Water Research, vol. 35, no. 1, p. 23–32.

Rositano, J., Nicholson, B. C., Pieronne, P. 1998. Destruction of cyanobacterial toxins by ozone. Ozone: Science & Engineering, vol. 20, no. 3, p. 223–238.

Rouquerol, J., Avnir, D., Fairbridge, C.W., Everett, D.H., Haynes, J.H., Pernicone, N., Ramsay, J.D.F., Sing, K.S.W., Unger, K.K. 1994. Recommendations for the characterization of porous solids. International Union of Pure and Applied Chemistry. Pure & Applied Chemistry, vol. 66, no. 8, p.1739-1758.

Rubio, F., Kamp, L., Carpino, J., Faltin, E., Loftin, K., Molgo, J., Araoz, R. 2014. Colorimetric Microtiter Plate Receptor-Binding Assay for the Detection of Freshwater and Marine Neurotoxins Targeting the Nicotinic Acetylcholine Receptors. Toxicon, vol. 91, p.45–56.

Ruiz, M., Galanti, L., Ruibal, A. L., Rodriguez, M. I., Wunderlin, D. A., Amé, M. V. 2013. First report of microcystins and anatoxin-a co-occurrence in san roque reservoir (Córdoba, Argentina). Water, Air, & Soil Pollution, vol. 224, no. 6, p. 1593.

Shams, S., Capelii, C., Cerasino, L., Ballot, A., Dietrich, D. R., Sivonen, K., Salmaso, N. 2015. Anatoxin-a producing *Tychonema* (Cyanobacteria) in European waterbodies. Water Research, vol. 69, p. 68-79

Sontheimer, H, Crittenden, J.C., Summers, R.S.. 1988. Activated carbon for water treatment. DVGW-Forschungsstelle, Engler-Bunte-Institut, Universitat Karlsruhe (TH), p. 1-722

Sorlini, S., Collivignarelli, C. 2011. Microcystin-LR removal from drinking water supplies by chemical oxidation and activated carbon adsorption. Journal of Water Supply: Research and Technology—AQUA, vol. 60, no. 7, p.403-411

Sorlini, S., Gialdini, F., Collivignarelli, C. 2013. Removal of Cyanobacterial Cells and Microcystin-LR from Drinking Water Using a Hollow Fiber Microfiltration Pilot Plant. Desalination, vol. 309, p.106–112.

Spoof, L. 2005. Microcystins and Nodularins. In Cyanobacterial Monitoring and Cyanotoxin Analysis, edited by Jussi Meriluoto and Codd. Åbo Akademis Forlang – Åbo Akademi University Press. p. 15–40.

Summers, R.S. 1986. Activated carbon adsorption of humic substances: Effect of molecular size and heterodispersity. PhD thesis, Department of Civil Engineering, Stanford University.

Stevens, D., Krieger, R. 1991. Stability studies on the cyanobacterial nicotinic alkaloid anatoxin-a. Toxicon, vol. 29, no. 2, p. 167–179.

Teixeira, M. R., Rosa, M. J. 2006. Neurotoxic and hepatotoxic cyanotoxins removal by nanofiltration. Water Research, vol. 40, no. 15, p. 2837–2846.

Teixeira, M. R., Rosa, M. J. 2011. Adsorption of microcystins and anatoxin-a on nanofiltration membranes. Proceedings, 6th IWA Specialist Conference on Membrane Technology for Water & Wastewater Treatment. International Water Association. Aachen, Germany.

Teixeira, M. R., Rosa, M. J. 2012. How does the adsorption of microcystins and anatoxin-a on nanofiltration membranes depend on their co-existence and on the water background matrix. Water Science & Technology, vol. 66, no. 5, p. 976–982.

Triantis, T., Tsimeli, K., Kaloudis, T., Thanassoulias, N, Lytras, E., Hiskia, A. 2010. Development of an Integrated Laboratory System for the Monitoring of Cyanotoxins in Surface and Drinking Waters. Toxicon, vol. 55, no. 5, p.979–989.

UKWIR. 1996. Pilot Scale GAC Tests to Evaluate Toxin Removal. Report Ref. No. 96/DW/07/1. UK Water Industry Research Limited. London, UK. p. 1–8.

USEPA. 2001. Creating a Cyanotoxin Target List for the Unregulated Contaminant Monitoring Rule, Report of the USEPA,Cincinnati.

USEPA. 2012. Contaminant Candidate List 3 – CCL. Water: Contaminant Candidate List. <water.epa.gov/scitech/drinkingwater/dws/ccl/ccl3.cfm#ccl3> (accessed November 10, 2013).

Valentine, W. M., Schaeffer, D. J., Beasley, V. R. 1991. Electromyographic assessment of the neuromuscular blockade produced in vivo by anatoxin-a in the rat. Toxicon, vol. 29, no. 3, p. 347–357.

van Apeldoorn, M., van Egmond, H., Speijers, G., Bakker, G. 2007. Toxins of cyanobacteria. Molecular Nutrition & Food Research, vol. 51, no. 1, p. 7-60

Vlad, S., Anderson, W.B., Peldszus, S., Huck, P.M. 2014. Removal of the cyanotoxin anatoxin-a by drinking water treatment processes: a review. Journal of Water and Health, vol. 12, no. 4, p. 601-617

Watanabe, M., Tsujimura, S., Oishi, S. 2003. Isolation and identification of homoanatoxin-a from a toxic strain of the cyanobacterium Raphidiopsis mediterranea Skuja isolated from Lake Biwa, Japan. Phycologia, vol. 42, no. 4, p. 364–369.

Westrick, J., Szlag, D. C., Southwell, B. J., Sinclair, J. 2010. A review of cyanobacteria and cyanotoxins removal/inactivation in drinking water treatment. Analytical and Bioanalytical Chemistry, vol. 397, no. 5, p.1705–1714

WHO. 1999. Toxic cyanobacteria in water: a guide to their public health consequences, monitoring and management. Available at:

<http://www.who.int/water_sanitation_health/resourcesquality/toxicyanbact/en/> (Accessed December 23, 2013).

Wonnacott, S., Swanson, K. 1992. Homoanatoxin: a potent analogue of anatoxin-a. Biochemical Pharmacology, vol. 43, no. 3, p. 419–423.

Wood, S. a., Rasmussen, J. P., Holland, P. T., Campbell, R., Crowe, A. L. M. 2007. First report of the cyanotoxin anatoxin-a from Aphanizomenon Issatschenkoi (cyanobacteria). Journal of Phycology, vol. 43, no. 2, p. 356–365.

Worch, E. 2012. Adsorption Technology in Water Treatment. p. 1–332. Germany: De Gruyter.

Xagoraraki, I., Harrington, G. W. 2006. Inactivation Kinetics of the Cyanobacterial Toxin Microcystin-LR by Free Chlorine. Journal of Environmental Engineering, vol. 132, no.7, p. 818–823.

Yang, X. 2007. Occurrence of the cyanobacterial neurotoxin, Anatoxin-a, in the Lower Great Lakes. PhD Thesis. Statue University of New York.

Yu, Z., Peldszus, S., Huck, P. M. 2009. Adsorption of Selected Pharmaceuticals and an Endocrine Disrupting Compound by Granular Activated Carbon. Environmental Science and Technology, vol. 29, no. 5, p. 1467-1473.

Zamyadi, A. MacLeod, S. L., Fan, Y., McQuaid, N., Dorner, S., Sauve, S., Prevost, M. 2012. Toxic Cyanobacterial Breakthrough and Accumulation in a Drinking Water Plant: A Monitoring and Treatment Challenge. Water Research, vol. 46, no. 5, p.1511–1523.

Zamyadi, A., Dorner, S., Sauve, S., Ellis, D., Bolduc, A., Bastien, C., Prevost, M. 2013. Species-Dependence of Cyanobacteria Removal Efficiency by Different Drinking Water Treatment Processes. Water Research, vol. 47, no. 8, p. 2689–2700.

Zhou, H., Smith, D. 2002. Advanced technologies in water and wastewater treatment. Journal of Environmental Engineering and Science, vol. 1, no. 4, p. 247–264.

Appendix A

Additional LC-MS/MS Method Validation Data

Table A-1: LC-MS/MS MDL data

Sample	Anatoxin-a Spiking Concentration (µg/L)	Concentration - average of triplicate measurements (µg/L)
1	5.0	4.618
2	5.0	4.642
3	5.0	4.354
4	5.0	4.388
5	5.0	4.618
6	5.0	4.484
7	5.0	4.058
	Cumulative average	**4.451**
	Standard deviation	**0.209**
	Relative standard deviation	**4.68%**

Table A-2: LC-MS/MS reproducibility data

Sample	Anatoxin-a Spiking Concentration (µg/L)	Concentration - average of triplicate measurements (µg/L)
1	10.0	10.05
2	10.0	9.79
3	10.0	9.66
4	10.0	9.77
5	10.0	9.85
6	10.0	9.83
7	10.0	9.94
	Cumulative average	**9.84**
	Standard deviation	**0.125**
	Relative standard deviation	**1.27%**

Appendix B
Linearly Determined Kinetic Parameters

Table B-1: Linearly determined pseudo-first order kinetic model parameters for virgin carbon in ultrapure water

Carbon	q_e experimental	ln q_e	q_e calculated	k_1	R^2
F400	1.99	0.64	1.90	0.04	0.9978
F300	1.99	0.72	2.05	0.06	0.9734
Aqua Carb	1.91	0.80	2.22	0.11	0.8778
C-Gran	1.96	-0.09	0.92	0.12	0.8928
WV B-30	1.99	-0.19	0.82	0.15	0.8698
PAC	2.00	-2.89	0.06	0.24	0.5698

Table B-22: Linearly determined pseudo-second order kinetic model parameters for virgin carbon in ultrapure water

Carbon	q_e (µg/mg)	q_e experimental	k_2 (mg/µg/day)	ϑ (µg/mg/day)	R^2
F400	2.11	1.99	0.066	0.29	0.9836
F300	2.08	1.99	0.046	0.20	0.9638
Aqua Carb	2.15	1.91	0.072	0.33	0.9914
C-Gran	1.99	1.96	0.695	2.76	0.9997
WV B-30	2.02	1.99	0.529	2.17	0.9996
PAC	1.99	2.00	55.867	222.22	1.0000

Table B-3: Linearly determined pseudo-second order kinetic model parameters for preloaded carbon in ultrapure water

Carbon	q_e (µg/mg)	q_e experimental	k_2 (mg/µg/day)	ϑ (µg/mg/day)	R^2
F400	2.20	1.96	0.115	0.56	0.9967
F300	2.27	1.93	0.064	0.33	0.9983
Aqua Carb	1.99	1.78	0.081	0.32	0.9787
C-Gran	2.02	1.89	0.486	1.99	0.9983
WV B-30	2.02	1.79	0.307	1.26	0.9937
F300 - utility	1.93	1.60	0.058	0.22	0.9797

Appendix C

Confidence Intervals and Joint Confidence Regions for Freundlich Isotherms

Additional Confidence Interval Data

Table C-1: Confidence intervals for the Freundlich coefficient (K_F) for isotherms determined using virgin carbon in ultrapure water

	90% confidence		80% confidence		70% confidence		60% confidence	
	K_F upper bound	K_F lower bound	K_F upper bound	K_F lower bound	K_F upper bound	K_F lower bound	K_F upper bound	K_F lower bound
F400	3.13	1.26	2.88	1.51	2.73	1.66	2.62	1.77
F300	2.94	0.62	2.64	0.92	2.46	1.10	2.33	1.23
Aqua Carb	1.65	0.65	1.52	0.78	1.44	0.86	1.38	0.92
C Gran	1.45	0.62	1.34	0.57	1.27	0.80	1.22	0.85
WV B-30	1.04	0.75	1.00	0.79	0.97	0.81	0.96	0.83
PAC	7.11	5.23	6.82	5.52	6.67	5.67	6.56	5.78

Table C-2: Confidence intervals for the Freundlich coefficient (K_F) for isotherms determined using preloaded carbon in ultrapure water

	90% confidence		80% confidence	
	K_F upper bound	K_F lower bound	K_F upper bound	K_F lower bound
F400	1.86	0.61	1.70	0.77
F300	1.51	0.85	1.42	0.93
F300 – utility preloaded	1.63	0.00	1.28	0.78
Aqua Carb	1.37	0.69	0.64	0.52
C Gran	0.67	0.50	0.71	0.40
WV B-30	0.76	0.34	1.16	0.27

Table C-3: Confidence intervals for the Freundlich power parameter (1/n) for isotherms determined using preloaded carbon in ultrapure water

	90% confidence		80% confidence	
	1/n upper bound	1/n lower bound	1/n upper bound	1/n lower bound
F400	0.45	0.13	0.41	0.20
F300	0.34	0.19	0.32	0.21
F300 – utility preloaded	0.61	0.00	0.31	0.17
Aqua Carb	0.33	0.15	0.62	0.56
C Gran	0.63	0.55	0.69	0.53
WV B-30	0.72	0.50	0.44	0.12

Table C-4: Confidence intervals for the Freundlich coefficient (K_F) for isotherms determined using virgin carbon in Grand River surface water

	90% confidence		80% confidence		70% confidence		60% confidence	
	K_F upper bound	K_F lower bound	K_F upper bound	K_F lower bound	K_F upper bound	K_F lower bound	K_F upper bound	K_F lower bound
F400	0.76	0.58	0.74	0.61	0.72	0.62	0.71	0.63
F300	0.72	0.61	0.70	0.63	0.69	0.64	0.69	0.64
Aqua Carb	0.78	0.49	0.74	0.53	0.71	0.55	0.70	0.57
C Gran	0.83	0.67	0.81	0.69	0.79	0.70	0.78	0.71
WV B-30	0.90	0.61	0.86	0.65	0.83	0.68	0.82	0.69
PAC	2.77	1.51	2.60	1.68	2.50	1.78	2.43	1.85

Table C-5: Confidence intervals for the Freundlich power parameter (1/n) for isotherms determined using virgin carbon in Grand River surface water

	90% confidence		80% confidence		70% confidence		60% confidence	
	1/n upper bound	1/n lower bound	1/n upper bound	1/n lower bound	1/n upper bound	1/n lower bound	1/n upper bound	1/n lower bound
F400	0.14	0.03	0.12	0.04	0.11	0.05	0.11	0.06
F300	0.09	0.02	0.08	0.03	0.07	0.03	0.07	0.04
Aqua Carb	0.30	0.11	0.27	0.13	0.26	0.15	0.24	0.16
C Gran	0.17	0.08	0.16	0.09	0.15	0.10	0.15	0.11
WV B-30	0.23	0.07	0.21	0.09	0.19	0.10	0.18	0.11
PAC	0.60	0.26	0.56	0.31	0.53	0.34	0.51	0.36

Joint Confidence Regions

Joint confidence regions for the two parameters in the Freundlich equation were calculated using a non-linear method, as per the following equations:

$$S(\theta) = \sum[y_i - f(x_i, \theta)]^2 \quad \text{(C-1)}$$

$$S(\theta) = S(\hat{\theta}) * [1 + \frac{p}{n-p} * f_{p,n-p,0.05}] \quad \text{(C-2)}$$

Where y_i is the matrix of q_e values in µg anatoxin-a/mg carbon, x_i is the matrix of equilibrium concentrations in µg/L, θ is the matrix of parameters (in this case, K_F and 1/n, the parameters of the Freundlich equation), $\hat{\theta}$ is a matrix of parameter value estimates based on the non-linear regression, p is the number of parameters (in this case, 2), n is the number of data points used to estimate the isotherm parameters, and $f_{p,n-p,0.05}$ is the f-statistic value. Combining equations C-1 and C-2 with the Freundlich equation yields:

$$\sum[y_i - K_F x_i^{1/n})]^2 = \left(\sum[y_i - f(x_i, \widehat{\theta})]^2\right) * \left(1 + \frac{p}{n-p} * f_{p,n-p,0.05}\right) \quad \text{(C-3)}$$

Solving equations C-3 for each isotherm yields a quadratic equation for 1/n in terms of K_F (or vice-versa), which defines the joint confidence region at a 95% confidence level.

Appendix D

Kinetic Data

Table D-1: Anatoxin-a kinetic data determined with virgin carbon in ultrapure water

	Time (hours)						
ANTX peak area	**0.1**	**1**	**2**	**4**	**6**	**9**	**12**
MilliQ control 1 (100 µg/L)	3910994	4171577	4088679	4254091	4480246	4877650	5110906
MilliQ control 2 (100 µg/L)	3893583	4092176	4106000	4247779	ND	ND	4985518
MilliQ control 3 (20 µg/L)	855056	915209	918864	977708	ND	ND	1151880
F400	3932727	3915864	3957866	3967911	4086254	4490062	4426044
F300	3959922	4033336	4004679	4037501	4214678	4549901	4534023
C Gran	3937486	3807844	3844035	3721606	3742344	3755657	3528510
WV B-30	3933409	3823472	3851567	3754060	3797562	3910510	3799735
PAC	1510971	249507	99358	139257	152710	113210	53858

ND – not determined

Table D-1 continued: Anatoxin-a kinetic data determined with virgin carbon in ultrapure water

	Time (d)											
ANTX peak area	**1**	**2**	**3**	**5**	**7**	**12**	**14**	**16**	**18**	**20**	**26**	29
MilliQ control 1 (100 µg/L)	4671648	3800540	3950640	4056808	4332461	4114079	4392420	4132688	5906393	5853894	4221086	4279636
MilliQ control 2 (100 µg/L)	ND	3811239	4205525	3952513	4284917	3995568	4359032	4028083	5971256	5800905	4281699	4099652
MilliQ control 3 (20 µg/L)	ND	875677	908921	902056	942644	887995	991593	943815	1435645	1366513	948180	948115
F400	3878566	3095732	3048860	2676131	2573242	1880964	1894594	1647540	2287612	1983135	992544	858076
F300	4063506	3298659	3265031	2992309	2917067	2291932	2325008	2121312	2890380	2640220	1449601	1334168
C Gran	2361759	1182376	758777	358484	244882	154653	152763	141194	199473	186701	122645	117814
WV B-30	2493589	1280630	910939	463856	359283	190478	177166	164914	206262	180256	81243	71961
PAC	34112	19701	14716	53966	8960	47115	4851	1086	ND	ND	ND	ND

ND – not determined

Table D-1 continued: Anatoxin-a kinetic data determined with virgin carbon in ultrapure water

	Time (d)										
ANTX peak area	**33**	**37**	**41**	**44**	**50**	**58**	**64**	**69**	**75**	**83**	**89**
MilliQ control 1 (100 µg/L)	4185968	3589846	3736842	3871428	3916135	3737635	3791949	4091678	4155130	4615500	4985944
MilliQ control 2 (100 µg/L)	4050936	3700668	3720264	3755794	3661477	3643275	3840821	3849411	4033530	4358258	4745600
MilliQ control 3 (20 µg/L)	911310	795753	833860	831067	841610	796918	804568	868849	907564	1001905	1032805
F400	668561	465282	413428	360803	261622	159218	111401	98992	65580	49524	30016
F300	1125927	900218	781220	696209	550866	396010	314824	280503	214470	179928	144832
C Gran	100481	68982	84353	80360	71845	66474	73299	ND	ND	ND	ND
WV B-30	55023	44380	39834	36460	34010	17819	13676	ND	ND	ND	ND
PAC	ND	ND	ND	ND	ND	ND	ND	ND	ND	ND	ND

ND – not determined

Table D-2: Anatoxin-a kinetic data for Aqua Carb GAC determined with virgin carbon in ultrapure water

ANTX concentration (µg/L)	Time (d)																
	0.004	0.25	0.5	1	4	7	10	13	16	19	22	26	28	33	36	40	43
MilliQ control 1 (100 µg/L)	102.2	102.4	100.1	99.6	105.3	101.9	101.5	91.8	95.0	96.1	95.5	97.9	98.7	97.7	99.4	98.4	97.6
MilliQ control 2 (100 µg/L)	100.8	101.5	99.1	99.1	91.3	101.7	101.4	91.4	95.0	95.0	94.8	97.2	97.8	98.4	98.6	98.0	97.4
MilliQ control 3 (100 µg/L)	21.9	22.5	21.7	21.3	22.0	21.2	20.5	18.1	21.7	20.9	19.8	20.6	20.4	20.3	20.6	20.1	19.9
Aqua Carb	101.2	93.8	88.1	82.5	65.5	50.2	38.9	28.7	26.9	24.7	17.9	14.3	13.2	9.8	8.0	5.2	4.6

Table D-3: Anatoxin-a kinetic data determined with preloaded carbon in ultrapure water

	Time (hours)		
ANTX concentration (µg/L)	0.1	6	12
MilliQ control 1 (100 µg/L)	102.2	102.4	100.1
MilliQ control 2 (100 µg/L)	100.8	101.5	99.1
MilliQ control 3 (20 µg/L)	21.9	22.5	21.7
F400	101.3	95.6	89.0
F300	100.9	96.8	92.4
Aqua Carb	101.5	91.1	80.8
C Gran	102.3	64.2	48.0
WV B-30	100.7	66.6	53.6
F300 – utility preloaded	100.4	95.0	92.9

ND – not determined

Table D-3 continued: Anatoxin-a kinetic data determined with preloaded carbon in ultrapure water

	Time (d)													
ANTX concentration (µg/L)	1	4	7	10	13	16	19	22	26	28	33	36	40	43
MilliQ control 1 (100 µg/L)	99.6	105.3	101.9	101.5	91.8	95.0	96.1	95.5	97.9	98.7	97.7	99.4	98.4	97.6
MilliQ control 2 (100 µg/L)	99.1	91.3	101.7	101.4	91.4	95.0	95.0	94.8	97.2	97.8	98.4	98.6	98.0	97.4
MilliQ control 3 (20 µg/L)	21.3	22.0	21.2	20.5	18.1	21.7	20.9	19.8	20.6	20.4	20.3	20.6	20.1	19.9
F400	78.8	45.2	27.6	16.2	10.5	6.5	5.4	4.6	3.0	2.6	2.1	2.0	1.9	ND
F300	84.4	59.3	43.0	31.1	22.2	18.7	16.3	12.6	9.4	8.9	6.0	4.7	3.4	3.2
Aqua Carb	77.6	62.8	56.4	46.4	35.0	35.0	33.0	25.4	19.6	19.5	15.2	13.4	11.3	10.9
C Gran	36.4	16.4	12.4	9.4	7.9	8.0	7.1	6.0	5.7	5.6	ND	ND	ND	ND
WV B-30	44.6	23.5	17.3	14.8	12.2	12.0	11.6	11.1	10.9	10.2	ND	ND	ND	ND
F300 – utility preloaded	88.4	76.9	64.7	53.2	40.6	40.9	39.3	30.6	26.3	25.2	23.5	22.0	20.1	19.3

ND – not determined

Table D-4: Anatoxin-a kinetic data determined with virgin carbon in Grand River surface water

	Time (d)								
ANTX concentration (µg/L)	**0.004**	**0.5**	**1**	**3**	**6**	**9**	**12**	**18**	**21**
Surface Water control 1 (100 µg/L)	100.6	98.5	96.2	83.9	84.3	56.7	47.2	34.7	32.8
Surface Water control 2 (100 µg/L)	97.9	96.2	95.9	87.0	85.1	64.4	53.6	40.1	40.6
Surface Water control 3 (20 µg/L)	20.7	20.0	20.5	16.9	15.2	11.2	9.3	6.8	6.7
MilliQ control 4 (100 µg/L)	101.9	96.8	100.6	100.1	97.2	94.9	94.1	98.0	98.8
MilliQ control 5 (100 µg/L)	97.2	95.5	99.9	101.5	98.0	95.2	96.6	97.4	98.2
MilliQ control 6 (20 µg/L)	20.3	20.1	20.3	21.0	18.6	19.3	19.5	20.2	20.5
F400	99.8	64.1	58.4	32.3	15.7	8.7	3.8	1.1	1.2
F300	99.5	76.4	70.8	41.0	27.1	17.3	8.9	2.9	2.8
Aqua Carb	100.3	68.4	60.2	21.3	10.0	2.9	0.9	0.2	0.2
C Gran	100.4	68.9	61.4	28.6	17.7	7.8	3.9	0.8	1.0
WV B-30	101.1	72.7	67.4	29.6	18.1	7.1	2.7	0.3	0.5
PAC	100.2	18.0	4.1	2.4	1.2	ND	ND	ND	ND

ND – not determined

Appendix E
Equilibrium Data

Virgin Carbon, Ultrapure Water

Table E.1: Equilibrium data for virgin F400 in ultrapure water

Sample	Carbon dose (mg/L)	Equilibrium anatoxin-a concentration (µg/L)	Equilibrium capacity, q_e (µg/mg)
F400-1	5.0	33.0	13.4
F400-2	9.9	11.5	8.9
F400-3	15.7	10.9	5.7
F400-4	21.8	3.1	4.4
F400-5	28.5	0.5	3.5
F400-6	32.8	0.8	3.0
F400-7	37.9	2.3	2.6
F400-8	44.2	0.4	2.3
F400-9	51.2	0.8	2.0

Table E.2: Equilibrium data for virgin F300 in ultrapure water

Sample	Carbon dose (mg/L)	Equilibrium anatoxin-a concentration (µg/L)	Equilibrium capacity, q_e (µg/mg)
F300-1	6.6	28.0	10.9
F300-2	10.3	28.3	7.0
F300-3	16.5	19.2	4.9
F300-4	21.2	6.7	4.4
F300-5	28.6	2.6	3.4
F300-6	31.8	10.5	2.8
F300-7	39.2	0.9	2.5
F300-8	43.2	1.2	2.3
F300-9	50.8	1.1	1.9

Table E.3: Equilibrium data for virgin Aqua Carb in ultrapure water

Sample	Carbon dose (mg/L)	Equilibrium anatoxin-a concentration (µg/L)	Equilibrium capacity, q_e (µg/mg)
AquaCarb-1	8.2	65.7	4.2
AquaCarb-2	13.4	55.0	3.4
AquaCarb-3	21	31.9	3.2
AquaCarb-4	24.6	35.2	2.6
AquaCarb-5	31.6	21.0	2.5
AquaCarb-6	37.2	17.7	2.2
AquaCarb-7	43.7	5.1	2.2
AquaCarb-8	49.8	4.6	1.9

Table E.4: Equilibrium data for virgin C Gran in ultrapure water

Sample	Carbon dose (mg/L)	Equilibrium anatoxin-a concentration (µg/L)	Equilibrium capacity, q_e (µg/mg)
C Gran-1	7.4	46.5	7.2
C Gran-2	12.7	36.5	5.0
C Gran-3	21	15.9	4.0
C Gran-4	30	7.7	3.1
C Gran-5	35.2	7.8	2.6
C Gran-6	43.2	4.0	2.2
C Gran-7	49.8	4.2	1.9

Table E.5: Equilibrium data for virgin C Gran in ultrapure water

Sample	Carbon dose (mg/L)	Equilibrium anatoxin-a concentration (µg/L)	Equilibrium capacity, q_e (µg/mg)
WV B-30-1	9.2	33.4	7.2
WV B-30-2	15.4	19.0	5.3
WV B-30-3	22.6	10.7	3.9
WV B-30-4	29.2	9.4	3.1
WV B-30-5	35.6	6.2	2.6
WV B-30-6	41.6	5.1	2.3
WV B-30-7	51.2	3.1	1.9

Table E.6: Equilibrium data for virgin C Gran in ultrapure water

Sample	Carbon dose (mg/L)	Equilibrium anatoxin-a concentration (µg/L)	Equilibrium capacity, q_e (µg/mg)
PAC-1	7.2	45.1	7.6
PAC-2	9.7	23.7	7.9
PAC-3	12	12.3	7.3
PAC-4	13.1	4.9	7.3
PAC-5	16.3	1.7	6.0

Preloaded Carbon, Ultrapure Water

Table E.7: Equilibrium data for pilot-preloaded F400 in ultrapure water

Sample	Carbon dose (mg/L)	Equilibrium anatoxin-a concentration (µg/L)	Equilibrium capacity, q_e (µg/mg)
F400-1	4.1	82.4	4.3
F400-2	10.7	45.6	5.1
F400-3	16.2	34.7	4.0
F400-4	22.3	28.7	3.2
F400-5	30.5	19.5	2.6
F400-6	35.9	9.0	2.5
F400-7	43.2	8.7	2.1
F400-8	49.9	2.8	1.9

Table E.8: Equilibrium data for pilot-preloaded F300 in ultrapure water

Sample	Carbon dose (mg/L)	Equilibrium anatoxin-a concentration (µg/L)	Equilibrium capacity, q_e (µg/mg)
F300-1	4.8	82.1	3.7
F300-2	10.6	61.1	3.7
F300-3	16.3	42.6	3.5
F300-4	19.4	37.1	3.2
F300-5	29.9	25.1	2.5
F300-6	36.5	15.3	2.3
F300-7	44.1	10.7	2.0
F300-8	49.8	3.1	1.9

Table E.9: Equilibrium data for pilot-preloaded Aqua Carb in ultrapure water

Sample	Carbon dose (mg/L)	Equilibrium anatoxin-a concentration (µg/L)	Equilibrium capacity, q_e (µg/mg)
Aqua Carb -1	8.9	71.7	3.2
Aqua Carb -2	15.8	60.7	2.5
Aqua Carb -3	21.6	46.6	2.5
Aqua Carb -4	26.1	37.8	2.4
Aqua Carb -5	33.2	23.3	2.3
Aqua Carb -6	37.8	18.3	2.2
Aqua Carb -7	44.5	16.9	1.9
Aqua Carb -8	50.2	9.2	1.8

Table E.10: Equilibrium data for pilot-preloaded C Gran in ultrapure water

Sample	Carbon dose (mg/L)	Equilibrium anatoxin-a concentration (µg/L)	Equilibrium capacity, q_e (µg/mg)
C Gran-1	8.6	50.4	5.8
C Gran-2	14.0	33.7	4.7
C Gran-3	19.6	23.3	3.9
C Gran-4	24.8	19.2	3.3
C Gran-5	31.4	13.3	2.8
C Gran-6	38.0	11.9	2.3
C Gran-7	45.0	7.8	2.0
C Gran-8	50.6	7.3	1.8

Table E.11: Equilibrium data for pilot-preloaded WV B-30 in ultrapure water

Sample	Carbon dose (mg/L)	Equilibrium anatoxin-a concentration (µg/L)	Equilibrium capacity, q_e (µg/mg)
WV B-30-1	7.6	53.3	6.1
WV B-30-2	12.4	36.7	5.1
WV B-30-3	20.0	20.7	4.0
WV B-30-4	25.8	14.6	3.3
WV B-30-5	33.0	13.2	2.6
WV B-30-6	37.8	11.7	2.3
WV B-30-7	44.0	9.6	2.1
WV B-30-8	50.0	10.7	1.8

Table E.12: Equilibrium data for utility-preloaded F300 in ultrapure water

Sample	Carbon dose (mg/L)	Equilibrium anatoxin-a concentration (µg/L)	Equilibrium capacity, q_e (µg/mg)
F300 utility preloaded-1	9.4	77.1	2.4
F300 utility preloaded-2	33.6	33.4	2.0
F300 utility preloaded-3	48.6	19.8	1.6

Virgin Carbon, Grand River Water

Table E.13: Equilibrium data for virgin F400 in Grand River water

Sample	Carbon dose (mg/L)	Equilibrium anatoxin-a concentration (µg/L)	Equilibrium capacity, q_e (µg/mg)
F400-1	8.6	43.3	-
F400-2	12.4	38.0	-
F400-3	18.4	20.6	0.9
F400-4	23.2	16.0	0.9
F400-5	29.2	12.9	0.8
F400-6	36.4	8.8	0.8
F400-7	44.2	5.1	0.7
F400-8	49.2	1.2	0.7

Table E.14: Equilibrium data for virgin F300 in Grand River water

Sample	Carbon dose (mg/L)	Equilibrium anatoxin-a concentration (µg/L)	Equilibrium capacity, q_e (µg/mg)
F300-1	8.0	40.4	-
F300-2	11.6	39.9	-
F300-3	18.8	35.5	-
F300-4	24.0	18.0	0.8
F300-5	30.6	13.6	0.8
F300-6	37.2	9.1	0.7
F300-7	41.8	5.3	0.8
F300-8	49.2	2.8	0.7

Table E.15: Equilibrium data for virgin Aqua Carb in Grand River water

Sample	Carbon dose (mg/L)	Equilibrium anatoxin-a concentration (µg/L)	Equilibrium capacity, q_e (µg/mg)
Aqua Carb-1	8.2	35.9	-
Aqua Carb-2	11.4	22.3	1.3
Aqua Carb-3	21	14.0	1.1
Aqua Carb-4	25.8	11.1	1.0
Aqua Carb-5	30.4	9.6	0.9
Aqua Carb-6	37	4.8	0.9
Aqua Carb-7	44.4	1.9	0.8
Aqua Carb-8	49.8	0.2	0.7

Table E.16: Equilibrium data for virgin C Gran in Grand River water

Sample	Carbon dose (mg/L)	Equilibrium anatoxin-a concentration (µg/L)	Equilibrium capacity, q_e (µg/mg)
C Gran-1	7.0	37.6	-
C Gran-2	12.4	23.5	1.1
C Gran-3	17.8	16.4	1.1
C Gran-4	24.4	12.0	1.0
C Gran-5	30.4	6.3	1.0
C Gran-6	36.6	5.3	0.9
C Gran-7	44.6	1.2	0.8
C Gran-8	49.6	1.0	0.7

Table E.17: Equilibrium data for virgin WV B-30 in Grand River water

Sample	Carbon dose (mg/L)	Equilibrium anatoxin-a concentration (µg/L)	Equilibrium capacity, q_e (µg/mg)
WV B-30-1	8.8	38.8	-
WV B-30-2	12.2	22.1	1.2
WV B-30-3	19.0	16.2	1.1
WV B-30-4	25.0	9.5	1.1
WV B-30-5	32.4	3.6	1.0
WV B-30-6	36.8	3.5	0.9
WV B-30-7	45.0	2.4	0.8
WV B-30-8	50.4	0.5	0.7

Table E.18: Equilibrium data for virgin PAC in Grand River water

Sample	Carbon dose (mg/L)	Equilibrium anatoxin-a concentration (µg/L)	Equilibrium capacity, q_e (µg/mg)
PAC-1	8.8	9.5	5.8
PAC-2	10.2	6.4	5.3
PAC-3	13.4	4.4	4.2
PAC-4	15.0	5.5	3.7
PAC-5	18.0	3.3	3.2
PAC-6	20.0	1.6	2.9
PAC-7	22.2	1.5	2.7
PAC-8	30.2	0.2	2.0

Appendix F

Details of Surface Area and Pore Volume Distribution Analysis

1. Filtrasorb 400 (F400)

Quantachrome® ASiQwin™- Automated Gas Sorption Data
Acquisition and Reduction
© 1994-2013, Quantachrome Instruments
version 3.01

Analysis				Report			
Operator:	lab	**Date:**	2014/07/03	**Operator:**	ra	**Date:**	2014/08/11
Sample ID:	F-400	**Filename:**		University of Waterloo_F400_070314.qps			
Sample Desc:	Activated carbon	**Comment:**		University of Waterloo, Lab #4549			
Sample Weight:	0.0315 g	**Instrument:**		Autosorb iQ Station 1			
Outgas Time:	16.0 hrs	**Outgas Temp.:**		300 °C			
Analysis gas:	Nitrogen	**Non-ideality:**		6.58e-05 1/Torr	**CellType:**		6mm w/o rod
Analysis Time:	30:50 hr:min	**Bath temp.:**		77.35 K			
Analysis Mode:	Standard				**VoidVol Remeasure:**		off
VoidVol. Mode:	He Measure	**Cold Zone V:**		6.11376 cc	**Warm Zone V:**		8.25039 cc

Multi-Point BET

Data Reduction Parameters Data

Adsorbate	**Thermal Transpiration:** on	**Eff. mol. diameter (D):** 3.54 Å		**Eff. cell stem diam. (d):** 4.0000 mm	
	Nitrogen	**Temperature**	298.150K		
	Molec. Wt.: 28.013	**Cross Section:**	16.200 A^2	**Liquid Density:**	0.806 g/cc

Multi-Point BET Data

Relative Pressure [P/Po]	Volume @ STP [cc/g]	1 / [W((Po/P) - 1)]	Relative Pressure [P/Po]	Volume @ STP [cc/g]	1 / [W((Po/P) - 1)]
9.02336e-03	195.4236	3.7280e-02	3.92911e-02	221.8808	1.4748e-01
1.00012e-02	197.0736	4.1015e-02	4.99157e-02	226.6923	1.8543e-01
2.13276e-02	210.1910	8.2955e-02	7.51901e-02	235.1808	2.7660e-01
2.92224e-02	216.1068	1.1145e-01			

BET summary

Slope =	3.612
Intercept =	5.286e-03
Correlation coefficient, r =	0.999983
C constant=	684.370
Surface Area =	962.621 m^2/g

Quantachrome® ASiQwin™- Automated Gas Sorption Data
Acquisition and Reduction
© 1994-2013, Quantachrome Instruments
version 3.01

Analysis			Report			
Operator:	lab	**Date:**2014/07/03	**Operator:**	ra	**Date:**2014/08/11	
Sample ID:	F-400	**Filename:**	University of Waterloo_F400_070314.qps			
Sample Desc:	Activated carbon	**Comment:**	University of Waterloo, Lab #4549			
Sample Weight:	0.0315 g	**Instrument:**	Autosorb iQ Station 1			
Outgas Time:	16.0 hrs	**Outgas Temp.:**	300 °C			
Analysis gas:	Nitrogen	**Non-ideality:**	6.58e-05 1/Torr	**CellType:**	6mm w/o rod	
Analysis Time:	30:50 hr:min	**Bath temp.:**	77.35 K			
Analysis Mode:	Standard			**VoidVol Remeasure:**	off	
VoidVol. Mode:	He Measure	**Cold Zone V:**	6.11376 cc	**Warm Zone V:**	8.25039 cc	

DFT method Pore Size Distribution (log)

Data Reduction Parameters Data

	Thermal Transpiration: on	**Eff. mol. diameter (D):** 3.54 Å		**Eff. cell stem diam. (d):** 4.0000 mm	
DFT method	**Calc. Model:** N2 at 77 K on carbon (slit pore, QSDFT equilibrium model)				
	Rel. press. range: 0.0000 - 1.0000			**Moving pt. avg:** 5	
Adsorbate	**Nitrogen**	**Temperature**	77.350K		
	Molec. Wt.: 28.013	**Cross Section:**	16.200 Å²	**Liquid Density:**	0.806 g/cc

DFT method Pore Size Distribution (log) Data

Pore width [Å]	Cumulative Pore Volume [cc/g]	Cumulative Surface Area [m²/g]	dV(log d) [cc/g]	dS(log d) [m²/g]
4.8400	9.5703e-02	4.2687e+02	5.6906e-01	2.1720e+03
5.2400	1.2054e-01	5.2316e+02	5.9059e-01	2.1428e+03
5.6700	1.4211e-01	6.0276e+02	5.4106e-01	1.8459e+03
6.1400	1.6105e-01	6.6610e+02	5.4267e-01	1.7177e+03
6.6600	1.8048e-01	7.2585e+02	5.2003e-01	1.5143e+03
7.2300	1.9822e-01	7.7583e+02	4.7763e-01	1.2840e+03
7.8500	2.1494e-01	8.1960e+02	4.6078e-01	1.1513e+03
8.5200	2.3176e-01	8.6067e+02	4.5906e-01	1.0548e+03
9.2600	2.4851e-01	8.9785e+02	4.5262e-01	9.3935e+02
10.0700	2.6462e-01	9.2995e+02	4.4720e-01	8.4503e+02
10.9600	2.8097e-01	9.6003e+02	4.6583e-01	8.1306e+02
11.9300	2.9886e-01	9.9051e+02	4.7976e-01	7.8038e+02
12.9900	3.1678e-01	1.0191e+03	4.4374e-01	6.7498e+02
14.1600	3.3278e-01	1.0428e+03	3.7804e-01	5.3373e+02
15.4300	3.4613e-01	1.0610e+03	3.1826e-01	4.1679e+02
16.8200	3.5778e-01	1.0759e+03	2.5326e-01	3.0710e+02
18.3400	3.6620e-01	1.0857e+03	1.8974e-01	2.0851e+02
20.0000	3.7270e-01	1.0925e+03	1.5665e-01	1.5568e+02
21.8300	3.7845e-01	1.0980e+03	1.4118e-01	1.2668e+02
23.8200	3.8363e-01	1.1025e+03	1.4066e-01	1.1273e+02
26.0000	3.8911e-01	1.1067e+03	1.6496e-01	1.1774e+02
28.3800	3.9583e-01	1.1114e+03	1.8860e-01	1.2384e+02
30.9900	4.0312e-01	1.1160e+03	1.9154e-01	1.1836e+02
33.8500	4.1049e-01	1.1205e+03	1.8662e-01	1.0874e+02
36.9800	4.1786e-01	1.1247e+03	1.7313e-01	9.4639e+01
40.3900	4.2447e-01	1.1283e+03	1.4087e-01	7.0506e+01
44.1300	4.2919e-01	1.1305e+03	1.1426e-01	5.0718e+01
48.2300	4.3346e-01	1.1323e+03	1.0701e-01	4.3027e+01
52.7000	4.3754e-01	1.1339e+03	1.0304e-01	3.7914e+01
57.6000	4.4150e-01	1.1353e+03	1.0214e-01	3.4261e+01
62.9600	4.4550e-01	1.1366e+03	1.0342e-01	3.1686e+01
68.8300	4.4956e-01	1.1378e+03	1.0088e-01	2.8352e+01
75.2400	4.5338e-01	1.1389e+03	9.5670e-02	2.4736e+01
82.2700	4.5708e-01	1.1398e+03	9.4646e-02	2.2437e+01
89.9500	4.6085e-01	1.1407e+03	9.7718e-02	2.0908e+01
98.3500	4.6470e-01	1.1415e+03	9.8502e-02	1.9076e+01
107.5500	4.6846e-01	1.1422e+03	9.7705e-02	1.7360e+01
117.6100	4.7228e-01	1.1428e+03	1.0324e-01	1.6883e+01
128.6100	4.7653e-01	1.1435e+03	1.0380e-01	1.5760e+01
140.6600	4.8050e-01	1.1441e+03	9.3441e-02	1.3067e+01
153.8300	4.8397e-01	1.1446e+03	8.7275e-02	1.1075e+01
168.2500	4.8742e-01	1.1450e+03	8.2566e-02	9.6743e+00
184.0200	4.9058e-01	1.1454e+03	7.1246e-02	7.6700e+00
201.2800	4.9313e-01	1.1456e+03	6.9704e-02	6.6600e+00
220.1600	4.9605e-01	1.1459e+03	7.8018e-02	6.7226e+00
240.8200	4.9916e-01	1.1461e+03	8.2465e-02	6.4144e+00
263.4300	5.0234e-01	1.1464e+03	9.4033e-02	6.6293e+00

Continued on next page

Analysis
Operator: lab **Date:**2014/07/03
Sample ID: F-400 **Filename:**

Report
Operator: ra **Date:**2014/08/11
University of Waterloo_F400_070314.qps

DFT method Pore Size Distribution (log) Data continued

Pore width [Å]	Cumulative Pore Volume [cc/g]	Cumulative Surface Area [m²/g]	dV(log d) [cc/g]	dS(log d) [m²/g]
288.1600	5.0631e-01	1.1467e+03	1.1305e-01	7.4529e+00
315.2200	5.1083e-01	1.1469e+03	1.2395e-01	7.5743e+00
344.8200	5.1645e-01	1.1473e+03	1.4408e-01	8.3586e+00

DFT method summary

Pore volume =	0.503 cc/g
Surface area =	1095.182 m²/g
Lower confidence limit =	4.840 Å
Fitting error =	0.241 %
Pore width (Mode(dLog)) =	5.240 Å
Moving point average :	5

2. Filtrasorb 300 (F300)

Quantachrome® ASiQwin™- Automated Gas Sorption Data Acquisition and Reduction
© 1994-2013, Quantachrome Instruments
version 3.01

Analysis				Report			
Operator:	lab	**Date:**	2014/07/08	**Operator:**	ra	**Date:**	2014/08/11
Sample ID:	Waterloo F300	**Filename:**		University of Waterloo_F300_070714.qps			
Sample Desc:		**Comment:**					
Sample Weight:	0.0309 g	**Instrument:**		Autosorb iQ Station 1			
Outgas Time:	16.0 hrs	**Outgas Temp.:**		300 °C			
Analysis gas:	Nitrogen	**Non-ideality:**		6.58e-05 1/Torr	**CellType:**		6mm w/o rod
Analysis Time:	34:04 hr:min	**Bath temp.:**		77.35 K			
Analysis Mode:	Standard				**VoidVol Remeasure:**		off
VoidVol. Mode:	He Measure	**Cold Zone V:**		6.17334 cc	**Warm Zone V:**		8.21885 cc

Multi-Point BET

Data Reduction Parameters Data

Adsorbate							
	Thermal Transpiration: on		**Eff. mol. diameter (D):** 3.54 Å		**Eff. cell stem diam. (d):** 4.0000 mm		
	Nitrogen		**Temperature**	77.350K			
	Molec. Wt.:	28.013	**Cross Section:**	16.200 Å²	**Liquid Density:**	0.806 g/cc	

Multi-Point BET Data

Relative Pressure [P/Po]	Volume @ STP [cc/g]	1 / [W((Po/P) - 1)]	Relative Pressure [P/Po]	Volume @ STP [cc/g]	1 / [W((Po/P) - 1)]
1.00588e-02	213.6259	3.8057e-02	4.94919e-02	247.8409	1.6810e-01
2.09500e-02	228.1217	7.5052e-02	7.43878e-02	257.9786	2.4925e-01
3.02214e-02	236.1278	1.0560e-01	1.00237e-01	265.4578	3.3578e-01
3.91881e-02	242.1898	1.3474e-01			

BET summary

Slope =	3.288
Intercept =	5.635e-03
Correlation coefficient, r =	0.999981
C constant=	584.548
Surface Area =	1057.287 m²/g

Quantachrome® ASiQwin™ - Automated Gas Sorption Data
Acquisition and Reduction
© 1994-2013, Quantachrome Instruments
version 3.01

Analysis				Report			
Operator:	lab	Date:2014/07/08		Operator:	ra	Date:2014/08/11	
Sample ID:	Waterloo F300	Filename:		University of Waterloo_F300_070714.qps			
Sample Desc:		Comment:					
Sample Weight:	0.0309 g	Instrument:		Autosorb iQ Station 1			
Outgas Time:	16.0 hrs	Outgas Temp.:		300 °C			
Analysis gas:	Nitrogen	Non-ideality:		6.58e-05 1/Torr	CellType:	6mm w/o rod	
Analysis Time:	34:04 hr:min	Bath temp.:		77.35 K			
Analysis Mode:	Standard				VoidVol Remeasure:	off	
VoidVol. Mode:	He Measure	Cold Zone V:		6.17334 cc	Warm Zone V:	8.21885 cc	

DFT method Pore Size Distribution (log)

Data Reduction Parameters Data

	Thermal Transpiration: on	Eff. mol. diameter (D): 3.54 Å		Eff. cell stem diam. (d): 4.0000 mm	
DFT method	Calc. Model: N2 at 77 K on carbon (slit pore, QSDFT equilibrium model)				
	Rel. press. range: 0.0000 - 1.0000			Moving pt. avg: 5	
Adsorbate	Nitrogen	Temperature	77.350K		
	Molec. Wt.: 28.013	Cross Section:	16.200 Å²	Liquid Density:	0.806 g/cc

DFT method Pore Size Distribution (log) Data

Pore width [Å]	Cumulative Pore Volume [cc/g]	Cumulative Surface Area [m²/g]	dV(log d) [cc/g]	dS(log d) [m²/g]
5.2400	1.0064e-01	4.0935e+02	1.2013e+00	4.2373e+03
5.6700	1.3811e-01	5.4454e+02	8.7750e-01	3.0048e+03
6.1400	1.6766e-01	6.4751e+02	7.1402e-01	2.3169e+03
6.6600	1.9174e-01	7.2395e+02	5.9118e-01	1.7572e+03
7.2300	2.1067e-01	7.7736e+02	5.0853e-01	1.3538e+03
7.8500	2.2807e-01	8.2202e+02	4.9883e-01	1.2232e+03
8.5200	2.4635e-01	8.6591e+02	5.1971e-01	1.1833e+03
9.2600	2.6579e-01	9.0904e+02	5.3171e-01	1.1096e+03
10.0700	2.8520e-01	9.4822e+02	5.3000e-01	1.0084e+03
10.9600	3.0452e-01	9.8381e+02	5.4343e-01	9.4697e+02
11.9300	3.2507e-01	1.0187e+03	5.5959e-01	9.0415e+02
12.9900	3.4603e-01	1.0518e+03	5.3390e-01	8.0602e+02
14.1600	3.6562e-01	1.0807e+03	4.7326e-01	6.6544e+02
15.4300	3.8265e-01	1.1039e+03	4.0250e-01	5.2627e+02
16.8200	3.9717e-01	1.1224e+03	3.1914e-01	3.8699e+02
18.3400	4.0796e-01	1.1350e+03	2.3841e-01	2.6406e+02
20.0000	4.1605e-01	1.1436e+03	1.8760e-01	1.8870e+02
21.8300	4.2279e-01	1.1501e+03	1.5892e-01	1.4423e+02
23.8200	4.2848e-01	1.1551e+03	1.5304e-01	1.2299e+02
26.0000	4.3441e-01	1.1596e+03	1.7954e-01	1.2780e+02
28.3800	4.4173e-01	1.1647e+03	2.0644e-01	1.3502e+02
30.9900	4.4969e-01	1.1698e+03	2.1109e-01	1.3016e+02
33.8500	4.5786e-01	1.1747e+03	2.0619e-01	1.2039e+02
36.9800	4.6601e-01	1.1794e+03	1.8757e-01	1.0320e+02
40.3900	4.7310e-01	1.1832e+03	1.4412e-01	7.3237e+01
44.1300	4.7776e-01	1.1855e+03	1.0865e-01	4.8981e+01
48.2300	4.8176e-01	1.1872e+03	9.9437e-02	4.0115e+01
52.7000	4.8554e-01	1.1887e+03	9.5248e-02	3.4802e+01
57.6000	4.8914e-01	1.1899e+03	9.5491e-02	3.1617e+01
62.9600	4.9289e-01	1.1911e+03	1.0365e-01	3.1402e+01
68.8300	4.9714e-01	1.1924e+03	1.0929e-01	3.0426e+01
75.2400	5.0135e-01	1.1935e+03	1.0865e-01	2.7721e+01
82.2700	5.0558e-01	1.1946e+03	1.1067e-01	2.5955e+01
89.9500	5.1001e-01	1.1956e+03	1.1598e-01	2.4829e+01
98.3500	5.1464e-01	1.1965e+03	1.1622e-01	2.2732e+01
107.5500	5.1906e-01	1.1974e+03	1.1157e-01	2.0027e+01
117.6100	5.2337e-01	1.1981e+03	1.1287e-01	1.8575e+01
128.6100	5.2794e-01	1.1989e+03	1.1050e-01	1.6824e+01
140.6600	5.3214e-01	1.1995e+03	9.8408e-02	1.3789e+01
153.8300	5.3579e-01	1.2000e+03	9.1149e-02	1.1582e+01
168.2500	5.3938e-01	1.2004e+03	8.5739e-02	1.0051e+01
184.0200	5.4265e-01	1.2008e+03	7.3830e-02	7.9485e+00
201.2800	5.4530e-01	1.2011e+03	7.0369e-02	6.7595e+00
220.1600	5.4820e-01	1.2013e+03	7.7708e-02	6.7240e+00
240.8200	5.5133e-01	1.2016e+03	8.4354e-02	6.5378e+00
263.4300	5.5462e-01	1.2018e+03	9.9782e-02	6.9679e+00
288.1600	5.5885e-01	1.2021e+03	1.2345e-01	8.0513e+00

Continued on next page

Analysis
Operator: lab **Date:**2014/07/08
Sample ID: Waterloo F300 **Filename:**

Report
Operator: ra **Date:**2014/08/11
University of Waterloo_F300_070714.qps

DFT method Pore Size Distribution (log) Data continued

Pore width [Å]	Cumulative Pore Volume [cc/g]	Cumulative Surface Area [m²/g]	dV(log d) [cc/g]	dS(log d) [m²/g]
315.2200	5.6404e-01	1.2025e+03	1.4417e-01	8.7978e+00
344.8200	5.7063e-01	1.2028e+03	1.6914e-01	9.8117e+00

DFT method summary

Pore volume =	0.551 cc/g
Surface area =	1131.053 m²/g
Lower confidence limit =	5.040 Å
Fitting error =	0.341 %
Pore width (Mode(dLog)) =	5.240 Å
Moving point average :	5

3. Aqua Carb CX 1230

Quantachrome® ASiQwin™- Automated Gas Sorption Data
Acquisition and Reduction
© 1994-2013, Quantachrome Instruments
version 3.01

Analysis				**Report**			
Operator:	lab	**Date:**	2014/07/24	**Operator:**	ra	**Date:**	2014/08/12
Sample ID:	CX-1230	**Filename:**		University of Waterloo_CX-1230_Lab 4549_072414.qps			
Sample Desc:	Carbon	**Comment:**		University of Waterloo, Lab #4549			
Sample Weight:	0.0212 g	**Instrument:**		Autosorb iQ Station 1			
Outgas Time:	16.0 hrs	**Outgas Temp.:**		300 °C			
Analysis gas:	Nitrogen	**Non-ideality:**		6.58e-05 1/Torr	**CellType:**	6mm w/o rod	
Analysis Time:	38:06 hr:min	**Bath temp.:**		77.35 K			
Analysis Mode:	Standard				**VoidVol Remeasure:**	off	
VoidVol. Mode:	He Measure	**Cold Zone V:**		5.98762 cc	**Warm Zone V:**	8.03141 cc	

Multi-Point BET

Data Reduction Parameters Data

	Thermal Transpiration: on	**Eff. mol. diameter (D):** 3.54 Å		**Eff. cell stem diam. (d):** 4.0000 mm	
Adsorbate	**Nitrogen**	**Temperature**	77.350K		
	Molec. Wt.: 28.013	**Cross Section:**	16.200 A^2	**Liquid Density:**	0.806 g/cc

Multi-Point BET Data

Relative Pressure [P/Po]	Volume @ STP [cc/g]	1 / [W((Po/P) - 1)]	Relative Pressure [P/Po]	Volume @ STP [cc/g]	1 / [W((Po/P) - 1)]
9.99997e-03	314.4565	2.5701e-02	4.95887e-02	365.8067	1.1412e-01
2.12483e-02	335.8874	5.1714e-02	7.44584e-02	381.7010	1.6863e-01
3.02151e-02	347.6580	7.1705e-02	1.00234e-01	393.3431	2.2660e-01
4.04748e-02	358.1800	9.4227e-02			

BET summary

Slope =	2.216
Intercept =	4.244e-03
Correlation coefficient, r =	0.999976
C constant=	523.263
Surface Area =	1568.317 m^2/g

Quantachrome® ASiQwin™- Automated Gas Sorption Data
Acquisition and Reduction
© 1994-2013, Quantachrome Instruments
version 3.01

Analysis			Report			
Operator:	lab	**Date:**2014/07/24	**Operator:**	ra	**Date:**2014/08/12	
Sample ID:	CX-1230	**Filename:**	University of Waterloo_CX-1230_Lab 4549_072414.qps			
Sample Desc:	Carbon	**Comment:**	University of Waterloo, Lab #4549			
Sample Weight:	0.0212 g	**Instrument:**	Autosorb iQ Station 1			
Outgas Time:	16.0 hrs	**Outgas Temp.:**	300 °C			
Analysis gas:	Nitrogen	**Non-ideality:**	6.58e-05 1/Torr	**CellType:**	6mm w/o rod	
Analysis Time:	38:06 hr:min	**Bath temp.:**	77.35 K			
Analysis Mode:	Standard			**VoidVol Remeasure:**	off	
VoidVol. Mode:	He Measure	**Cold Zone V:**	5.98762 cc	**Warm Zone V:**	8.03141 cc	

DFT method Pore Size Distribution (log)

Data Reduction Parameters Data

	Thermal Transpiration: on	**Eff. mol. diameter (D):** 3.54 Å		**Eff. cell stem diam. (d):** 4.0000 mm	
DFT method	**Calc. Model:** N2 at 77 K on carbon (slit pore, QSDFT equilibrium model)				
	Rel. press. range: 0.0000 - 1.0000			**Moving pt. avg:** 5	
Adsorbate	**Nitrogen**	**Temperature**	77.350K		
	Molec. Wt.: 28.013	**Cross Section:**	16.200 Å²	**Liquid Density:**	0.806 g/cc

DFT method Pore Size Distribution (log) Data

Pore width [Å]	Cumulative Pore Volume [cc/g]	Cumulative Surface Area [m²/g]	dV(log d) [cc/g]	dS(log d) [m²/g]
5.2400	1.3299e-01	5.2740e+02	1.9731e+00	6.9596e+03
5.6700	1.9118e-01	7.3912e+02	1.2627e+00	4.3639e+03
6.1400	2.3718e-01	9.0019e+02	1.1148e+00	3.5860e+03
6.6600	2.7512e-01	1.0189e+03	9.5342e-01	2.7679e+03
7.2300	3.0493e-01	1.1002e+03	8.5182e-01	2.2264e+03
7.8500	3.3496e-01	1.1770e+03	8.7548e-01	2.1648e+03
8.5200	3.6812e-01	1.2580e+03	9.0478e-01	2.0974e+03
9.2600	4.0175e-01	1.3338e+03	8.6583e-01	1.8280e+03
10.0700	4.3197e-01	1.3951e+03	8.0382e-01	1.5304e+03
10.9600	4.6046e-01	1.4473e+03	8.2557e-01	1.4320e+03
11.9300	4.9231e-01	1.5011e+03	8.9134e-01	1.4333e+03
12.9900	5.2632e-01	1.5547e+03	8.6999e-01	1.3051e+03
14.1600	5.5797e-01	1.6010e+03	7.7943e-01	1.0874e+03
15.4300	5.8619e-01	1.6393e+03	6.8316e-01	8.9015e+02
16.8200	6.1137e-01	1.6713e+03	5.5252e-01	6.7248e+02
18.3400	6.3018e-01	1.6934e+03	3.9982e-01	4.4705e+02
20.0000	6.4330e-01	1.7075e+03	2.8971e-01	2.9607e+02
21.8300	6.5341e-01	1.7175e+03	2.1510e-01	2.0171e+02
23.8200	6.6062e-01	1.7239e+03	1.5955e-01	1.3582e+02
26.0000	6.6616e-01	1.7285e+03	1.3721e-01	1.0375e+02
28.3800	6.7131e-01	1.7322e+03	1.2759e-01	8.6701e+01
30.9900	6.7592e-01	1.7352e+03	1.1165e-01	7.0280e+01
33.8500	6.7999e-01	1.7377e+03	9.7978e-02	5.7795e+01
36.9800	6.8375e-01	1.7399e+03	8.6818e-02	4.8290e+01
40.3900	6.8712e-01	1.7417e+03	6.4855e-02	3.3322e+01
44.1300	6.8908e-01	1.7427e+03	4.4245e-02	1.9917e+01
48.2300	6.9064e-01	1.7433e+03	3.7962e-02	1.5444e+01
52.7000	6.9207e-01	1.7439e+03	3.4082e-02	1.2767e+01
57.6000	6.9334e-01	1.7444e+03	3.0706e-02	1.0539e+01
62.9600	6.9451e-01	1.7447e+03	2.8614e-02	8.9161e+00
68.8300	6.9561e-01	1.7451e+03	2.6841e-02	7.5704e+00
75.2400	6.9661e-01	1.7453e+03	2.5304e-02	6.4923e+00
82.2700	6.9758e-01	1.7456e+03	2.4849e-02	5.8573e+00
89.9500	6.9857e-01	1.7458e+03	2.4892e-02	5.3828e+00
98.3500	6.9954e-01	1.7460e+03	2.3824e-02	4.7150e+00
107.5500	7.0044e-01	1.7462e+03	2.1954e-02	3.9815e+00
117.6100	7.0128e-01	1.7463e+03	2.1550e-02	3.5594e+00
128.6100	7.0214e-01	1.7465e+03	2.1016e-02	3.1871e+00
140.6600	7.0294e-01	1.7466e+03	1.9109e-02	2.6577e+00
153.8300	7.0366e-01	1.7467e+03	1.8298e-02	2.3064e+00
168.2500	7.0438e-01	1.7468e+03	1.7742e-02	2.0677e+00
184.0200	7.0507e-01	1.7469e+03	1.5240e-02	1.6471e+00
201.2800	7.0561e-01	1.7469e+03	1.2880e-02	1.2809e+00
220.1600	7.0611e-01	1.7470e+03	1.0499e-02	9.5082e-01
240.8200	7.0642e-01	1.7470e+03	7.8893e-03	6.5494e-01

Quantachrome® ASiQwin™- Automated Gas Sorption Data Acquisition and Reduction
© 1994-2013, Quantachrome Instruments
version 3.01

Analysis
Operator: lab **Date:**2014/07/24
Sample ID: CX-1230 **Filename:**

Report
Operator: ra **Date:**2014/08/12
University of Waterloo_CX-1230_Lab 4549_072414.qps

DFT method summary

Pore volume =	0.672 cc/g
Surface area =	1617.270 m^2/g
Lower confidence limit =	5.040 Å
Fitting error =	0.306 %
Pore width (Mode(dLog)) =	5.240 Å
Moving point average :	5

4. Norit C Gran

Quantachrome® ASiQwin™- Automated Gas Sorption Data
Acquisition and Reduction
© 1994-2013, Quantachrome Instruments
version 3.01

Analysis			Report		
Operator:	lab	**Date:**2014/08/05	**Operator:** ra		**Date:**2014/09/03
Sample ID:	C-Gran	**Filename:**	University of Waterloo_C-Gran_Lab 4549_080514.qps		
Sample Desc:		**Comment:**			
Sample Weight:	0.0198 g	**Instrument:**	Autosorb iQ Station 1		
Outgas Time:	16.0 hrs	**Outgas Temp.:**	300 °C		
Analysis gas:	Nitrogen	**Non-ideality:**	6.58e-05 1/Torr	**CellType:**	6mm w/o rod
Analysis Time:	34:24 hr:min	**Bath temp.:**	77.35 K		
Analysis Mode:	Standard			**VoidVol Remeasure:**	off
VoidVol. Mode:	He Measure	**Cold Zone V:**	6.37455 cc	**Warm Zone V:**	7.86744 cc

Multi-Point BET

Data Reduction Parameters Data

	Thermal Transpiration: on	**Eff. mol. diameter (D):** 3.54 Å		**Eff. cell stem diam. (d):** 4.0000 mm	
Adsorbate	**Nitrogen**	**Temperature**	77.350K		
	Molec. Wt.: 28.013	**Cross Section:**	16.200 Å²	**Liquid Density:**	0.808 g/cc

Multi-Point BET Data

Relative Pressure [P/Po]	Volume @ STP [cc/g]	1 / [W((Po/P) - 1)]	Relative Pressure [P/Po]	Volume @ STP [cc/g]	1 / [W((Po/P) - 1)]
2.00791e-02	347.5754	4.7170e-02	7.45749e-02	423.5633	1.5223e-01
2.98109e-02	368.0253	6.6803e-02	1.00332e-01	444.5681	2.0071e-01
3.92023e-02	383.2026	8.5194e-02	1.49421e-01	475.8800	2.9536e-01
4.95444e-02	397.1373	1.0502e-01			

BET summary

Slope =	1.911
Intercept =	9.703e-03
Correlation coefficient, r =	0.999977
C constant=	197.921
Surface Area =	1813.488 m²/g

Analysis			Report		
Operator:	lab	**Date:**2014/08/05	**Operator:** ra	**Date:**2014/09/03	
Sample ID:	C-Gran	**Filename:**	University of Waterloo_C-Gran_Lab 4549_080514.qps		
Sample Desc:		**Comment:**			
Sample Weight:	0.0198 g	**Instrument:**	Autosorb iQ Station 1		
Outgas Time:	16.0 hrs	**Outgas Temp.:**	300 °C		
Analysis gas:	Nitrogen	**Non-ideality:**	6.58e-05 1/Torr	**CellType:**	6mm w/o rod
Analysis Time:	34:24 hr:min	**Bath temp.:**	77.35 K		
Analysis Mode:	Standard			**VoidVol Remeasure:**	off
VoidVol. Mode:	He Measure	**Cold Zone V:**	6.37455 cc	**Warm Zone V:**	7.86744 cc

DFT method Pore Size Distribution (log)

Data Reduction Parameters Data

DFT method	**Thermal Transpiration:** on	**Eff. mol. diameter (D):** 3.54 Å		**Eff. cell stem diam. (d):** 4.0000 mm	
	Calc. Model: N2 at 77 K on carbon (slit/cylindr. pores, QSDFT adsorption branch)				
	Rel. press. range: 0.0000 - 1.0000			**Moving pt. avg:** 5	
Adsorbate	**Nitrogen**	**Temperature**	77.350K		
	Molec. Wt.: 28.013	**Cross Section:**	16.200 Å²	**Liquid Density:**	0.808 g/cc

DFT method Pore Size Distribution (log) Data

Pore width [Å]	Cumulative Pore Volume [cc/g]	Cumulative Surface Area [m²/g]	dV(log d) [cc/g]	dS(log d) [m²/g]
5.0400	5.0293e-02	2.0960e+02	1.2367e+00	4.7202e+03
5.2400	6.9804e-02	2.8406e+02	1.1635e+00	4.3386e+03
5.4500	8.6754e-02	3.4718e+02	9.1161e-01	3.3373e+03
5.6700	1.0099e-01	3.9894e+02	6.8103e-01	2.4478e+03
5.9000	1.1106e-01	4.3470e+02	4.3952e-01	1.5435e+03
6.1400	1.1698e-01	4.5515e+02	2.3028e-01	7.8867e+02
6.4000	1.1967e-01	4.6419e+02	8.6353e-02	2.8823e+02
6.6600	1.2031e-01	4.6628e+02	1.6759e-02	5.4590e+01
6.9400	1.2031e-01	4.6628e+02	0.0000e+00	0.0000e+00
7.2300	1.2031e-01	4.6628e+02	0.0000e+00	0.0000e+00
7.5300	1.2031e-01	4.6628e+02	1.4418e-02	3.3846e+01
7.8500	1.2080e-01	4.6741e+02	8.1667e-02	1.8652e+02
8.1800	1.2301e-01	4.7243e+02	2.4063e-01	5.3461e+02
8.5200	1.2880e-01	4.8521e+02	5.0334e-01	1.0880e+03
8.8900	1.4033e-01	5.0992e+02	8.4687e-01	1.7834e+03
9.2600	1.5806e-01	5.4694e+02	1.2195e+00	2.5017e+03
9.6600	1.8326e-01	5.9819e+02	1.5427e+00	3.0770e+03
10.0700	2.1340e-01	6.5766e+02	1.7474e+00	3.3793e+03
10.5100	2.4699e-01	7.2180e+02	1.8043e+00	3.3740e+03
10.9600	2.7998e-01	7.8261e+02	1.7351e+00	3.1298e+03
11.4400	3.1143e-01	8.3841e+02	1.5881e+00	2.7557e+03
11.9300	3.3923e-01	8.8578e+02	1.4226e+00	2.3668e+03
12.4500	3.6434e-01	9.2672e+02	1.2773e+00	2.0317e+03
12.9900	3.8693e-01	9.6193e+02	1.1676e+00	1.7739e+03
13.5600	4.0795e-01	9.9323e+02	1.0841e+00	1.5760e+03
14.1600	4.2778e-01	1.0215e+03	1.0100e+00	1.4089e+03
14.7800	4.4605e-01	1.0466e+03	9.2849e-01	1.2444e+03
15.4300	4.6278e-01	1.0686e+03	8.3379e-01	1.0733e+03
16.1100	4.7766e-01	1.0874e+03	7.2721e-01	8.9825e+02
16.8200	4.9043e-01	1.1029e+03	6.1979e-01	7.3435e+02
17.5600	5.0123e-01	1.1154e+03	5.1614e-01	5.8740e+02
18.3400	5.1018e-01	1.1254e+03	3.9787e-01	4.4131e+02
19.1500	5.1674e-01	1.1326e+03	2.7838e-01	3.0497e+02
20.0000	5.2117e-01	1.1374e+03	1.7509e-01	1.8959e+02
21.2063	5.2477e-01	1.1412e+03	9.1643e-02	1.0030e+02
21.9485	5.2570e-01	1.1423e+03	2.9311e-02	3.6317e+01
22.7167	5.2581e-01	1.1425e+03	4.1351e-03	7.7998e+00
23.5118	5.2581e-01	1.1425e+03	0.0000e+00	0.0000e+00
24.3347	5.2581e-01	1.1425e+03	0.0000e+00	0.0000e+00
25.1864	5.2581e-01	1.1425e+03	1.2499e-03	1.7901e+00
26.0679	5.2584e-01	1.1425e+03	1.1673e-02	1.6276e+01
26.9803	5.2613e-01	1.1429e+03	4.5296e-02	6.1667e+01
27.9246	5.2712e-01	1.1443e+03	1.1496e-01	1.5278e+02
28.9020	5.2940e-01	1.1473e+03	2.1948e-01	2.8523e+02
29.9136	5.3341e-01	1.1524e+03	3.4072e-01	4.3366e+02
30.9605	5.3929e-01	1.1599e+03	4.5559e-01	5.6775e+02
32.0442	5.4680e-01	1.1692e+03	5.4381e-01	6.6200e+02

Continued on next page

Analysis
Operator: lab **Date:**2014/08/05
Sample ID: C-Gran **Filename:**

Report
Operator: ra **Date:**2014/09/03
University of Waterloo_C-Gran_Lab 4549_080514.qps

DFT method Pore Size Distribution (log) Data continued

Pore width [Å]	Cumulative Pore Volume [cc/g]	Cumulative Surface Area [m²/g]	dV(log d) [cc/g]	dS(log d) [m²/g]
33.1657	5.5542e-01	1.1796e+03	5.9618e-01	7.0591e+02
34.3265	5.6459e-01	1.1903e+03	6.2787e-01	7.1892e+02
35.5279	5.7418e-01	1.2011e+03	6.6721e-01	7.3564e+02
36.7714	5.8447e-01	1.2122e+03	7.2766e-01	7.7232e+02
38.0584	5.9578e-01	1.2241e+03	8.0188e-01	8.2180e+02
39.3905	6.0825e-01	1.2367e+03	8.7414e-01	8.6788e+02
40.7691	6.2178e-01	1.2499e+03	9.3029e-01	8.9563e+02
42.1960	6.3601e-01	1.2635e+03	9.5798e-01	8.9359e+02
43.6729	6.5043e-01	1.2767e+03	9.5800e-01	8.6449e+02
45.2015	6.6470e-01	1.2894e+03	9.4523e-01	8.2426e+02
46.7835	6.7874e-01	1.3015e+03	9.2386e-01	7.7895e+02
48.4209	6.9238e-01	1.3128e+03	8.9270e-01	7.2799e+02
50.1157	7.0551e-01	1.3234e+03	8.6951e-01	6.8481e+02
51.8700	7.1846e-01	1.3334e+03	8.6197e-01	6.5475e+02
53.6900	7.3135e-01	1.3430e+03	8.6396e-01	6.3252e+02
55.5600	7.4423e-01	1.3523e+03	8.8498e-01	6.2480e+02
57.5100	7.5772e-01	1.3617e+03	9.1862e-01	6.2698e+02
59.5200	7.7166e-01	1.3711e+03	9.4768e-01	6.2570e+02
61.6000	7.8598e-01	1.3804e+03	9.9571e-01	6.3417e+02
63.7600	8.0137e-01	1.3900e+03	1.0738e+00	6.5904e+02
65.9900	8.1795e-01	1.4001e+03	1.1407e+00	6.7617e+02
68.3000	8.3528e-01	1.4102e+03	1.1920e+00	6.8407e+02
70.6900	8.5347e-01	1.4205e+03	1.2610e+00	7.0074e+02
73.1700	8.7298e-01	1.4312e+03	1.3217e+00	7.1009e+02
75.7300	8.9299e-01	1.4418e+03	1.3305e+00	6.9067e+02
78.3790	9.1270e-01	1.4519e+03	1.3110e+00	6.5856e+02
81.1220	9.3220e-01	1.4615e+03	1.3066e+00	6.3557e+02
83.9610	9.5188e-01	1.4710e+03	1.3337e+00	6.2560e+02
86.9000	9.7212e-01	1.4803e+03	1.3855e+00	6.2469e+02
89.9410	9.9314e-01	1.4896e+03	1.4450e+00	6.2811e+02
93.0890	1.0151e+00	1.4990e+03	1.5035e+00	6.3330e+02
96.3470	1.0380e+00	1.5085e+03	1.5444e+00	6.3173e+02
99.7200	1.0613e+00	1.5180e+03	1.5412e+00	6.1064e+02
103.2100	1.0842e+00	1.5269e+03	1.5175e+00	5.7955e+02
106.8200	1.1068e+00	1.5354e+03	1.5211e+00	5.5926e+02
110.5600	1.1296e+00	1.5436e+03	1.5357e+00	5.4548e+02
114.4300	1.1526e+00	1.5517e+03	1.5225e+00	5.2432e+02
118.4360	1.1752e+00	1.5594e+03	1.4842e+00	4.9570e+02
122.5810	1.1972e+00	1.5666e+03	1.4157e+00	4.5762e+02
126.8710	1.2178e+00	1.5732e+03	1.3180e+00	4.1117e+02
131.3120	1.2368e+00	1.5790e+03	1.2305e+00	3.7013e+02
135.9080	1.2547e+00	1.5843e+03	1.1700e+00	3.4005e+02
140.6640	1.2719e+00	1.5892e+03	1.0945e+00	3.0822e+02
145.5880	1.2876e+00	1.5936e+03	9.9250e-01	2.7084e+02
150.6830	1.3018e+00	1.5974e+03	8.9366e-01	2.3588e+02
155.9570	1.3146e+00	1.6007e+03	8.0470e-01	2.0488e+02
161.4160	1.3261e+00	1.6036e+03	7.2710e-01	1.7828e+02
167.0650	1.3365e+00	1.6061e+03	6.7314e-01	1.5915e+02
172.9120	1.3463e+00	1.6084e+03	6.3405e-01	1.4510e+02
178.9640	1.3555e+00	1.6105e+03	5.9674e-01	1.3209e+02
185.2280	1.3643e+00	1.6124e+03	5.6883e-01	1.2141e+02
191.7110	1.3726e+00	1.6141e+03	5.3490e-01	1.1022e+02
198.4210	1.3803e+00	1.6157e+03	4.9930e-01	9.9420e+01
205.3660	1.3876e+00	1.6171e+03	4.8658e-01	9.3561e+01
212.5530	1.3949e+00	1.6185e+03	4.6907e-01	8.7305e+01
219.9930	1.4017e+00	1.6197e+03	4.2775e-01	7.6979e+01
227.6930	1.4078e+00	1.6208e+03	4.0073e-01	6.9612e+01
235.6620	1.4137e+00	1.6218e+03	3.7609e-01	6.3341e+01
243.9100	1.4191e+00	1.6227e+03	3.2425e-01	5.2950e+01
252.4470	1.4235e+00	1.6234e+03	2.7616e-01	4.3624e+01
261.2820	1.4274e+00	1.6241e+03	2.4401e-01	3.7287e+01
270.4270	1.4309e+00	1.6246e+03	2.0775e-01	3.0585e+01
279.8920	1.4337e+00	1.6250e+03	1.7385e-01	2.4633e+01
289.6890	1.4361e+00	1.6253e+03	1.5768e-01	2.1589e+01
299.8280	1.4385e+00	1.6256e+03	1.6676e-01	2.1842e+01

Continued on next page

Analysis
Operator: lab **Date:**2014/08/05
Sample ID: C-Gran **Filename:**

Report
Operator: ra **Date:**2014/09/03
University of Waterloo_C-Gran_Lab 4549_080514.qps

DFT method Pore Size Distribution (log) Data continued

Pore width [Å]	Cumulative Pore Volume [cc/g]	Cumulative Surface Area [m²/g]	dV(log d) [cc/g]	dS(log d) [m²/g]
310.3220	1.4411e+00	1.6260e+03	1.9158e-01	2.4090e+01
321.1830	1.4439e+00	1.6263e+03	2.1851e-01	2.6641e+01
332.4240	1.4484e+00	1.6269e+03	3.0715e-01	3.6957e+01

DFT method summary

Pore volume =	1.444 cc/g
Surface area =	1617.289 m²/g
Lower confidence limit =	5.040 Å
Fitting error =	0.229 %
Pore width (Mode(dLog)) =	10.510 Å
Moving point average :	5

5. WV B-30

Quantachrome® ASiQwin™- Automated Gas Sorption Data Acquisition and Reduction
© 1994-2013, Quantachrome Instruments
version 3.01

Analysis				Report			
Operator:	lab	**Date:**	2014/07/14	**Operator:**	ra	**Date:**	2014/09/03
Sample ID:	WV-B 30	**Filename:**		University of Waterloo_WV-B 30_071414.qps			
Sample Desc:	Carbon	**Comment:**		University of Waterloo, Lab #4549			
Sample Weight:	0.0341 g	**Instrument:**		Autosorb iQ Station 1			
Outgas Time:	16.0 hrs	**Outgas Temp.:**		300 °C			
Analysis gas:	Nitrogen	**Non-ideality:**		6.58e-05 1/Torr	**CellType:**		6mm w/o rod
Analysis Time:	33:07 hr:min	**Bath temp.:**		77.35 K			
Analysis Mode:	Standard				**VoidVol Remeasure:**		off
VoidVol. Mode:	He Measure	**Cold Zone V:**		6.10131 cc	**Warm Zone V:**		8.27629 cc

Multi-Point BET

Data Reduction Parameters Data

Adsorbate	**Thermal Transpiration:** on		**Eff. mol. diameter (D):**	3.54 Å	**Eff. cell stem diam. (d):**	4.0000 mm	
	Nitrogen		**Temperature**	77.350K			
	Molec. Wt.:	28.013	**Cross Section:**	16.200 Å²	**Liquid Density:**	0.806	g/cc

Multi-Point BET Data

Relative Pressure [P/Po]	Volume @ STP [cc/g]	1 / [W((Po/P) - 1)]	Relative Pressure [P/Po]	Volume @ STP [cc/g]	1 / [W((Po/P) - 1)]
3.01882e-02	293.1375	8.4963e-02	1.01416e-01	367.5144	2.4571e-01
4.05497e-02	307.9722	1.0980e-01	1.49100e-01	402.1852	3.4860e-01
4.96019e-02	319.0014	1.3090e-01	1.99732e-01	433.5316	4.6062e-01
7.64121e-02	346.4072	1.9109e-01			

BET summary

Slope =	2.205
Intercept =	2.071e-02
Correlation coefficient, r =	0.999945
C constant=	107.499
Surface Area =	1564.560 m²/g

Analysis			Report		
Operator:	lab	**Date:** 2014/07/14	**Operator:** ra	**Date:** 2014/09/03	
Sample ID:	WV-B 30	**Filename:**	University of Waterloo_WV-B 30_071414.qps		
Sample Desc:	Carbon	**Comment:**	University of Waterloo, Lab #4549		
Sample Weight:	0.0341 g	**Instrument:**	Autosorb iQ Station 1		
Outgas Time:	16.0 hrs	**Outgas Temp.:**	300 °C		
Analysis gas:	Nitrogen	**Non-ideality:**	6.58e-05 1/Torr	**CellType:**	6mm w/o rod
Analysis Time:	33:07 hr:min	**Bath temp.:**	77.35 K		
Analysis Mode:	Standard			**VoidVol Remeasure:**	off
VoidVol. Mode:	He Measure	**Cold Zone V:**	6.10131 cc	**Warm Zone V:**	8.27629 cc

DFT method Pore Size Distribution (log)

Data Reduction Parameters Data

	Thermal Transpiration: on	**Eff. mol. diameter (D):** 3.54 Å		**Eff. cell stem diam. (d):** 4.0000 mm	
DFT method	**Calc. Model:** N2 at 77 K on carbon (slit/cylindr. pores, QSDFT adsorption branch)				
	Rel. press. range: 0.0000 - 1.0000			**Moving pt. avg:** 5	
Adsorbate	**Nitrogen**	**Temperature**	77.350K		
	Molec. Wt.: 28.013	**Cross Section:**	16.200 Å²	**Liquid Density:**	0.806 g/cc

DFT method Pore Size Distribution (log) Data

Pore width [Å]	Cumulative Pore Volume [cc/g]	Cumulative Surface Area [m²/g]	dV(log d) [cc/g]	dS(log d) [m²/g]
5.0400	3.8109e-02	1.6696e+02	3.9765e-01	1.5178e+03
5.2400	4.4464e-02	1.9134e+02	3.3303e-01	1.2469e+03
5.4500	4.9283e-02	2.0955e+02	2.3141e-01	8.5777e+02
5.6700	5.2725e-02	2.2224e+02	1.5188e-01	5.5422e+02
5.9000	5.4777e-02	2.2962e+02	8.1140e-02	2.8881e+02
6.1400	5.5709e-02	2.3287e+02	3.1588e-02	1.0963e+02
6.4000	5.5964e-02	2.3373e+02	6.5126e-03	2.2077e+01
6.6600	5.5964e-02	2.3373e+02	0.0000e+00	0.0000e+00
6.9400	5.5964e-02	2.3373e+02	0.0000e+00	0.0000e+00
7.2300	5.5964e-02	2.3373e+02	0.0000e+00	0.0000e+00
7.5300	5.5964e-02	2.3373e+02	8.4511e-03	1.9838e+01
7.8500	5.6247e-02	2.3440e+02	4.9633e-02	1.1330e+02
8.1800	5.7598e-02	2.3747e+02	1.5130e-01	3.3582e+02
8.5200	6.1278e-02	2.4557e+02	3.2691e-01	7.0558e+02
8.8900	6.8840e-02	2.6175e+02	5.6708e-01	1.1915e+03
9.2600	8.0824e-02	2.8672e+02	8.4118e-01	1.7205e+03
9.6600	9.8380e-02	3.2230e+02	1.0961e+00	2.1788e+03
10.0700	1.2002e-01	3.6486e+02	1.2784e+00	2.4641e+03
10.5100	1.4487e-01	4.1218e+02	1.3576e+00	2.5314e+03
10.9600	1.6998e-01	4.5835e+02	1.3393e+00	2.4103e+03
11.4400	1.9452e-01	5.0180e+02	1.2519e+00	2.1687e+03
11.9300	2.1661e-01	5.3941e+02	1.1384e+00	1.8921e+03
12.4500	2.3681e-01	5.7234e+02	1.0330e+00	1.6420e+03
12.9900	2.5517e-01	6.0093e+02	9.5484e-01	1.4495e+03
13.5600	2.7246e-01	6.2665e+02	9.0209e-01	1.3089e+03
14.1600	2.8910e-01	6.5035e+02	8.6382e-01	1.2008e+03
14.7800	3.0494e-01	6.7197e+02	8.2834e-01	1.1044e+03
15.4300	3.2019e-01	6.9195e+02	7.9087e-01	1.0110e+03
16.1100	3.3474e-01	7.1020e+02	7.4786e-01	9.1567e+02
16.8200	3.4840e-01	7.2662e+02	7.0079e-01	8.2191e+02
17.5600	3.6115e-01	7.4130e+02	6.4389e-01	7.2525e+02
18.3400	3.7281e-01	7.5421e+02	5.4141e-01	5.9861e+02
19.1500	3.8212e-01	7.6446e+02	4.1185e-01	4.5593e+02
20.0000	3.8900e-01	7.7200e+02	2.8094e-01	3.1189e+02
21.2063	3.9500e-01	7.7860e+02	1.5887e-01	1.8143e+02
21.9485	3.9671e-01	7.8058e+02	5.8926e-02	7.8927e+01
22.7167	3.9704e-01	7.8120e+02	1.4338e-02	2.6730e+01
23.5118	3.9713e-01	7.8137e+02	2.8270e-03	5.1516e+00
24.3347	3.9713e-01	7.8137e+02	4.4224e-03	6.5568e+00
25.1864	3.9726e-01	7.8155e+02	2.8435e-02	4.1176e+01
26.0679	3.9793e-01	7.8252e+02	9.5030e-02	1.3429e+02
26.9803	3.9994e-01	7.8534e+02	2.2458e-01	3.0972e+02
27.9246	4.0432e-01	7.9134e+02	4.2688e-01	5.7483e+02
28.9020	4.1220e-01	8.0186e+02	6.8716e-01	9.0392e+02
29.9136	4.2425e-01	8.1759e+02	9.6131e-01	1.2350e+03
30.9605	4.4034e-01	8.3808e+02	1.1979e+00	1.5014e+03
32.0442	4.5962e-01	8.6202e+02	1.3607e+00	1.6611e+03

Continued on next page

Analysis
Operator: lab **Date:**2014/07/14
Sample ID: WV-B 30 **Filename:**

Report
Operator: ra **Date:**2014/09/03
University of Waterloo_WV-B 30_071414.qps

DFT method Pore Size Distribution (log) Data continued

Pore width [Å]	Cumulative Pore Volume [cc/g]	Cumulative Surface Area [m²/g]	dV(log d) [cc/g]	dS(log d) [m²/g]
33.1657	4.8082e-01	8.8760e+02	1.4402e+00	1.7079e+03
34.3265	5.0268e-01	9.1319e+02	1.4598e+00	1.6762e+03
35.5279	5.2454e-01	9.3792e+02	1.4586e+00	1.6172e+03
36.7714	5.4634e-01	9.6171e+02	1.4582e+00	1.5600e+03
38.0584	5.6813e-01	9.8467e+02	1.4571e+00	1.5060e+03
39.3905	5.8989e-01	1.0068e+03	1.4445e+00	1.4451e+03
40.7691	6.1138e-01	1.0280e+03	1.4083e+00	1.3647e+03
42.1960	6.3215e-01	1.0479e+03	1.3439e+00	1.2604e+03
43.6729	6.5177e-01	1.0660e+03	1.2633e+00	1.1449e+03
45.2015	6.7012e-01	1.0824e+03	1.1841e+00	1.0361e+03
46.7835	6.8734e-01	1.0972e+03	1.1095e+00	9.3795e+02
48.4209	7.0345e-01	1.1106e+03	1.0351e+00	8.4622e+02
50.1157	7.1845e-01	1.1227e+03	9.6328e-01	7.6155e+02
51.8700	7.3243e-01	1.1336e+03	8.9638e-01	6.8466e+02
53.6900	7.4546e-01	1.1434e+03	8.3731e-01	6.1697e+02
55.5600	7.5756e-01	1.1521e+03	7.9433e-01	5.6431e+02
57.5100	7.6925e-01	1.1603e+03	7.6773e-01	5.2645e+02
59.5200	7.8058e-01	1.1680e+03	7.5172e-01	4.9791e+02
61.6000	7.9173e-01	1.1752e+03	7.5054e-01	4.7974e+02
63.7600	8.0304e-01	1.1824e+03	7.6625e-01	4.7219e+02
65.9900	8.1463e-01	1.1894e+03	7.8720e-01	4.6802e+02
68.3000	8.2651e-01	1.1963e+03	8.0827e-01	4.6448e+02
70.6900	8.3874e-01	1.2033e+03	8.3005e-01	4.6169e+02
73.1700	8.5134e-01	1.2102e+03	8.3950e-01	4.5203e+02
75.7300	8.6389e-01	1.2168e+03	8.2367e-01	4.2913e+02
78.3790	8.7601e-01	1.2231e+03	7.9186e-01	3.9907e+02
81.1220	8.8764e-01	1.2288e+03	7.6211e-01	3.7129e+02
83.9610	8.9889e-01	1.2342e+03	7.4242e-01	3.4897e+02
86.9000	9.0991e-01	1.2393e+03	7.3283e-01	3.3192e+02
89.9410	9.2081e-01	1.2442e+03	7.2890e-01	3.1859e+02
93.0890	9.3168e-01	1.2489e+03	7.2494e-01	3.0662e+02
96.3470	9.4250e-01	1.2534e+03	7.1445e-01	2.9276e+02
99.7200	9.5311e-01	1.2577e+03	6.9343e-01	2.7492e+02
103.2100	9.6332e-01	1.2617e+03	6.7182e-01	2.5693e+02
106.8200	9.7325e-01	1.2654e+03	6.6233e-01	2.4401e+02
110.5600	9.8312e-01	1.2690e+03	6.5830e-01	2.3415e+02
114.4300	9.9292e-01	1.2724e+03	6.4678e-01	2.2277e+02
118.4360	1.0025e+00	1.2757e+03	6.2738e-01	2.0946e+02
122.5810	1.0118e+00	1.2787e+03	5.9807e-01	1.9329e+02
126.8710	1.0205e+00	1.2815e+03	5.5813e-01	1.7417e+02
131.3120	1.0285e+00	1.2840e+03	5.2080e-01	1.5674e+02
135.9080	1.0361e+00	1.2862e+03	4.9559e-01	1.4399e+02
140.6640	1.0434e+00	1.2883e+03	4.7225e-01	1.3270e+02
145.5880	1.0503e+00	1.2902e+03	4.4316e-01	1.2050e+02
150.6830	1.0567e+00	1.2919e+03	4.1427e-01	1.0890e+02
155.9570	1.0628e+00	1.2935e+03	3.8845e-01	9.8601e+01
161.4160	1.0684e+00	1.2949e+03	3.6372e-01	8.9085e+01
167.0650	1.0737e+00	1.2962e+03	3.4122e-01	8.0700e+01
172.9120	1.0787e+00	1.2973e+03	3.2096e-01	7.3452e+01
178.9640	1.0833e+00	1.2984e+03	3.0238e-01	6.6917e+01
185.2280	1.0877e+00	1.2993e+03	2.8705e-01	6.1285e+01
191.7110	1.0919e+00	1.3002e+03	2.6976e-01	5.5591e+01
198.4210	1.0958e+00	1.3010e+03	2.5319e-01	5.0409e+01
205.3660	1.0995e+00	1.3017e+03	2.4498e-01	4.7125e+01
212.5530	1.1032e+00	1.3024e+03	2.3441e-01	4.3633e+01
219.9930	1.1066e+00	1.3030e+03	2.1524e-01	3.8739e+01
227.6930	1.1097e+00	1.3036e+03	2.0319e-01	3.5282e+01
235.6620	1.1127e+00	1.3041e+03	1.9713e-01	3.3059e+01
243.9100	1.1156e+00	1.3046e+03	1.8180e-01	2.9485e+01
252.4470	1.1181e+00	1.3050e+03	1.6389e-01	2.5737e+01
261.2820	1.1205e+00	1.3054e+03	1.5142e-01	2.3054e+01
270.4270	1.1227e+00	1.3057e+03	1.3535e-01	1.9939e+01
279.8920	1.1246e+00	1.3060e+03	1.1415e-01	1.6224e+01
289.6890	1.1262e+00	1.3062e+03	1.0170e-01	1.3909e+01
299.8280	1.1277e+00	1.3064e+03	1.0704e-01	1.4003e+01

Continued on next page

Quantachrome® ASiQwin™- Automated Gas Sorption Data
Acquisition and Reduction
© 1994-2013, Quantachrome Instruments
version 3.01

Analysis
Operator: lab **Date:**2014/07/14
Sample ID: WV-B 30 **Filename:**

Report
Operator: ra **Date:**2014/09/03
University of Waterloo_WV-B 30_071414.qps

DFT method Pore Size Distribution (log) Data continued

Pore width [Å]	Cumulative Pore Volume [cc/g]	Cumulative Surface Area [m²/g]	dV(log d) [cc/g]	dS(log d) [m²/g]
310.3220	1.1294e+00	1.3066e+03	1.2109e-01	1.5237e+01
321.1830	1.1311e+00	1.3068e+03	1.3882e-01	1.6953e+01
332.4240	1.1339e+00	1.3072e+03	1.8356e-01	2.2086e+01

DFT method summary

Pore volume =	1.130 cc/g
Surface area =	1298.492 m²/g
Lower confidence limit =	5.040 Å
Fitting error =	0.291 %
Pore width (Mode(dLog)) =	34.326 Å
Moving point average :	5

6. Standard Purification Aquacarb 800 PAC

Quantachrome® ASiQwin™- Automated Gas Sorption Data Acquisition and Reduction
© 1994-2013, Quantachrome Instruments
version 3.01

Analysis				Report			
Operator:	lab	**Date:**	2014/07/10	**Operator:**	ra	**Date:**	2014/08/11
Sample ID:	PAC	**Filename:**		University of Waterloo_PAC_071014.qps			
Sample Desc:	Carbon	**Comment:**		University of Waterloo, Lab #4549			
Sample Weight:	0.026 g	**Instrument:**		Autosorb iQ Station 1			
Outgas Time:	16.0 hrs	**Outgas Temp.:**		300 °C			
Analysis gas:	Nitrogen	**Non-ideality:**		6.58e-05 1/Torr	**CellType:**		6mm w/o rod
Analysis Time:	38:00 hr:min	**Bath temp.:**		77.35 K			
Analysis Mode:	Standard				**VoidVol Remeasure:**		off
VoidVol. Mode:	He Measure	**Cold Zone V:**		6.31563 cc	**Warm Zone V:**		8.17507 cc

Multi-Point BET

Data Reduction Parameters Data

Adsorbate							
	Thermal Transpiration: on		**Eff. mol. diameter (D):** 3.54 Å		**Eff. cell stem diam. (d):** 4.0000 mm		
	Nitrogen		**Temperature**	77.350K			
	Molec. Wt.:	28.013	**Cross Section:**	16.200 Å²	**Liquid Density:**	0.806 g/cc	

Multi-Point BET Data

Relative Pressure [P/Po]	Volume @ STP [cc/g]	1 / [W((Po/P) - 1)]	Relative Pressure [P/Po]	Volume @ STP [cc/g]	1 / [W((Po/P) - 1)]
1.00250e-02	154.5473	5.2426e-02	4.92626e-02	175.2934	2.3651e-01
2.09032e-02	163.3077	1.0460e-01	7.42661e-02	182.0475	3.5259e-01
3.04160e-02	168.2316	1.4920e-01	9.95200e-02	187.4264	4.7180e-01
4.07059e-02	172.3668	1.9697e-01			

BET summary

Slope =	4.673
Intercept =	6.430e-03
Correlation coefficient, r =	0.999991
C constant=	727.664
Surface Area =	744.273 m²/g

Quantachrome® ASiQwin™- Automated Gas Sorption Data
Acquisition and Reduction
© 1994-2013, Quantachrome Instruments
version 3.01

Analysis				Report			
Operator:	lab	Date:2014/07/10		Operator:	ra	Date:2014/08/11	
Sample ID:	PAC	Filename:	University of Waterloo_PAC_071014.qps				
Sample Desc:	Carbon	Comment:	University of Waterloo, Lab #4549				
Sample Weight:	0.026 g	Instrument:	Autosorb iQ Station 1				
Outgas Time:	16.0 hrs	Outgas Temp.:	300 °C				
Analysis gas:	Nitrogen	Non-ideality:	6.58e-05 1/Torr	CellType:	6mm w/o rod		
Analysis Time:	38:00 hr:min	Bath temp.:	77.35 K				
Analysis Mode:	Standard			VoidVol Remeasure:	off		
VoidVol. Mode:	He Measure	Cold Zone V:	6.31563 cc	Warm Zone V:	8.17507 cc		

DFT method Pore Size Distribution (log)

Data Reduction Parameters Data

DFT method	Thermal Transpiration: on	Eff. mol. diameter (D): 3.54 Å		Eff. cell stem diam. (d): 4.0000 mm
	Calc. Model: N2 at 77 K on carbon (slit pore, QSDFT equilibrium model)			
	Rel. press. range: 0.0000 - 1.0000			Moving pt. avg: 5
Adsorbate	Nitrogen	Temperature	77.350K	
	Molec. Wt.: 28.013	Cross Section:	16.200 Å²	Liquid Density: 0.806 g/cc

DFT method Pore Size Distribution (log) Data

Pore width [Å]	Cumulative Pore Volume [cc/g]	Cumulative Surface Area [m²/g]	dV(log d) [cc/g]	dS(log d) [m²/g]
4.8400	8.4591e-02	3.7120e+02	8.8399e-01	3.3740e+03
5.2400	1.1346e-01	4.8428e+02	6.3384e-01	2.3540e+03
5.6700	1.3456e-01	5.6503e+02	4.6604e-01	1.6692e+03
6.1400	1.4946e-01	6.1746e+02	3.4480e-01	1.1416e+03
6.6600	1.5980e-01	6.4975e+02	2.7035e-01	7.8755e+02
7.2300	1.6878e-01	6.7460e+02	2.6344e-01	6.9093e+02
7.8500	1.7839e-01	6.9915e+02	2.8161e-01	6.8535e+02
8.5200	1.8878e-01	7.2389e+02	2.9514e-01	6.6781e+02
9.2600	1.9967e-01	7.4793e+02	2.9876e-01	6.2425e+02
10.0700	2.1064e-01	7.7020e+02	2.9212e-01	5.6296e+02
10.9600	2.2128e-01	7.9015e+02	2.8826e-01	5.0901e+02
11.9300	2.3204e-01	8.0855e+02	2.9263e-01	4.7257e+02
12.9900	2.4298e-01	8.2571e+02	2.8733e-01	4.2774e+02
14.1600	2.5358e-01	8.4107e+02	2.7474e-01	3.7714e+02
15.4300	2.6377e-01	8.5465e+02	2.6541e-01	3.3675e+02
16.8200	2.7383e-01	8.6712e+02	2.4756e-01	2.9047e+02
18.3400	2.8285e-01	8.7736e+02	2.2081e-01	2.3676e+02
20.0000	2.9082e-01	8.8561e+02	2.0259e-01	1.9837e+02
21.8300	2.9850e-01	8.9290e+02	1.9397e-01	1.7322e+02
23.8200	3.0579e-01	8.9918e+02	2.0564e-01	1.6390e+02
26.0000	3.1401e-01	9.0548e+02	2.5708e-01	1.8161e+02
28.3800	3.2464e-01	9.1273e+02	2.9912e-01	1.9474e+02
30.9900	3.3603e-01	9.2002e+02	2.9905e-01	1.8494e+02
33.8500	3.4754e-01	9.2704e+02	2.8243e-01	1.6723e+02
36.9800	3.5869e-01	9.3356e+02	2.4418e-01	1.3749e+02
40.3900	3.6781e-01	9.3857e+02	1.6888e-01	8.8009e+01
44.1300	3.7275e-01	9.4098e+02	1.0560e-01	4.8299e+01
48.2300	3.7632e-01	9.4253e+02	8.4921e-02	3.4698e+01
52.7000	3.7947e-01	9.4377e+02	7.5537e-02	2.8187e+01
57.6000	3.8229e-01	9.4479e+02	6.9609e-02	2.3656e+01
62.9600	3.8496e-01	9.4566e+02	6.7382e-02	2.0818e+01
68.8300	3.8758e-01	9.4645e+02	6.4760e-02	1.8230e+01
75.2400	3.9002e-01	9.4711e+02	6.1310e-02	1.5775e+01
82.2700	3.9238e-01	9.4770e+02	6.0657e-02	1.4320e+01
89.9500	3.9479e-01	9.4826e+02	6.1999e-02	1.3326e+01
98.3500	3.9724e-01	9.4877e+02	6.1070e-02	1.1952e+01
107.5500	3.9955e-01	9.4920e+02	5.8629e-02	1.0514e+01
117.6100	4.0182e-01	9.4960e+02	6.0599e-02	9.9304e+00
128.6100	4.0430e-01	9.4999e+02	6.0932e-02	9.2103e+00
140.6600	4.0663e-01	9.5034e+02	5.5815e-02	7.7546e+00
153.8300	4.0872e-01	9.5062e+02	5.3540e-02	6.7567e+00
168.2500	4.1085e-01	9.5088e+02	5.1778e-02	6.0494e+00
184.0200	4.1285e-01	9.5111e+02	4.5358e-02	4.8776e+00
201.2800	4.1449e-01	9.5128e+02	4.8283e-02	4.5386e+00
220.1600	4.1659e-01	9.5147e+02	5.8305e-02	4.9301e+00
240.8200	4.1891e-01	9.5166e+02	6.3172e-02	4.8693e+00
263.4300	4.2137e-01	9.5184e+02	7.2879e-02	5.1472e+00

Continued on next page

Quantachrome® ASiQwin™- Automated Gas Sorption Data
Acquisition and Reduction
© 1994-2013, Quantachrome Instruments
version 3.01

Analysis
Operator: lab **Date:**2014/07/10
Sample ID: PAC **Filename:**

Report
Operator: ra **Date:**2014/08/11
University of Waterloo_PAC_071014.qps

DFT method Pore Size Distribution (log) Data continued

Pore width [Å]	Cumulative Pore Volume [cc/g]	Cumulative Surface Area [m²/g]	dV(log d) [cc/g]	dS(log d) [m²/g]
288.1600	4.2446e-01	9.5205e+02	8.7618e-02	5.8214e+00
315.2200	4.2778e-01	9.5226e+02	9.0783e-02	5.5477e+00
344.8200	4.3189e-01	9.5250e+02	1.0540e-01	6.1131e+00

DFT method summary

Pore volume =	0.416 cc/g
Surface area =	887.333 m²/g
Lower confidence limit =	4.660 Å
Fitting error =	0.300 %
Pore width (Mode(dLog)) =	4.840 Å
Moving point average :	5